DAMPING OF POWER SYSTEM HARMONIC RESONANCES USING FIRING ANGLE MODULATION OF THE THYRISTOR CONTROLLED REACTOR OF A STATIC VAR COMPENSATOR

by

Ronald Wayne Mazur

A Thesis
Submitted to the Faculty of Graduate Studies
in Partial fulfillment of the
Requirements for the Degree of

MASTER OF SCIENCE

Department of Electrical and Computer Engineering
University of Manitoba
Winnipeg, Manitoba

September, 1989

ISBN 0-315-54912-2

Canada

DAMPING OF POWER SYSTEM HARMONIC RESONANCES USING FIRING ANGLE MODULATION OF THE THYRISTOR CONTROLLED REACTOR OF A STATIC VAR COMPENSATOR

BY

RONALD WAYNE MAZUR

A thesis submitted to the Faculty of Graduate Studies of the University of Manitoba in partial fulfillment of the requirements of the degree of

MASTER OF SCIENCE

ABSTRACT

Weak ac systems which interface to a dc link can form a parallel resonance with the ac harmonic filters or with the ac filters plus a static var compensator (fixed capacitor and thyristor-controlled reactor). The resonant frequency is of low harmonic order, usually near the second or third harmonic. Harmonic current, coincident with the resonant frequency, can generate a large harmonic voltage component due to the high parallel resonant impedance. Severe harmonic distortion of the fundamental frequency voltage waveforms can result.

A concern common to most static var compensator (SVC) applications is the interaction of the thyristor-controlled reactor (TCR) of the SVC with the ac system when a low frequency resonance occurs. Equidistant firing of the TCR when the terminal voltage is distorted by a second harmonic voltage component, generates a dc component and a second harmonic component in the positive sequence TCR line current. The second harmonic current component can enhance a system resonance whose resonant frequency is near the second harmonic, and possibly cause harmonic instability of a lightly damped power system.

The feasibility of damping system harmonic resonances (near the second harmonic) by modulating the firing angle of the TCR is examined. The second harmonic phasor component in the positive sequence TCR line current is measured and processed by a firing angle modulation controller. The firing of the TCR antiparallel thyristors is modulated sinusoidally such that a harmonic phasor component of appropriate magnitude and phase is generated with the objective of cancelling the undesired harmonic component.

Computer models were developed for the digital time domain simulation program EMTDC in order to study several system parallel resonant configurations. These study systems were resonant near the second harmonic.

The simulation results showed that modulation of the TCR firing angle reduced the system resonant frequency. Consequently, damping of the second harmonic voltage component was achieved for systems resonant at or below 120 Hz. The modulation enhanced the second harmonic voltage component if the system resonance was just above 120 Hz. Under this condition, TCR firing angle modulation control of the dc component of TCR line current would be more beneficial to avoid excessive saturation of the SVC step-up transformer.

ACKNOWLEDGEMENTS

The author wishes to express his appreciation to Dr. R.W. Menzies, the author's thesis supervisor, for his suggestions and valuable discussions throughout this project.

The author also wishes to thank Professor D.A. Woodford of the Manitoba HVDC Research Centre for his helpful suggestions in the application of the EMTDC program to this endeavor.

The author is indebted to Manitoba Hydro for allowing the use of the Prime Computer for the digital simulation required for this project.

The author would like to thank Ms. E. Zimmer for her untiring effort in typing this manuscript.

Finally, the author expresses his sincere appreciation to his wife, Ilonka and his three sons, Jonathan, Daniel and Michael for their understanding, support and encouragement.

TABLE OF CONTENTS

TABLE OF CONTENTS (Cont'd)

TABLE OF CONTENTS (Cont'd)

TABLE OF CONTENTS (Cont'd)

LIST OF FIGURES

LIST OF FIGURES (Cont'd)

LIST OF FIGURES (Cont'd)

LIST OF FIGURES (Cont'd)

LIST OF FIGURES (Cont'd)

LIST OF FIGURES (Cont'd)

LIST OF FIGURES (Cont'd)

LIST OF FIGURES (Cont'd)

LIST OF FIGURES (Cont'd)

LIST OF FIGURES (Cont'd)

LIST OF FIGURES (Cont'd)

LIST OF FIGURES (Cont'd)

LIST OF TABLES

LIST OF TABLES (Cont'd)

LIST OF TABLES (Cont'd)

LIST OF TABLES (Cont'd)

CHAPTER ONE

INTRODUCTION

1.1 Objectives and Outline of the Thesis

This thesis is a simulation study which investigates the feasibility of damping power system resonances by sinusoidally modulating the firing angle of the thyristor-controlled reactor (TCR) of a static var compensator (SVC). An undesired harmonic phasor component of a system current or voltage is measured and processed by a modulation controller such that a phasor component of appropriate magnitude and phase is generated in the TCR line current with the objective of cancelling the undesired harmonic.

In Chapter 1, a brief description is given of the second harmonic resonance problem often encountered when applying a SVC in a power system. The concept of applying TCR firing angle modulation to solve this resonance problem [3,4] is described.

The digital time domain simulation program EMTDC [7] is used to investigate the performance of a TCR with firing angle modulation under a variety of harmonic resonant network configurations and conditions. The scope of the work

includes the development of the EMTDC models required to simulate firing angle modulation control of a TCR. The EMTDC models that were developed and the network configurations investigated are described in Chapter 2.

In Chapters 3-7, the performance of the TCR with firing angle modulation, as observed from the simulation results, is presented and analyzed. Chapter 3 analyzes the TCR performance with firing angle modulation using a simple model with the TCR represented on the high voltage bus. This simple model is the same as that used in previously published work [3] on this subject. The simulation results are presented as a base case for the following chapters in this manuscript, and to check the simulation model and results for consistency with the published work. Chapter 4 examines the effect of the SVC step-up transformer and transformer saturation on the modulation. Chapter 5 examines TCR firing angle modulation performance with the SVC connected to a system which is in second harmonic parallel resonance. Chapter 6 examines the TCR firing angle modulation performance with the SVC connected to the system where a second harmonic parallel resonance exists between the system and the SVC fixed capacitor. Chapter 7 examines TCR firing angle modulation performance for the case where the SVC is connected to a network where a second harmonic parallel

resonance exists between the network and the SVC (fixed capacitor plus TCR).

In Chapter 8, some conclusions are presented on the feasibility of using a TCR with firing angle modulation to damp power system harmonic resonances. The effectiveness of using signals other than the TCR line currents as the control parameter is discussed. The current on the high voltage side of the SVC transformer, or the high side compensator bus voltage potentially could be used as the control input signal. The feasibility of eliminating more than one problem harmonic is discussed. Finally some comments are offered with regard to the speed of controller response that is required.

The appendices consist of program listings for the digital simulation models.

1.2 Problem Description

Static var compensators (SVC) have been installed in power transmission systems where rapid and continuous control of reactive power is required in response to changing system conditions.

Static compensators have been primarily applied in power transmission networks to provide dynamic reactive power compensation and rapid transient voltage control at the receiving end of a long high voltage ac transmission line, or at the interface of a dc transmission line feeding into a weak ac system. For example, two static compensators consisting of thyristor-controlled reactors (TCR) and thryistor-switched capacitors (TSC) are installed at Chateauguay on the 120 kV ac system side of the Hydro Quebec HVdc back-to-back tie to the United States to maintain stringent voltage control and reactive power balance [9].

The installation of a SVC at the midpoint of a long ac transmission line to enhance power transfer capability and transient stability is also feasible [10].

Static compensators with individual phase control have also been applied in the Republic of South Africa on the ESCOM 132 kV and 400 kV transmission systems for line voltage

balancing and voltage level control necessitated by the single phase electric railway loads [5,6].

A concern common to most of the SVC applications is the interaction of the SVC with the ac system in the presence of a low frequency system harmonic resonance condition such as a second harmonic resonance condition.

The general equivalent circuit at an ac/dc interface is shown in Figure 1.1. The quantities Vs and Zs are respectively the Thevenin source voltage and Thevenin impedance of the ac system as viewed from the interface bus. For a fully compensated system, the interface voltage, Vc and the Thevenin voltage, Vs both are assumed to be 1.0 pu in steady state. Therefore, the short circuit capacity of the ac network is equal to:

$$S = \frac{kV^2}{|Zs|} = \frac{1}{|Zs|} \quad pu \qquad (1.1)$$

Zs is normally inductive at 60 Hz and at the low order harmonic frequencies.

The parameter, Qc represents the reactive power of the ac harmonic filters (essentially capacitive at frequencies

below the tuned frequency) and shunt capacitors connected at the interface bus. For some system conditions the ac system inductive reactance can be in parallel resonance with the ac harmonic filters at a particular harmonic of the supply frequency. The harmonic resonance frequency can be expressed approximately as:

$$w_r = w_o \sqrt{\frac{S}{Qc}} \quad \text{rad/s} \qquad (1.2)$$

where w_o is the fundamental frequency in radians/second.

If Qc approaches a value of S/4, conditions for a resonance near second harmonic would exist. Such a resonance was observed at Chateauguay when all the reactive compensation (filters and static compensators operating fully capacitive) was connected and the ac system configuration was such that the short circuit capacity at the converter bus was at a minimum.

A system disturbance, such as the energization of a large transformer, or the clearing of a system fault, or a load rejection, can cause harmonic currents to flow in the ac system. Transformer saturation is a typical source of harmonic current. If one of these harmonic current components coincides with a system parallel resonant frequency, a

harmonic voltage of high amplitude will build up and cause an overvoltage condition to occur due to superposition of the harmonic voltage on the system fundamental frequency voltage.

The severity and duration of such system overvoltages is dependent on the system damping. The ac system impedance or damping angle is given by:

$$\phi = \tan^{-1} \frac{(w_o Ls)}{(Rs)} \qquad (1.3)$$

where the system Thevenin impedance is $Zs = Rs + jw_oLs$.

A damping angle of 90° indicates an undamped system while a damping angle of 75° indicates a reasonably well damped system.

Low harmonic frequency resonant problems are not restricted to locations where a dc link interfaces to a weak ac system. The line capacitance or reactive compensation of a high voltage ac transmission line, shown in Figure 1.2, can also form resonances with the ac system as the ac system impedance changes due to line switching, or the addition or removal of generators. Harmonic overvoltages can similarly

be generated by system disturbances which produce low order harmonic currents that coincide with the system resonances.

The normal sources of harmonic current in the ac system may decay naturally to negligible levels within a few cycles, or as in the case of transformer inrush current, may decay slowly over several seconds.

The TCR of a static compensator can enhance second harmonic instability since harmonic voltage distortion can cause large firing asymmetries. Firing asymmetries even with equidistant phase-locked loop (PLL) firing controls, can produce non-characteristic even harmonic currents, the most significant being the dc component and the second harmonic component [3,4]. The TCR can be considered as a sustained source of both characteristic and non-characteristic harmonic currents. Second harmonic instability was experienced during commission of a FC-TCR type static compensator on the ESCOM 132 kV system [5].

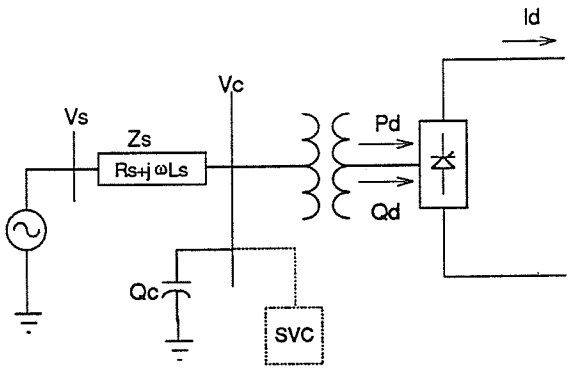

Figure 1.1 Equivalent at an AC/DC Interface

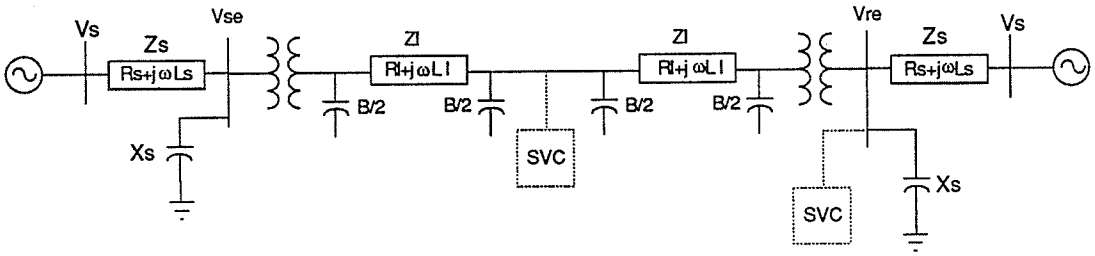

Figure 1.2 Equivalent Circuit of a High Voltage AC Transmission Link

1.3 SVC Generation of Non-Characteristic Harmonics

When the compensator bus voltages are balanced and consist only of the fundamental frequency component, the TCR line current contains only characteristic harmonics of order $n = pq \pm 1$, $q = 0, 1, 2, 3...$ and p is the pulse number. The dominant low order harmonic currents are prevented from flowing into the system by a combination of filtering and the use of the twelve pulse ($p = 12$) TCR configuration.

With balanced ac system voltages non-characteristic odd and even harmonic can also appear in the TCR line current due to normal tolerances in transformer and reactor impedances and due to firing asymmetries between the TCR phases and between the positive and negative half cycle thyristors in one phase [2]. These harmonics are generally an order of magnitude smaller than the dominant characteristic harmonics; however, some of the lower order ones may cause problems. For example, the dc component generated by firing asymmetry of the anti-parallel thyristors in one phase may cause the SVC step-up transformer to saturate. The saturation current contains harmonic components which may excite system resonances.

Under most conditions phase-locked loop equidistant firing controls reduce firing asymmetries such that the magnitudes of the non-characteristic harmonic currents are negligible.

However, if the compensator bus voltage is severely distorted due to the presence of a second harmonic voltage, the zero crossings of the source voltage waveforms will no longer be equidistant. Firing of the thyristor valves equidistantly will result in TCR phase current waveforms which are not symmetrical with respect to the zero current axis. Numerical Fourier analysis of the TCR line current waveforms shows that large non-characteristic dc and second harmonic components exist [4].

These harmonic components in the TCR line currents flow through the ac system harmonic impedances, thereby creating harmonic voltage components which can add to the source voltage distortion, and can lead to harmonic instability, especially if a parallel resonance condition exists near the point of connection of the SVC. The dc component can cause transformer saturation, which will result in additional harmonic currents being generated.

1.4 TCR With Firing Angle Modulation Control

As discussed above, ac system parallel resonance conditions can result in severe harmonic distortion of the source voltage. Equidistant firing of the TCR in the presence of distorted voltage waveforms produces low order non-characteristic even harmonics which can cause saturation of the SVC transformer, and can lead to harmonic instability.

Firing angle modulation of the anti-parallel thyristors of the TCR has been applied in the ESCOM system [5,6] to eliminate the dc component from the TCR line current to avoid saturating the SVC transformer.

The concept of using sinusoidal modulation of the TCR firing angle to generate TCR line currents having a harmonic component with the appropriate magnitude and phase to cancel a problem harmonic has been developed and demonstrated using digital simulation [3,4]. The three phase instantaneous values of the measured TCR line current are converted to their equivalent (α ,β) - components using the (a,b,c) to (α ,β) - transformation. The TCR PLL signals are then used to identify the positive and negative sequence phasors of a desired harmonic component. The measured phasor quantity is

input to a modulation controller which generates the firing angle modulation signal required to eliminate the measured harmonic phasor component from the TCR line current. The firing angle modulation signal is based on sinusoidal modulation of the anti-parallel thyristor valves about the nominal firing angle. Digital simulation was used to demonstrate that the dc component or second harmonic component could be eliminated from the positive sequence TCR line currents. The simulations were conducted on a simple system where the TCR was connected directly to a high voltage infinite bus.

In Reference [3] the author recommended that additional work be done with a more detailed model in order to assess the effect of the SVC step-up transformer on the firing angle modulation controller performance. Further, it was recommended that the ac system be represented such that a parallel resonance exists between the ac system and the SVC fixed capacitors in order to see if TCR firing angle modulation can damp the harmonic resonance.

The digital simulation program [3,4] could not be easily applied to a more complex ac system with the SVC connected through a step-up transformer. Further the models were not compatible with digital simulation programs, such as EMTDC

or EMTP (Electromagnetic Transients Program), that have the capability to model the ac system to any level of detail desired.

A major contribution of this work was the development of digital models, compatible with the EMTDC program, that could be used to simulate sinusoidal firing angle modulation of a general six pulse thyristor valve group. These EMTDC models were then applied to study the performance of sinusoidal firing angle modulation of a TCR with the ac system represented in varying detail. The system parameters were adjusted such that a parallel resonance was formed between the system inductance and the SVC capacitors, or the system inductance and system shunt connected capacitors, to determine if the modulation could damp the resonance. The effect of the SVC step-up transformer and transformer saturation on the modulation effectiveness was also analyzed.

CHAPTER TWO

STUDY TOOLS AND MODELS

2.1 Digital Simulation Program

The Electromagnetic Transient Program for DC (EMTDC) [7] was used to perform the digital simulation described in this manuscript. This time domain digital simulation program was developed at Manitoba Hydro with contributions from the University of Manitoba, and is currently available from the Manitoba HVDC Research Centre.

The EMTDC program is structured such that a main program coordinates all the activities of input, output, network solution and interfacing to available models or user written models through calls to subroutines. The user interacts with the EMTDC program through three files:

(i) A "DATA" file which defines the electrical network,

(ii) A Fortran subroutine "DSDYN" which contains the user defined dynamics, and

(iii) A Fortran subroutine "DSOUT" which contains the user defined output variables.

The rules required to assemble each of these files are described in detailed in the EMTDC USER'S MANUAL [8].

Figure 2.1 contains a flow chart of the dynamic simulation models used for this study. The dynamic models are called from within the EMTDC subroutine "DSDYN". Appendix A contains the "DATA" file, "DSDYN" file and "DSOUT" file necessary for EMTDC simulation of the circuit shown in Figure 2.2.

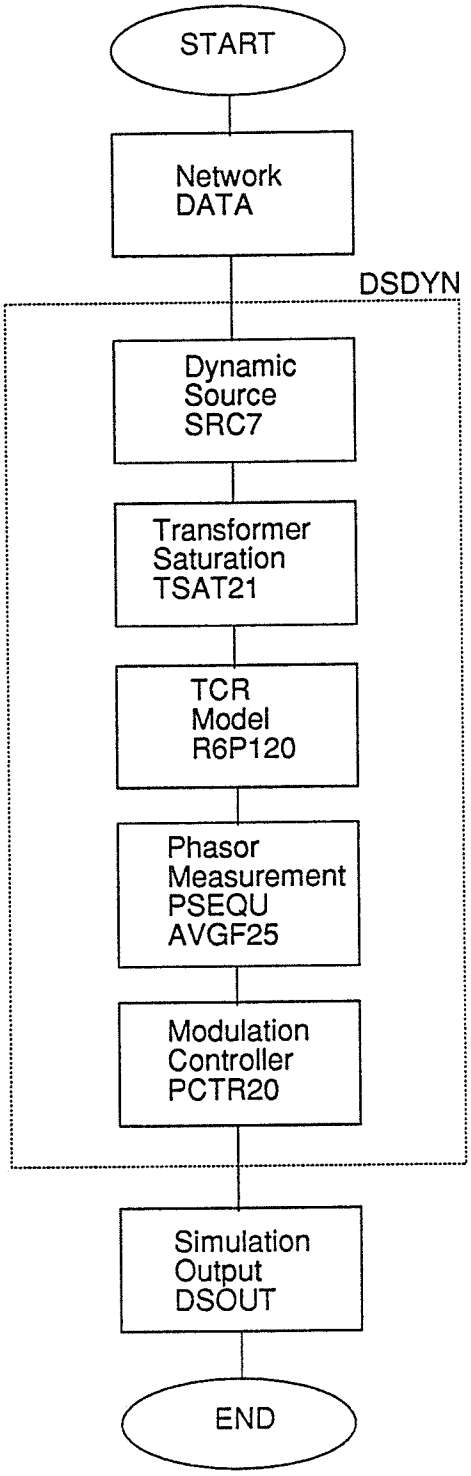

Figure 2.1 Flow Diagram of the EMTDC Simulation Model

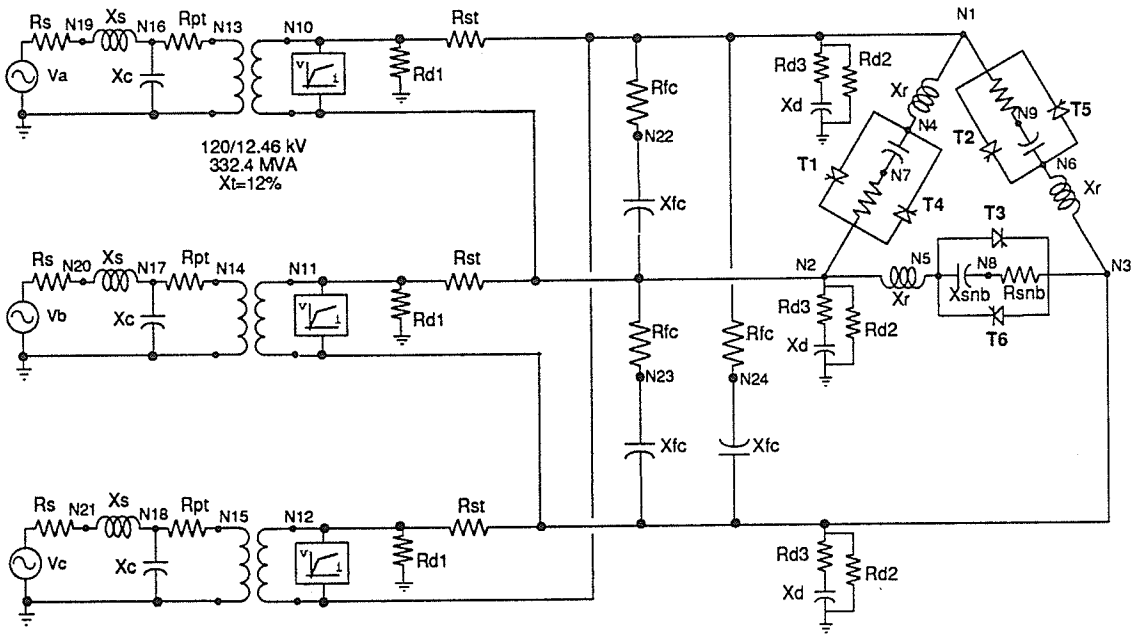

Xs - Thevenin Impedance of the AC System
Xr - Reactance of the TCR Reactor
Xt - SVC Transformer Leakage Reactance
Xfc - Capacitive Reactance of the SVC Fixed Capacitor
Xc - Equivalent System Capacitive Reactance
Xsnb - Snubber Circuit Capacitive Reactance
Xd - Numerical Damping Circuit Capacitive Reactance
Rs - Thevenin Resistance of the AC System
Rpt,Rst - SVC Transformer Primary & Secondary Winding Resistances
Rd1,Rd2,Rd3 - Numerical Damping Circuit Resistance
Rsnb - Snubber Circuit Resistance
Rfc - Fixed Capacitor Internal Resistance
Va ,Vb,Vc - Thevenin Voltage behind Reactance

Figure 2.2 Detailed EMTDC Simulation Circuit

2.2 Description of the Electrical Network

The detailed three phase EMTDC simulation network, shown in Figure 2.2, consists of a Thevenin equivalent representation of the high voltage system, high voltage shunt capacitors and a SVC of the FC + TCR type.

The EMTDC "DATA" file defines the connectivity and parameter values of the network components.

The Thevenin voltage source is defined by a source subroutine, SRC7, which is described in Section 2.3.

The high voltage system at the point of connection of the SVC is represented in varying detail as shown by the single line diagrams of Figures 2.3 to 2.6.

In Figure 2.3 the delta connected TCR is modelled on the high voltage bus by reflecting the SVC parameter values to the high voltage side of the transformer. The SVC transformer and the high voltage system equivalent shunt admittance are ignored. The high voltage network is represented by a simple Thevenin reactance and Thevenin voltage source. The concept of sinusoidal firing angle modulation of the TCR was studied in previous work [3] using this simple system. The equivalent system is assumed to be resonant at the second harmonic, causing severe distortion

of the voltage waveforms at the point of connection of the SVC. This condition is modelled by adding a balanced second harmonic component to the fundamental frequency component of the source voltage. The second harmonic component magnitude is 30% of the fundamental, with a phase displacement of -30°. The Thevenin reactance is assumed to be small to represent a strong (high short circuit capacity) system relative to the SVC rating.

In Figure 2.4 the SVC step-up transformer, fixed capacitors and the TCR are represented explicitly. The system equivalent is assumed to be the same as in Figure 2.3.

In Figure 2.5 the high voltage shunt capacitors, such as the ac filters of a HVdc converter, are represented explicitly in addition to the SVC. The values of the Thevenin reactance and the shunt capacitance are selected such that a second harmonic parallel resonance exists in the network as observed from the point of connection of the SVC to the high voltage system. The Thevenin voltage source is assumed to have a small second harmonic component, about 2% to 3% in magnitude with respect to the fundamental and phase displaced by -30°, superimposed on the fundamental. The effect of the parallel resonant system is to amplify the small second harmonic source voltage at the high voltage SVC

bus by injecting a second harmonic current into the high second harmonic impedance.

In Figure 2.6 the SVC is connected to an equivalent network with a parallel resonance near the second harmonic. The addition of the fixed capacitor type SVC shifts the resonant frequency such that a second harmonic parallel resonance is formed between the system and SVC fixed capacitor, or the system and the SVC (fixed capacitor plus TCR).

Additional detail of the characteristics of the system equivalent representation will be given in the appropriate chapters with the discussion of the simulation results.

The SVC modelled is of the fixed capacitor, thryistor-controlled reactor type. The SVC reactive power range applied in the simulations was 180 Mvar capacitive to 120 Mvar reactive.

The magnitude of the Thevenin voltage was adjusted to establish an initial condition fundamental frequency system voltage of 1.0 pu at the point of connection of the SVC.

The FC and TCR were both modelled as delta connected elements. Small resistors were required in series with the FC to avoid numerical problems in the solution due to a purely capacitive loop. The resistors were sized to represent the capacitor bank losses, taking care that the time constant of the branch was not less than the solution time step.

The TCR was modelled in the network as a linear reactor in series with a resistor, which represented the antiparallel thyristors. The "ON" and "OFF" resistances, 0.025 ohms and 1000 ohms respectively, are altered by the TCR dynamic model (described in Section 2.5) to simulate thyristor switching.

The thyristor on-off resistor is paralleled by a series resistor-capacitor circuit called a snubber circuit. The snubber circuit is required to absorb the energy associated with the thyristor recovery current, and to limit the resultant voltage rise and the rate of rise of this voltage. The recovery current, which appears as the thyristor changes from a conducting to a non-conducting state, is trapped in the TCR inductance and is forced to commutate to the RC snubber circuit. A series resonant circuit, damped by the snubber resistance, R is formed by the TCR induc-

tance, L and the snubber capacitance, C. The undamped natural frequency of this circuit is:

$$w_n = 1 / \sqrt{LC} \quad \text{rad/s.} \tag{2.1}$$

The time constant of the circuit is:

$$T = 2L/R \quad \text{s.} \tag{2.2}$$

The selection of the snubber circuit resistor and capacitor values for the model also required that the snubber circuit time constant be greater than the simulation time step by a factor of three or more [8], in order to avoid numerical integration error.

The chosen snubber circuit parameters of R = 100 ohms and C = 1.5 μF resulted in a snubber circuit time constant of:

$$T = RC = 150 \quad \mu s \tag{2.3}$$

This RC time constant of 150 μs and a simulation time step of 50 μs were found to produce satisfactory results. The inductance of the TCR reactor was 4.12 mH.

A 332.4 MVA, 120/12.46 kV wye-delta connected three phase transformer was modelled as the SVC step-up transformer. Three single phase coupled windings, connected in wye-delta were used. A transformer leakage reactance of 12% on transformer base, and a rated magnetizing current of 2% of rated full load current were assumed. Transformer saturation was represented as described in Section 2.4. The low voltage delta connected windings required large stabilizing resistors connected to ground to prevent dc offset voltage buildup. These resistors were also required for numerical stability when transformer saturation was modelled. The resistors served as the Norton conductance for the saturation current which was injected into the terminals of the low voltage winding. The resistors were sized to represent the transformer core losses which typically are one-half to one percent of transformer rating. A stabilizing resistor sized on the basis of one-half percent losses draws a current of about 0.60% of the TCR line current. Consequently, the current drawn by the numerical damping resistors had negligible impact on the simulation accuracy.

A series RC shunt was placed in parallel with the stabilizing resistor to smooth numerical voltage chatter at the nodes of the delta connected TCR. The time constant of this circuit was 250 us, five times the simulation time step.

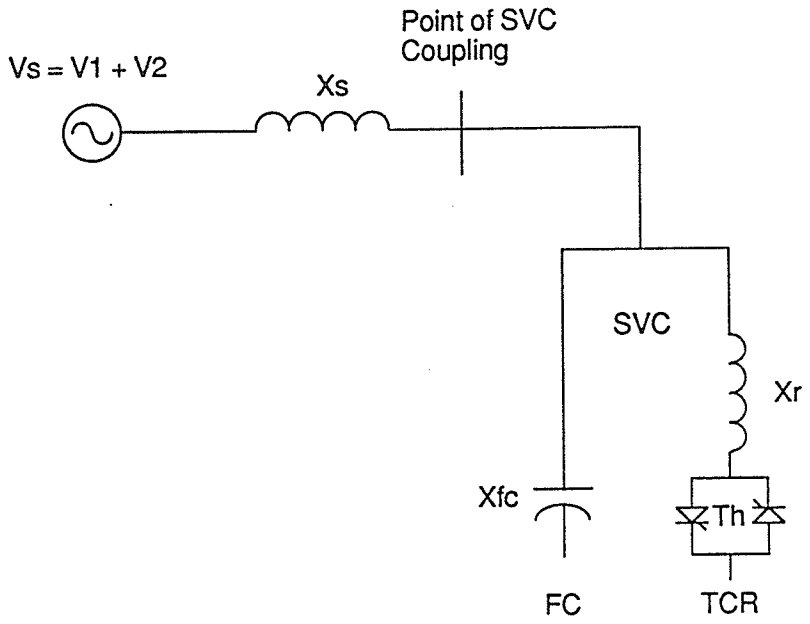

Vs = System Thevenin Voltage Source
V1 = Fundamental Frequency Voltage Source
V2 = Second Harmonic Voltage Source
Xs = System Thevenin Reactance
Xr = Reactance of TCR Reactor
Xfc = Reactance of Fixed Capacitor
TCR = Thyristor Controlled Reactor
Th = Thyristor Valve
FC = Fixed Capacitor
SVC = Static Var Compensator

Figure 2.3 Equivalent Circuit of a SVC Modelled on the High Voltage Bus

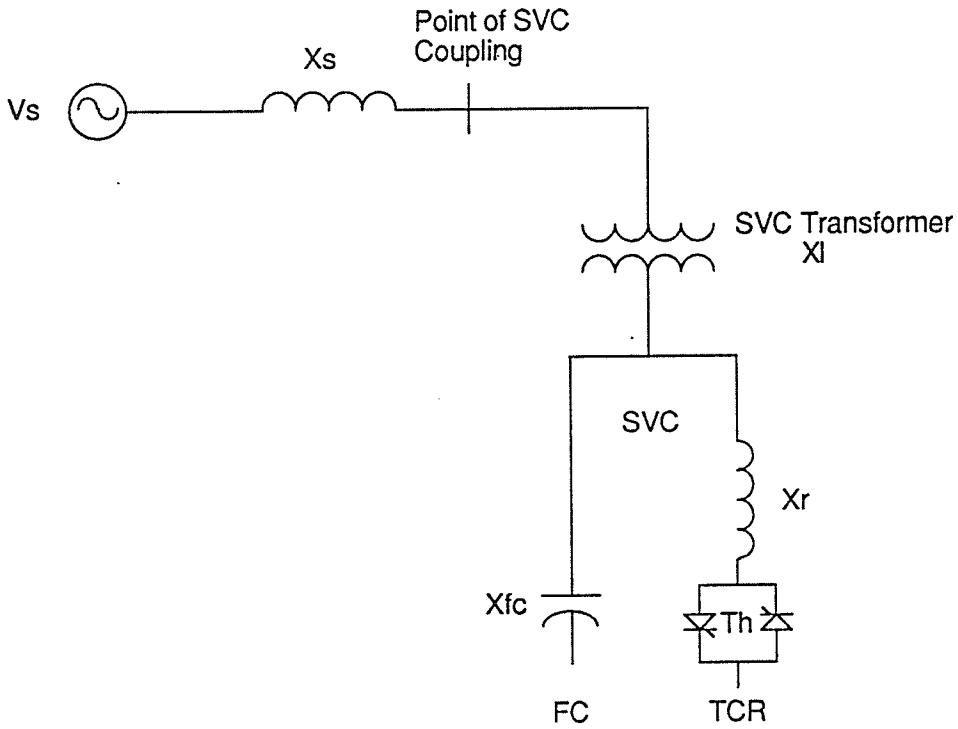

Vs = System Thevenin Voltage Source
Xs = System Thevenin Reactance
Xr = Reactance of TCR reactor
Xfc = Reactance of Fixed Capacitor
Xl = Transformer Leakage Reactance
TCR = Thyristor Controlled Reactor
Th = Thyristor Valve
FC = Fixed Capacitor
SVC = Static Var Compensator

Figure 2.4 Equivalent Circuit of a SVC with a Step-up Transformer

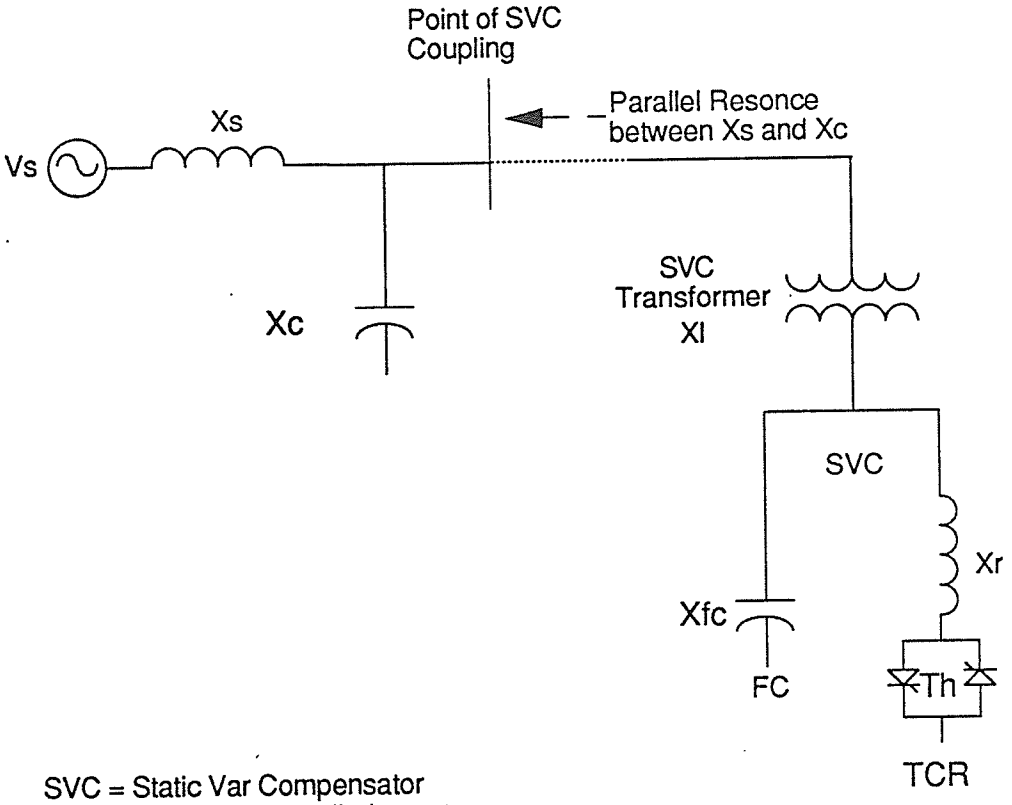

SVC = Static Var Compensator
TCR = Thyristor-controlled reactor
FC = Fixed Capacitor
Vs = System Thevenin voltage
Xs = Equivalent system reactance
Xc = Equivalent system capacitive reactance
Xfc = Fixed capacitor reactance
Xl = Transformer leakage reactance
Th = Thyristor valve

Figure 2.5 Equivalent Circuit of a SVC Connected to a Parallel Resonant Network

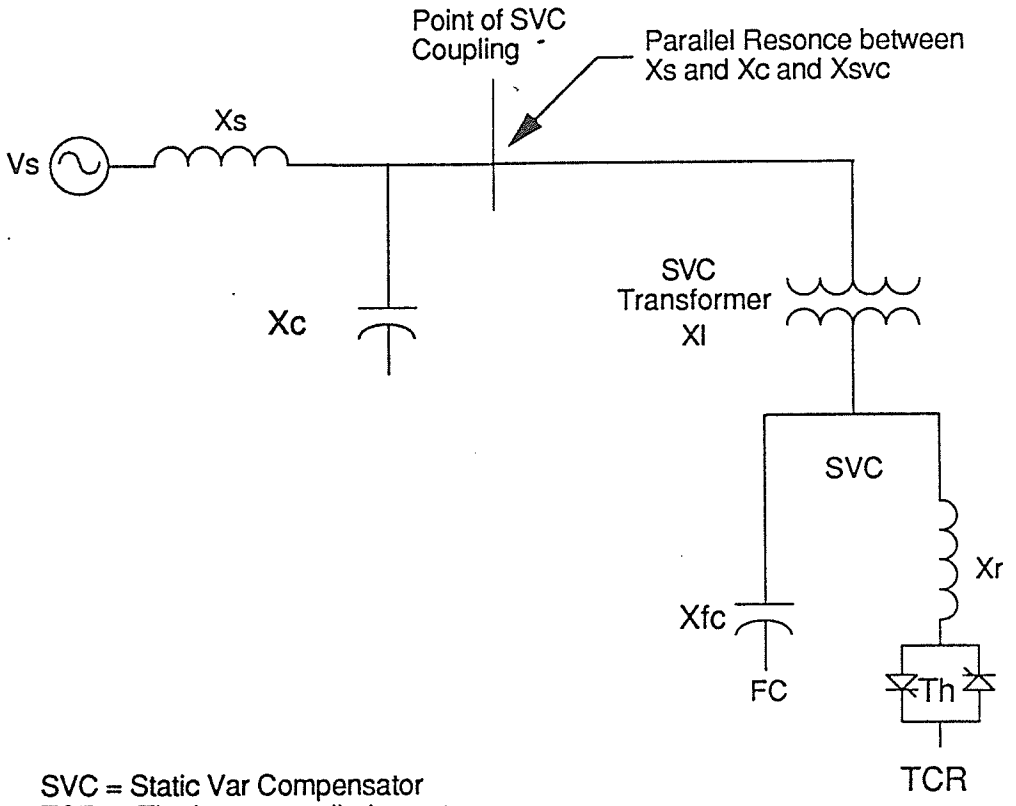

SVC = Static Var Compensator
TCR = Thyristor-controlled reactor
FC = Fixed Capacitor
Vs = System Thevenin voltage
Xs = Equivalent system reactance
Xc = Equivalent system capacitive reactance
Xfc = Fixed capacitor reactance
Xl = Transformer leakage reactance
Th = Thyristor valve

Figure 2.6 Equivalent Circuit of a SVC Connected to a Network in Parallel Resonance with the SVC

2.3 Three Phase Voltage Source Model

Subroutine SRC7 models a sinusoidal three phase star connected Thevenin voltage source which consists of a fundamental frequency sinusoidal source and provision for specifying a second harmonic component.

The EMTDC network DATA file allows for the specification of one Thevenin voltage source per node. This source can be connected in series with either a resistor, inductor or capacitor as the Thevenin impedance. The Thevenin voltage, as shown in Figure 2.7(a) is defined as e = ES (k,m) at each node, k in subsystem, m. The subroutine SRC7 calculates the value of the Thevenin voltage each time step, and interfaces to the network via the parameter ES (k,m).

Figure 2.7(b) shows the phase displacement relationship between the fundamental frequency source vectors and the second harmonic source vectors in Subroutine SRC7.

The subroutine source listing is included in APPENDIX B1.

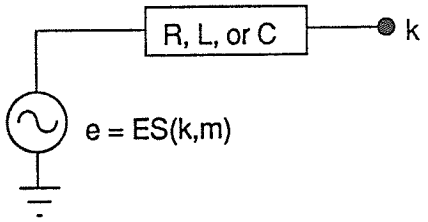

k = Node Number
m = Subsystem Number

(a) EMTDC Thevenin Voltage Source Representation

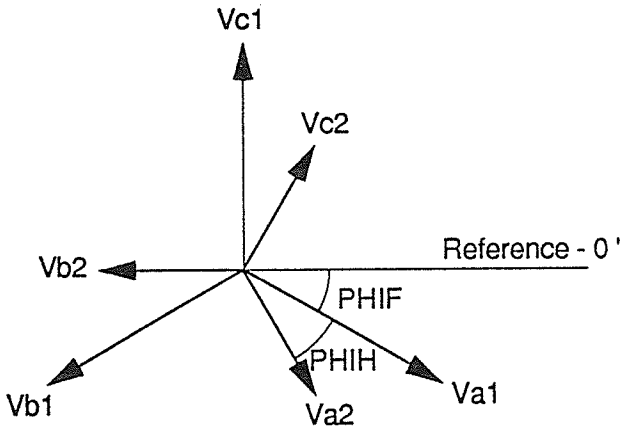

(b) Positive Sequence Vector Relationships

Figure 2.7 Three Phase Voltage Source
Subroutine SRC7

2.4 SVC Transformer Model

The three phase SVC step-up transformer was represented by interconnecting three single phase transformers in a wye-delta configuration as shown in Figure 2.2. This representation is valid for any three phase transformer with a shell form core design, any three phase transformer with a positive sequence impedance equal to the zero sequence impedance, or a three phase bank consisting of three single phase transformers.

The EMTDC program represents a single phase two winding transformer as two mutually coupled coils as shown in Figure 2.8(a). The relationship between the voltage across each winding and the current is:

$$\begin{bmatrix} V_1 - V_2 \\ V_3 - V_4 \end{bmatrix} = \begin{bmatrix} L_{11} & M_{12} \\ M_{12} & L_{22} \end{bmatrix} \begin{bmatrix} di_1/dt \\ di_2/dt \end{bmatrix} \qquad (2.4)$$

The winding self-inductances (L_{11} and L_{22}) and the mutual inductance (M_{12}) between each winding are required for the model. These parameters can be calculated from manufacturers test data or alternatively from data obtained from transformer open circuit and short circuit tests. The

procedure and formulae are described in detail in the EMTDC User's Manual [8].

The equivalent circuit for the two mutually coupled windings is shown in figure 2.8(b).

Adding transformer saturation effects to the equivalent circuit of Figure 2.8(b) involves modelling the shunt magnetizing reactance, Xm as a non-linear element. Alternatively the saturation current can be modelled as a current source, Is(t) connected across one of the windings as shown in Figure 2.9. This is the method used in the EMTDC program [8]. The saturation current Is(t) is a function of the voltage across the winding V(t), where Is(t) is the current flowing in the transformer magnetizing branch.

The flux in the transformer magnetizing branch is calculated as the integral of the voltage.

$$\phi s(t) = \int V(t)\, dt \qquad (2.5)$$

The current, Is(t) flowing in the magnetizing branch is related to the flux, $\phi s(t)$ by the non-linear saturating inductance Ls(t) such that

$$\phi s(t) = Ls(t) \cdot Is(t) \qquad (2.6)$$

The non-linear inductance, Ls shown in Figure 2.10, represents the transformer saturation characteristic which can be approximated by either a two slope characteristic using the non-saturated inductance (Lm) and the saturated inductance (La - air core inductance), or by using a mathematical expression relating the magnetizing current as a function of the flux.

The following mathematical expression, used in the EMTDC program, gives a saturation curve which is asymptotic to the vertical flux axis and the sloping air core inductance characteristic.

$$Is(\phi) = \frac{\Delta\phi + \sqrt{\Delta\phi^2 + 4DLa}}{2La} - \frac{D}{\phi k^2} \qquad (2.7)$$

where: $\Delta\phi = \phi s - \phi k$

$$A = \frac{La}{\phi k^2}$$

$$B = \frac{La\ Im - \phi m}{\phi k}$$

$$C = Im\ (La\ Im - \phi m + \phi k)$$

$$D = \frac{-B - \sqrt{B^2 - 4AC}}{2A}$$

$$\phi k = K\ \phi m \qquad 1.15 < K < 1.25$$

$$\phi m = \frac{\sqrt{2}\ Vm}{w_o}$$

ϕs = flux (webers)

ϕk = knee point flux

ϕm = flux at rated winding voltage

K = per unit knee point

L_A = air core inductance (henries)

w_o = rated frequency (rad/s)

Vm = winding rated rms voltage (volts)

Im = rms magnetizing current at rated voltage (amperes)

The EMTDC subroutine TSAT 21 uses equations (2.5) and (2.6), as shown in Figure 2.9, to approximate the effect of transformer saturation. The saturation current is injected into the network at the winding nodes. To maintain numerical stability of the solution, a large resistor must be connected to ground at these nodes. The value of these resistors was chosen to approximate the transformer core losses.

When the voltage across the transformer winding is sinusoidal then the flux will also be sinusoidal. Large currents will flow through the magnetizing branch when the flux exceeds the knee value. The shape of the current waveform depends on the parameters of the transformer

saturation curve and on the amount by which the flux exceeds the knee point value.

Figure 2.11 shows the winding voltage, the flux and the saturation current waveforms of one phase for the condition where the SVC transformer is subjected to a balanced three phase overvoltage of 1.25 pu. The transformer rating is 332.4 MVA, 120/12.46 kV wye-delta connected, with a 12% leakage reactance. The rated magnetizing current was assumed to be 2% of rated winding current. The air core reactance was assumed to be 40%. The saturation was applied to the low voltage secondary winding. A saturation flux knee point of 1.15 pu was used.

In general, the saturation current contains not only a fundamental component but also harmonic components. If the saturation characteristic is symmetrical and the flux is not offset there will be no even harmonic components present in the saturation current.

Numerical Fourier analysis of the magnetizing current waveform of Figure 2.11 indicates the presence of harmonic components as tabulated in Table 2.1. The current contains a large 60 Hz component and a seventh harmonic component. The TCR was fired equidistantly at a firing angle of 30°.

The rated transformer winding magnitizing current of 251.5 A peak was used as the per unit base current. The per unit base used for the transformer flux was 46.74 Volt-seconds.

TABLE 2.1 Transformer Saturation Current of Figure 2.11 Positive Sequence Harmonic Components Due to 60 Hz Balanced Three Phase Overvoltage

Component	Magnitude - pu	Phase
dc	0.0019	134.5°
1	3.0867	97.0°
2	0.0029	43.9°
3	0.0031	83.9°
4	0.0038	160.5°
5	0.0047	-105.3°
6	0.0051	-16.2°
7	0.6076	-44.2°

Harmonic currents flowing in the magnetizing branch must also flow in the ac system and will produce harmonic voltages. The magnitude and phase angle of each harmonic voltage depends on both the harmonic current and the harmonic impedance of the ac system. The harmonic voltages add to the fundamental frequency voltage at the transformer terminals and modify the flux and the saturation current which is responsible for the harmonic voltages in the first place.

If the voltages at the terminals of the transformer are distorted due to the presence of a large second harmonic, the flux will be offset, and the saturation current will also contain even harmonics. Figures 2.12, 2.13 and 2.14 respectively show the Phase A,B and C transformer secondary winding voltage, flux, and saturation current for the case where the fundamental frequency energizing voltage was 1.0 pu in magnitude @ 0° but contained a second harmonic component of 30% @ -30°.

The Fourier components in the positive sequence of the saturation current are tabulated in Table 2.2.

TABLE 2.2 Transformer Saturation Current Positive Sequence Harmonic Components Due to Second Harmonic Voltage Distortion

Component	Magnitude	Phase
dc	0.1394	133.4°
1	0.8578	97.1°
2	0.3806	60.4°
3	0.1167	23.9°
4	0.0335	-9.0°
5	0.0150	-9.0°
6	0.0322	-16.6°
7	0.0699	-47.4°

The secondary winding flux is now offset and a dc, second and third harmonic components are evident in the magnetizing current. The TCR was fired equidistantly at 30° as in the case shown in Table 2.1.

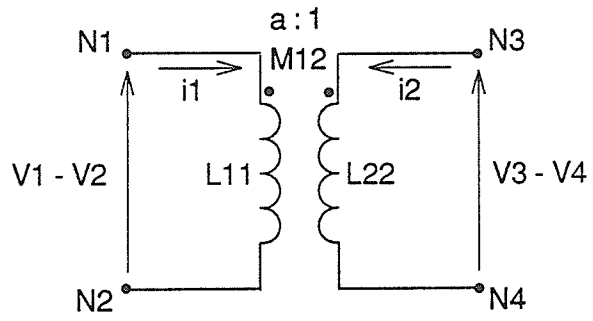

L11 = Self Inductance of Winding 1
L22 = Self Inductance of Winding 2
M12 = Mutual Inductance between Winding 1 & 2
a : 1 = Turns Ratio between Windings 1 & 2

$$a = \frac{V1 - V2}{V3 - V4} = \sqrt{\frac{L11}{L22}}$$

(a) Two Mutually Coupled Windings

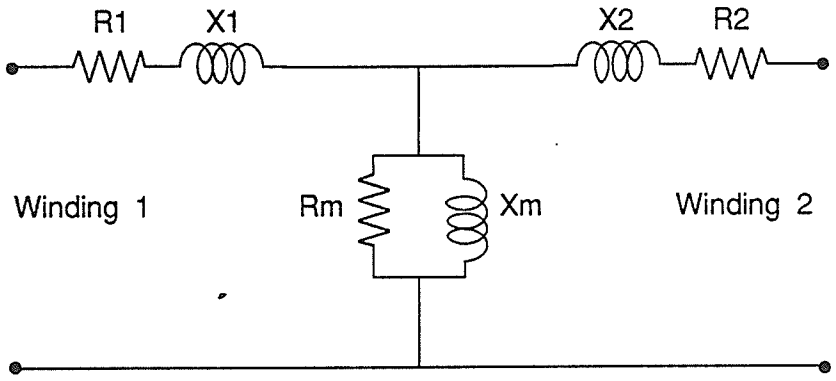

R1 = Resistance of Winding 1
R2 = Resistance of Winding 2
Rm = Resistance of Magnetizing Branch
X1 = Reactance of Winding 1
X2 = Reactance of Winding 2
Xm = Reactance of Magnetizing Branch

(b) Equivalent Circuit of Two Mutually Coupled Windings

Figure 2.8 EMTDC Two Winding Transformer Model

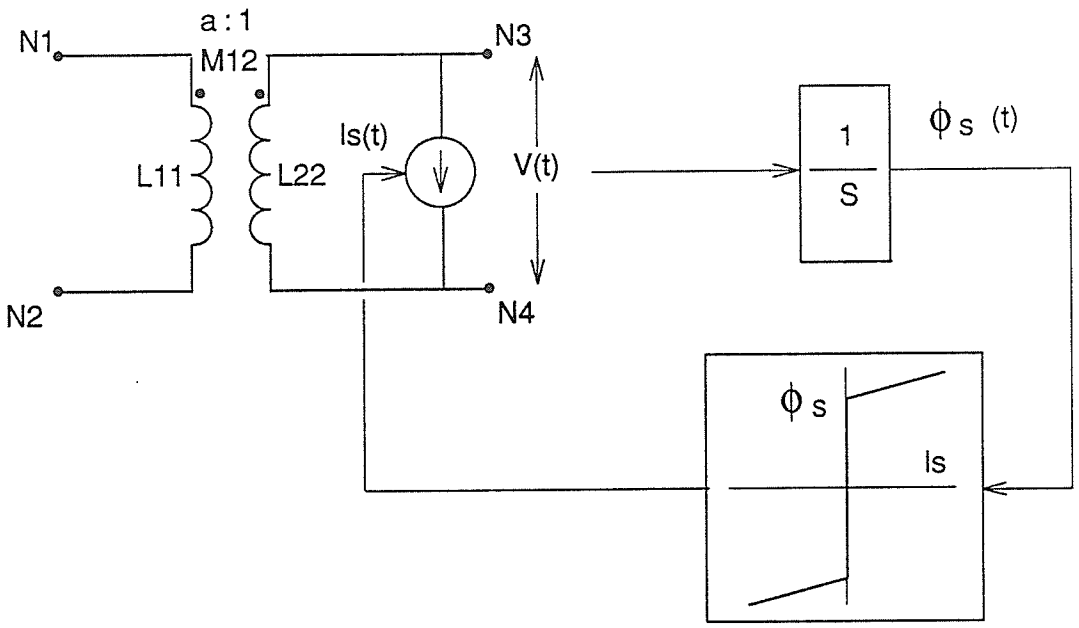

Figure 2.9 EMTDC Implimentation of Transformer Saturation

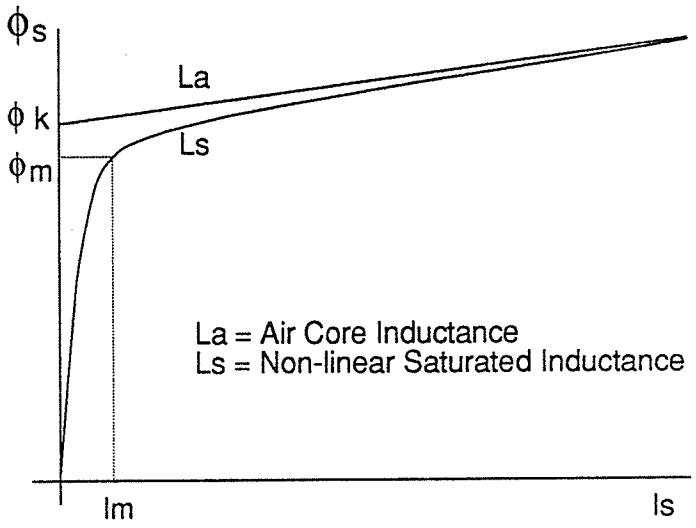

Figure 2.10 EMTDC Transformer Saturation Characteristic

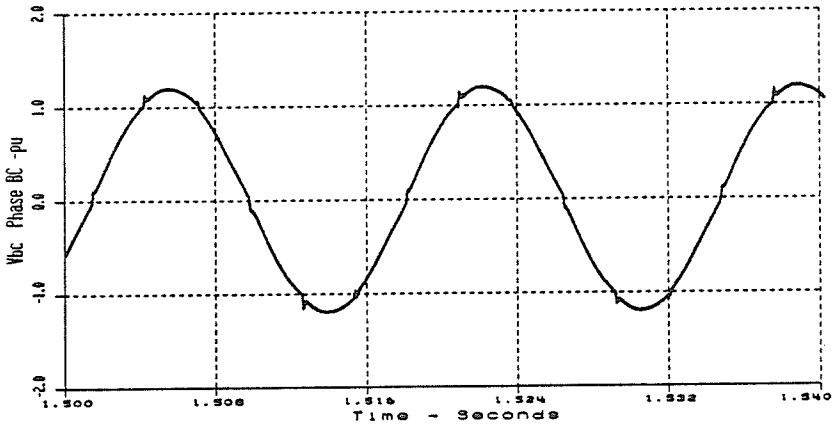

a) Winding Voltage

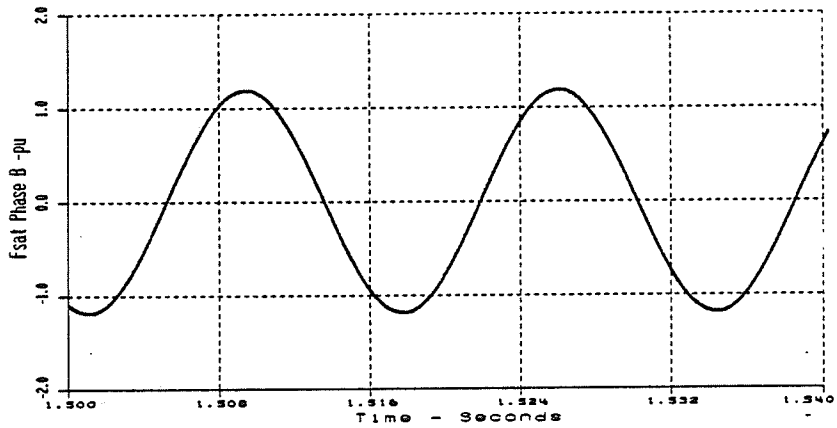

b) Winding Flux

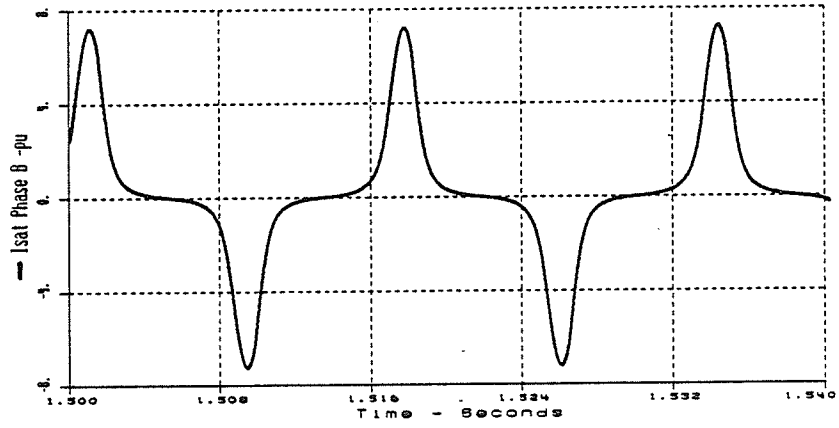

c) Saturation Current

Figure 2.11 Transformer Winding Voltage, Flux and Saturation Current for a Balanced Three Phase Overvoltage.

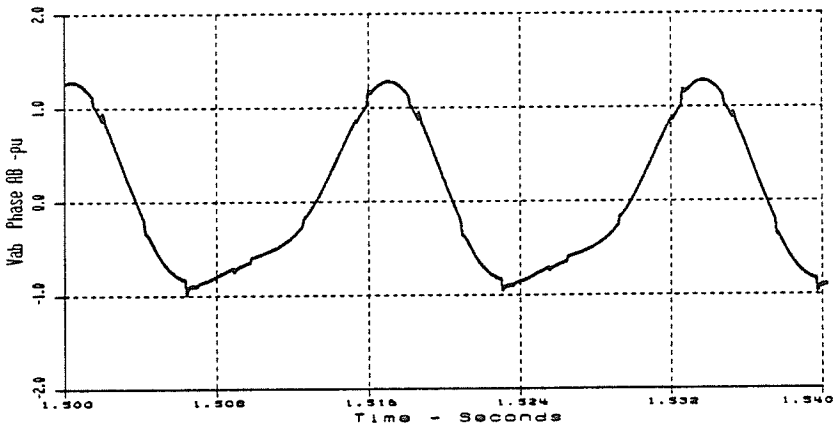

a) Winding Voltage

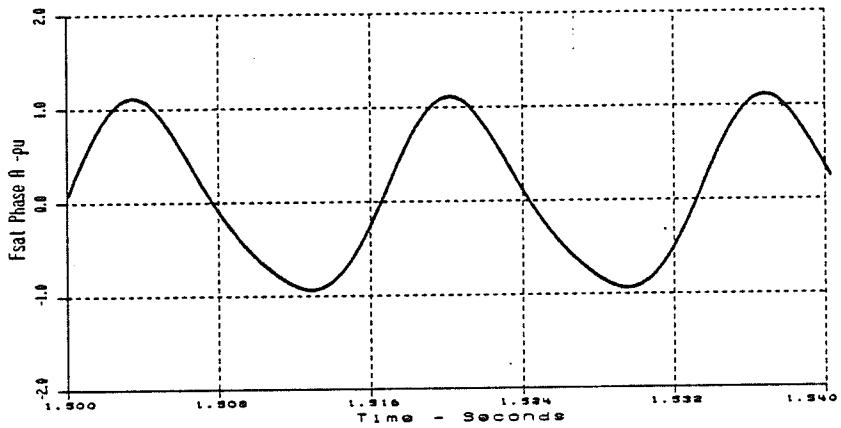

b) Winding Flux

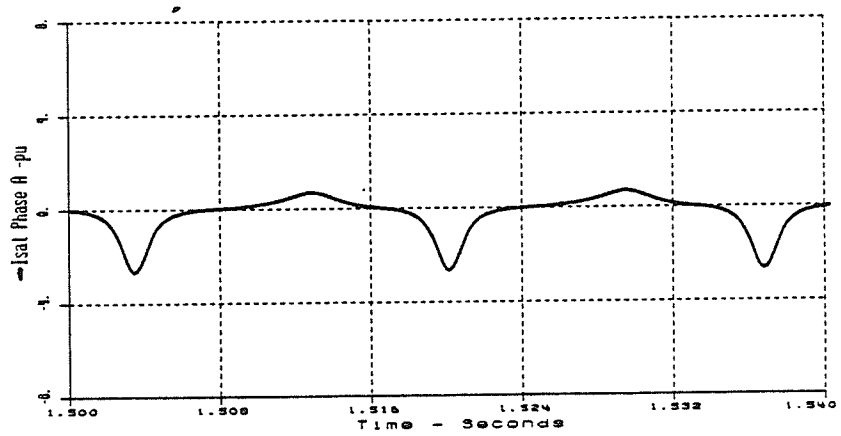

c) Saturation Current

Figure 2.12 Transformer Phase A Winding Voltage, Flux and Saturation Current for Overvoltage Due to 2nd Harmonic Distortion

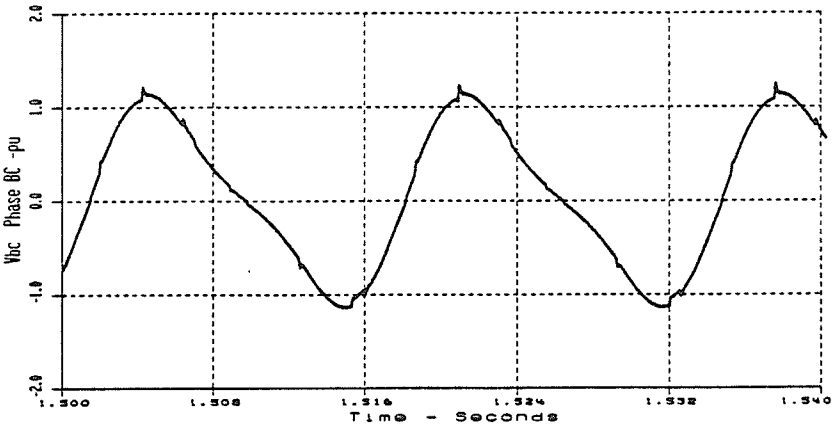

a) Winding Voltage

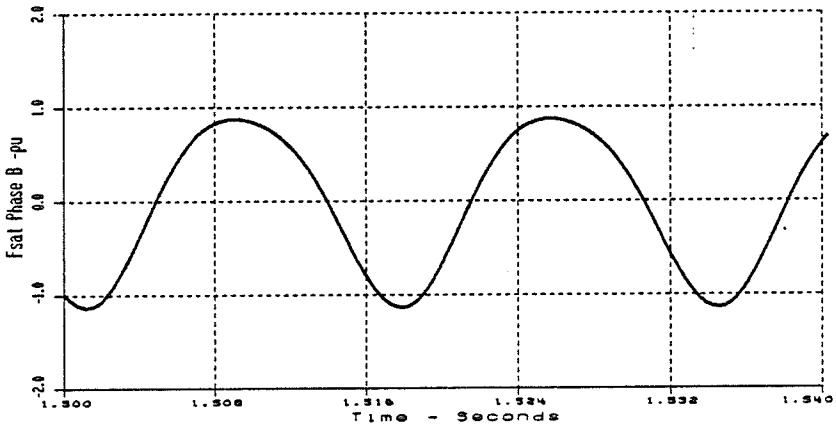

b) Winding Flux

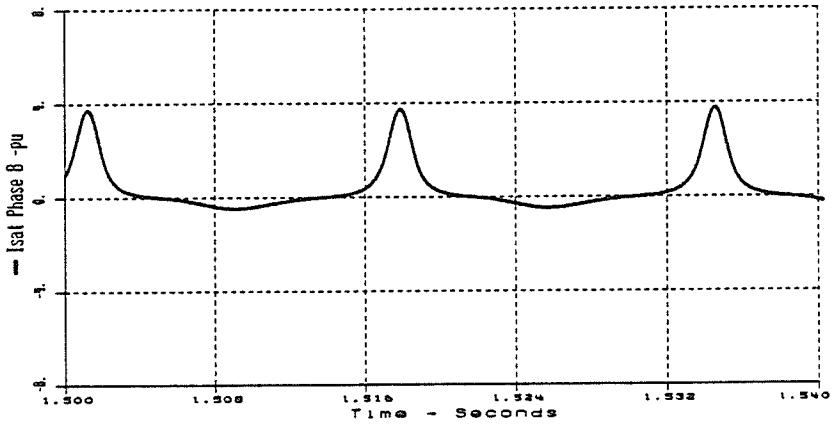

c) Saturation Current

Figure 2.13 Transformer Phase B Winding Voltage, Flux and Saturation Current for Overvoltage Due to 2nd Harmonic Distortion

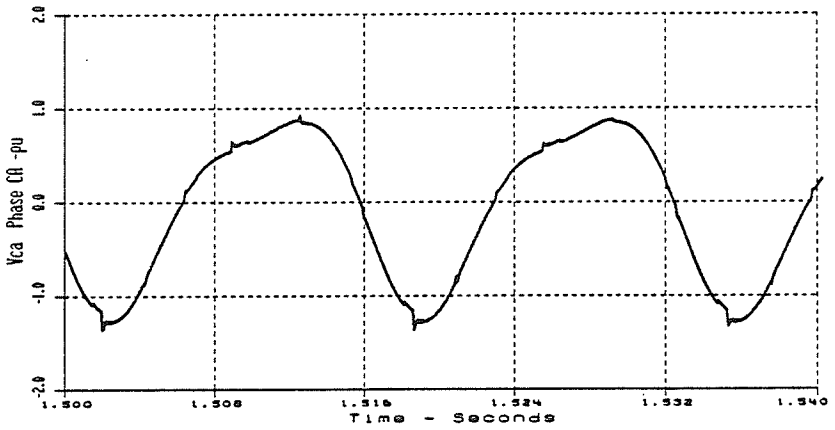

a) Winding Voltage

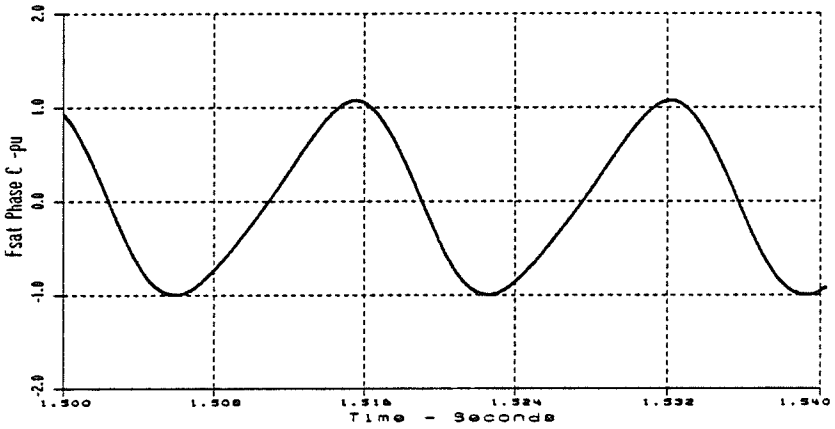

b) Winding Flux

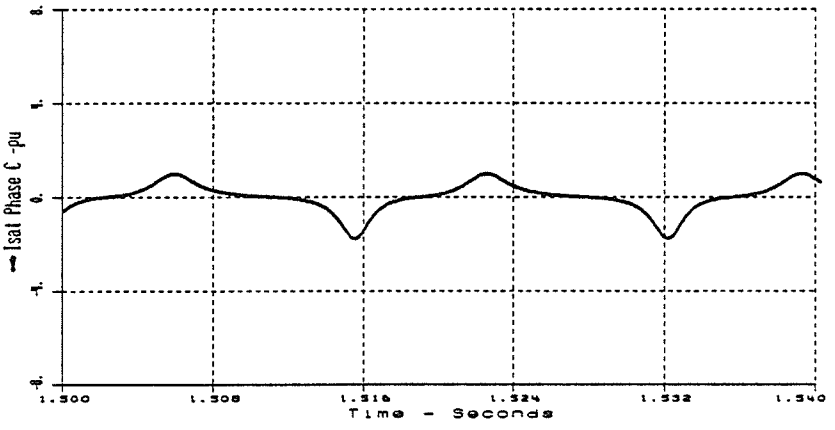

c) Saturation Current

Figure 2.14 Transformer Phase C Winding Voltage, Flux and Saturation Current for Overvoltage Due to 2nd Harmonic Distortion

2.5 TCR Model

Subroutine R6P120 models the operation of a six pulse thyristor controlled reactor complete with a phase-locked-loop equidistant firing control system and thyristor switching logic. The subroutine also has provision to allow the user to modulate the firing of each anti-parallel thyristor pair. The nominal firing angle (α o) and the modulating angle (Δ) are determined externally and passed to the subroutine.

Figure 2.15 shows the three phase representation of the TCR to illustrate the node naming convention required by the model.

The appropriate circuit node numbers are passed to the model via the subroutine call statement in the EMTDC user defined dynamics subroutine DSDYN.

The numbering of the circuit nodes is arbitrary. The inductance of the TCR reactor, the thyristor snubber circuits, the SVC step-up transformer, the capacitance of fixed capacitors and circuit damping resistances that make up the SVC circuit are entered into the EMTDC "DATA" file as network data. Each anti-parallel thyristor pair in each phase of the delta connected TCR is represented as a

resistance between positive node numbers. Each thyristor has the anode identified as node NxF and the cathode identified as NxT. The thyristor firing pulses are referenced to a three phase reference voltage waveform which is generated by a phase-locked oscillator. The firing sequence shown in Figure 2.15 (T1, T2, T3, T4, T5, T6) assumes that the PLL reference voltage waveforms are synchronized to a positive sequence (anti-clockwise A,B,C phase rotation) three phase voltage source. The thyristor nodes must be numbered such that N1F=N4, N1T=N2, N2F=N1, N2T=N6, etc., to ensure the proper firing sequence.

The positive sequence three phase voltage source to which the PLL oscillator is synchronized is the AC commutating voltage measured across each phase of the TCR. In subroutine R6P120, the commutating voltage is derived from the phase-to-ground voltage measured at the high voltage bus to which the SVC is connected. The measured voltages are VDC(NA,MA), VDC(NB,MA) and VDC(NC,MA), which requires that node NA=N13, NB=N14 and NC=N15 for the node numbering sequence used in Figure 2.15.

The phase relationship between the measured high voltage bus waveforms and the TCR commutating voltage is shown in Figure 2.16. For a wye-delta connected SVC transformer the ac

commutating voltage (Vab) is in phase with the high side voltage since:

$$\bar{V}ab = \frac{\bar{V}A}{n} \angle 0^\circ \text{ , where } \bar{V}ab = \bar{V}a - \bar{V}b. \tag{2.8}$$

For a wye-wye connected SVC transformer, the ac commutating bus voltage leads the high side voltage by 30° since

$$\bar{V}ab = \frac{\sqrt{3}}{n} \bar{V}_A \angle 30^\circ \tag{2.9}$$

The logic contained in subroutine R6P120 is shown in Figures 2.17, 2.18 and 2.19 in block diagram form. The Fortran code for subroutine R6P120 is included in Appendix B2.1.

A proportional-integral controller is used to synchronize the phase-locked oscillator voltage waveforms to the measured commutating voltage waveforms.

The phase-locked oscillator generates a three phase set of reference voltages having the form:

$$\begin{aligned} V_A &= V_{REFM} \sin \theta_r \\ V_B &= V_{REFM} \sin (\theta_r - 120) \\ V_C &= V_{REFM} \sin (\theta_r + 120^\circ) \end{aligned} \tag{2.10}$$

$$\theta_r = w_r t \tag{2.11}$$

where θ_r is the phase position of the PLL.

The zero crossings ($\theta_r = 0$) of the PLL reference voltage waveforms, shown in Table 2.3, are constant.

Table 2.3 PLL Reference Voltage Zero Crossings		
PLL Voltage Phase	Crossing -/+	Crossing +/-
A	0°	180°
B	120°	300°
C	240°	60°

The model requires the source voltage to be a cosine function. Consequently the commutating voltage is of the form:

$$V_A = \sqrt{2}\ V_1 \cos(\theta_s + \phi_1)$$
$$V_B = \sqrt{2}\ V_1 \cos(\theta_s - 120° + \phi_1) \qquad (2.12)$$
$$V_C = \sqrt{2}\ V_1 \cos(\theta_s + 120° + \phi_1)$$
$$\theta_s = w_s t + \phi_1 \qquad (2.13)$$

where θ_s is the system phase position at time "t",

ϕ_1 is the initial phase position (t=o),

V_1 is the rms fundamental frequency voltage magnitude,

w_s = 377 rad/s is the system angular velocity assuming a frequency of 60 Hz.

The reference (α o = o) for the nominal firing angle is defined to be the peak of phase "A" (θ s = o) of the fundamental frequency component of the system voltage. The system commutating voltage, the PLL reference voltage, and the nominal firing angle reference are shown for phase A in Figure 2.20. The reference voltage waveform is synchronized to the system voltage, but there is a 90° phase difference between θ s and θ r.

A proportional-integral (PI) controller synchronizes the PLL reference voltage waveform to the system commutating voltage waveforms by acting to reduce the total phase error. The total phase error per cycle is defined as:

$$ETOT = \sum_{j=1}^{6} ERR(j) = \sum_{j=1}^{6} [\theta r(j) - \theta s(j)] \qquad (2.14)$$

The zero crossings of the measured commutating voltage are determined by checking if a polarity change has occurred. When a zero crossing is detected, linear interpolation is used to reduce the sensitivity of the measurement to the solution time step, and the storage register, ERR (j) is updated. The total error is then calculated and passed to the PI controller.

The firing pulses are issued to each thyristor whenever the PLL phase position, θr satisfies the logic shown in Table 2.4, where the thyristor arrangement is as in Figure 2.15.

Table 2.4 Thyristor Firing Pulse Logic	
Thyristor	Range of θr
1	$\alpha o + 90° \leq \theta r < 180°$
2	$\alpha o + 150° \leq \theta r < 240°$
3	$\alpha o + 210° \leq \theta r < 300°$
4	$\alpha o + 270° \leq \theta r < 360°$
5	$0° \leq \theta r < 60°$, or $\alpha o + 330° \leq \theta r < 360°$
6	$\alpha o + 30° \leq \theta r < 120°$

The PLL position, θr is calculated with modulus 2π, as is the system phase position, θs to avoid computational problems. Referring to Figure 2.20, thyristor, T1 can only be fired when the voltage, Vab across it is positive and $\alpha o + 90° \leq \theta r < 180°$ ($\alpha o \leq \theta s < 90°$). Thyristor, T4 can only be fired when voltage, Vab is negative and $\alpha o + 270° \leq \theta r < 360°$.

Firing angle modulation logic is provided for each anti-parallel thyristor pair to allow one thyristor to be fired at $\alpha o + \Delta_{xy}$ and the opposite thyristor to be fired at

$\alpha_o - \Delta_{xy}$. The modulation angle, Δ_{xy} is calculated externally and passed to the subroutine, as is α_o.

Input filtering is provided to filter the higher frequency ripple arising from time step discretization, computational voltage and current chatter and the presence of higher order harmonics due to system unbalances. A filter gain of 1.0 [unit less] and a filter time constant of 0.0083s (one-half cycle) were found to be suitable. Figure 2.21 compares the unfiltered and filtered PLL steady state error for the case where the TCR is fired at $\alpha_o = 30°$ in the presence of severely distorted system voltage waveforms due to second harmonic voltages. The PI controller minimizes the total phase error between the phase-locked oscillator voltage waveforms and the system voltage waveforms by varying the angular frequency, w_r of the oscillator. The PLL steady state error was within ± 0.006°. The controller gain settings were chosen minimize the synchronization time following large phase errors such as encountered during system startup or following a step change in the phase (generation - load unbalance) of the measured voltage. A minimum response time of about 300 ms was achieved using the parameters listed in Table 2.5.

Table 2.5 PLL Control Parameter Settings	
Parameters	Value
Input Filter Gain	Gf = 1.0
Input Filter Time Constant	Tf = 0.0083 s
Proportional Gain	Kp = 10 s^{-1}
Integral Gain (slow)	Kis = 100 s^{-2}
(fast)	Kif = 250 s^{-2}
Integral Gain Switching Pickup Level	Vset = 0.2618 rad (15°)
Hysteresis	Hyst = 0.1745 rad (10°)
Time Delay Pick Up	Tdpu = 0.01s
Time Delay Drop Out	Tddo = 1.00s

The response of the PLL was slightly underdamped using these settings as observed in Figure 2.22 which shows the input error, integral output, and PLL output, w_r for a step change in system phase of 90° (at t = 0.75s). A normal integral gain of 100 s^{-2} was found necessary to quickly minimize the steady state error due to proportional action following small phase changes. A steady state error of less than ± 0.006° was obtained within 300 ms of a system phase deviation.

Integral gain switching was used to increase the gain from 100 s^{-2} to 250 s^{-2} for phase changes exceeding 15°. Gain switching allowed fast settling time to be achieved following large changes in system phase, and also allowed the PLL to remain in phase-lock during system frequency changes. The gain switching logic in the TCR model requires

the modelling of a relay with a time delay on pickup and dropout. The Fortran code for this subroutine, T1MD5 is included in Appendix B2.2.

Figure 2.23 shows the input error, integral output, and PLL output following a system frequency increase (starting at t = 0.5s) at a rate of 10 Hz/s. The integral output produces a steady state output, Δw_r = 62.8 rad/s to augment the PLL base frequency of 377 rad/s (60 Hz) in order to remain synchronized to the system whose frequency has increased to 439.8 rad/s (70 Hz).

Figure 2.24 shows the TCR system voltages, the PLL reference voltages, the TCR phase currents, and the thyristor firing pulses for TCR operation at a firing angle of 30 degrees in the presence of an sinusoidal 60 Hz source voltage. The PLL reference voltages are observed to be in phase with the fundamental frequency system voltage. The firing pulses are equidistant and the TCR phase currents are symmetrical.

Each thyristor is modelled as a resistor. The switching logic changes the value of the resistance from R_{on} to R_{off} to turn the thyristor off, and vice versa. The logic first checks the status of the thyristor from the previous time step. Due to numerical constraints the thyristor switch model is not ideal. Consequently, when the voltage

across the thyristor becomes positive, some current will flow in the forward direction. The value of ROFF must be large enough so that the error is insignificant with respect to the full load current.

The thyristor current, Ivj(t) is used in the model to determine when to turn the thyristor off. In order that the thyristor remain conducting (on), the current must exceed a "holding current" level > Chold. When the current falls below this level, the thyristor is turned off, the system conductance matrix is inverted, and the time the thyristor is turned off is recorded. Also, the thyristor current turn off level Ivoff(t) is set to zero. When the thyristor is turned off, there will be a small negative current through the thyristor due to the finite value of Roff.

During the next cycle, when the thyristor becomes forward biased, there will be a small positive current through the thyristor. This current exceeds the current turn off level which is zero when the thyristor is off. If the firing pulse exists the thyristor is turned on, the system conductance matrix is inverted, and the identity of the thyristor is recorded; otherwise the thyristor remains off. When the thyristor is on, the current turn off level Ivoff(t) is set to Chold.

The thyristor current is calculated each time step by the relationship:

$$Ivj(t) = Gvj(t) * Vj(t),\ j = 1,6 \qquad (2.15)$$

where Gvj(t) is the thyristor conductance (Gon or Goff)

Vj(t) is the forward voltage across the thyristor.

The model interfaces to the network by calculating the conductance element for each anti-parallel thyristor pair between nodes I and J each time step.

$$\begin{aligned} GDC\ (I,J,M) &= 0 \\ GDC\ (I,J,M) &= GDC\ (I,J,M) + Gvj(t)\ ,\ j = 1,6,1 \\ GDC\ (J,I,M) &= G(I,J,M) \end{aligned} \qquad (2.16)$$

The EMTDC program requires the conductance to be initialized to zero each time step.

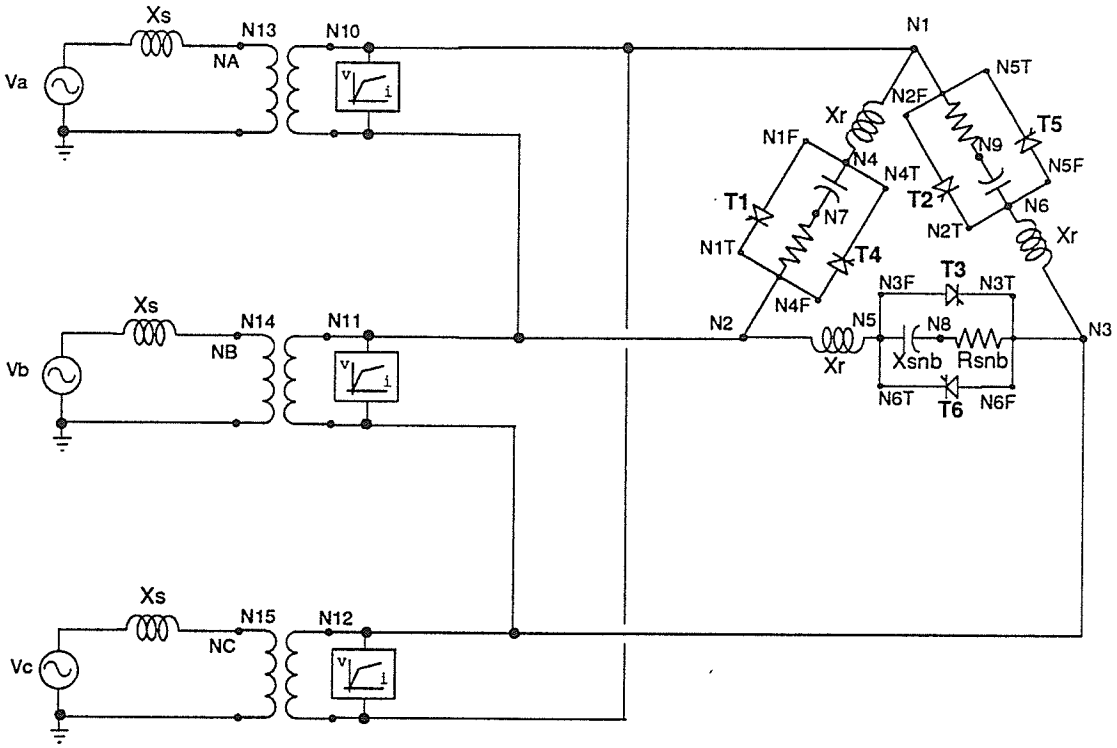

Subroutine R6P120 (MA, NA, NB, NC, N1T, N1F, N2T, N2F, N3T, N4F, N5T, N5F, KV, KB, ROFF, RON, CTO, ALPHO, VREFM, FREQS, WR, G, TI, TIF, YO, TLO, THI, GL, TL, VSET, HYST, TDPU, TDDO, RPUL24, DELTR, DELST, DELTR)

Figure 2.15 TCR Model Interface to the Electrical Network

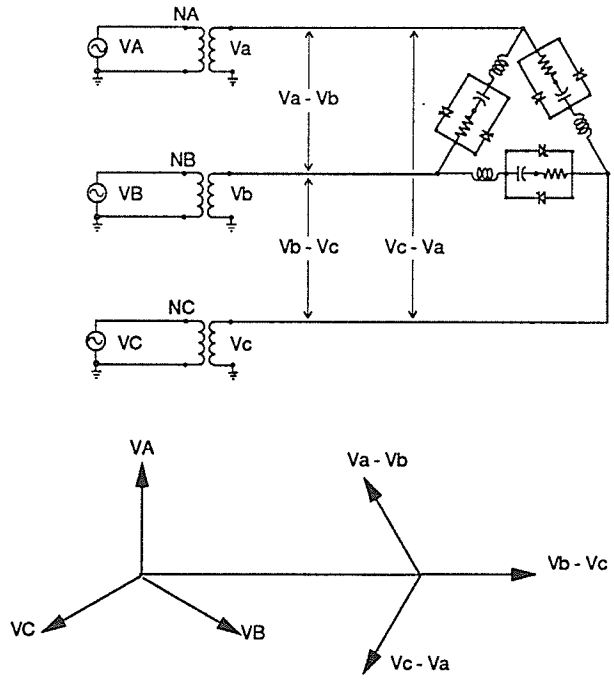

(a) SVC Transformer Y - Y Connected - PLL Reference Voltage Lags TCR Commutating Voltage by 30'

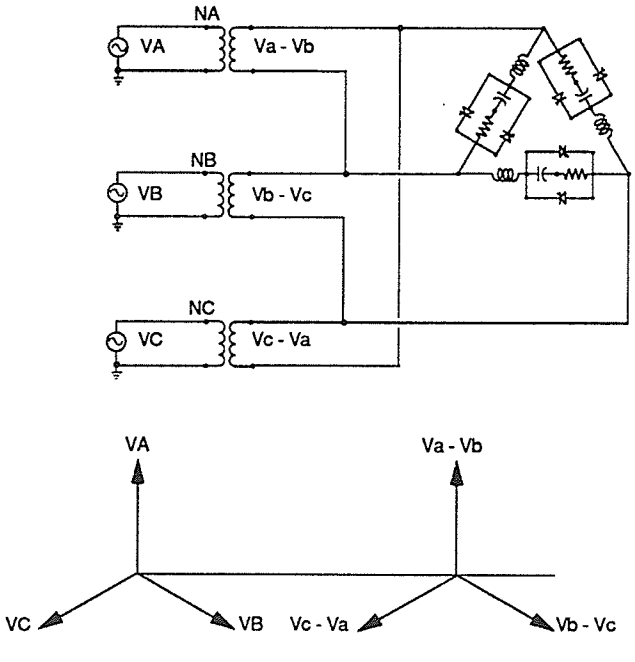

(b) SVC Transformer Y - ΔConnected - PLL Reference Voltage in Phase with TCR Commutating Voltage

Figure 2.16 Relationship between PLL Reference Voltage Phasors and TCR Commutating Voltage Phasors

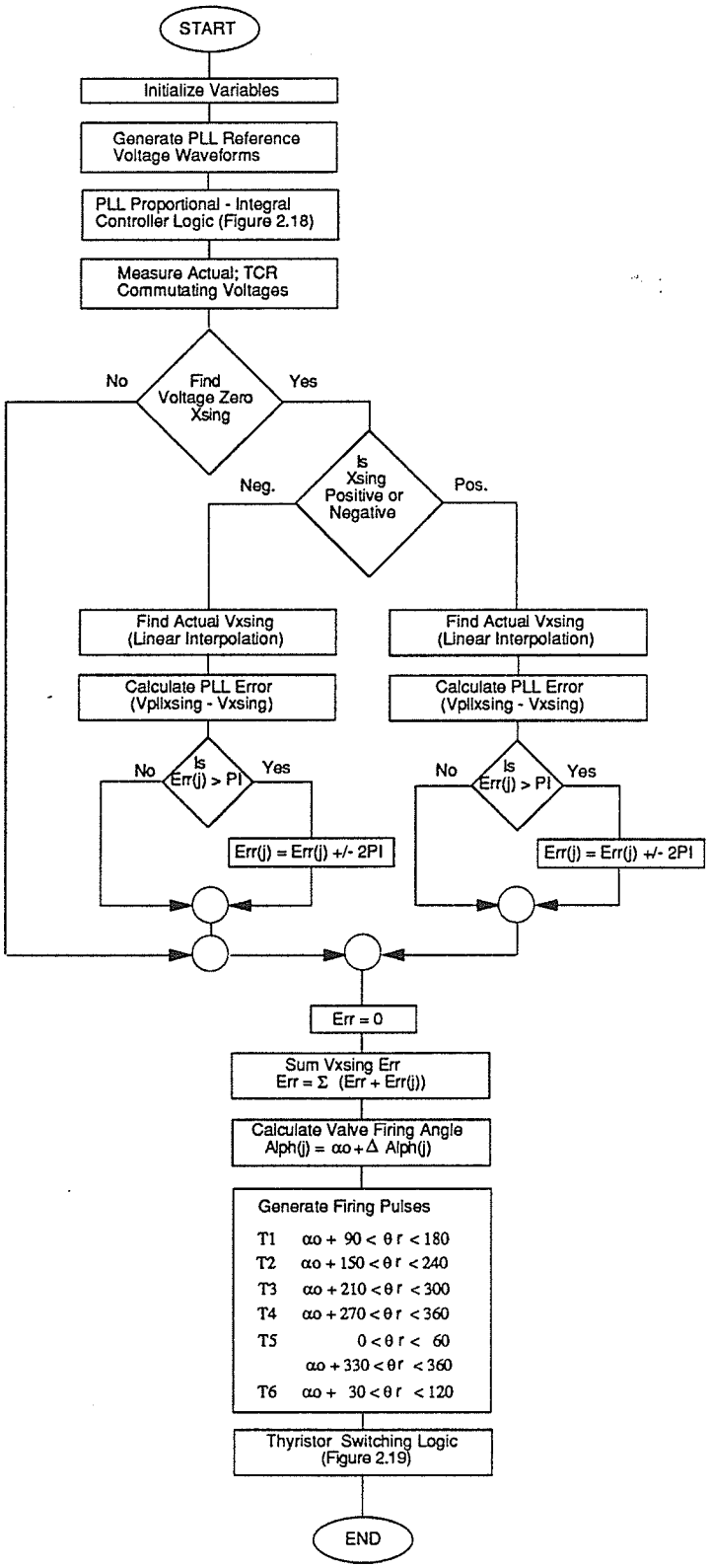

Figure 2.17 TCR Model Block Diagram Showing Thyristor Firing Pulse Logic Subroutine R6P120

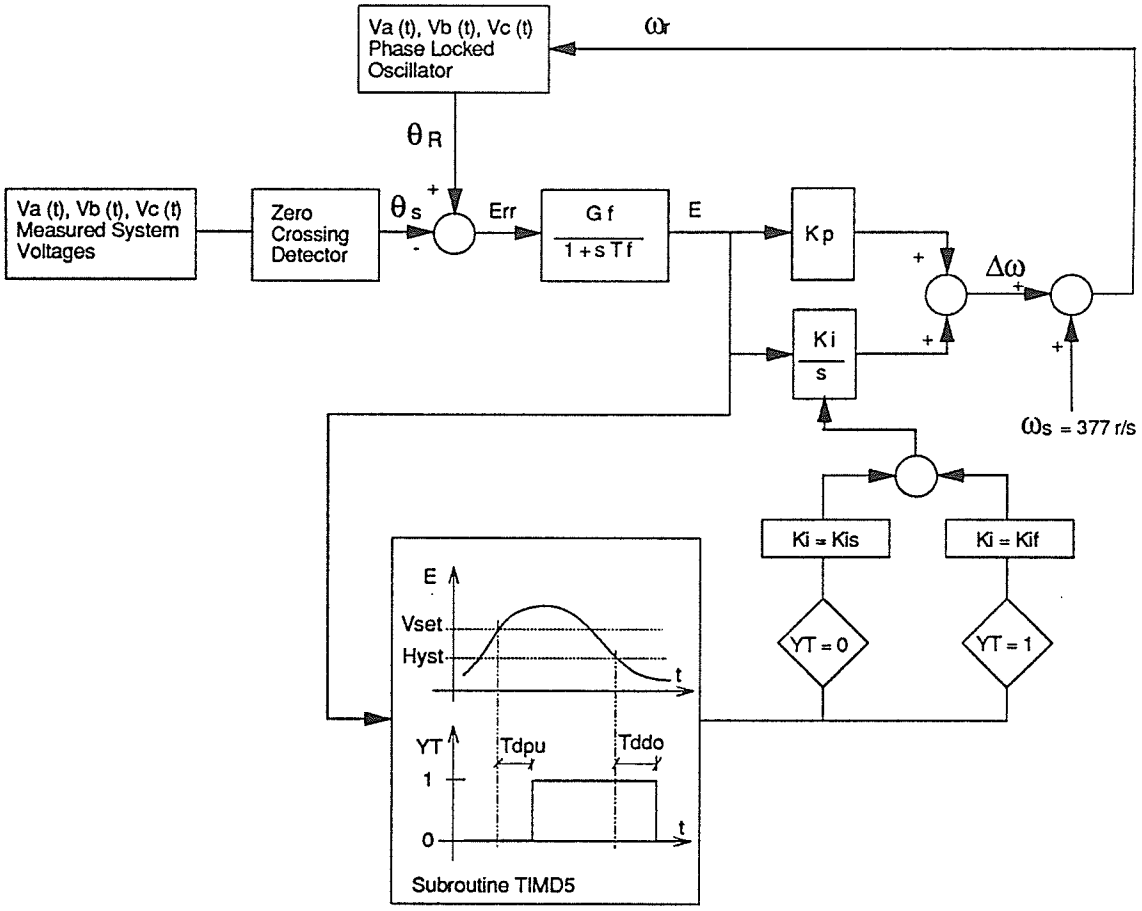

Gf = Input Filter Gain [-]
Tf = Input Filter Time Constant [s]
Kp = Proportional Gain [1/s]
Ki = Integral Gain [1/s*2]
Vset = Integral Gain Switching Pickup Setting [rad]
Hyst = Integral Gain Switching Dropout Setting [rad]
Tdpu = Time Delay On Pickup [s]
Tddo = Time Delay On Dropout [s]
Kis = Low Integral Gain [1/s*2]
Kif = High Integral Gain [1/s*2]

Figure 2.18 TCR Model Phase - Locked Loop Block Diagram
Subroutine R6P120

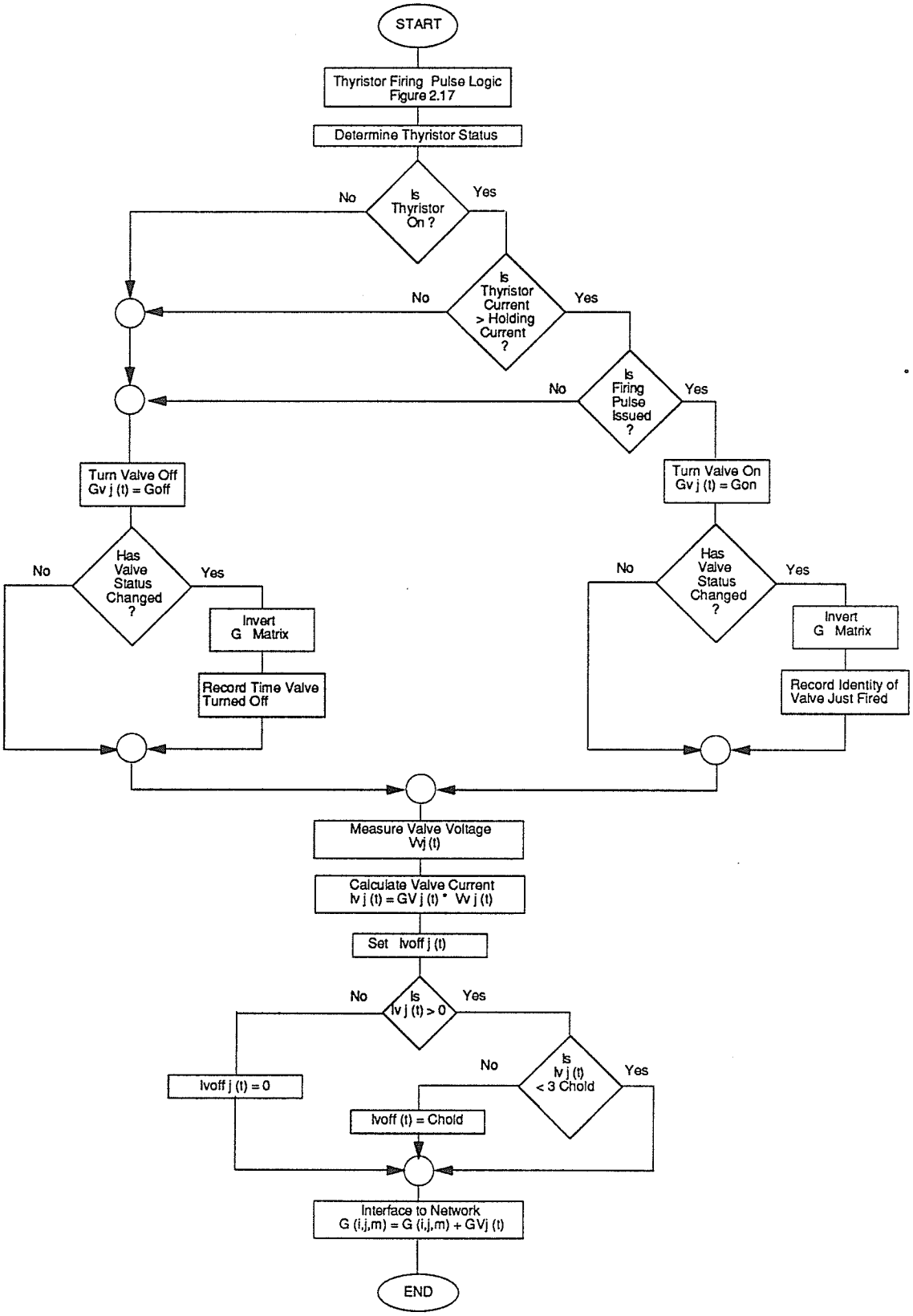

Figure 2.19 TCR Model Block Diagram Showing Thyristor Switching Logic Subroutine R6P120

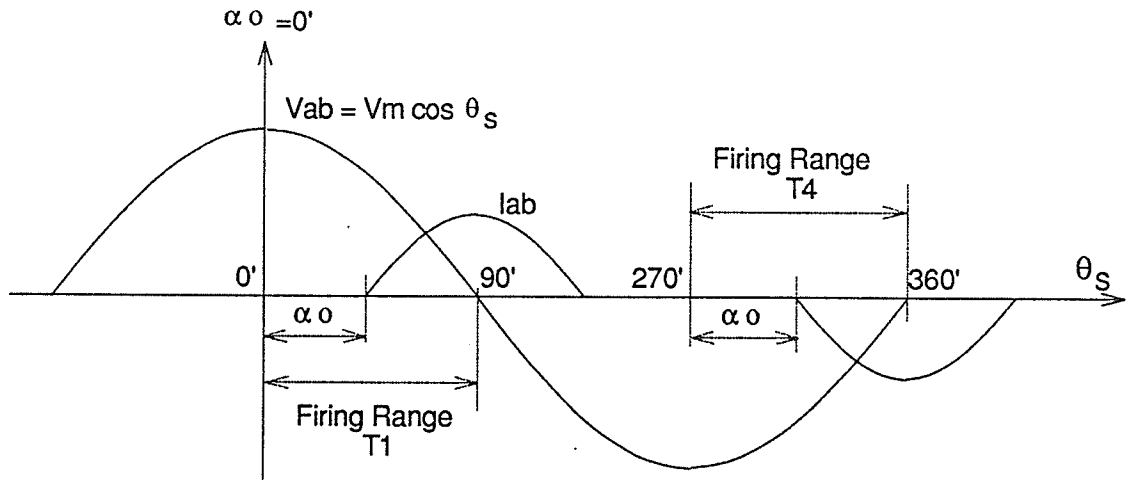

(a) System Angle Reference

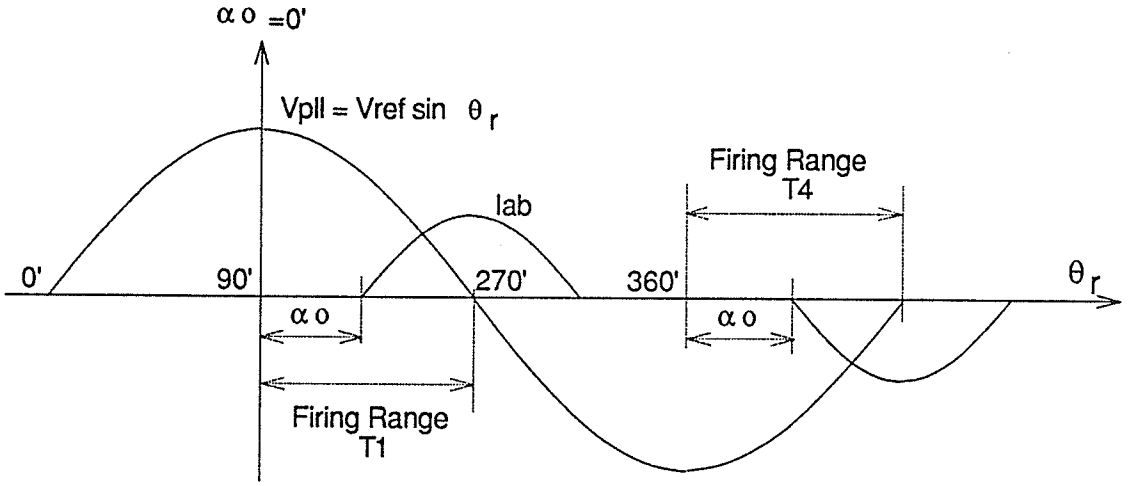

(b) PLL Angle Reference

Figure 2.20 TCR Model Nominal Fiiring Angle Reference
Subroutine R6P120

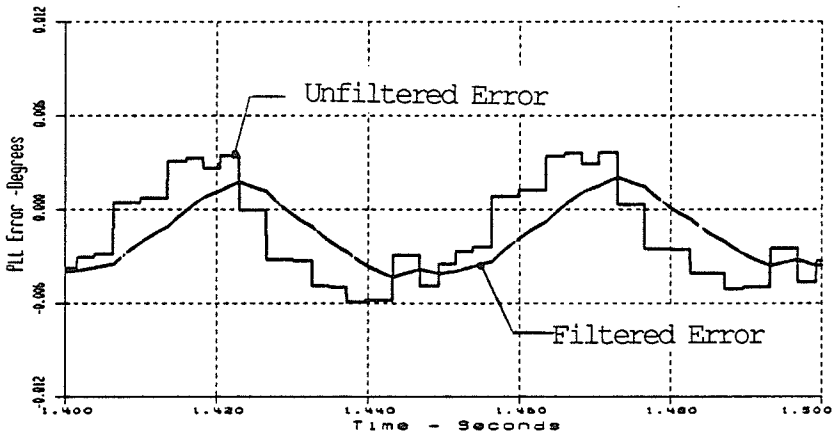

Figure 2.21 PLL Steady State Error, **Equidistant** Firing with Alpha = 30°, Source 2nd Harmonic Voltage 30% @ -30°

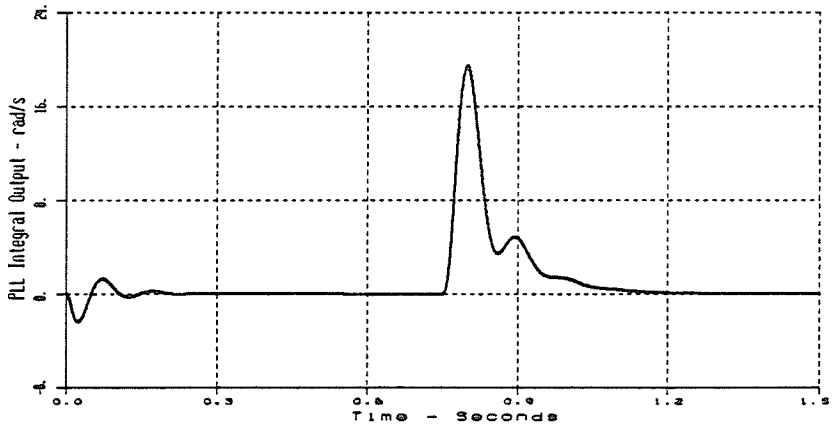

a) PLL Integral Output - rad/s

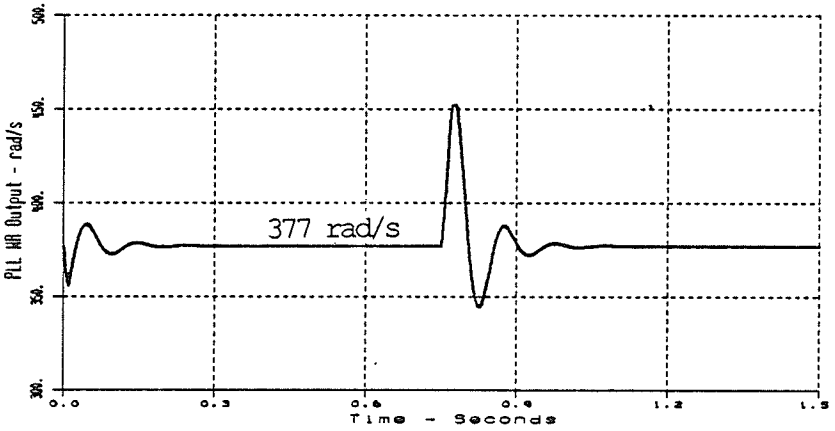

b) PLL Output - Wr - rad/s

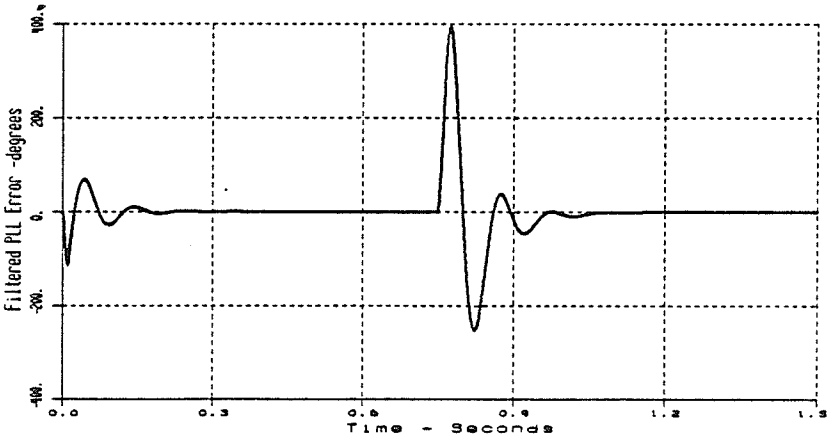

c) PLL Filtered Error - Degrees

Figure 2.22 TCR PLL Response to a 90° Step Increase in System Phase, Equidistant Firing with Alpha = 30°, Source 2nd Harmonic Voltage 30% @ -30°

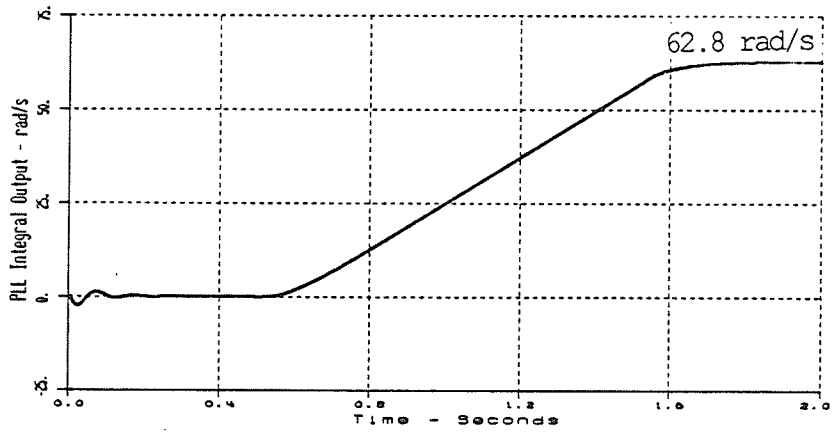

a) PLL Integral Output - rad/s

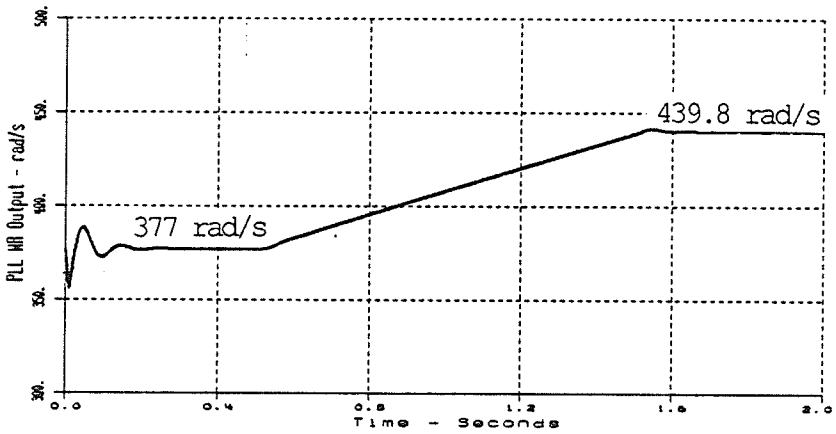

b) PLL Output - Wr - rad/s

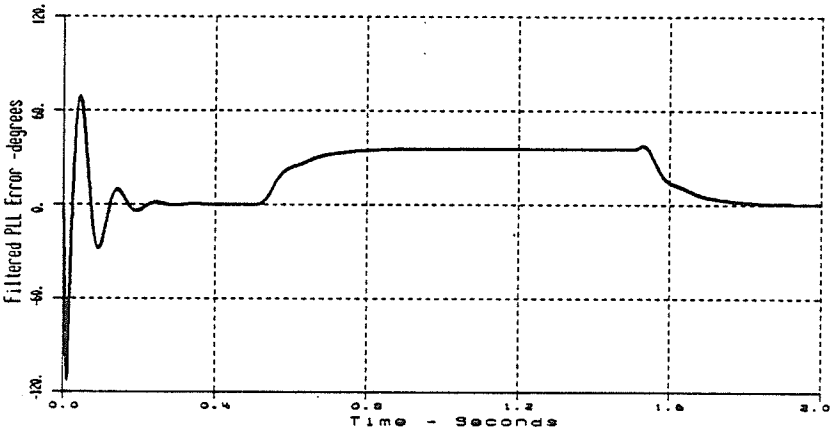

c) PLL Filtered Error - Degrees

Figure 2.23 TCR PLL Response to a 10 Hz/s Ramp in System Frequency, Equidistant Firing with Alpha = 30°, Source: 2nd Harmonic Voltage 30% @ -30°

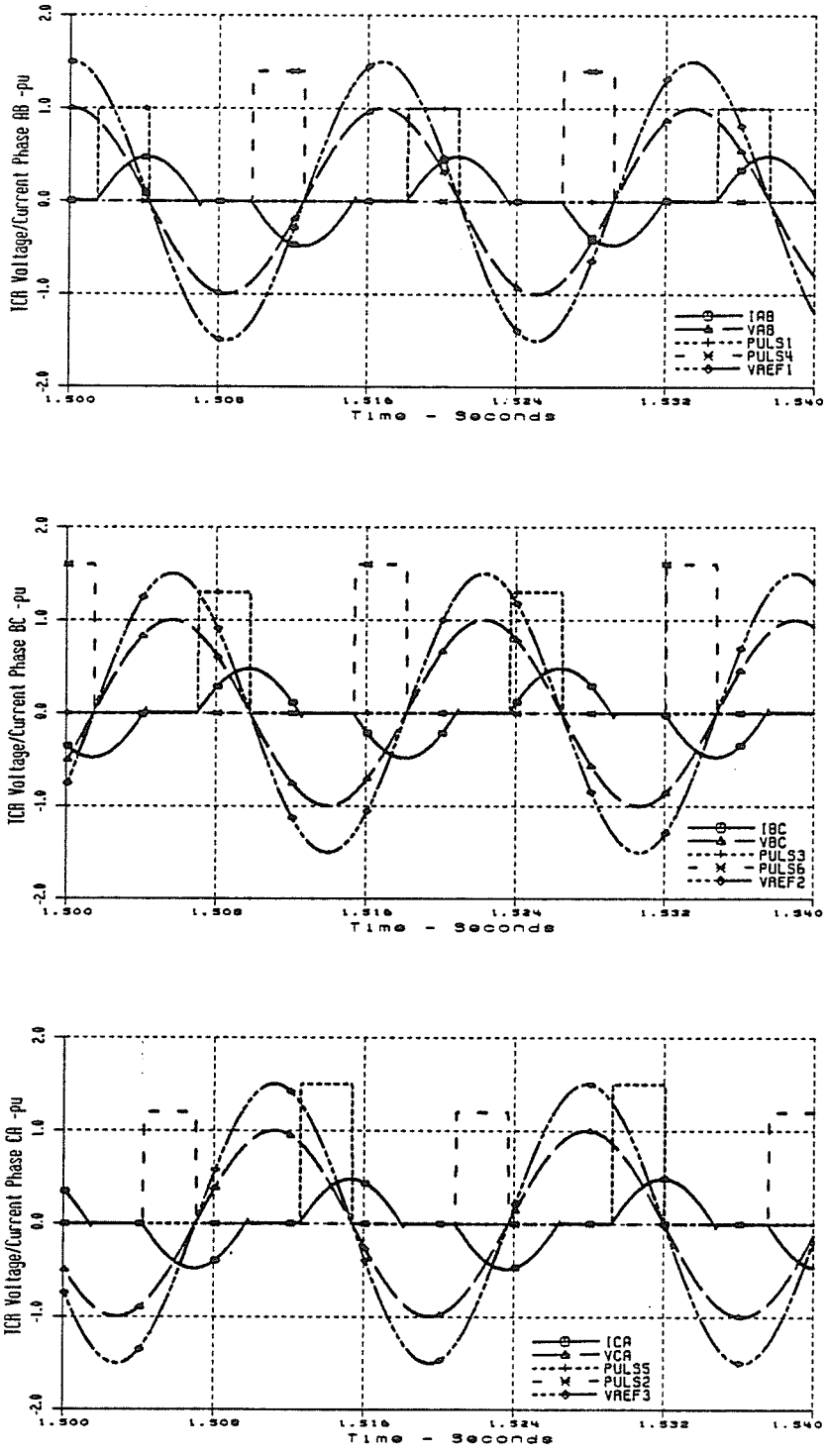

Figure 2.24 TCR Voltages, Phase Currents, Firing Pulses and PLL Reference Voltages during Balanced Voltage Operation with Firing Angle 30°

2.6 Phasor Measurement of Control Parameters

If a troublesome harmonic is to be eliminated from the TCR line current, this quantity must be measured and processed by the TCR firing angle modulation controller. The phasor value of the positive sequence second harmonic component must be measured if the second harmonic is to be controlled. Similarly, if the dc component of the TCR line current is to be eliminted, the phasor value of the dc component in the positive sequence line current must be measured.

In the presence of distorted system voltage waveforms due to a second harmonic system resonance, the TCR line current can have the form:

$$i(t) = \sum_{i=1}^{n} \hat{i}_n \cos (n\, w_o t + \phi\, n) \qquad (2.17)$$

To obtain an accurate phasor measurement of any desired harmonic component of this current, a reference phasor is required. The reference phasor must remain constant in phase position and frequency with respect to the signals to be identified as phasors.

The control parameter measurement method used in this analysis transforms the instantaneously measured current into its phasor equivalent by using the TCR firing system

PLL to provide the reference phasor [3]. The PLL can provide a reference harmonic phasor of the form.

$$A\, e^{j(n\, w_r t + \phi\, r)} = A\, [\cos(n\, w_r\, t + \phi\, r) + j\, \sin(n\, w_r t + \phi\, r)] \qquad (2.18)$$

where w_r is the PLL frequency and $\phi\, r$ is the PLL phase position and n is the desired harmonic number.

The reference phasor is locked onto the positive sequence of the system voltage, and consequently remains constant in phase and frequency with respect to the system quantities to be identified as phasors even in the presence of system unbalances and frequency excursions.

The measured instantaneous values of the three phase currents are converted to their equivalent two phase set of instantaneous values using the scalar (a,b,c) to (α, β) transformation defined by:

$$\begin{bmatrix} i\ \alpha\ (t) \\ i\ \beta\ (t) \end{bmatrix} = \frac{1}{3} \begin{bmatrix} 2 & -1 & -1 \\ 0 & \sqrt{3} & -\sqrt{3} \end{bmatrix} \begin{bmatrix} ia\ (t) \\ ib\ (t) \\ ic\ (t) \end{bmatrix} \qquad (2.19)$$

The symmetrical components of the instantaneous values are required. Before the vector symmetrical component transformation can be applied, the instantaneous values of the

(α , β) - components must be translated to their phasor equivalents. The symmetrical component transformation can be applied as follows:

$$\begin{bmatrix} I_1 \\ I_2 \end{bmatrix} = \frac{1}{2} \begin{bmatrix} 1 & j \\ 1 & -j \end{bmatrix} \begin{bmatrix} I_\alpha \\ I_\beta \end{bmatrix} \qquad (2.20)$$

The symbols I_1 and I_2 denote the positive and negative sequence phasors respectively, and I_α and I_β denote the phasor values of the instantaneous signals $i_\alpha(t)$ and $i_\beta(t)$ respectively.

To compute the sequence components directly from the instantaneous values of the (α, β) - components a transformation, T is required which is defined symbolically by:

$$\begin{bmatrix} I_1 \\ I_2 \end{bmatrix} = \begin{bmatrix} T_{11} & T_{12} \\ T_{21} & T_{22} \end{bmatrix} \begin{bmatrix} i_\alpha(t) \\ i_\beta(t) \end{bmatrix} \qquad (2.21)$$

The transformation T is defined by the requirement to extract from a time varying signal the phasor component of a specified frequency as a dc value.

It has been shown [3] that the elements of transformation T are:

$$T11 = \cos w_r t - j \sin w_r t, \tag{2.22}$$

$$T12 = j\, T11, \tag{2.23}$$

$$T21 = T11, \text{ and} \tag{2.24}$$

$$T22 = -j\, T11. \tag{2.25}$$

Consequently, the real and imaginary parts of the k_{th} harmonic positive sequence phasor are given as:

$$\begin{bmatrix} \text{Re } [I_1] \\ \text{Im } [I_1] \end{bmatrix} = \begin{bmatrix} \cos w_r t & \sin w_r t \\ -\sin w_r t & \cos w_r t \end{bmatrix} \begin{bmatrix} i_{\alpha}(t) \\ i_{\beta}(t) \end{bmatrix} \tag{2.26}$$

The real and imaginary parts of the k_{th} harmonic negative sequence phasor are given as:

$$\begin{bmatrix} \text{Re } [I_2] \\ \text{Im } [I_2] \end{bmatrix} = \begin{bmatrix} \cos w_r t & -\sin w_r t \\ -\sin w_r t & -\cos w_r t \end{bmatrix} \begin{bmatrix} i_{\alpha}(t) \\ i_{\beta}(t) \end{bmatrix} \tag{2.27}$$

Figure 2.25 shows the implementation of the harmonic phasor measurement system for measuring the positive sequence real and imaginary components of the n^{th} harmonic phasor of the TCR line currents.

Subroutine PSEQU converts the measured instantaneous values of the TCR line curent to the equivalent instantaneous (α, β) - component values as per equation (2.19). The positive sequence real and imaginary phasor components are calculated as in equation (2.26). The sine/cosine oscillator, which generates the reference phasor, remains in phase-lock with the system voltages since the phase position, θ_r is generated by the TCR phase-locked loop. The PLL phase position is adjusted by $\phi r = -90°$ to coincide with the reference coordinate system ($\alpha o = 0°$ is defined to be the peak of the system phase A voltage waveform). The input currents, PLL phase position and desired harmonic number are passed to the subroutine via the call statement. If the harmonic number N=o, the dc component phasor is calculated, if N=1 the fundamental frequency phasor is calculated, if N=2 the second harmonic phasor is calculated, and so on.

Subroutine PSEQU outputs the (α , β) - components and the unfiltered real and imginary components of the positive sequence n^{th} harmonic phasor. The listing for subroutine PSEQU in included in Appendix B3.

Filtering to eliminate the sinusoidal terms which arise when extracting the n^{th} harmonic component from the instantaneous current is accomplished using a digital averaging filter. The real and imaginary components output

from subroutine PSEQU are sampled 24 times per cycle and stored in a shift-register containing 24 registers. Each new sample is stored in register #1, and the previous samples are shifted up one register. The output is calculated by summing the contents of the 24 registers and averaging the result (1/24) after each sampling pulse. The output is the dc value of any sinusoid whose period is a multiple of the fundamental period. The sampling pulse train is generated by the PLL and therefore remains constant in phase position with respect to the measured currents.

The sampling rate of 24 samples per second is adequate for the harmonic components of interest in this analysis. If higher frequency components are to be measured, the sampling rate may have to be increased so that the sampling interval is less than the Nyquist interval.

The filtering is done by subroutine AVGF25, whose Fortran coding is included in Appendix B4.

Figure 2.26 shows the positive sequence dc, 60 Hz, and second harmonic real and imaginary phasor components respectively of the TCR line currents as measured by subroutines PSEQU and AVGF25. The measurements were made for the case where the TCR firing angle, $\alpha_o = 30°$, with the source voltage containing a second harmonic component of 30%

magnitude at a phase displacement of -30° with respect to the fundamental frequency voltage source.

Table 2.6 shows a comparison of the steady state output of the phasor mesurement system with the output from numerical Fourier analysis of the TCR line currents for the case shown in Figure 2.26.

TABLE 2.6
Comparsion of Model Phasor Measurement
to Numerical Fourier Analysis
for TCR Line Currents,
Alpha = 30°, Source 2nd Harmonic 30% @ -30°

	Measured		Fourier Analysis	
+ve Seq.	Magnitude (pu)	Phase (degrees)	Magnitude (pu)	Phase (degrees)
dc	0.0543	-133.1	0.0537	-132.3
60 Hz	0.3718	-120.4	0.3701	-120.8
120 Hz	0.1086	-131.5	0.1093	-133.0

Figure 2.27 shows the phasor measurement system response to a step change in system phase of 90° at t = 0.75 seconds. The real and imaginary components of the dc, 60 Hz and second harmonic positive sequence phasors of the TCR line current are shown for the case where the TCR is fired at α_o = 30° in the presence of a source voltage with a second harmonic component of 30% @ -30°. The measurement system adjusted to the system phase error within 150 ms. Note that

the magnitudes of the harmonic phasors are the same before and after the system phase change. Only the phase position is altered as the reference phasor, generated by the PPL, adjusts to remain locked onto the system voltage waveforms.

Figure 2.28 shows the measurement system response during a 10 Hz/s ramp in system frequency.

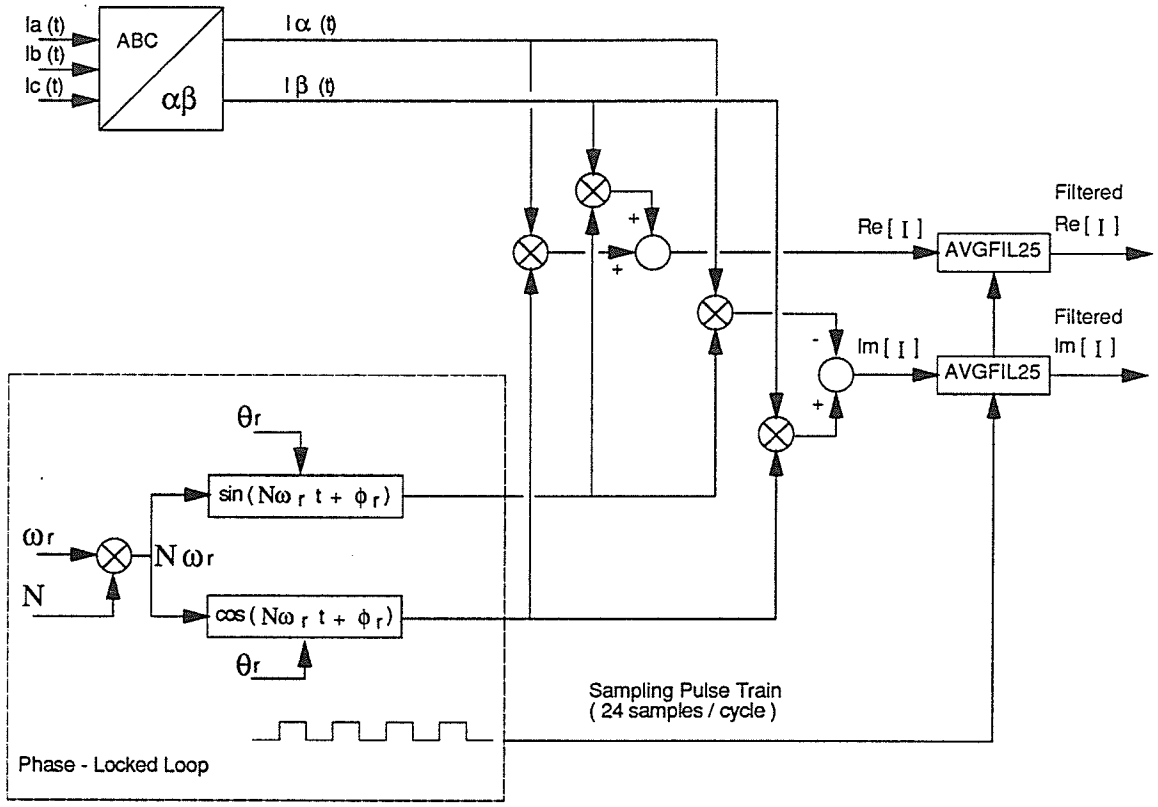

Figure 2.25 Block Diagram for Measurement of the Nth Harmonic Positive Sequence Phasor Component of the TCR Line Current

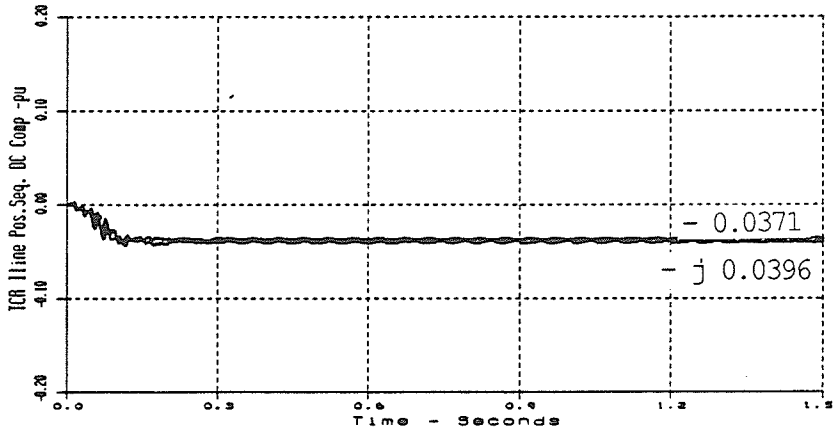

a) Real/Imaginary DC Component - pu

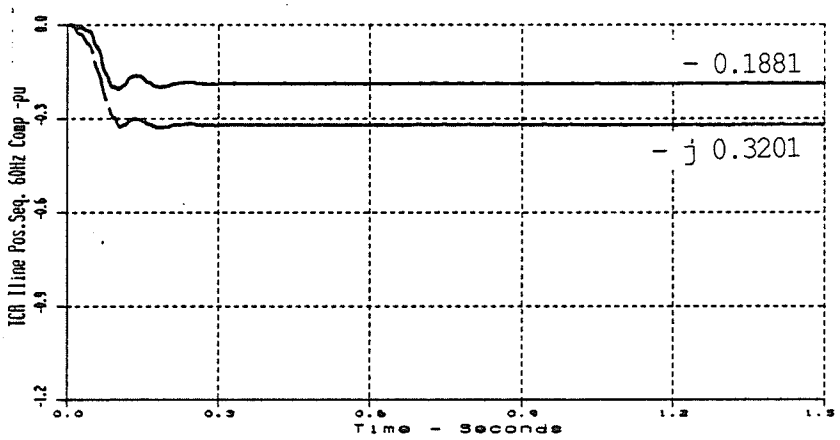

b) Real/ Imaginary 60 Hz Component - pu

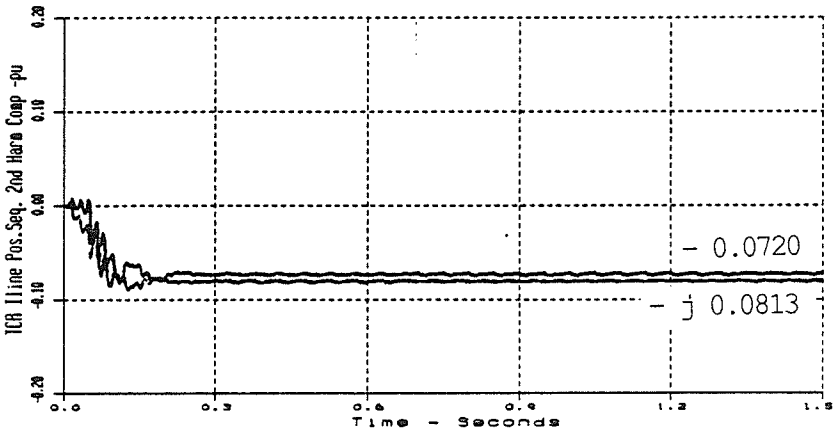

c) Real/Imaginary 2nd Harmonic Component - pu

Figure 2.26 Measured Positive Sequence DC, 60 Hz, and 2nd Harmonic Components of TCR Line Current, Equidistant TCR Firing at Alpha = 30°, Source: 2nd Harmonic Voltage 30% @ -30°

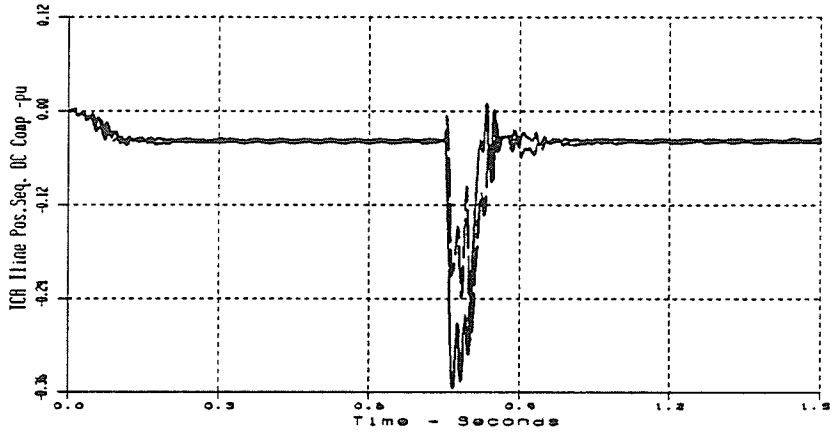

a) Real/Imaginary DC Component - pu

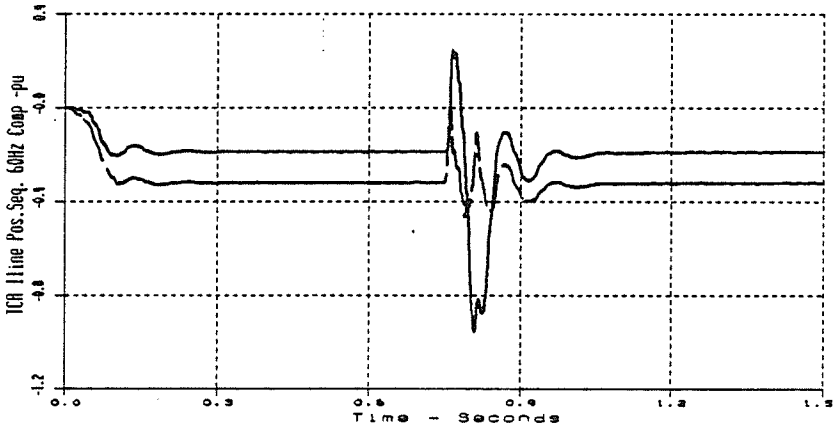

b) Real/ Imaginary 60 Hz Component - pu

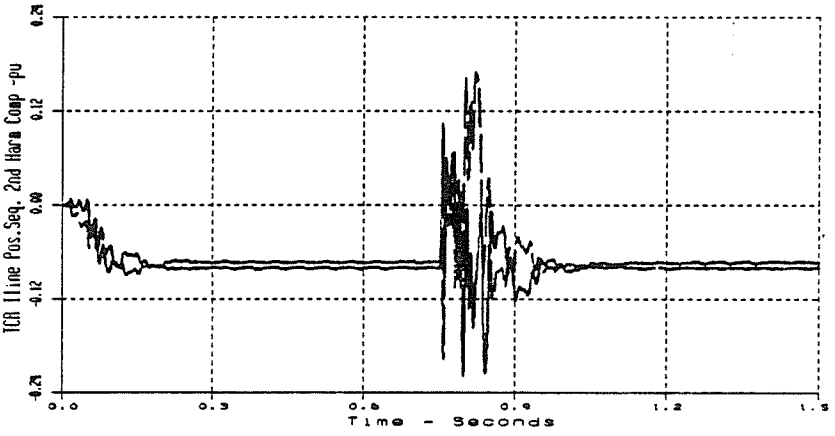

c) Real/Imaginary 2nd Harmonic Component - pu

Figure 2.27 Measurement System Response to a Step Change in System Phase of 90°, Equidistant TCR Firing at Alpha = 30°, Source: 2nd Harmonic Voltage 30% @ -30°

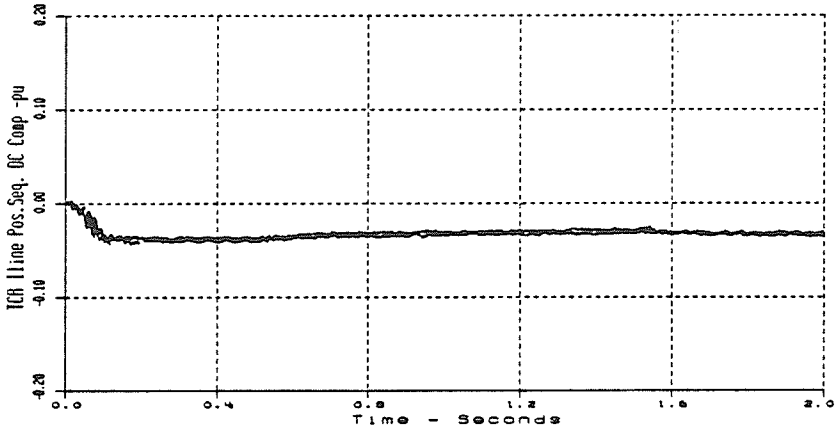

a) Real/Imaginary DC Component - pu

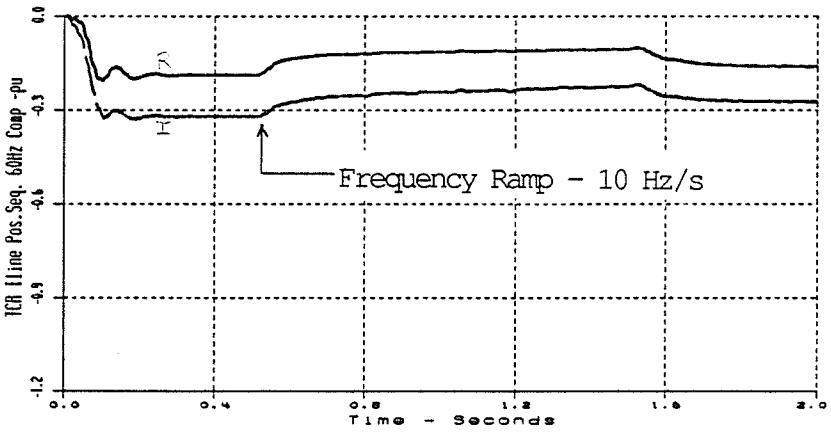

b) Real/ Imaginary 60 Hz Component - pu

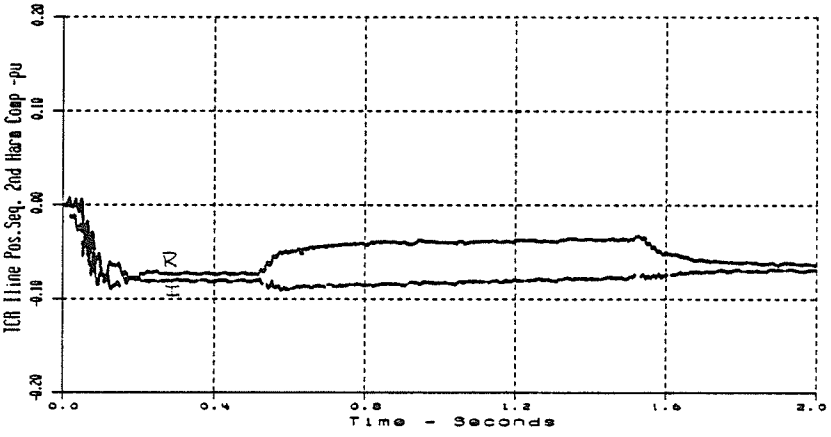

c) Real/Imaginary 2nd Harmonic Component - pu

Figure 2.28 Measurement System Response to a System Frequency Ramp of 10 Hz/s, Equidistant TCR Firing at Alpha = 30°, **Source:** 2nd Harmonic Voltage 30% @ -30°

2.7 Firing Angle Modulation Controller Model

The TCR firing angle modulation controller consists of one real-pole type input filter, one proportional-integral controller for each component (real or imaginary) of the measured input phasor, and a control algorithm to generate the modulation signal. The modulation controller block diagram is shown in Figure 2.29 and is implemented by subroutine PCTR20. The Fortran code for subroutine PCTR20 is included in Appendix B5.

Filtering of the real and imaginary components of the measured harmonic phasor allows averaging the input signal over several cycles. The reference values for the real and imaginary components of current are zero, therefore the PI controller adjusts the firing angle modulation until the measured components are reduced to zero.

The modulation controller outputs a phasor quantity, expressed in terms of its real component, CRL and imaginary component, CIMG:

$$\bar{\Delta} = CRL + j\ CIMG = \hat{\Delta} \angle \delta \qquad (2.28)$$

where $$\hat{\Delta} = \sqrt{CRL^2 + CIMG^2} \qquad (2.29)$$

and $$\delta = \tan^{-1} \frac{CIMG}{CRL} \qquad (2.30)$$

A sinusoidal signal, Δ at frequency, w_r can be derived from this phasor information where

$$\Delta = \hat{\Delta} \cos (w_r t + \delta) \qquad (2.31)$$

and w_r is the signal frequency.

Since the firing of the thyristor normally occurs at 60° intervals, with firing of each anti-parallel pair of thyristors in each TCR phase occurring at 180° intervals, the modulation sinusoid can be described by:

$$\Delta xy = \hat{\Delta} \cos (\theta r + (k-1)\ 120° + \delta) \qquad (2.32)$$

where $\theta r = w_r t$.

The reference frame for firing angle modulation is defined as shown in Figure 2.30 by arbitrarily setting $\theta r = 0°$ and defining k as in Table 2.7.

TABLE 2.7
Firing Angle Definition for Sinusoidal Modulation

xy	k	Δ xy	Firing Angle α i = α o + Δ xy
ab	1	$\hat{\Delta}$ cos δ	α 1 = α o + Δ ab α 4 = α o - Δ ab
bc	2	$\hat{\Delta}$ cos δ + 120°	α 3 = α o + Δ bc α 6 = α o - Δ bc
ca	3	$\hat{\Delta}$ cos δ + 240°	α 5 = α o + Δ ca α 2 = α o - Δ ca

The thyristor configuration and numbering is as shown in Figure 2.15. The equations in Table 2.7 (column 3) are used in subroutine PCTR20 to compute the modulation angle, Δ_{xy} for each anti-parallel thyristor pair. These phase modulation angles are passed to the TCR model R6P120 where the individual thyristor firing angles are computed (column 4).

Alternately, the modulation sinusoid can be constructed from the phasor output of the modulation controller using two phase-locked loop oscillator signals, one in quadrature with the other, as shown in Figure 2.29. Expansion of equation (2.31) produces the result:

$$\Delta = \hat{\Delta} \cos \delta \, (\cos w_r t) + \hat{\Delta} \sin \delta \, (-\sin w_r t) \quad (2.33)$$

where CRL = $\hat{\Delta} \cos \delta$ and CIMG = $\hat{\Delta} \sin \delta$. Sampling the modulation sinusoid at 60° intervls for each fundamental frequency cycle defines the firing angle modulation for each thyristor.

Figure 2.31 shows the response of the firing angle modulation controller when controlling the second harmonic component of TCR line current. The TCR was fired at a nominal firing angle $\alpha o = 30°$, for the case where the source voltage contained a second harmonic component of 30% magnitude at -30° with respect to the fundamental frequency source. The controller was turned on at 0.25 s and eliminated the second harmonic component of the TCR line in less than 300 ms.

Figure 2.31 also shows the controller response to a step change in system phase of 90° at 0.75 seconds when controlling the second harmonic component of TCR line current. The controller reduced the second harmonic component to zero within 200 ms after the phase shift.

Similarly, Figure 2.32 demonstrates that the firing angle modulation controller maintained control of the second harmonic component of TCR line current during a system frequency ramp of 10 Hz/s. The frequency ramp starts at t = 0.50s, just after the controller has reduced the second harmonic component of the positive sequence TCR line current to zero.

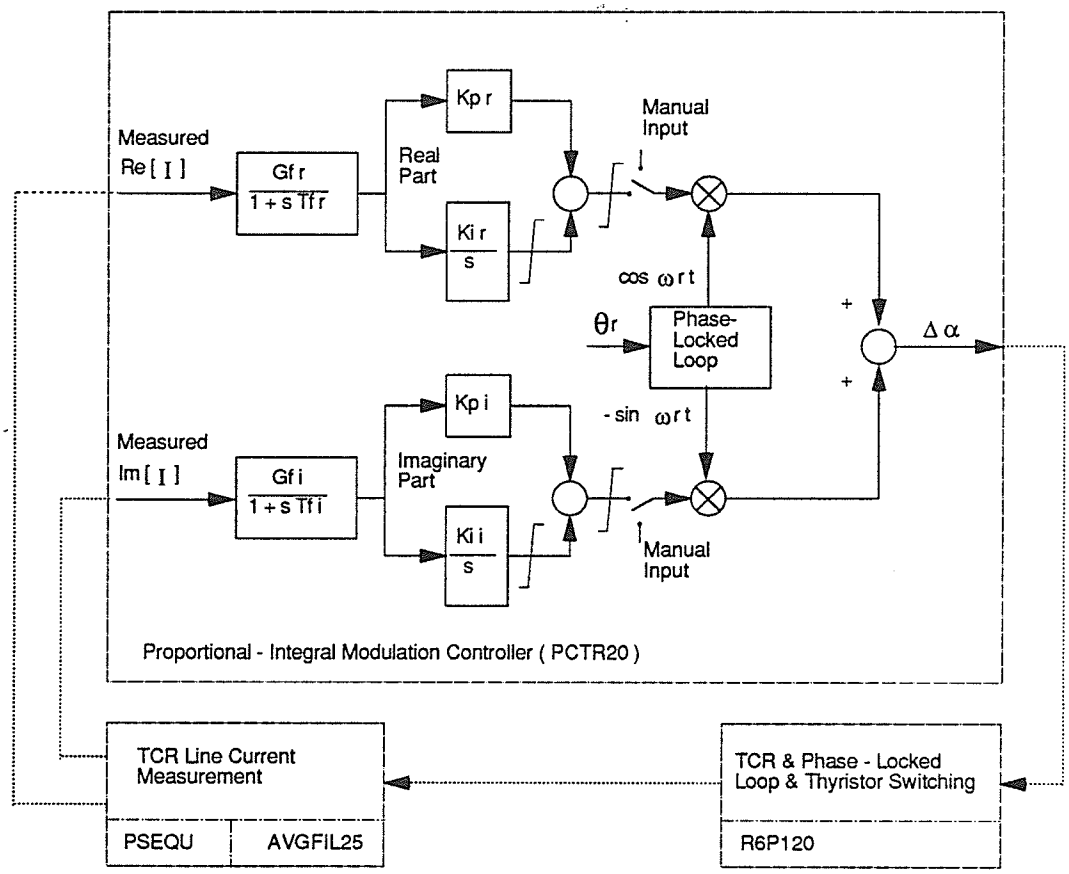

Figure 2.29 Block Diagram of the Proportional - Integral Controller for Sinusoidal Firing Angle Modulation of a TCR

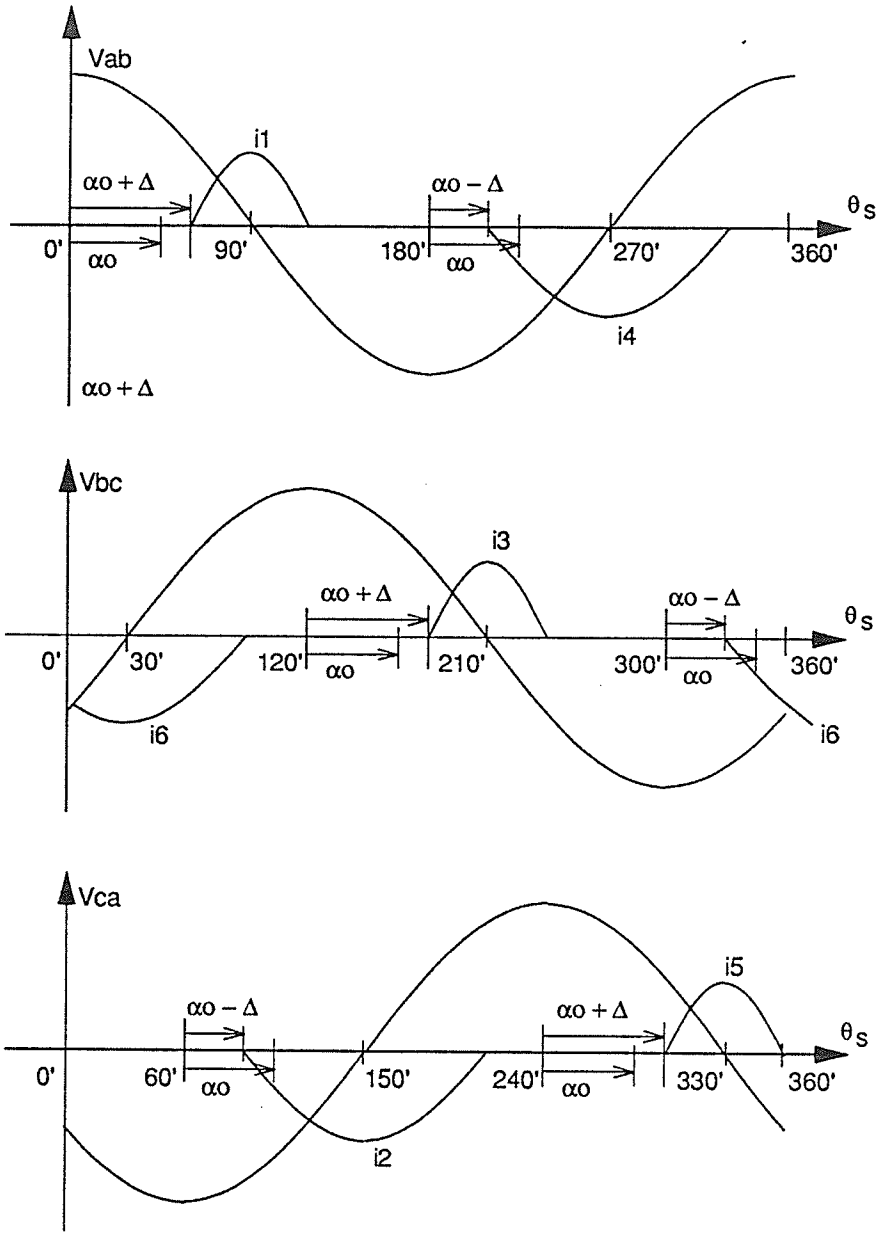

Figure 2.30 Phase Reference Frame for Sinusoidal Modulation

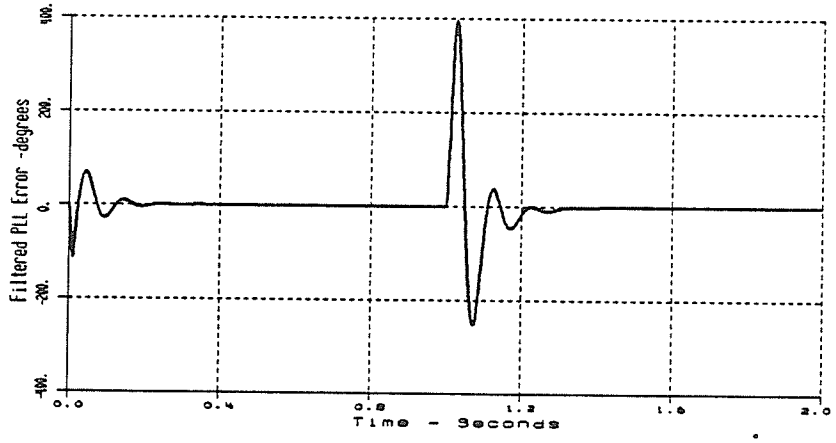

a) PLL Error - Degrees

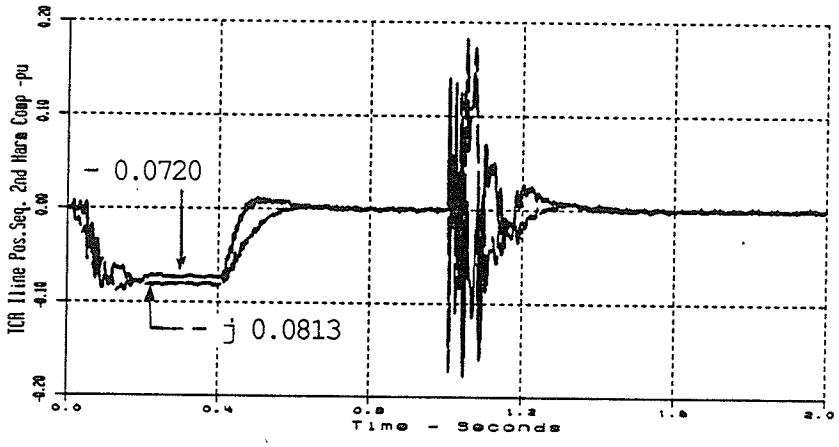

b) Real/Imaginary 2nd Harmonic Component - pu

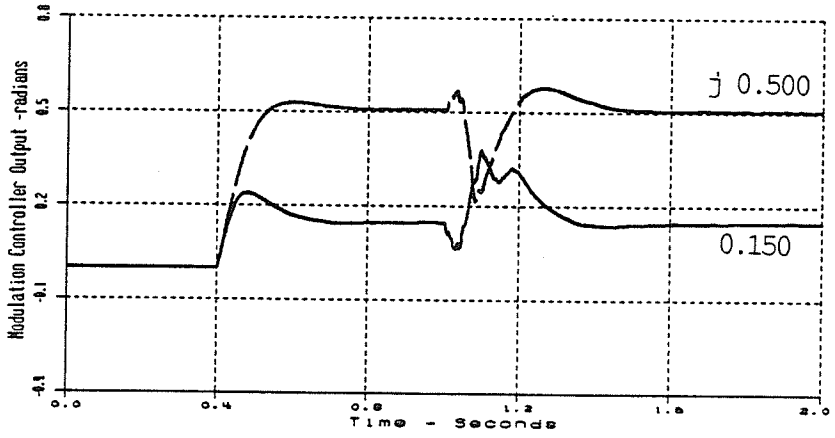

c) Real/Imaginary Modulation Output - radians

Figure 2.31 Modulation Control of Positive Sequence 2nd Harmonic Component of TCR Line Current, Response for a Step Change in System Phase of 90°, Alpha = 30°, Source: 2nd Harmonic Voltage 30% @ -30°

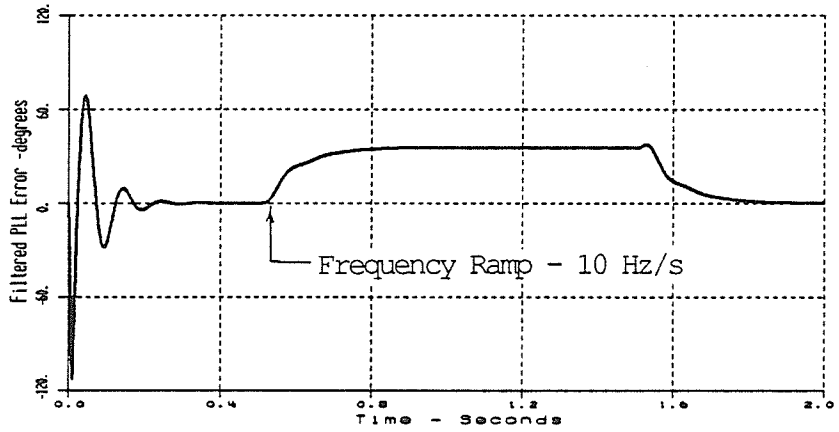

a) PLL Error - Degrees

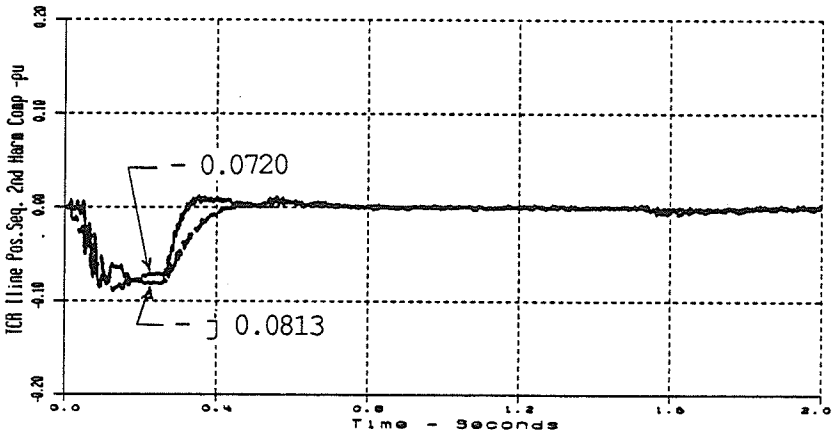

b) Real/Imaginary 2nd Harmonic Component - pu

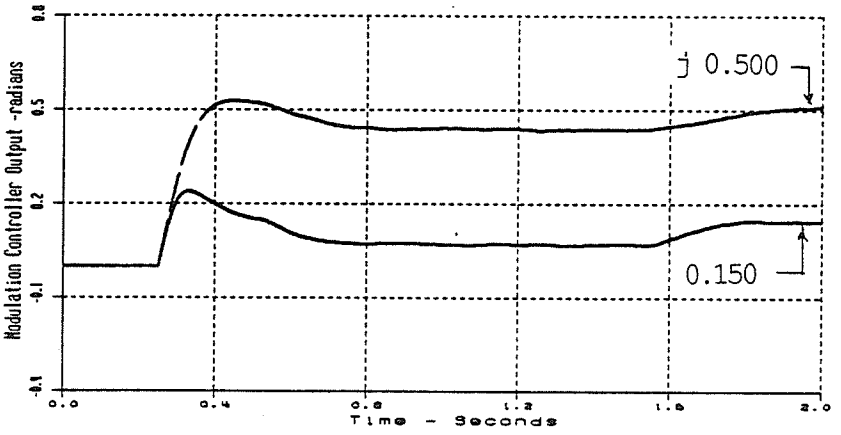

c) Real/Imaginary Modulation Output - radians

Figure 2.32 Modulation Control of Positive Sequence 2nd Harmonic Component of TCR Line Current, 10 Hz/s Ramp Increase in System Frequency, Alpha = 30°, Source: 2nd Harmonic Voltage 30% @ -30°

2.8 Numerical Fourier Analysis

A program called FOURIER was written to perform a numerical Fourier analysis on any periodic waveform stored in any one of the ten possible channels in the EMTDC simulation output file. The program requires that one of the output channels contains period markers. The PLL reference pulse, generated once per cycle, is used as the period marker.

The numercial Fourier analysis is based on the supposition that a function i(t) of period T has the expansion:

$$i(t) = \frac{ao}{2} + \sum_{n=1}^{\infty} (a_n \cos nwt + b_n \sin nwt), \qquad (2.34)$$

for $to < t < to + T$,

where $a_n = \frac{2}{T} \int_{to}^{(to+T)} i(t) \cos nwt \, dt \quad (n=0,1,2,...)$ (2.35)

$$b_n = \frac{2}{T} \int_{to}^{(to+T)} i(t) \sin nwt \, dt \quad (n=1,2,3,...) \qquad (2.36)$$

Letting $f(t) = i(t) \cos nwt$, (2.37)

then $an = \int_{to}^{to+T} f(t) \, dt \quad (n=o,1,2,...)$ (2.38)

The function f(t) is shown in Figure 2.33 for the interval (to<t<to+T). Since the integral of f(t) exists over the interval [to, to+T], the integration may be carried out over N equal subintervals, each of duration Δ t such that

$$\Delta t = \frac{T}{N} = t_{k+1} - t_k \qquad (2.39)$$

$$\text{Therefore} \quad a_n = \frac{2}{T} \left[\sum_{n=1}^{N} \int_{t_{n-1}}^{t_n} f(t)dt \right] \qquad (2.40)$$

Applying the trapezoidal rule of numerical integration

$$\int_{t_{n-1}}^{t_n} f(t)dt \simeq \frac{\Delta t}{2} \left[f(t_n) + f(t_{n-1}) \right] , \qquad (2.41)$$

and substituting into (2.40) yields

$$a_n \simeq \frac{1}{N} \left[\sum_{n=o}^{N} f(t_n) + f(t_{n-1}) \right]$$

$$= \frac{1}{N} \left[f(t_o) + f(t_N) + 2 \sum_{n=1}^{N-1} f(t_n) \right] \qquad (2.42)$$

Substituting for f(t) using 2.37:

$$a_n \approx \frac{1}{N} \left[i(t_o) \cos nwt_o + i(t_N) \cos Nwt_N + 2 \sum_{n=1}^{N-1} i(t_n) \cos nwt_n \right] \quad (n=0,\ 1,2,..) \qquad (2.43)$$

Similarly

$$b_n \approx \frac{1}{N} \left[i(t_o) \sin nwt_o + i(t_N) \sin Nwt_N + 2 \sum_{n=1}^{N-1} i(t_n) \sin nwt_n \right] \quad (n=\ \ 1,2,..) \qquad (2.44)$$

Where N is the number of samples of the waveform and w = 376.99 radians/second.

The program outputs the Fourier coefficients in terms of their magnitude and angle.

$$i(t) = C_n \cos (nwt + \phi\, n) \qquad (2.45)$$

where $C_n = \sqrt{a_n 2 + b_n 2}$, (2.46)

$$\phi\, n = \tan^{-1} \frac{(-b_n)}{(a_n)} . \qquad (2.47)$$

A symmetrical component analysis of the waveform is also calculated using the transformation.

$$\begin{bmatrix} Io \\ I1 \\ I2 \end{bmatrix} = \frac{1}{3} \begin{bmatrix} 1 & 1 & 1 \\ 1 & a & a^2 \\ 1 & a^2 & a \end{bmatrix} \begin{bmatrix} Ia \\ Ib \\ Ic \end{bmatrix} \qquad (2.48)$$

where $a = -0.5 + j0.866 = 1.0 \angle 120°$ (2.49)

$a^2 = -0.5 - j0.866 = 1.0 \angle 240°$ (2.50)

The Fortran code for the program is included as Appendix B6.

A sample interval of 50 us (the simulation time step) was rised throughout this study to compute the Fourier coefficients of the voltage and current waveforms.

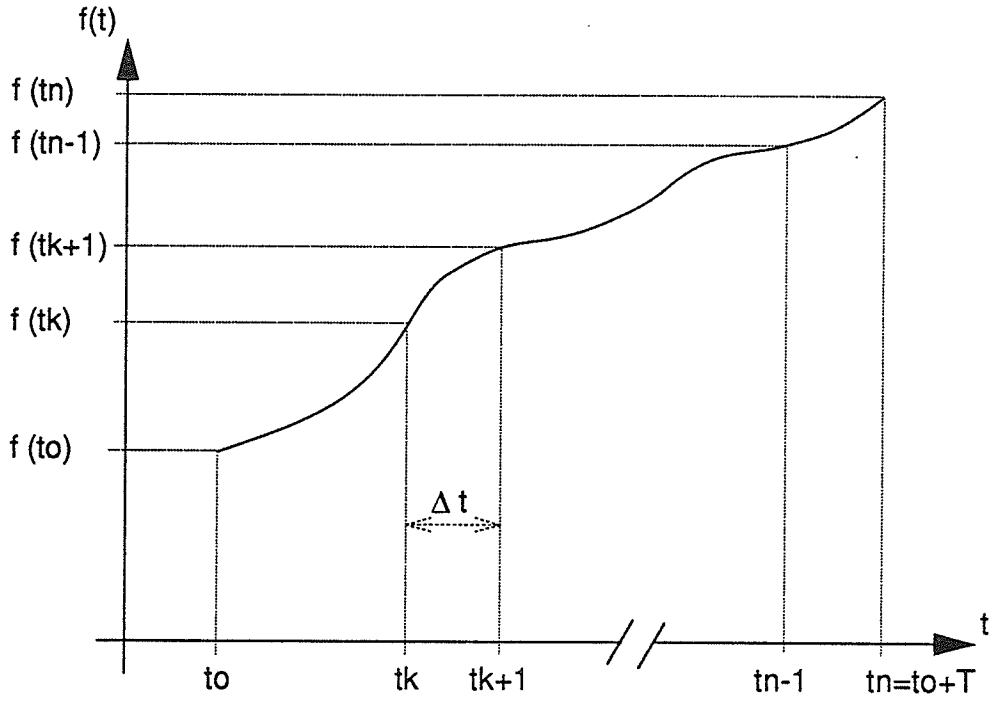

T = Period of f(t)

n = number of samples of f (t)

Δ t = duration between samples

Figure 2.33 Periodic Function f (t)

CHAPTER THREE

SIMPLE SVC MODEL CONNECTED TO THE HIGH VOLTAGE SYSTEM

3.1 Study Network

The performance of the TCR with firing angle modulation is evaluated with a FC + TCR type SVC modelled directly on the high voltage bus as shown in Figure 2.3. The SVC step up transformer was not modelled. This case was identical to the simple model that was used [3] to demonstrate the concept of using firing angle modulation of the TCR firing angle to control a given harmonic component of the positive sequence TCR line current.

The SVC nominally rated 120 kV, 180 Mvar production to 120 Mvar absorption, consisted of a 180 Mvar fixed capacitor and a 300 Mvar thyristor-controlled reactor. The fixed capacitor and the reactor were connected in a delta configuration as shown in the detailed simulation circuit of Figure 3.1. The fixed capacitor, although often tuned to filter the 5th and 7th harmonic, was modelled as a simple capacitor in this study.

The equivalent system at the point of connection of the SVC was assumed to be resonant at the second harmonic, resulting

in the presence of a large second harmonic voltage. This condition was modelled by superimposing a balanced 120 Hz three phase set of voltage waveforms on the Thevenin fundamental frequency voltage source. The second harmonic source was adjusted to produce a second harmonic voltage magnitude of 30% with a phase displacement of -30° relative to the fundamental at the point of SVC coupling.

The fundamental frequency Thevenin voltage source magnitude was adjusted to maintain 1.0 pu system voltage on the SVC bus. The performance of the TCR with firing angle modulation was evaluated at firing angles of 0°, 20°, 30° and 45°. The SVC configuration and steady state system conditions are shown in Figure 3.2 for each firing angle.

The results are presented as a base case for comparison to results obtained in the following chapters with various system representations. The results and conclusions are compared for consistency with previously published work [3,4].

3.2 Per Unit System

The TCR reactor rating was used to define the per unit (pu) base parameters listed in Table 3.1.

Table 3.1 Per Unit System

Base Parameter	Value
MVA	300 MVA
Line Voltage	169.7 kV
Phase Voltage	97.98 kV
Line Current	2041.2 A
Phase Current	1178.5 A

The voltage and current per unit bases are expressed as peak values. The magnitudes of the harmonic phasor components of the measured currents and the computed Fourier components are also expressed as peak values.

With the per unit system chosen, the TCR line current was 1.0 pu at alpha = 0° assuming a TCR line voltage of 1.0 pu.

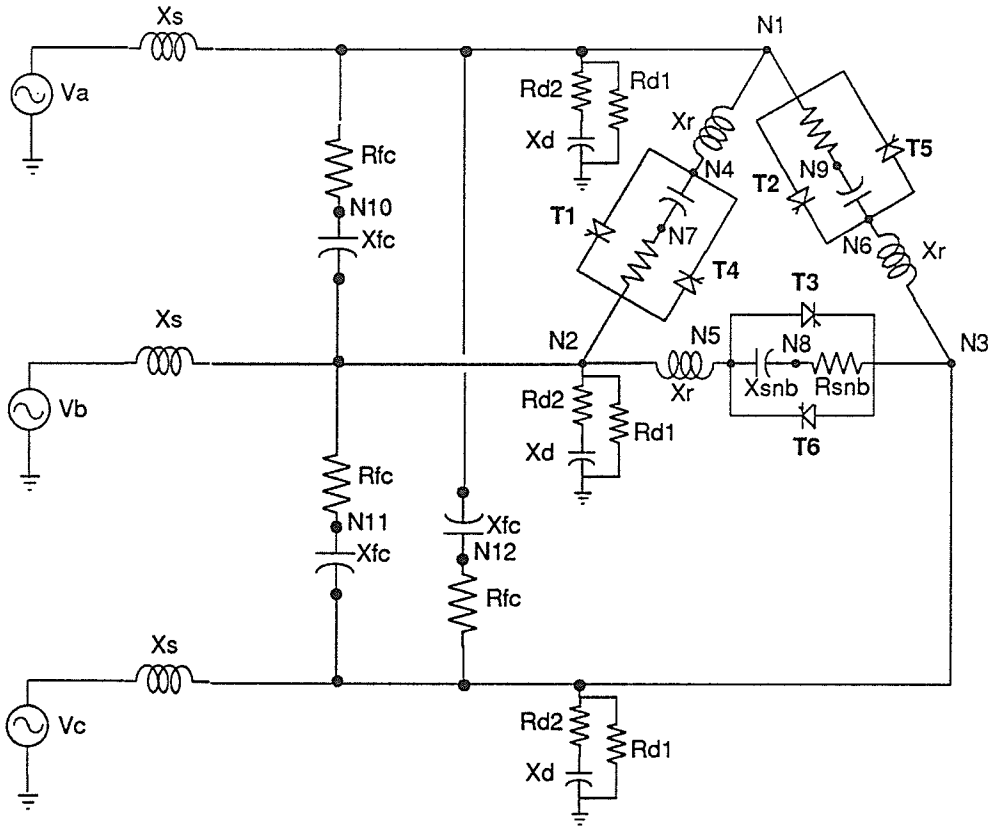

Xs - Thevenin Impedance of the AC System
Xr - Reactance of the TCR Reactor
Xfc - Capacitive Reactance of the SVC Fixed Capacitor
Xsnb - Snubber Circuit Capacitive Reactance
Xd - Numerical Damping Circuit Capacitive Reactance
Rd1,Rd2 - Numerical Damping Circuit Resistance
Rsnb - Snubber Circuit Resistance
Rfc - Fixed Capacitor Internal Resistance
Va ,Vb,Vc - Thevenin Voltage behind Reactance

Figure 3.1 Three Phase Equivalent Circuit of a SVC Modelled on the High Voltage Bus

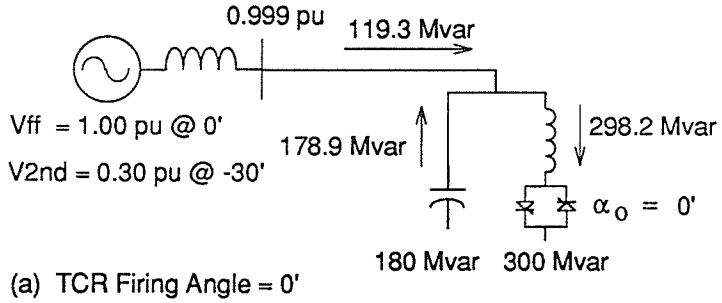

(a) TCR Firing Angle = 0'

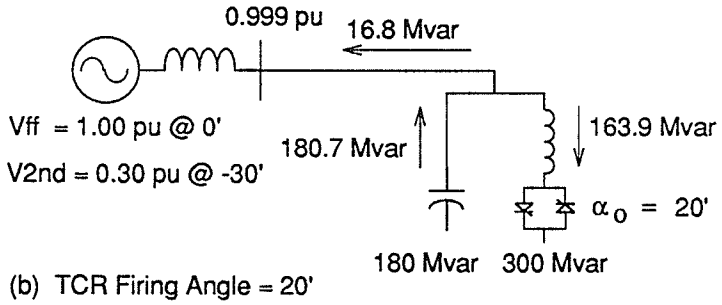

(b) TCR Firing Angle = 20'

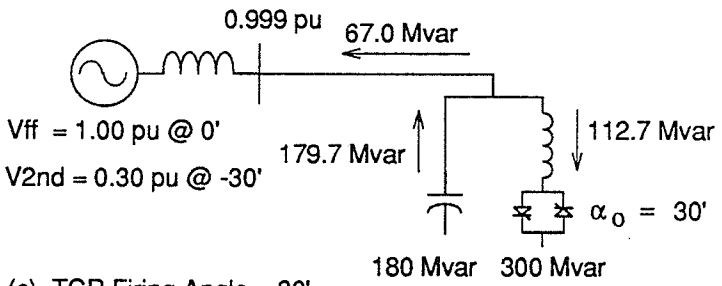

(c) TCR Firing Angle = 30'

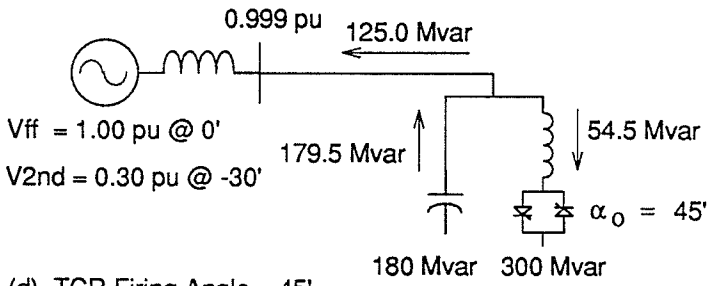

(d) TCR Firing Angle = 45'

Figure 3.2 Study System Steady State Conditions

3.3 TCR Performance With Equidistant Firing

The steady state positive sequence harmonic phasor components of some SVC variables are listed in Table 3.2 for TCR firing angles of 0°, 20°, 30° and 45°. Tnese components are computed by performing a numerical Fourier analysis on the voltage and current waveforms.

The magnitude of the dc component is observed to remain relatively constant over the firing angle range, varying from 0.041 pu to 0.070 pu. The second harmonic component variation was somewhat greater varying from 0.082 pu to 0.148 pu over the firing angle range. The TCR fundamental frequency var absorption was not significantly effected by the harmonic voltage distortion as it was within 5% of the ideal output at 1.0 pu voltage. The ideal output is the calculated output at a given firing angle based on the effective reactance of the TCR assuming perfectly sinusoidal 60 Hz commutating voltage waveforms.

Figure 3.3 shows the steady state TCR waveforms for the case where the firing angle $\alpha o = 30°$ and the voltage waveforms are distorted by a second harmonic component of 30% at -30° relative to the fundamental. The TCR line voltage waveform zero crossings are not equidistant as can be observed by comparison to the PLL reference voltage waveforms (VREF1,

VREF2, VREF3). The line voltages reach a peak magnitude of about 1.3 pu (V_{AB} and V_{CA}) due to the second harmonic distortion. The thyristor firing pulses, measured from the peak of the PLL reference voltage waveforms, are equidistant. The TCR phase currents are not symmetrical with respect to the zero current axis. A dc component is apparent in the TCR line current waveforms shown in Figure 3.4.

The measured real and imaginary parts of the dc, 60 Hz and second harmonic components of the positive sequence TCR line current are shown from system startup in Figure 3.5. The system voltage was ramped up in the first 0.10s and an additional 0.05s were required for the PLL to settle out and allow the measurement system to initialize. The voltage and current phasor magnitude and phase, for the case where alpha = 30°, agree closely with the Fourier coefficients shown in Table 3.2.

Table 3.2 Positive Sequence SVC Variables
with Equidistant Firing of the TCR
Source 2nd Harmonic Voltage 30% @ -30°

Firing Angle	Alpha = 0°	Alpha = 20°	Alpha = 30°	Alpha = 45°
Variable	pu /-°	pu /-°	pu /-°	pu /-°
TCR Line Current				
DC Comp.	0.070/-93°	0.070/-123°	0.059/-134°	0.041/-149°
60 Hz Comp.	0.995/-119°	0.547/-120°	0.376/-121°	0.182/-123°
120 Hz Comp.	0.148/-150°	0.139/-140°	0.120/-132°	0.082/-117°
SVC Line Current				
DC Comp.	0.070/-93°	0.069/-123°	0.059/-134°	0.041/-149°
60 Hz Comp.	0.398/-115°	0.056/ 38°	0.223/ 56°	0.417/ 58°
120 Hz Comp.	0.212/ 24°	0.227/ 18°	0.252/ 16°	0.298/ 17°
TCR Line Voltage				
DC Comp.	0.0005/75°	0.0005/75°	0.0005/75°	0.0005/75°
60 Hz Comp.	0.999/ 0°	0.999/ 0°	0.999/ 0°	0.999/ 0°
120 Hz Comp.	0.300/-31°	0.300/-31°	0.300/-31°	0.300/-31°
TCR 60 Hz Absorption	Mvar (%)	Mvar (%)	Mvar (%)	Mvar (%)
Actual (% Ideal)	298.2 (99.4)	163.9 (95.3)	112.7 (96.1)	54.5 (100.0)

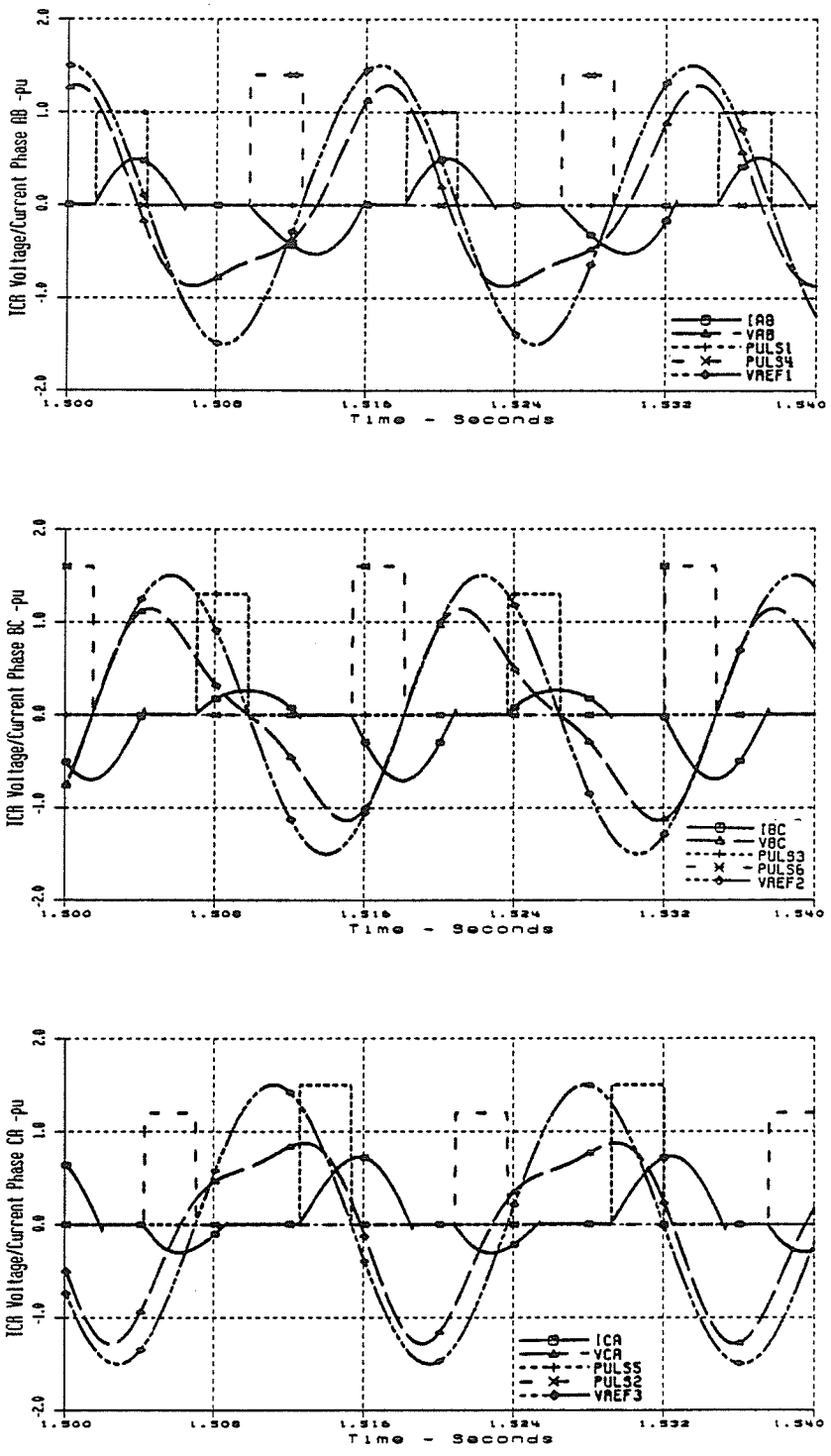

Figure 3.3 TCR Waveforms with Equidistant Firing at Alpha = 30°, Source: 2nd Harmonic Voltage of 30% @ -30°

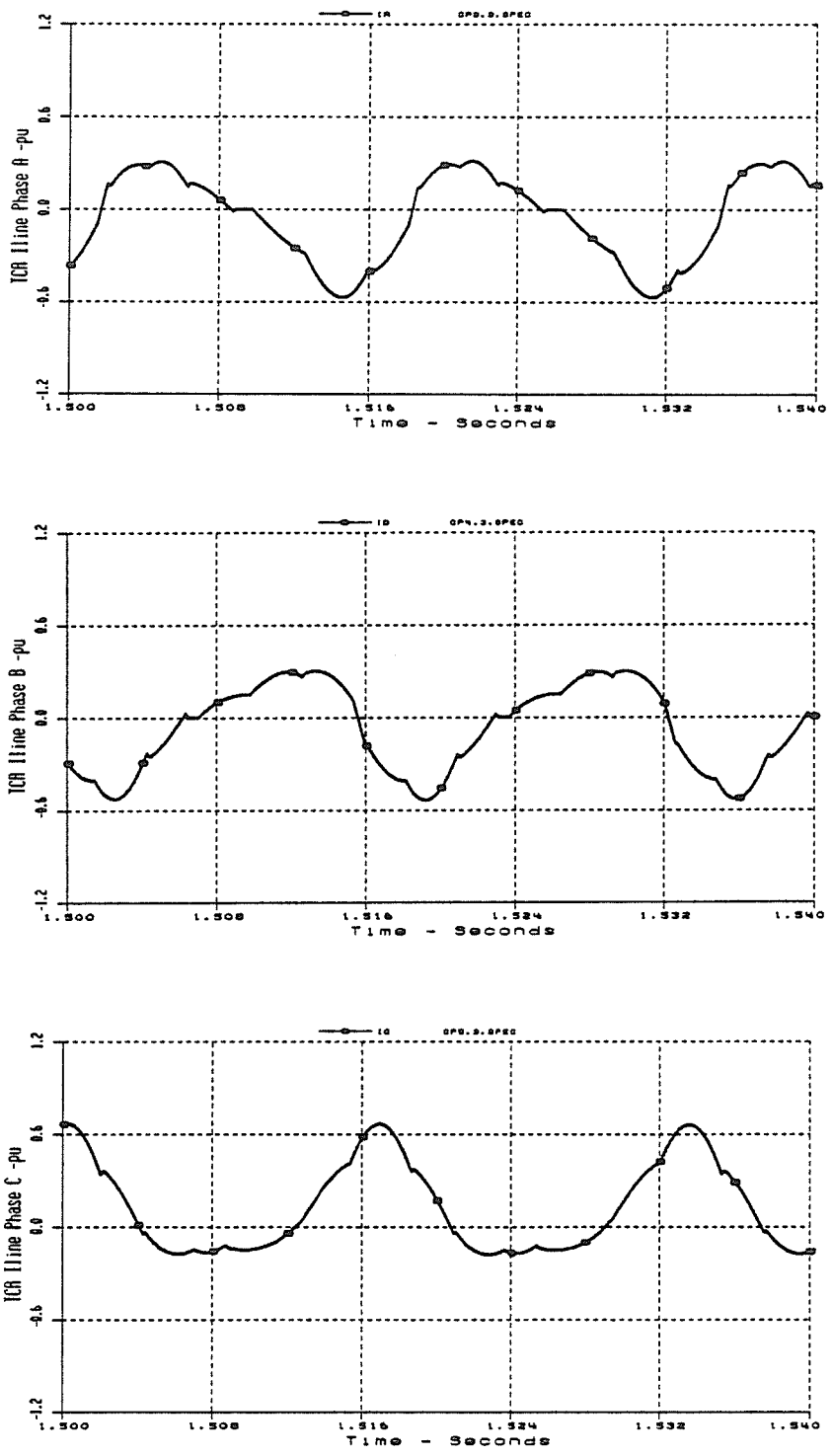

Figure 3.4 TCR Line Current Waveforms with Equidistant Firing at Alpha = 30°, Source: 2nd Harmonic Voltage of 30% @ -30°

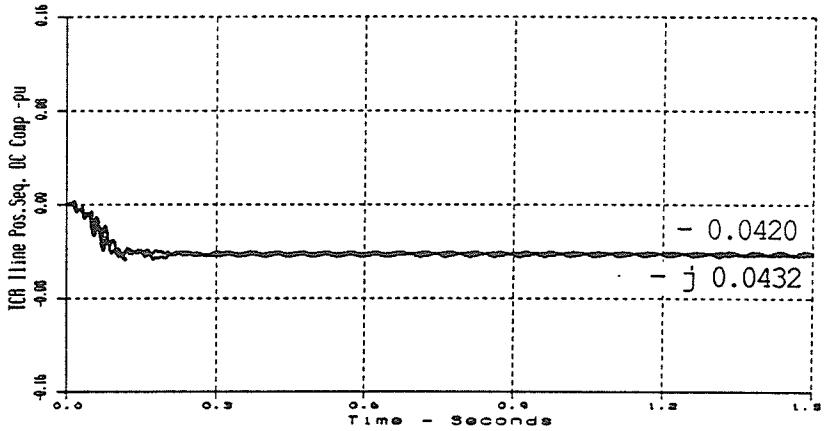

a) Real/Imaginary DC Components - pu

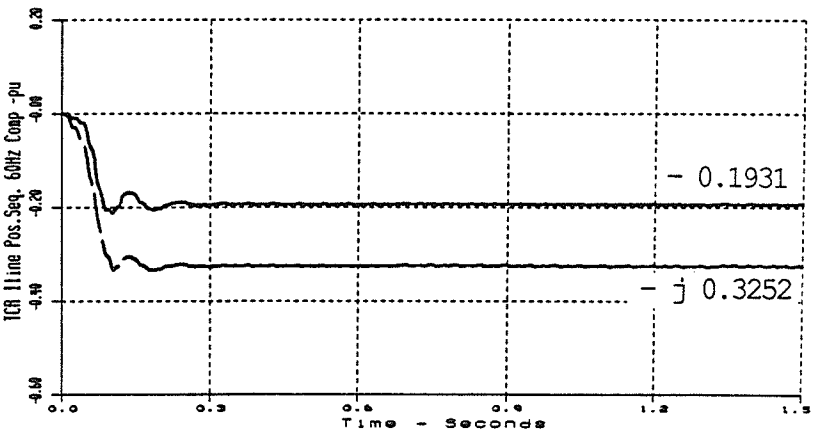

b) Real/Imaginary 60 Hz Components - pu

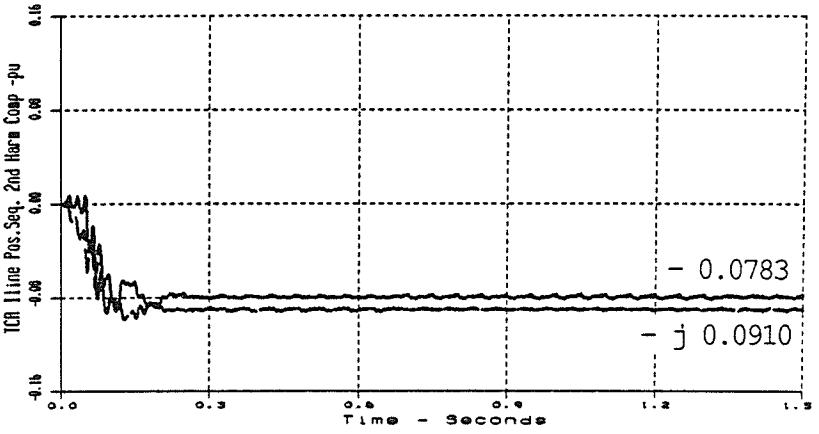

c) Real/Imaginary 2nd Harmonic Components - pu

Figure 3.5 Positive Sequence Phasor Components of TCR Line Current with Alpha = 30°, Source: 2nd Harmonic Voltage of 30% @ -30°

3.4 TCR Performance Using Firing Angle Modulation to Control the Positive Sequence Second Harmonic Phasor Component of the TCR Line Current.

The measured real and imaginary positive sequence second harmonic phasor components of TCR line current were input into the modulation controller using the controller parameter settings listed in Table 3.3. The variables are defined in Figure 2.29.

Table 3.3 Modulation Controller Settings with the Second Harmonic Component of TCR Line Current as the Control Parameter

Parameter	Real Part	Imaginary Part
G (-)	1.00	1.00
T (s)	0.032	0.032
Kp (rad/pu)	-1.00	-1.00
KI (rad/pu-s)	-90.0	-90.0
Limits (rad)	± 1.5	± 1.5

These controller gains were to chosen to give a slightly under damped response to minimize the settling time.

The steady state phasor components of some SVC variables and modulation parameters are listed in Table 3.4 for TCR firing angles of 0°, 20°, 30° and 45°. Comparison of Table 3.4 to the "no modulation" cases in Table 3.2 illustrates that elimination of the second harmonic component from the TCR line current approximately doubled the dc component at all firing angles except $\alpha o = 45°$ where it was reduced by 12%.

Firing angle limits, encountered for the cases where alpha = 0° and 20°, restricted the sinusoidal modulation on one side. The second harmonic component was still eliminated, however, large modulation magnitudes were required. Furthermore, the modulation significantly reduced the fundamental frequency absorption of the TCR to 51% at alpha = 0° and 88% at alpha = 20°. The reactive power absorption of the TCR was not significantly reduced when firing angle limits were not encountered.

Figure 3.6 shows the measured second harmonic component of the TCR line current and the controller output for alpha = 30°. The second harmonic component was reduced to zero in about 325 ms after the modulation controller was turned on at t = 0.25s. The required modulation controller output of 0.150 + j0.521 radians corresponded to a modulation peak of 31.0° and a modulation phase of 74.0°.

Figure 3.7 shows the effect of the firing angle modulation on the dc and 60 Hz components of the TCR line current for the case where alpha = 30°. The dc component increased by 80% from 0.059 pu @ -134° to 0.106 pu @ 88°. The fundamental frequency component increased by 4% from 0.377 pu @ -120° to 0.392 pu @ -119°.

Figure 3.8 shows the steady state TCR waveforms for the case where alpha = 30°. The thyristor firing pulses are no longer equidistant due to the modulation. The actual firing angles, measured from the peak of the PLL reference voltage waveforms, correspond to the nominal firing angle plus or minus Δ_{xy}, the modulation angle in each phase.

The TCR phase currents are not symmetrical relative to the zero current axis. The TCR line current waveforms plotted in Figure 3.9 clearly show the existance of a dc component.

Table 3.4 Positive Sequence SVC Variables with Control of Positive Sequence 2nd Harmonic Component of TCR Line Current, Source 2nd Harmonic Voltage 30% @ -30°

Firing Angle	Alpha = 0°	Alpha = 20°	Alpha = 30°	Alpha = 45°
Variable	pu /-°	pu /-°	pu /-°	pu /-°
TCR Line Current				
DC Comp.	0.134/ 91°	0.129/ 87°	0.106/ 88°	0.036/ 89°
60 Hz Comp.	0.505/-119°	0.479/-119°	0.393/-119°	0.177/ -119°
120 Hz Comp. **	0.0004/ 21°	0.002/ 55°	0.001/ 29°	0.0005/-117°
SVC Line Current				
DC Comp.	0.134/ 91°	0.130/ 87°	0.106/ 88°	0.036/ 89°
60 Hz Comp.	0.099/ 44°	0.123/ 46°	0.207/ 52°	0.423/ 56°
120 Hz Comp.	0.360/ 26°	0.361/ 26°	0.361/ 26°	0.359/ 26°
TCR Line Voltage				
DC Comp.	0.0005/75°	0.0005/75°	0.0005/75°	0.0005/75°
60 Hz Comp.	0.999/ 0°	0.999/ 0°	0.999/ 0°	0.999/ 0°
120 Hz Comp.	0.300/-31°	0.300/-31°	0.300/-31°	0.300/-31°
TCR 60 Hz Absorption	Mvar (%)	Mvar (%)	Mvar (%)	Mvar (%)
Actual (% No Modulation Case)	151.5 (50.8)	143.6 (87.6)	117.8 (104.5)	53.1 (97.4)
Modulation				
Peak/Phase	77°/65.9°	44.1°/71.3°	31°/74°	22.9°/90.0°
Δ ab	31.4°	14.1°	8.6°	0.0°
Δ bc	-76.6°	-43.3°	-30.2°	-19.9°
Δ ca	45.2°	29.1°	21.5°	19.9°

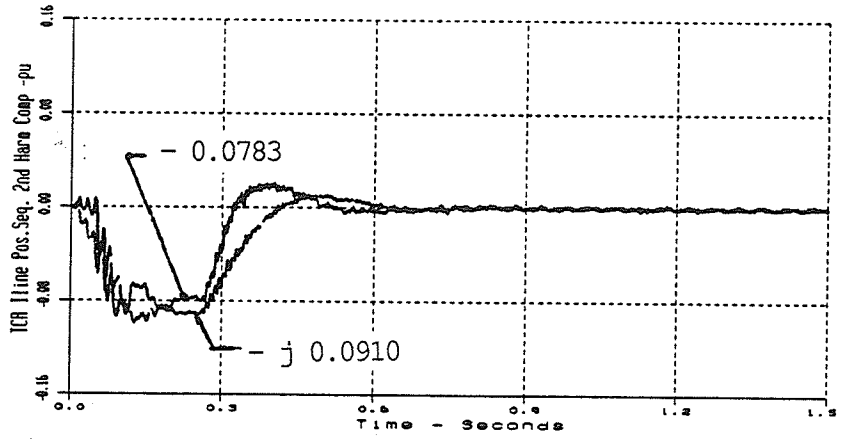

a) Real/Imaginary 2nd Harmonic Components - pu

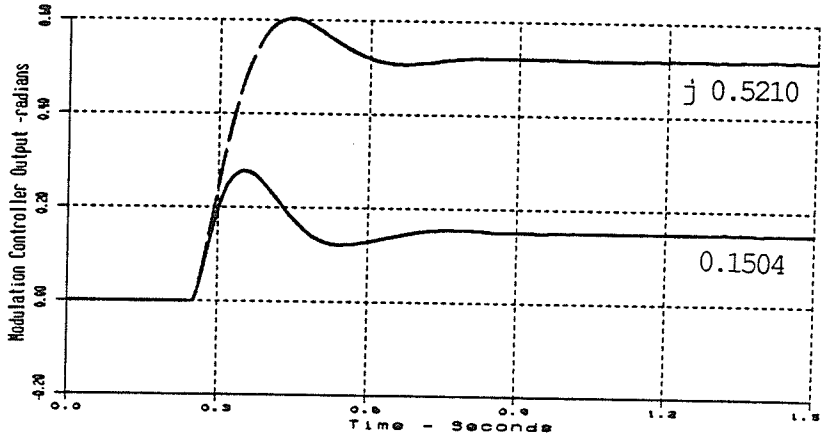

b) Real/Imaginary Modulation Controller Components - radians

Figure 3.6 Control of Positive Sequence 2nd Harmonic Component of TCR Line Current, Alpha = 30°, Source: 2nd Harmonic Voltage 30% @ -30°

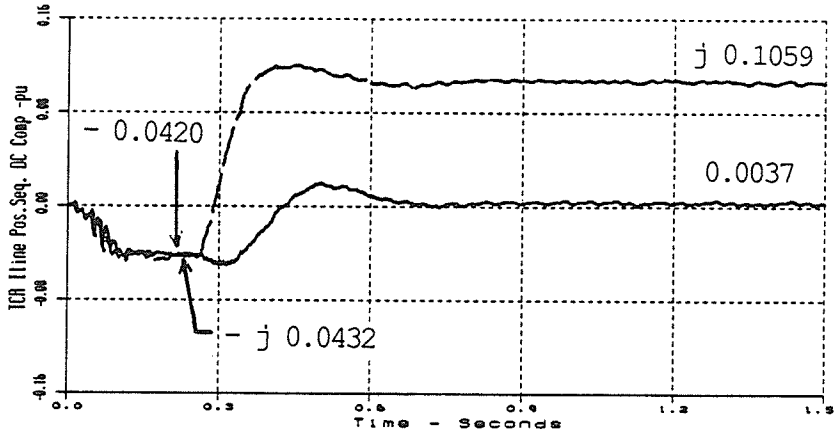

a) Real/Imaginary DC Components - pu

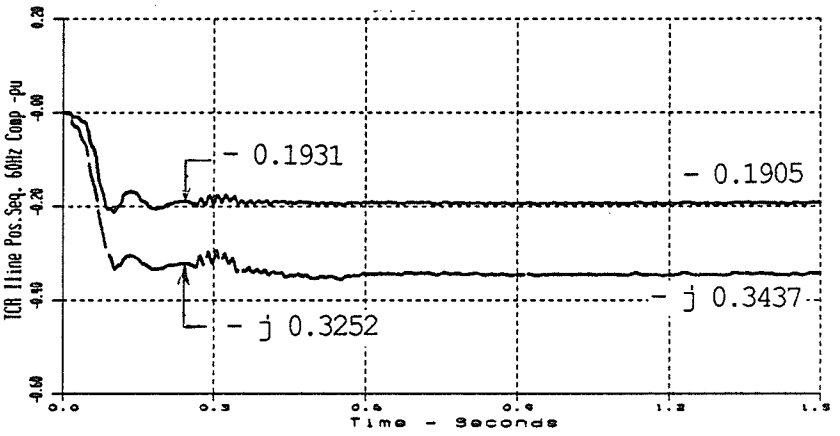

b) Real/Imaginary 60 Hz Components - pu

Figure 3.7 Effect of Control of the Positive Sequence 2nd Harmonic Component of TCR Line Current on the DC and 60 Hz Components, Alpha = 30°, Source: 2nd Harmonic Voltage 30% @ -30°

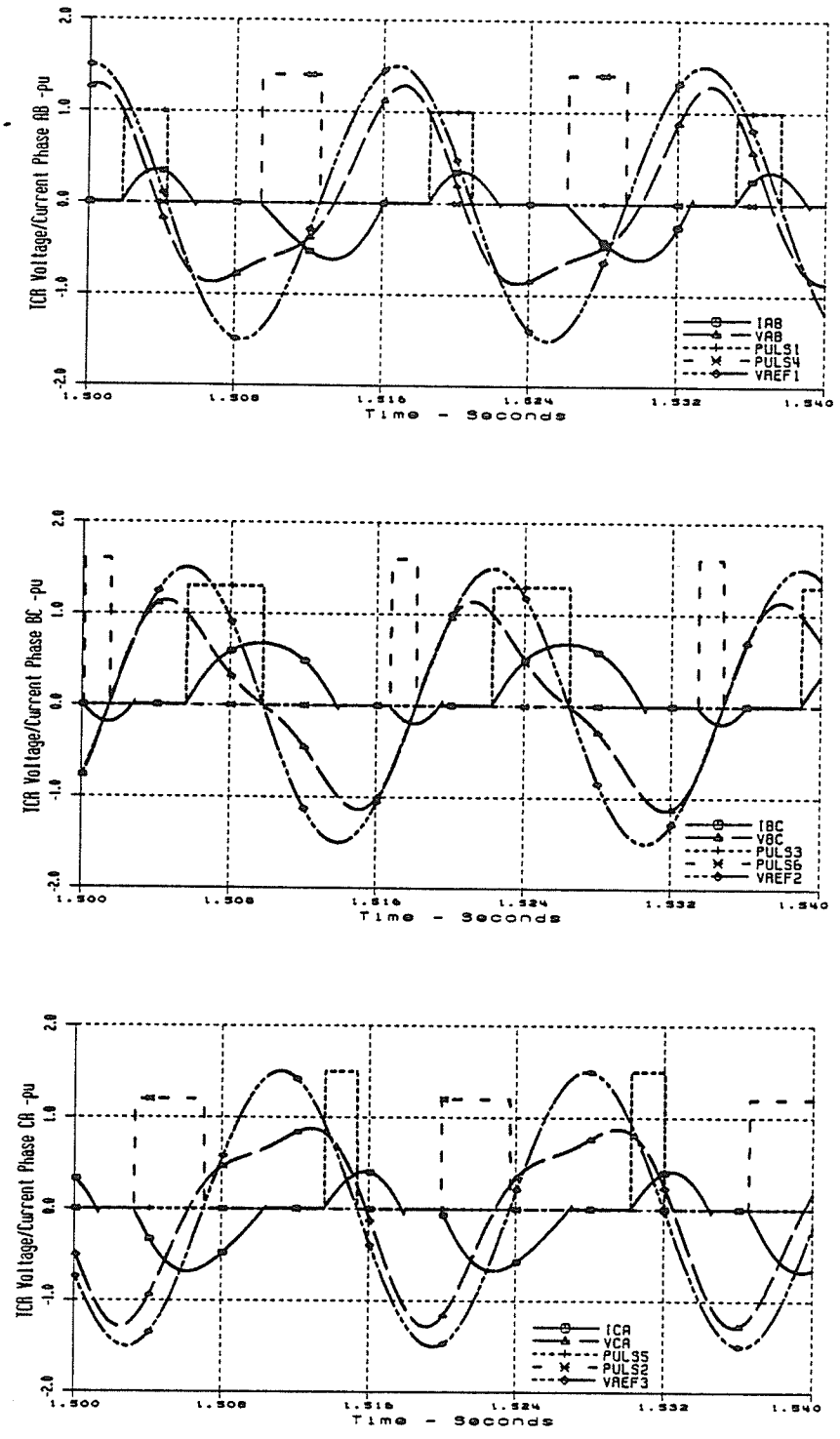

Figure 3.8 TCR Waveforms, Control of the Positive Sequence 2nd Harmonic Component of TCR Line Current, Alpha = 30°, Source: 2nd Harmonic Voltage 30% @ -30°

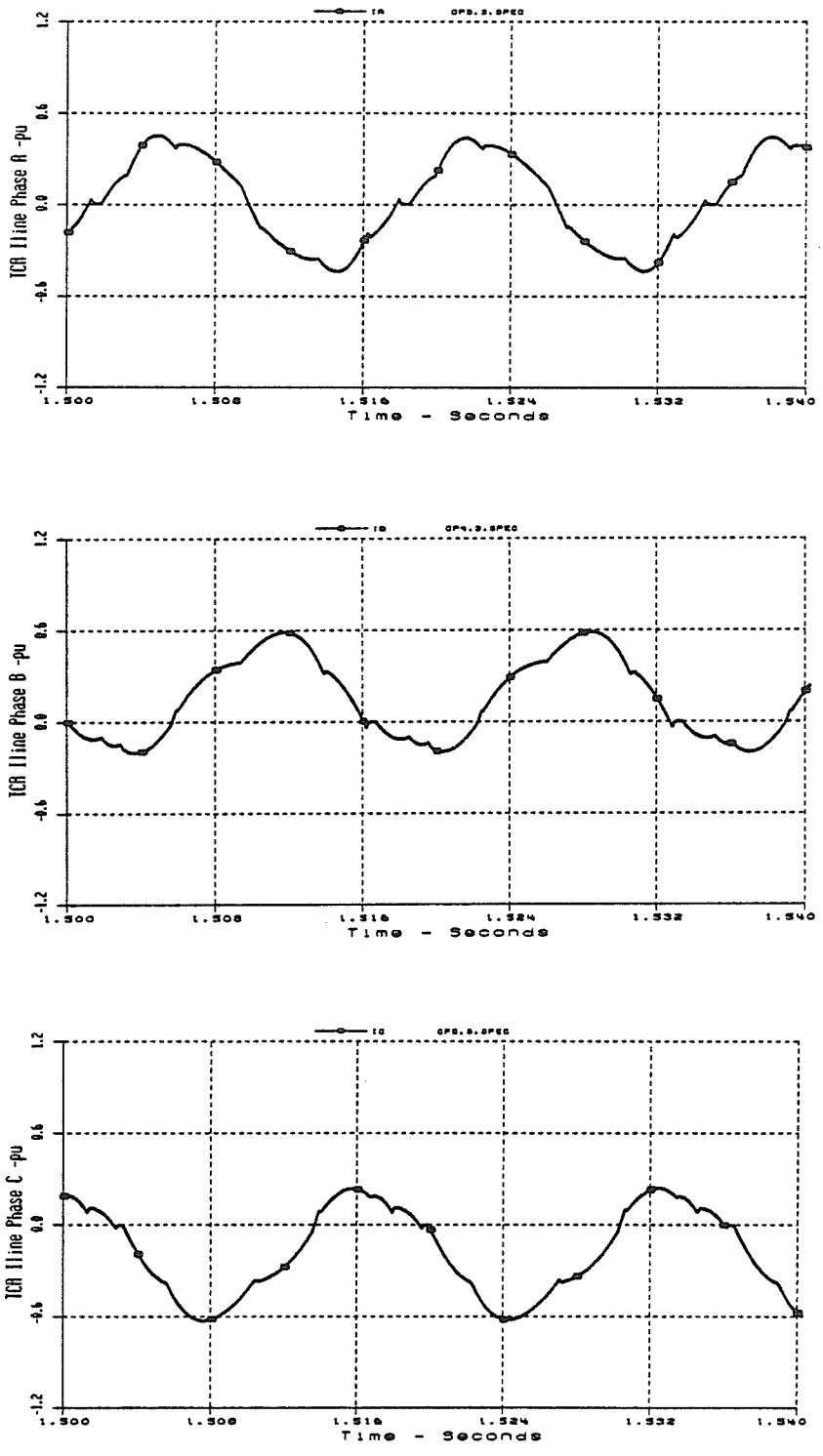

Figure 3.9 TCR Line Current Waveforms, Control of the Positive Sequence 2nd Harmonic Component of TCR Line Current, Alpha = 30°, Source: 2nd Harmonic Voltage 30% @ -30°

3.5 TCR Performance using Firing Angle Modulation to Control the Positive Sequence DC Component of the TCR Line Current

The measured real and imaginary dc phasor components of the positive sequence TCR line current were input into the modulation controller using the controller parameter settings listed in Table 3.5. The variables are defined in Figure 2.29.

Table 3.5 Modulation Controller Settings With the DC Component of TCR Line Current as the Control Parameter

Parameter	Real Part	Imaginary Part
G (-)	1.00	1.00
T (s)	0.032	0.032
Kp (rad/pu)	+1.00	-1.00
KI (rad/pu-s)	+60.00	-60.00
Limits (rad)	± 1.50	± 1.50

These controller gains were chosen to give a slightly under damped response to minimize settling time.

The steady state phasor components of some SVC variables and the modulation parameter are listed in Table 3.6 for TCR firing angles of 0°, 20°, 30° and 45°. Comparison of Table 3.6 to the "no modulation" cases in Table 3.2 illustrates that elimination of the dc component from the TCR line current also reduced the second harmonic component

The second harmonic component was reduced by 11% at 0°, 24% at 20°, 33% at 30° and 46% at 45°.

Firing angle limits, encountered at alpha = 0°, restricted the sinusoidal modulation on one side. The dc component was still satisfactorily eliminated although a larger modulation magnitude was required to cancel the dc component magnitude of 0.07 pu as compared to the case where alpha = 20°. Furthermore, the modulation reduced the reactive absorption of the TCR by 16% relative to the "no modulation" case. The reactive absorption capability was only minimally reduced when firing angle limits were not encountered.

Figure 3.10 shows the measured dc component of the TCR line current and the controller output for alpha = 30°. The dc component was reduced to zero in about 325 ms after the controller was turned on at t = 0.25s. The modulation controller output of -0.0513 + j0.2070 radians corresponded to a modulation peak of 12.2° and a modulation phase of 103.9°.

Figure 3.11 shows the effect of the firing angle modulation on the 60 Hz and 120 Hz components of the TCR line current. The fundamental component was only reduced by 2% from 0.376 pu @ -121° to 0.368 pu @ -119°. The second harmonic

component was reduced by 34% from 0.120 pu @ -132° to 0.079 pu @ -150°.

Figure 3.12 shows the steady state TCR waveforms for the case where alpha = 30°.

The TCR phase currents shown in Figure 3.12, and the TCR line currents shown in Figure 3.13, appear to be symmetrical relative to the zero current axis.

Table 3.6 Positive Sequence SVC Variables with Control of the Positive Sequence DC Component of TCR Line Current, Source 2nd Harmonic Voltage 30% @ -30°

Firing Angle	Alpha = 0°	Alpha = 20°	Alpha = 30°	Alpha = 45°
Variable	pu /-°	pu /-°	pu /-°	pu /-°
TCR Line Current				
DC Comp. **	0.001/-117°	0.002/78°	0.001/-107°	0.0007/ 64°
60 Hz Comp.	0.834/-119°	0.548/-119°	0.368/-119°	0.170/-119°
120 Hz Comp.	0.133/-150°	0.104/-150°	0.079/-150°	0.044/-149°
SVC Line Current				
DC Comp.	0.001/-127°	0.002/78°	0.001/-10°	0.0005/-63°
60 Hz Comp.	0.227/-112°	0.058/31°	0.232/ 54°	0.430/ 57°
120 Hz Comp.	0.227/ 24°	0.256/25°	0.281/ 25°	0.315/ 26°
TCR Line Voltage				
DC Comp.	0.0005/75°	0.0005/75°	0.0005/75°	0.0005/75°
60 Hz Comp.	0.999/ 0°	0.999/ 0°	0.999/ 0°	0.999/ 0°
120 Hz Comp.	0.300/-31°	0.300/-31°	0.300/-31°	0.300/-31°
TCR 60 Hz Absorption	Mvar (%)	Mvar (%)	Mvar (%)	Mvar (%)
Actual (% No Modulation Case)	249.9 (83.8)	164.2 (100.2)	110.3 (97.9)	50.9 (93.4)
Modulation				
Peak/Phase	18.6°/70.6°	11.0°/92.5°	12.2°/103.9°	13.9°/118.5°
Δ ab	6.2°	-0.5°	-2.9°	-6.6°
Δ bc	-18.3°	-9.2°	-8.8°	-7.3°
Δ ca	12.1°	9.7°	11.7°	13.9°

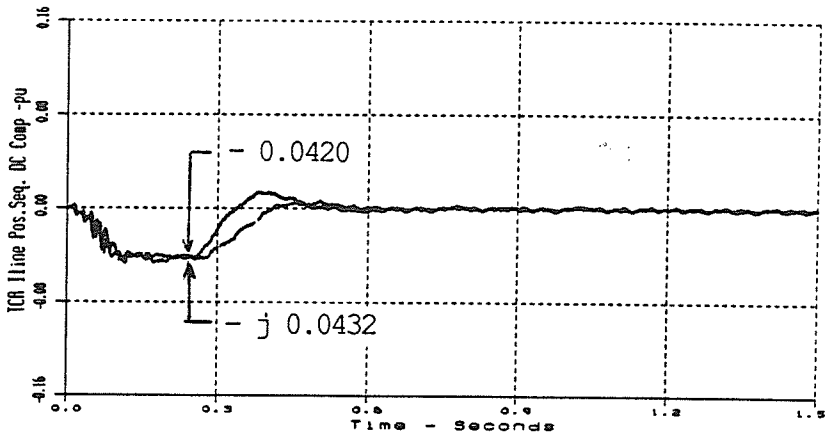

a) Real/Imaginary DC Components - pu

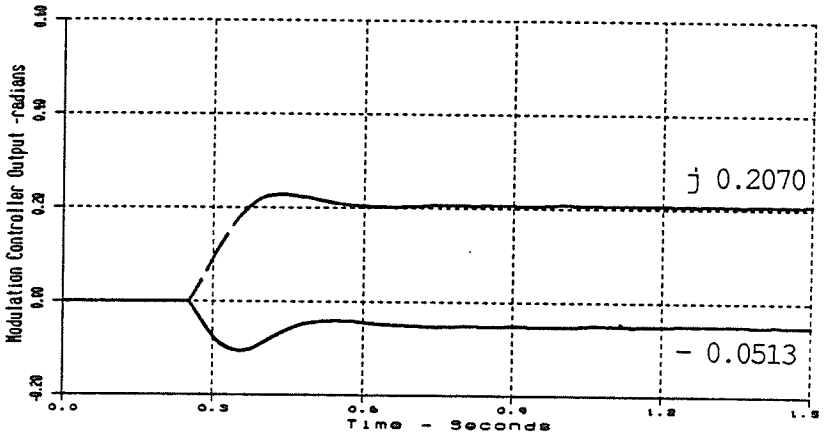

b) Real/Imaginary Modulation Controller Components - radians

Figure 3.10 Control of Positive Sequence DC Component of TCR Line Current, Alpha = 30°, Source: 2nd Harmonic Voltage 30% @ - 30°

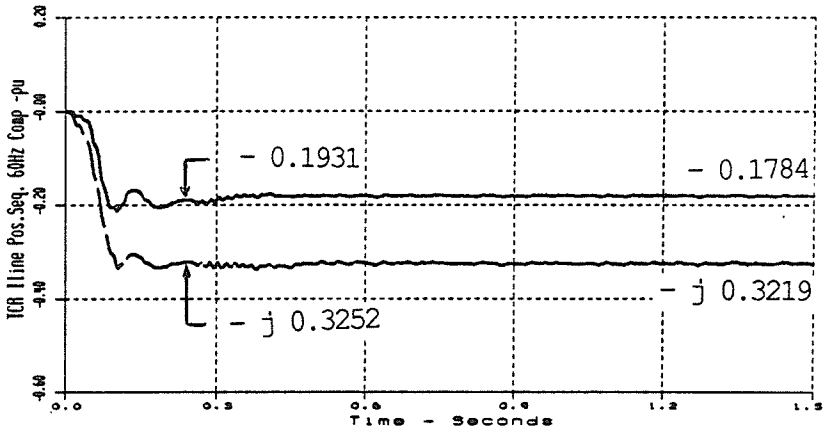

a) Real/Imaginary 60 Hz Components - pu

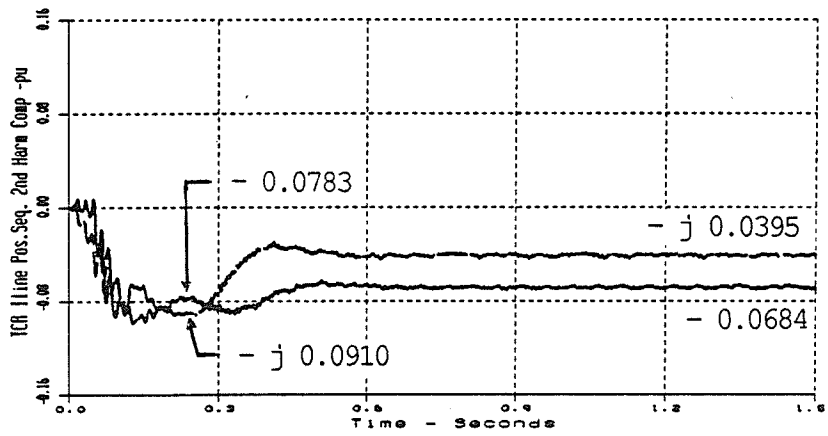

b) Real/Imaginary 2nd Harmonic Components - pu

Figure 3.11 Effect of Control of Positive Sequence DC Component of TCR Line Current on 60 Hz and 120 Hz Components, Alpha = 30°, Source 2nd Harmonic Voltage 30% @ -30

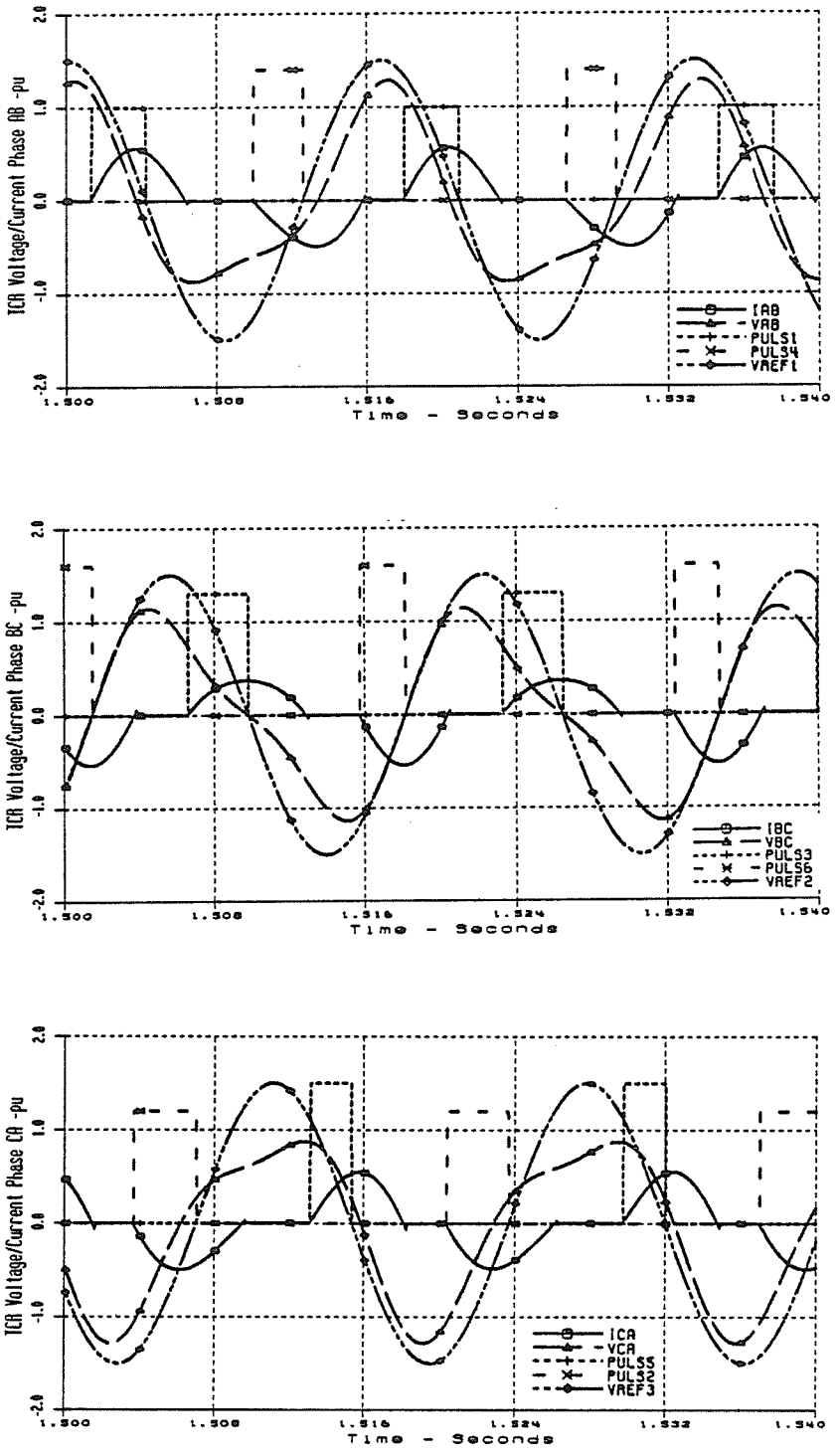

Figure 3.12 TCR Waveforms, Control of the Positive Sequence DC Component of TCR Line Current, Alpha = 30°, Source: 2nd Harmonic Voltage 30% @ -30°

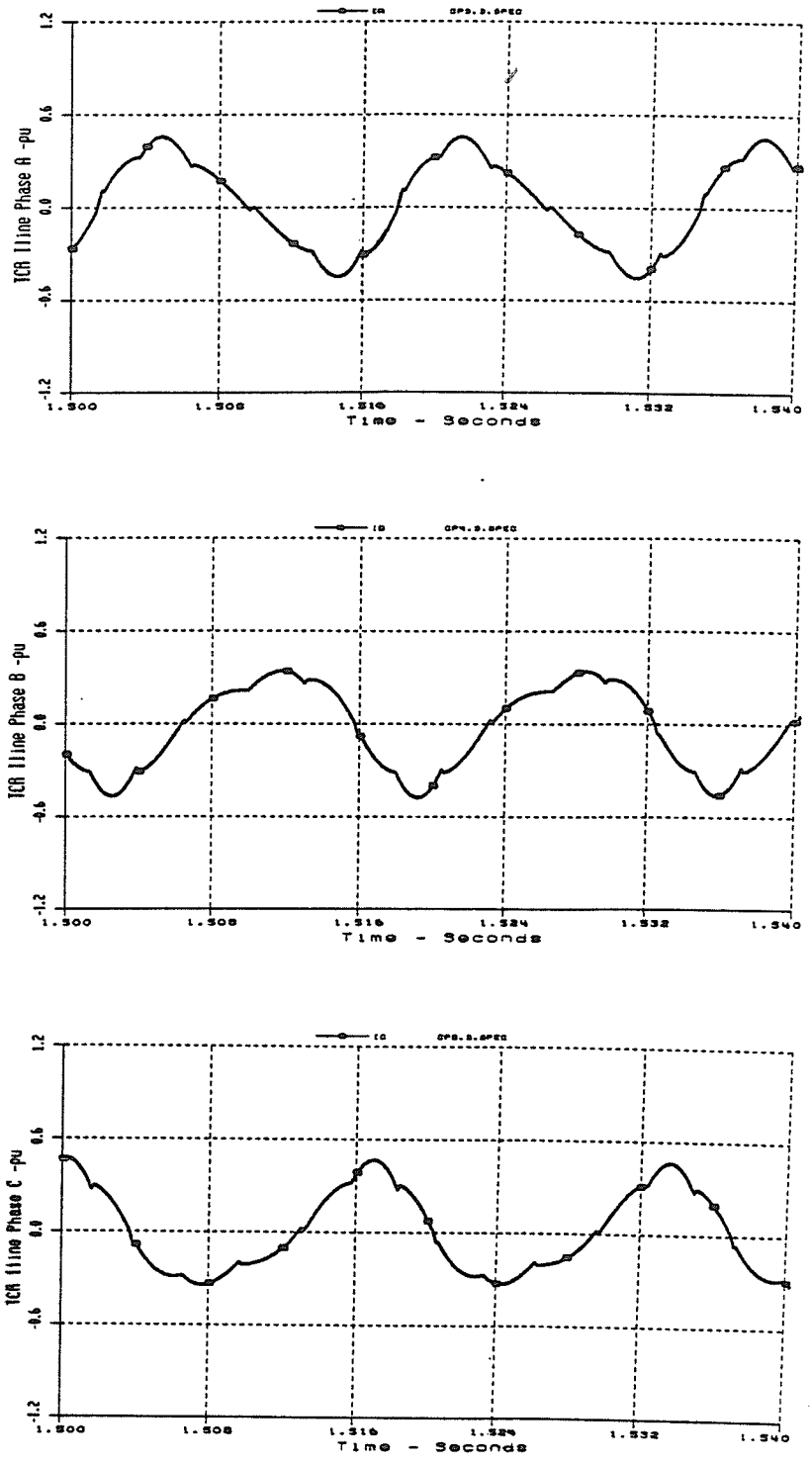

Figure 3.13 TCR Line Current Waveforms, Control of the Positive Sequence DC Component of TCR Line Current, Alpha = 30°, Source: 2nd Harmonic Voltage 30% @ -30°

3.6 Summary and Conclusions

Distortion of the TCR voltage waveforms due to a large second harmonic component caused a large non-characteristic dc component (4-7% of fundamental) and a large non-characteric second harmonic component (8-15% of fundamental) to appear in the positive sequence of the TCR line current when the TCR was fired equidistantly. These currents can aggravate an existing system resonant condition.

Sinusoidal modulation of the TCR firing angle was successfully applied to eliminate the dc or second harmonic component from the positive sequence of the TCR line current, even in cases where firing angle limits were encountered. A larger modulation signal was required when firing angle limitations made the modulation "one sided". It was demonstrated the the TCR firing could be controlled to prevent injection of an undesired harmonic current into the system.

Elimination of the second harmonic component from the positive sequence of the TCR line current caused the dc component to approximately double in magnitude.

Elimination of the dc component from the positive sequence of the TCR line current also reduced the second harmonic

component. The amount of reduction increased from 11% to 46% with increasing firing angle.

Elimination of both the dc and second harmonic components simultaneously was not possible since the dc component phasor has the opposite phase rotation relative to the second harmonic component phasor. Consequently the gain of either the real or imaginary portion of the controller must be of opposite sign for the dc component relative to the second harmonic component.

Firing angle modulation reduced the fundamental frequency TCR output by 3-7% when firing angle limits were not encountered. The reduction was much more severe when firing angle limits were encountered. The reduction was more severe for second harmonic modulation (49% at alpha = 0°) as compared to dc modulation (17% at alpha = 20°). This was only due to the fact that a smaller modulation signal was required to eliminate the dc component for the conditions analyzed. This reduction in reactive power absorption capability would be in conflict with the normal fundamental frequency reactive power controls that establish the nominal firing angle. A strategy would have to be devised to avoid operating conditions such that firing angle limits would severely restrict the sinuoidal modulation.

The modulation controller gains were selected to provide the fastest response to step changes without encountering excessive overshoot. The error to a step input was eliminated by the controller in about 325 ms.

The results were consistent with previous work [3] which concluded that a simple representation of the TCR on the high voltage bus was adequate to simulate actual TCR wave-form forms measured during a second harmonic resonance condition at the Hydro-Quebec installation at Chateauguay.

CHAPTER FOUR

SVC WITH STEP-UP TRANSFORMER

4.1 Study Network

The performance of the TCR with firing angle modulation is evaluated with a FC + TCR type SVC with a step-up transformer modelled as shown in the single line diagram of Figure 2.4. The three phase EMTDC simulation circuit is shown in Figure 4.1.

A wye-delta connected transformer, rated 332.4 MVA, 120 kV wye/12.46 kV delta, with a leakage reactance of 12% was modelled. The rated magnetizing current was assumed to be 2% of the rated full load current of the transformer. Transformer saturation was modelled as a current injection into the low voltage winding. An air core reactance of 40% and a knee point flux of 1.15 pu were used to represent the transformer saturation characteristic.

The SVC (FC + TCR type), nominally rated 180 Mvar production to 120 Mvar absorption, was the same as in Chapter 3 except that it was rated 12.4 kV and connected to the 120 kV system through a 120 kV/12.46 kV step-up transformer.

The equivalent system at the point of connection of the SVC was the same as that used in Chapter 3.

The performance of the TCR with firing angle modulation was evaluated at firing angles of 0°, 20°, 30° and 45°. The SVC configuration and steady state system conditions are shown in Figure 4.2 for each firing angle. A system voltage of 1.0 pu was maintained at the point of SVC connection for each of the TCR firing angles examined.

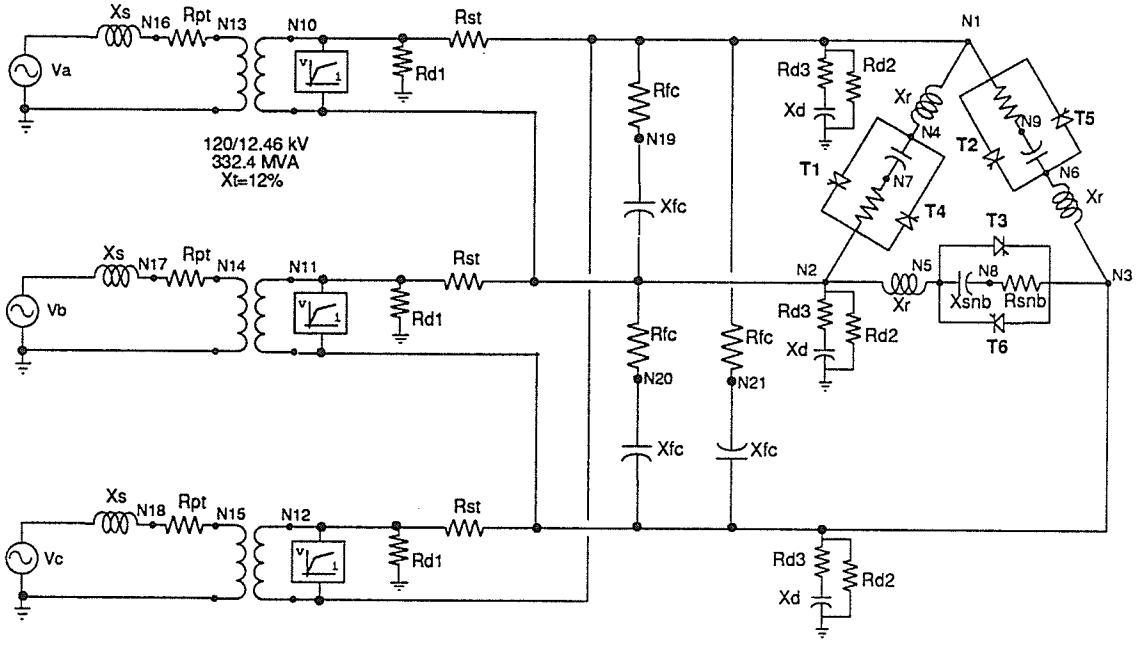

Xs - Thevenin Impedance of the AC System
Xr - Reactance of the TCR Reactor
Xt - SVC Transformer Leakage Reactance
Xfc - Capacitive Reactance of the SVC Fixed Capacitor
Xsnb - Snubber Circuit Capacitive Reactance
Xd - Numerical Damping Circuit Capacitive Reactance
Rpt,Rst - SVC Transformer Primary & Secondary Winding Resistances
Rd1,Rd2,Rd3 - Numerical Damping Circuit Resistance
Rsnb - Snubber Circuit Resistance
Rfc - Fixed Capacitor Internal Resistance
Va ,Vb,Vc - Thevenin Voltage behind Reactance

Figure 4.1 Study Network Three Phase EMTDC Simulation Circuit

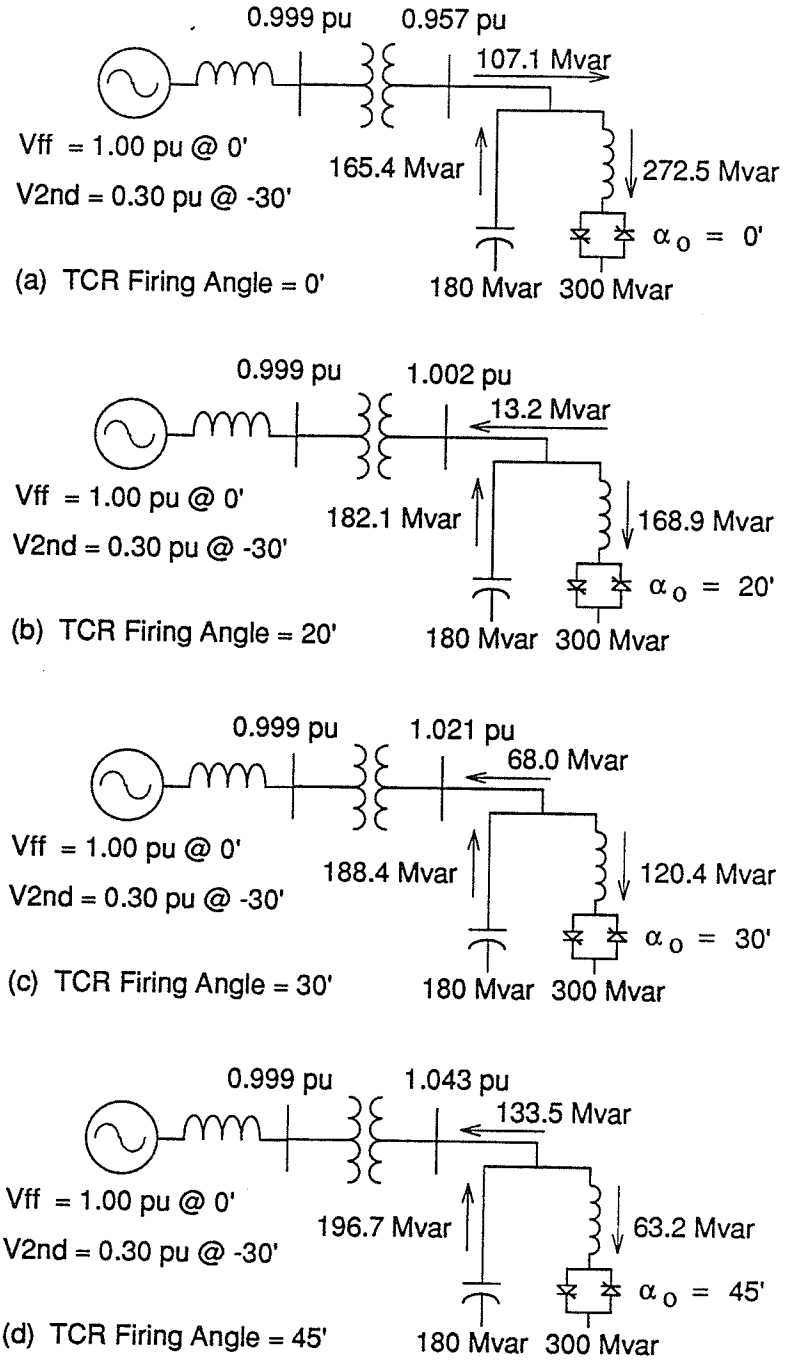

Figure 4.2 Study System Steady State Conditions

4.2 Per Unit System

The TCR reactor rating was used to define the per unit base quantities listed in Table 4.1.

Table 4.1 Per Unit System

Base Parameter	Value
MVA	300.0 MVA
Primary Voltage (LL)	169.7 kV
Primary Voltage (LG)	97.98 kV
Secondary Voltage (LL)	17.62 kV
Primary Line Current	2 041.2 A
Secondary Line Current	19 658.8 A
Secondary Phase Current	11 350.0 A
Transformer Magnetizing Current	251.5 A
Transformer Flux	46.7 V-s

The phasor magnitudes of the measured currents and the magnitudes of the Fourier components are expressed as peak values. The transformer magnetizing current base equals 2% of the rated transformer secondary winding current of 12 575.9 A peak.

4.3 TCR Performance with Equidistant Firing

The steady state positive sequence harmonic phasor components of several SVC variables are tabulated in Tables 4.2 and 4.3 for TCR firing angles of 0°, 20°, 30° and 45° in the presence of a second harmonic voltage of 30% @

-30° at the high voltage bus. Table 4.2 contains the results obtained without transformer saturation modelled and Table 4.3 contains the results with transformer saturation.

Some effects of representing the SVC transformer are observed by comparing Table 4.2 to Table 3.2. With the TCR represented directly on the high voltage bus, the second harmonic source was effectively an infinite source. The fundamental and second harmonic voltage magnitudes at the TCR terminals remained constant over the TCR firing angle range. With the transformer modelled, the 60 Hz voltage magnitude at the TCR terminals varied from 0.955 pu to 1.039 pu as the firing angle varied from 0° to 45°. This variation is characteristic of an FC & TCR type SVC when operated to maintain a constant system voltage. However, the second harmonic voltage component magnitude at the TCR terminal increased from 17.7% to 26% relative to the Table 3.2 (and the magnitude at the high voltage bus in Table 4.2). This increase in second harmonic voltage component caused an increase in the dc and second harmonic components of the positive sequence TCR line current. For example, at alpha = 30°, the dc component increased 13% and the second harmonic component increased 18% relative to the case without the transformer (Table 3.2).

Comparison of Tables 4.1 and 4.2 indicates that modelling of transformer saturation had little effect on the steady state components of the TCR line current.

Figure 4.3 shows the steady state TCR waveforms for equidistant TCR firing at alpha = 30°. Transformer saturation was modelled. Peak voltage magnitudes of 1.3 pu were observed on two phases. The TCR line current waveforms plotted in Figure 4.4, are non-symmetrical relative to the zero current axis. The waveforms of Figures 4.3 and 4.4 are very similar to the corresponding case in Figures 3.3 and 3.4, where the SVC was modelled on the high voltage bus without a step-up transformer.

The dc component magnitude of the positive sequence TCR line current varied from 8.5% to 24.8% of the fundamental as the firing angle was varied from 0° to 45° (Table 4.3). Similarly, the second harmonic component varied from 18.5% to 50%. The measured real and imaginary parts of the dc, 60 Hz and 120 Hz phasor components of the positive sequence TCR line current are shown in Figure 4.5 for a TCR firing angle of 30°. The measured quantities correspond closely to the components in Table 4.3 which are obtained from a numerical Fourier analysis of the voltage and current waveforms.

All components of the positive sequence transformer saturation current in Table 4.3 increased as the firing angle range increased from 0° to 45°. This increase was excepted since the secondary winding voltage increased. Figures 4.6 and 4.7 show the saturation current for TCR firing angles of 30° and 0° respectively. The waveforms are shown from system startup. The saturation current is initially limited to +/- Im, the rated magnetizing current, and then released at time t = 0.25s. The current in each phase is offset relative to the zero axis due to the offset in the transformer secondary voltage waveforms caused by the second harmonic distortion. A peak steady state saturation current of about 3.5 pu is observed in the alpha = 0° case. The peak magnitude approached 6.0 pu in the alpha = 30° case.

Table 4.2 Positive Sequence SVC Variables with Equidistant Firing of the TCR, Transformer Saturation Not Modelled, Source 2nd Harmonic Voltage 30% @ -30°

Firing Angle	Alpha = 0°	Alpha = 20°	Alpha = 30°	Alpha = 45°
Variable	pu /-°	pu /-°	pu /-°	pu /-°
TCR Line Current				
DC Comp.	0.077/-87°	0.076/-118°	0.068/-132°	0.052/-146°
60 Hz Comp.	0.949/-120°	0.562/-120°	0.393/-122°	0.202/-125°
120 Hz Comp.	0.178/-151°	0.162/-143°	0.142/-135°	0.103/-121°
Xfmr Primary Line Current				
DC Comp.	0.077/-58°	0.076/-88°	0.068/-102°	0.052/-116°
60 Hz Comp.	0.397/-86°	0.025/ 43°	0.198/ 87°	0.402/ 89°
120 Hz Comp.	0.242/ 52°	0.269/ 47°	0.306/ 43°	0.372/ 43°
Xfmr Saturation Current				
DC Comp.	-	-	-	-
60 Hz Comp.	-	-	-	-
120 Hz Comp.	-	-	-	-
Primary Line Voltage				
DC Comp.	0.0005/74°	0.0005/ 75°	0.0005/ 75°	0.0005/ 75°
60 Hz Comp.	0.999 / 0°	0.999 / 0°	0.999 / 0°	0.999 / 0°
120 Hz Comp.	0.300/-31°	0.300 /-31°	0.300 /-31°	0.300 /-31°
Secondary Line Voltage				
DC Comp.	0.0009/106°	0.0009/ 85°	0.0009/ 73°	0.0008/ 68°
60 Hz Comp.	0.957 / 0°	1.002 / 0°	1.021 / 0°	1.043 / 0°
120 Hz Comp.	0.353 /-32°	0.357 /-33°	0.364 /-34°	0.378 /-34°
TCR 60 Hz Absorption Mvar	272.5	168.9	120.4	63.2

Table 4.3 Positive Sequence SVC Variables with Equidistant Firing of the TCR, Transformer Saturation Modelled, Source 2nd Harmonic Voltage 30% @ -30°

Firing Angle	Alpha = 0°	Alpha = 20°	Alpha = 30°	Alpha = 45°
Variable	pu /-°	pu /-°	pu /-°	pu /-°
TCR Line Current				
DC Comp.	0.080/-88°	0.076/-118°	0.067/-132°	0.050/-147°
60 Hz Comp.	0.945/-119°	0.561/-120°	0.392/-122°	0.202/-125°
120 Hz Comp.	0.175/-88°	0.161/-143°	0.140/-135°	0.101/-121°
Xfmr Primary Line Current				
DC Comp.	0.083/-57°	0.079/-86°	0.070/-98°	0.053/-108°
60 Hz Comp.	0.412/-85°	0.021/-15°	0.171/ 85°	0.365/ 88°
120 Hz Comp.	0.235/ 52°	0.255/ 46°	0.288/ 43°	0.345/ 42°
Xfmr Saturation Current				
DC Comp.	0.122/133°	0.188/135°	0.255/137°	0.402/138°
60 Hz Comp.	0.712/ 97°	0.968/ 98°	1.185/ 98°	1.585/ 98°
120 Hz Comp.	0.354/ 61°	0.530/ 60°	0.694/ 59°	1.011/ 58°
Primary Line Voltage				
DC Comp.	0.0005/ 75°	0.0005/ 75°	0.0005/ 75°	0.0005/ 75°
60 Hz Comp.	0.999 / 0°	0.999 / 0°	0.999 / 0°	0.999 / 0°
120 Hz Comp.	0.300 /-31°	0.300 /-31°	0.300 /-31°	0.300 /-31°
Secondary Line Voltage				
DC Comp.	0.0010/ 95°	0.0009/ 85°	0.0008/ 72°	0.0008/ 69°
60 Hz Comp.	0.955 / 0°	0.999 / 0°	1.018 / 0°	1.039 / 0°
120 Hz Comp.	0.351 /-32°	0.354 /-33°	0.360 /-34°	0.372 /-34°
TCR 60 Hz Absorption Mvar	270.7	168.1	119.7	63.0

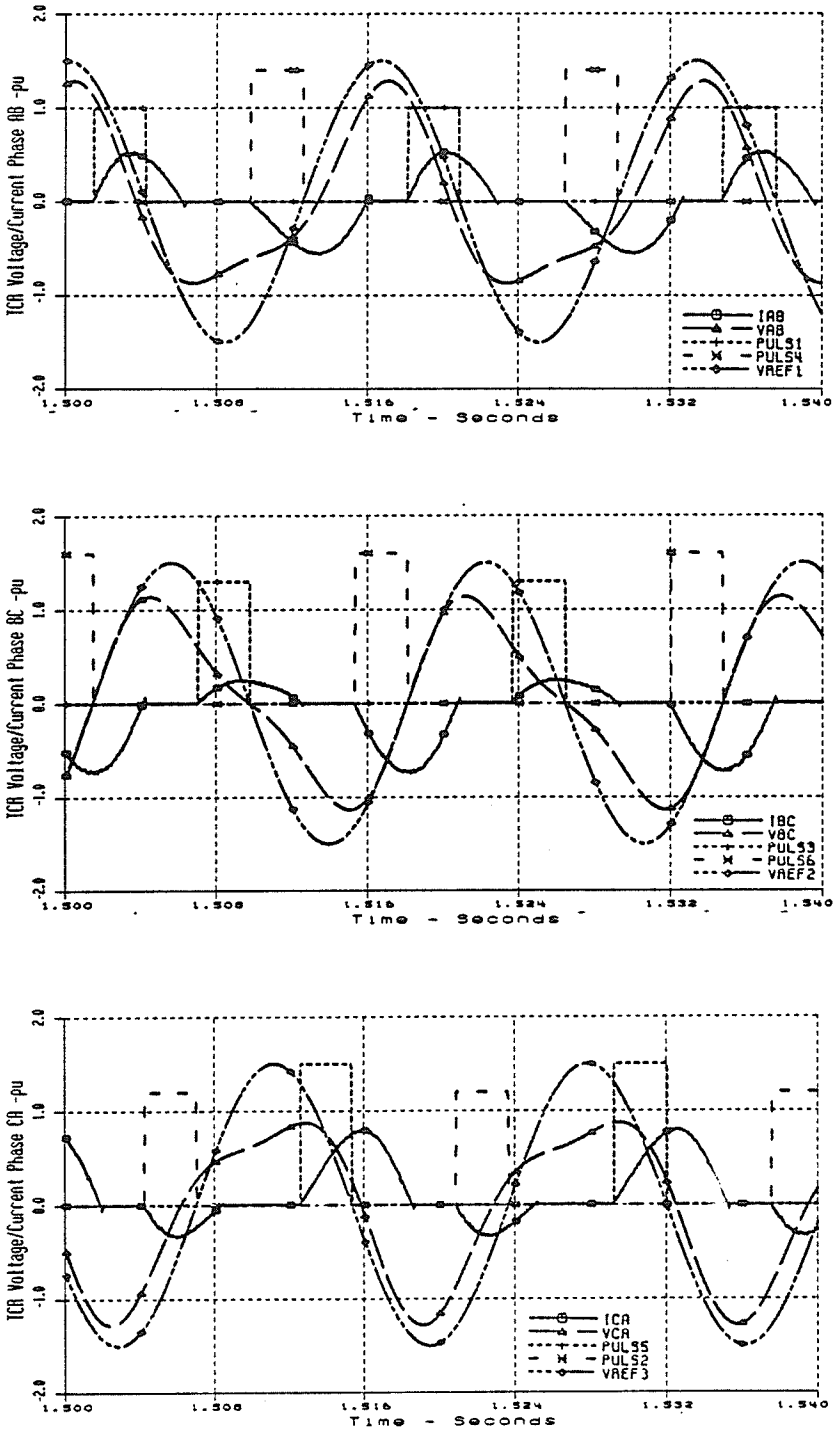

Figure 4.3 TCR Waveforms with Equidistant Firing, Alpha = 30°, Transformer Saturation Modelled, Source: 2nd Harmonic Voltage 30% @ -30°

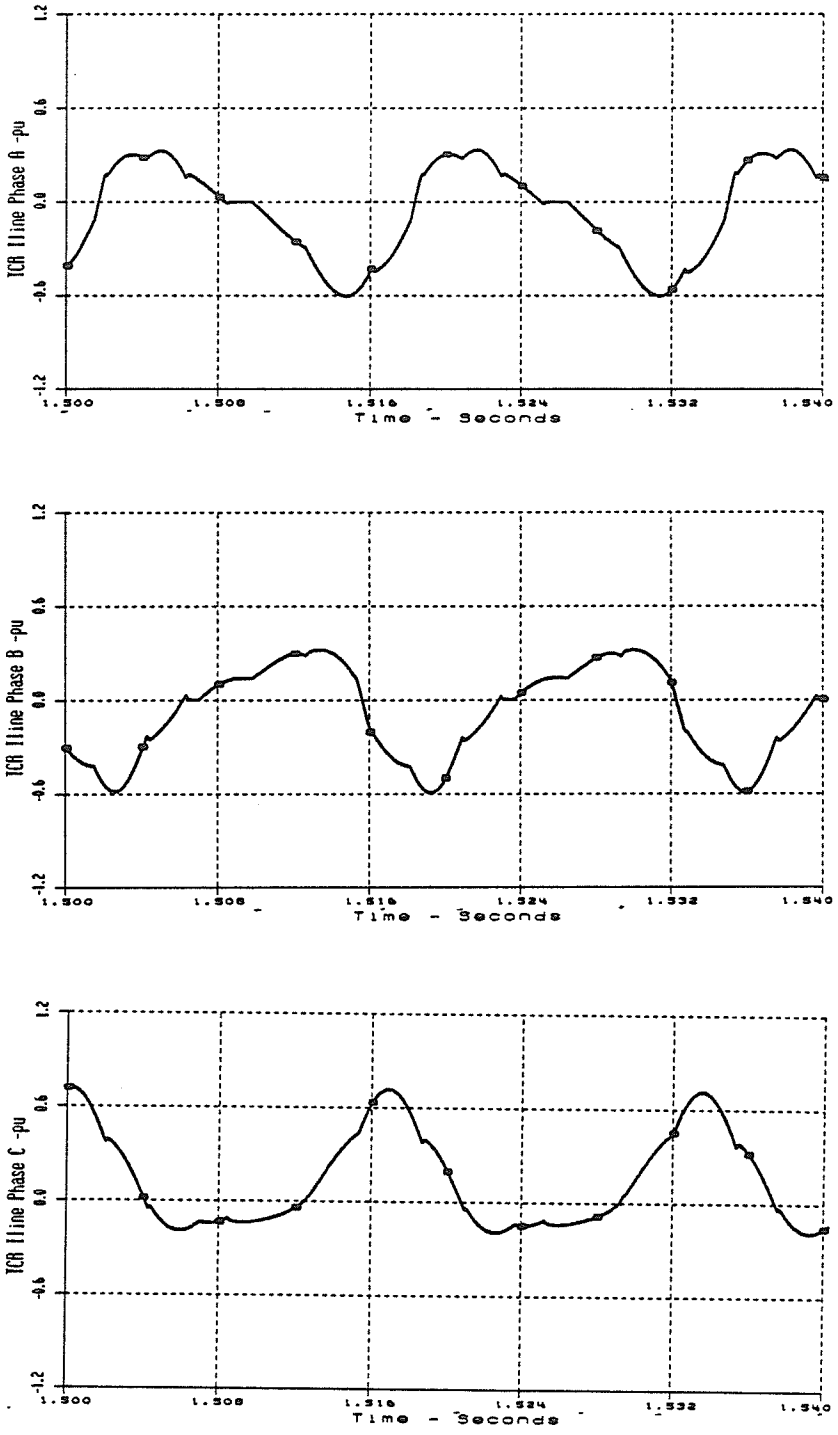

Figure 4.4 TCR Line Current Waveforms with Equidistant Firing, Alpha = 30°, Transformer Saturation Modelled, Source: 2nd Harmonic Voltage 30% @ -30°

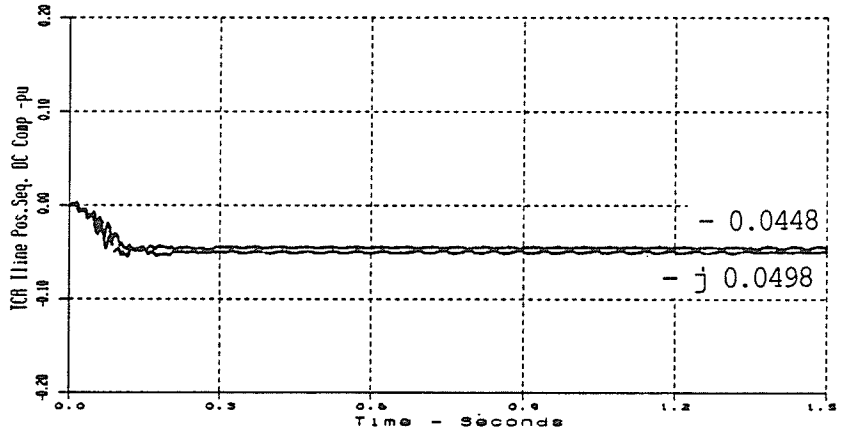

a) Real/Imaginary DC Components - pu

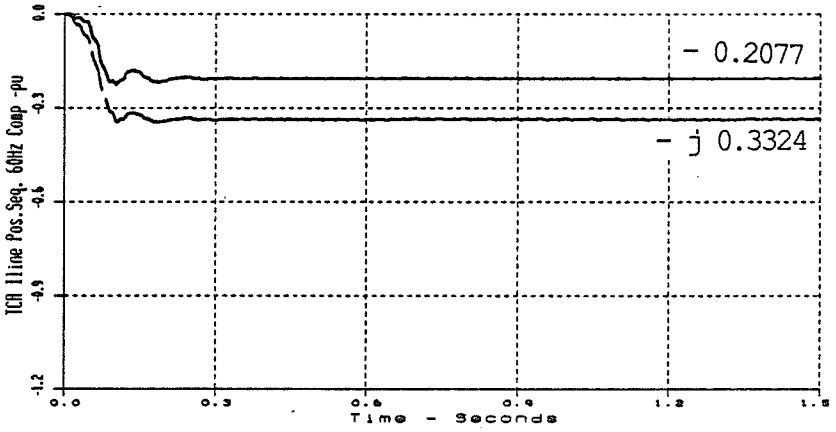

b) Real/Imaginary 60 Hz Components - pu

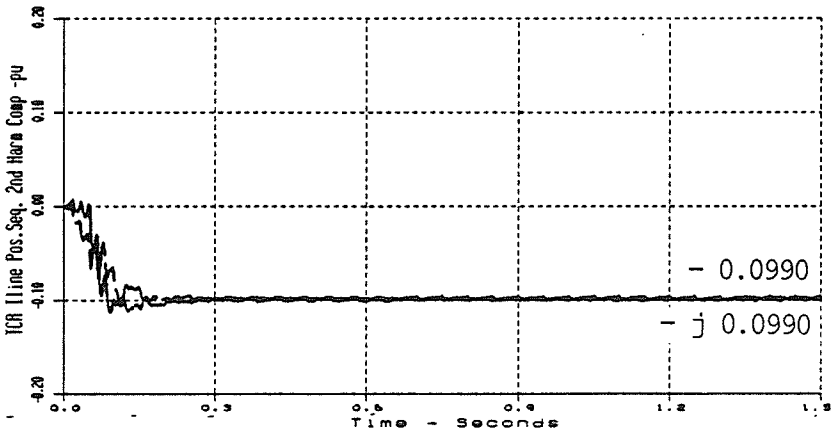

c) Real/Imaginary 2nd Harmonic Components - pu

Figure 4.5 Positive Sequence Phasor Components of TCR Line Current with Equidistant Firing, Alpha = 30°, Transformer Saturation Modelled, Source: 2nd Harmonic Voltage 30% @ -30°

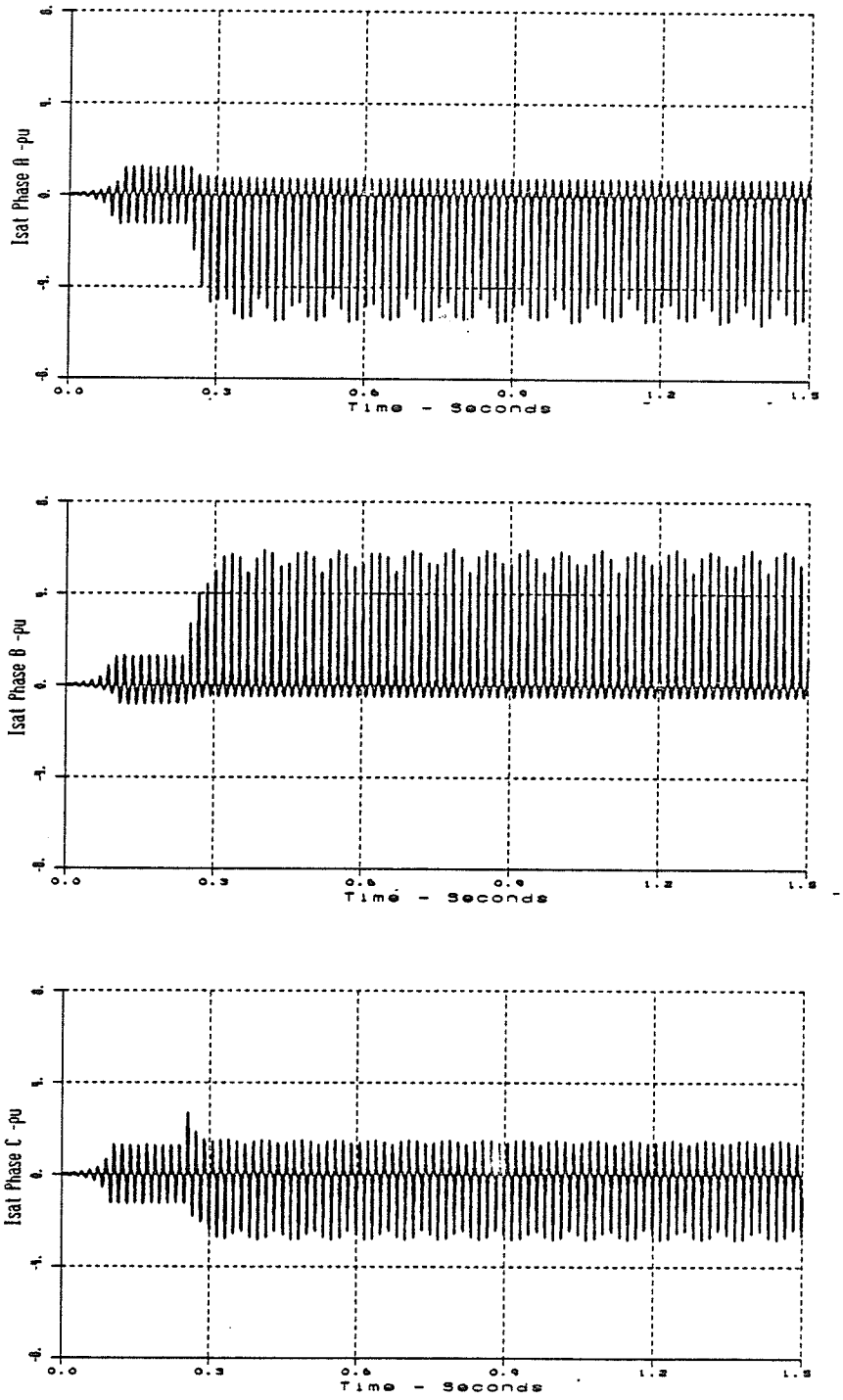

Figure 4.6 Transformer Saturation Current Waveforms with Equidistant TCR Firing, Alpha = 30°, Source 2nd Harmonic Voltage 30% @ -30°

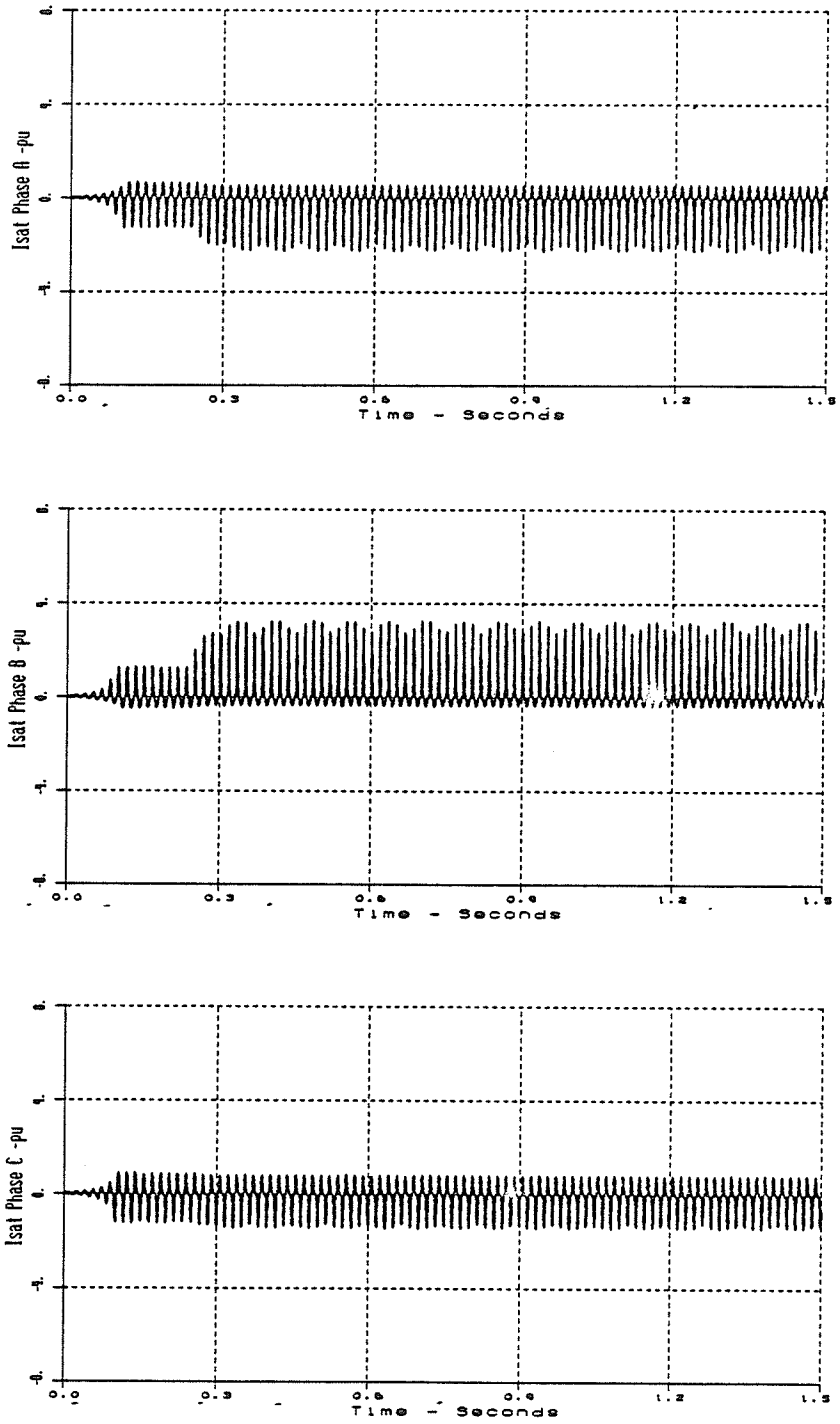

Figure 4.7 Transformer Saturation Current Waveforms with Equidistant TCR Firing, Alpha = 0°, Source 2nd Harmonic Voltage 30% @ -30°

4.4 TCR Performance using Firing Angle Modulation to Control the Positive Sequence Second Harmonic Phasor Component of the TCR Line Current

The measured real and imaginary second harmonic phasor components of the positive sequence TCR line currents were input to the TCR firing angle modulation controller to generate a modulation signal in order to cancel the second harmonic component. The controller settings that were applied are listed in Table 3.3

The steady state harmonic phasor components of some SVC variables and the modulation parameters obtained from the EMTDC simulations are presented in Table 4.4 for the cases without transformer saturation modelled, and in Table 4.5 for the cases with transformer saturation modelled. Nominal TCR firing angles of 0°, 20°, 30° and 45° were considered. The source voltage contained a second harmonic voltage component such that a second harmonic voltage of 30% at -30° phase displacement relative to the fundamental source existed at the point of SVC coupling to the system.

The firing angle modulation controller successfully cancelled the second harmonic component from the positive sequence of the TCR line current at nominal TCR firing angles of 20°, 30° and 45°. The modulation controller was unable to completely eliminate the second harmonic component

with the TCR firing angle = 0°. The 0.178 pu magnitude of the second harmonic component required a modulation angle of 90° in one phase, resulting in 'one-sided' firing of the antiparallel thyristors. Without the step-up transformer modelled in Chapter 3 (Table 3.4) the modulation controller was able to cancel the second harmonic component; however, the magnitude was only 0.148 pu.

Figure 4.8 shows the measured positive sequence second harmonic component of the TCR line current and the modulation controller output for the nominal TCR firing angle of 30° (with saturation modelled). The second harmonic component was reduced from the "no modulation" case magnitude of 0.140 pu/-135° to zero in about 350 ms. after the controller was turned on. The modulation controller output of 0.243 + j0.713 radians corresponds to a modulation peak of 43.2° at a phase displacement of 71.2°. The corresponding firing angle modulation in each phase is:

$$\Delta ab = 13.9°, \quad \Delta bc = -42.4° \text{ and } \Delta ca = 28.4°.$$

Figure 4.9 shows the effect of the modulation on the dc and 60 Hz components of the TCR line current (alpha = 30°). The dc component increased to 182% while the 60 Hz component decreased to 97% of the corresponding "no modulation" values. Tables 4.4 and 4.5 show that modulation of the TCR

firing angle to control the second harmonic component of the TCR line current caused the dc component to increase by 160% to 180% of the "no modulation" values in Tables 4.2 and 4.3, except at alpha = 45° where the dc component marginally increased to 112% of the "no modulation value". The 60 Hz component of TCR line current was only marginally effected by the modulation when TCR firing angle limits were not encountered (alpha = 30° or 45°). When TCR firing angles were encountered, as at alpha = 20°, the TCR line current was reduced to 76% of the "no modulation" case. At alpha = 0°, the sinusoidal modulation becomes one sided, and the TCR line current dropped to 48% of the no modulation case.

Figure 4.10 shows the steady state TCR waveforms for the case where alpha = 30° with transformer saturation modelled. The reduction of the second harmonic component by firing angle modulation caused the peak magnitudes of the TCR line voltage to increase slightly due to the increased dc component in TCR Line current. The thyristor firing was no longer equidistant. The actual firing angle of each thyristor, measured from the figure, agrees with the firing angles obtained by adjusting the nominal firing angle by the modulation angle Δ xy given above for each phase. The TCR phase current waveforms clearly contained a dc component, which was also observed in the TCR line current waveforms plotted in Figure 4.11.

A comparison of Table 4.4 (no saturation) with Table 4.5 shows that transformer saturation did not significantly alter the results as the overvoltages caused by the second harmonic distortion were only 10% to 15% above the knee point (115%) of the saturation characteristic.

However, a comparison of the cases in Table 4.5 to the "no modulation" cases in Table 4.3 clearly illustrates that TCR firing angle modulation control of the second harmonic component of the positive sequence TCR line current caused a large increase in all components of the positive sequence SVC transformer saturation current. The dc component increase ranged from 120% (alpha = 45°) to 339% (alpha = 0°) of the 'no modulation" saturation current components. Similarly the 60 Hz component increase ranged from 112% (alpha = 45°) to 207% (alpha = 0°) and the second harmonic component increase ranged from 120% (alpha = 45°) to 284% (alpha = 0°). The increase is less pronounced as the TCR firing angle is increased from 0° to 45° and is attributed to the increase in the dc component of the TCR line current that is brought about by the modulation.

Figure 4.12 shows the SVC transformer saturation current waveforms for the alpha = 30° case. The modulation controller caused a large increase in the peak saturation

current waveforms of phases A and B when the controller was turned on at 0.25s. The change in transformer saturation current due to the modulation can be more clearly seen when Figure 4.12 is compared to Figure 4.6, the corresponding "no modulation" case saturation current waveforms. The peak value of saturation current increased from about 5.0 pu to 10.0 pu due to the modulation. Figure 4.13 shows the transformer saturation current waveforms for the case where the TCR firing angle = 0°. The one sided firing angle modulation caused the saturation current to increase dramatically to peak values approaching 10 p.u. or 20% of rated transformer secondary winding current. The peak saturation currents at TCR firing angles of 0° (Figure 4.13) and 45° (Figure 4.12) are approximately the same in magnitude. The one sided modulation at alpha = 0° increased the dc component of the TCR line current, thereby driving the transformer further into saturation.

The modelling of the SVC step-up transformer resulted in a larger second harmonic voltage component present at the TCR terminals as compared to the simple model of Chapter 3 (about 0.351 pu as compared to 0.300 pu). The modulation reduced but could not totally eliminate the second harmonic component from the positive sequence TCR line current at the

TCR firing angle of 0°. Reducing the magnitude of the second harmonic voltage component to 0.300 pu produced similar results to that of Chapter 3 (Table 3.4).

Table 4.4 Positive Sequence SVC Variables with Control of the Positive Sequence Second Harmonic Component of TCR Line Current, Transformer Saturation Not Modelled, Source 2nd Harmonic Voltage 30% @ -30°

Firing Angle	Alpha = 0°	Alpha = 20°	Alpha = 30°	Alpha = 45°
Variable	pu /-°	pu /-°	pu /-°	pu /-°
TCR Line Current				
DC Comp.	0.131/ 102°	0.138/ 92°	0.124/ 83°	0.056/ 89°
60 Hz Comp.	0.458/-120°	0.423/-119°	0.383/-119°	0.203/-119°
120 Hz Comp. **	0.022/- 91°	0.001/ 48°	0.003/ 113°	0.001/ 67°
	* not cancelled*			
Xfmr Primary Line Current				
DC Comp.	0.131/ 132°	0.138/122°	0.124/ 113°	0.056/ 119°
60 Hz Comp.	0.129/ 80°	0.163/ 79°	0.211/ 82°	0.402/ 86°
120 Hz Comp.	0.468/ 52°	0.483/ 55°	0.481/ 55°	0.482/ 55°
Xfmr Saturation Current				
DC Comp.	-	-	-	-
60 Hz Comp.	-	-	-	-
120 Hz Comp.	-	-	-	-
Primary Line Voltage				
DC Comp.	0.0005/ 75°	0.0005/ 75°	0.0005/ 75°	0.0005/ 75°
60 Hz Comp.	0.999 / 0°	0.999 / 0°	0.999 / 0°	0.999 / 0°
120 Hz Comp.	0.300 /-31°	0.300 /-31°	0.300 /-31°	0.300 /-31°
Secondary Line Voltage				
DC Comp.	0.0008/-14°	0.0007/-24°	0.0006/-23°	0.0004/ 21°
60 Hz Comp.	1.014 /- 1°	1.017 / -1°	1.022 / -1°	1.043 / -1°
120 Hz Comp.	0.401 /-33°	0.405 /-32°	0.404 /-32°	0.405 /-32°
TCR 60 Hz Absorption Mvar (% No Mod. Case)	139.3 (51.1)	129.0 (76.4)	117.4 (97.5)	63.5 (100.5)
Modulation				
Peak/Phase	87.3°/58.6°	60.8°/69.2°	43.4°/71.2°	31.1°/87°
Δ ab	45.4°	21.6°	14.0°	1.6°
Δ bc	-87.0°	-60.0°	-42.6°	-27.7°
Δ ca	41.8°	38.4°	28.6°	26.1°

Table 4.5 Positive Sequence SVC Variables with Control of the Positive Sequence Second Harmonic Component of TCR Line Current, Transformer Saturation Modelled, Source 2nd Harmonic Voltage 30% @ -30°

Firing Angle	Alpha = 0°	Alpha = 20°	Alpha = 30°	Alpha = 45°
Variable	pu /-°	pu /-°	pu /-°	pu /-°
TCR Line Current				
DC Comp.	0.130/ 102°	0.137/ 92°	0.122/ 84°	0.056/ 90°
60 Hz Comp.	0.454/-120°	0.425/-119°	0.381/-119°	0.202/ -119°
120 Hz Comp. **	0.026/- 90°	0.002/ 50°	0.002/ 116°	0.0009/ 22°
	Not Cancelled			
Xfmr Primary Line Current				
DC Comp.	0.121/131°	0.128/120°	0.113/ 111°	0.046/ 117°
60 Hz Comp.	0.102/ 74°	0.133/ 74°	0.177/ 79°	0.361/ 85°
120 Hz Comp.	0.439/ 51°	0.453/ 55°	0.449/ 55°	0.446/ 55°
Xfmr Saturation Current				
DC Comp.	0.414/143°	0.421/142°	0.444/141°	0.481/134°
60 Hz Comp.	1.476/ 99°	1.512/ 98°	1.576/ 98°	1.775/ 97°
120 Hz Comp.	1.008/ 56°	1.033/ 57°	1.081/ 58°	1.212/ 61°
Primary Line Voltage				
DC Comp.	0.0005/ 75°	0.0005/ 75°	0.0005/ 75°	0.0005/ 75°
60 Hz Comp.	0.999 / 0°	0.999 / 0°	0.999 / 0°	0.999 / 0°
120 Hz Comp.	0.300 /-31°	0.300 /-31°	0.300 /-31°	0.300 /-31°
Secondary Line Voltage				
DC Comp.	0.0008/-13°	0.0007/-22°	0.0006/-22°	0.0003/ 23°
60 Hz Comp.	1.010 / 0°	1.013 /- 1°	1.018 /- 1°	1.039 /- 1°
120 Hz Comp.	0.395 /-33°	0.398 /-32°	0.397 /-32°	0.397 /-32°
TCR 60 Hz Absorption Mvar (% No Mod. Case)	137.6 (50.8)	129.2 (76.8)	116.4 (97.2)	63.0 (104.1)
Modulation				
Peak/Phase	87.0°/58.9°	60.5°/69.1°	43.2°/71.2°	30.9°/86.4°
Δ ab	45.0°	21.6°	13.9°	2.0°
Δ bc	-87.0°	-59.7°	-42.4°	-27.6°
Δ ca	42.0°	38.2°	28.4°	25.7°

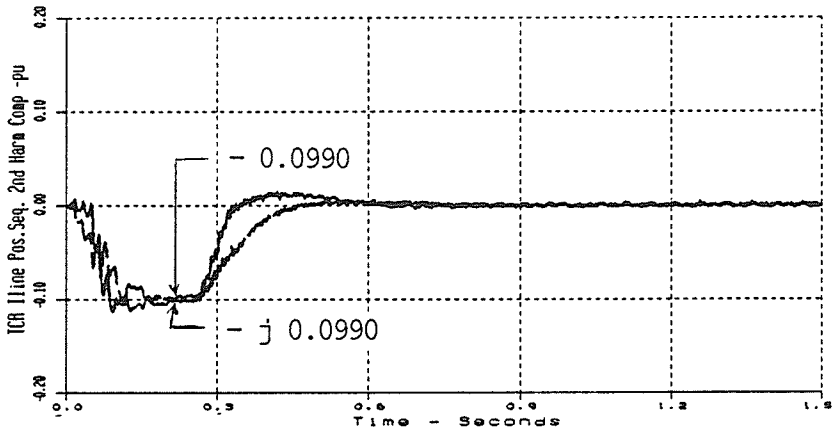

a) Real/Imaginary 2nd Harmonic Components - pu

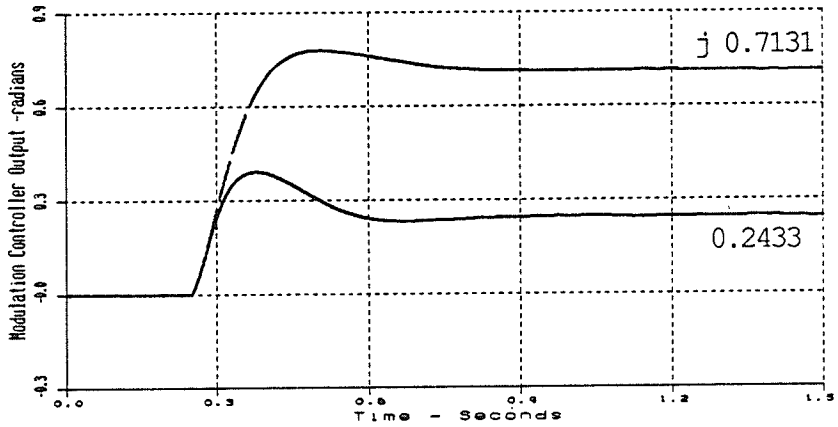

b) Real/Imaginary Modulation Controller Components - radians

Figure 4.8 Control of Positive Sequence 2nd Harmonic Component of TCR Line Current, Alpha = 30°, Transformer Saturation Modelled, Source 2nd Harmonic Voltage 30% @ -30°

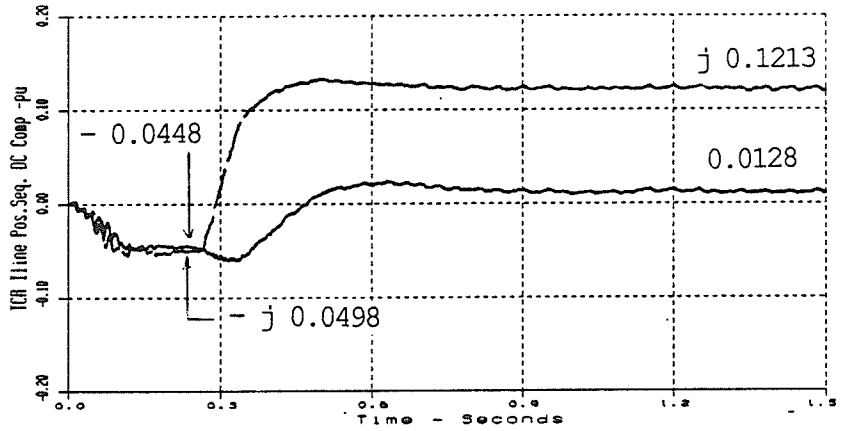

a) Real/Imaginary DC Components - pu

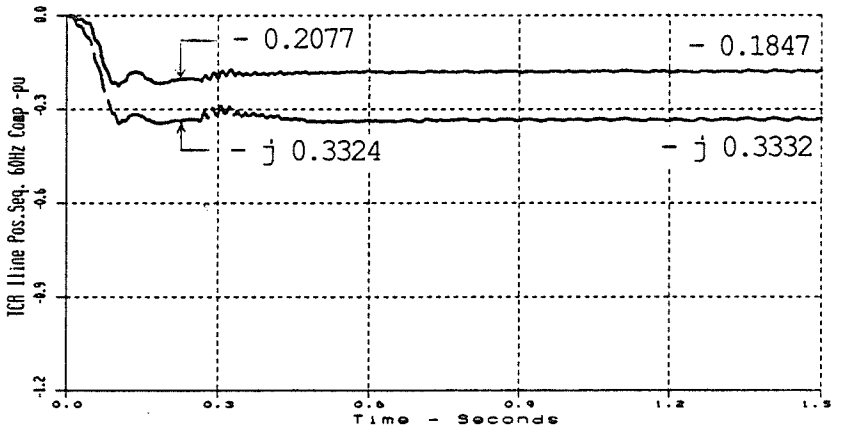

b) Real/Imaginary 60 Hz Components - pu

Figure 4.9 Effect of Control of the Positive Sequence 2nd Harmonic Component of TCR Line Current on the DC and 60 HZ Components, Alpha = 30°, Transformer Saturation Modelled, Source: 2nd Harmonic Voltage 30% @ -30°

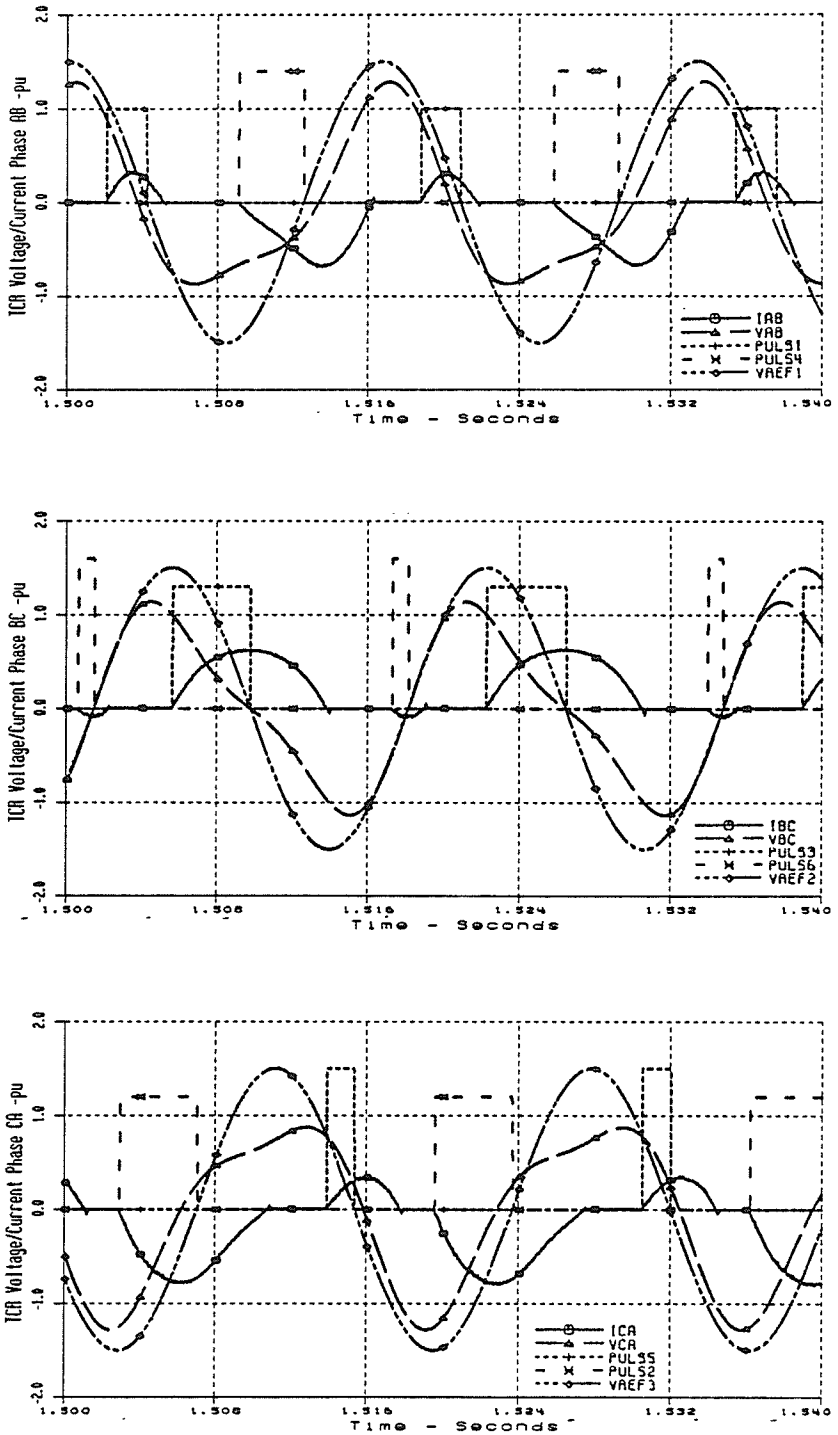

Figure 4.10 TCR Waveforms, Control of the Positive Sequence 2nd Harmonic Component of TCR Line Current, Alpha = 30°, Transformer Saturation Modelled, Source 2nd Harmonic Voltage 30% @ -30°

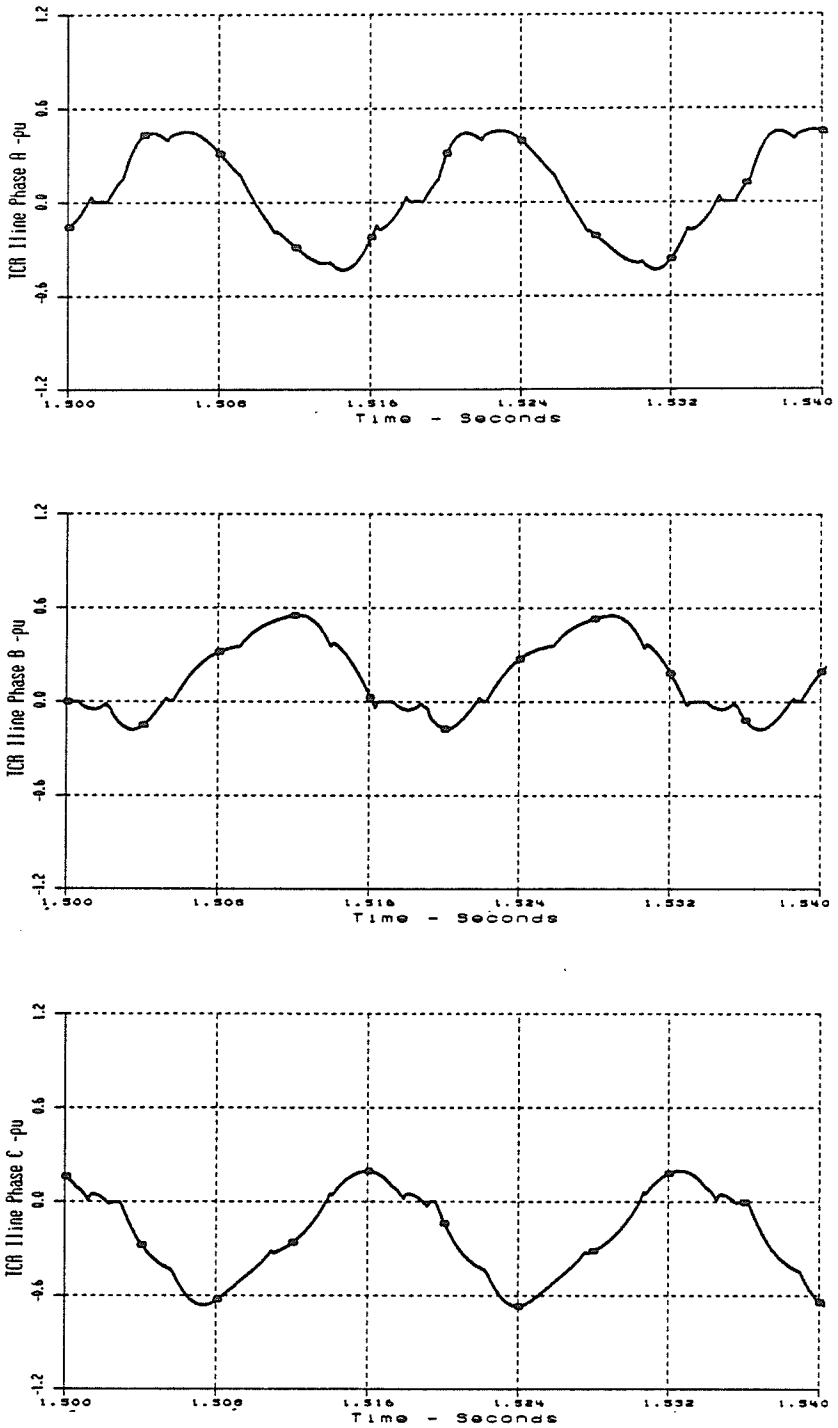

Figure 4.11 TCR Line Current Waveforms, Control of the Positive Sequence 2nd Harmonic Component of TCR Line Current, Alpha = 30°, Transformer Saturation Modelled, Source: 2nd Harmonic Voltage 30% @ -30°

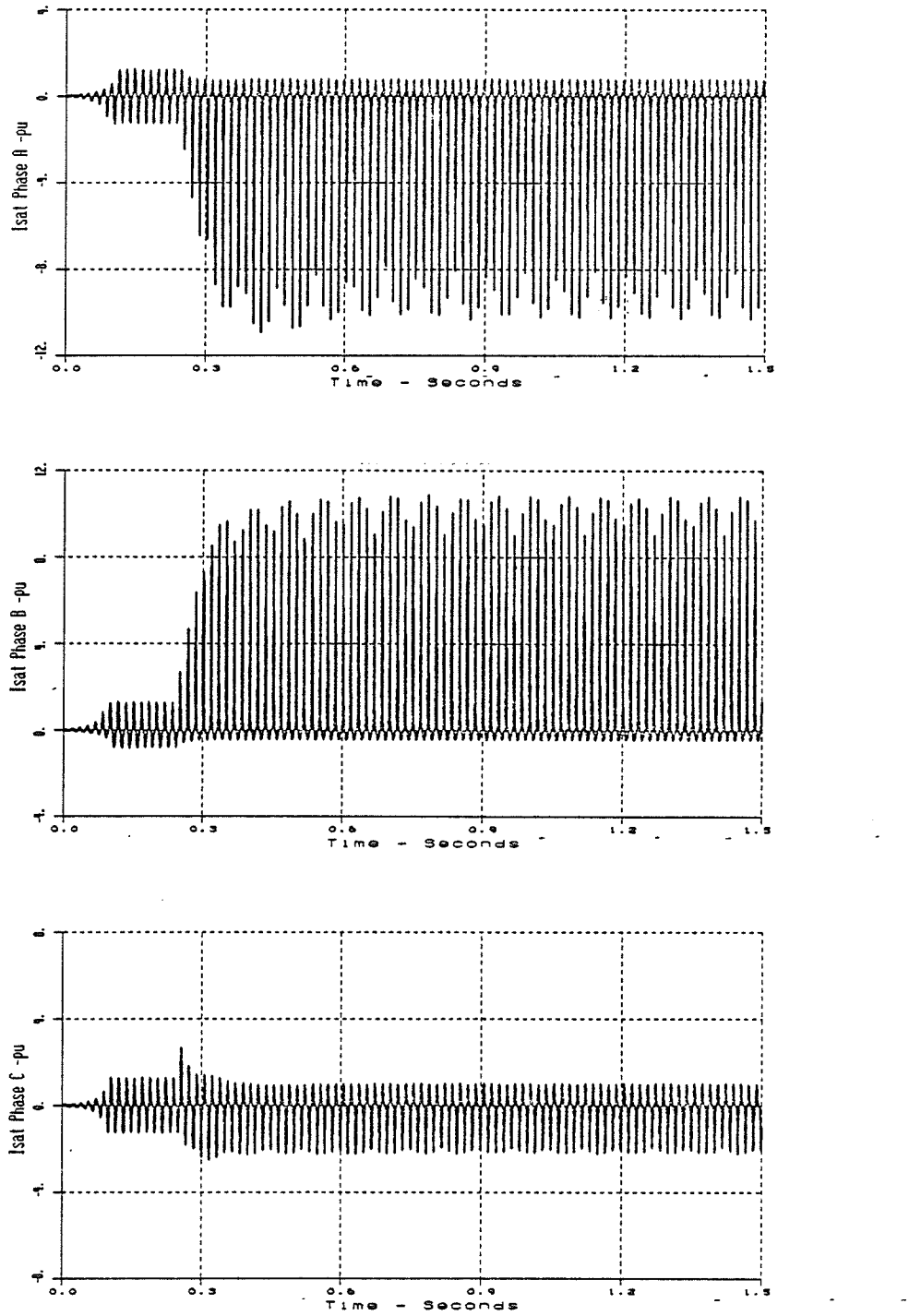

Figure 4.12 Transformer Saturation Current Waveforms, Control of the Positive Sequence 2nd Harmonic Component of TCR Line Current, Alpha = 30°, Source: 2nd Harmonic Voltage 30% @ -30°

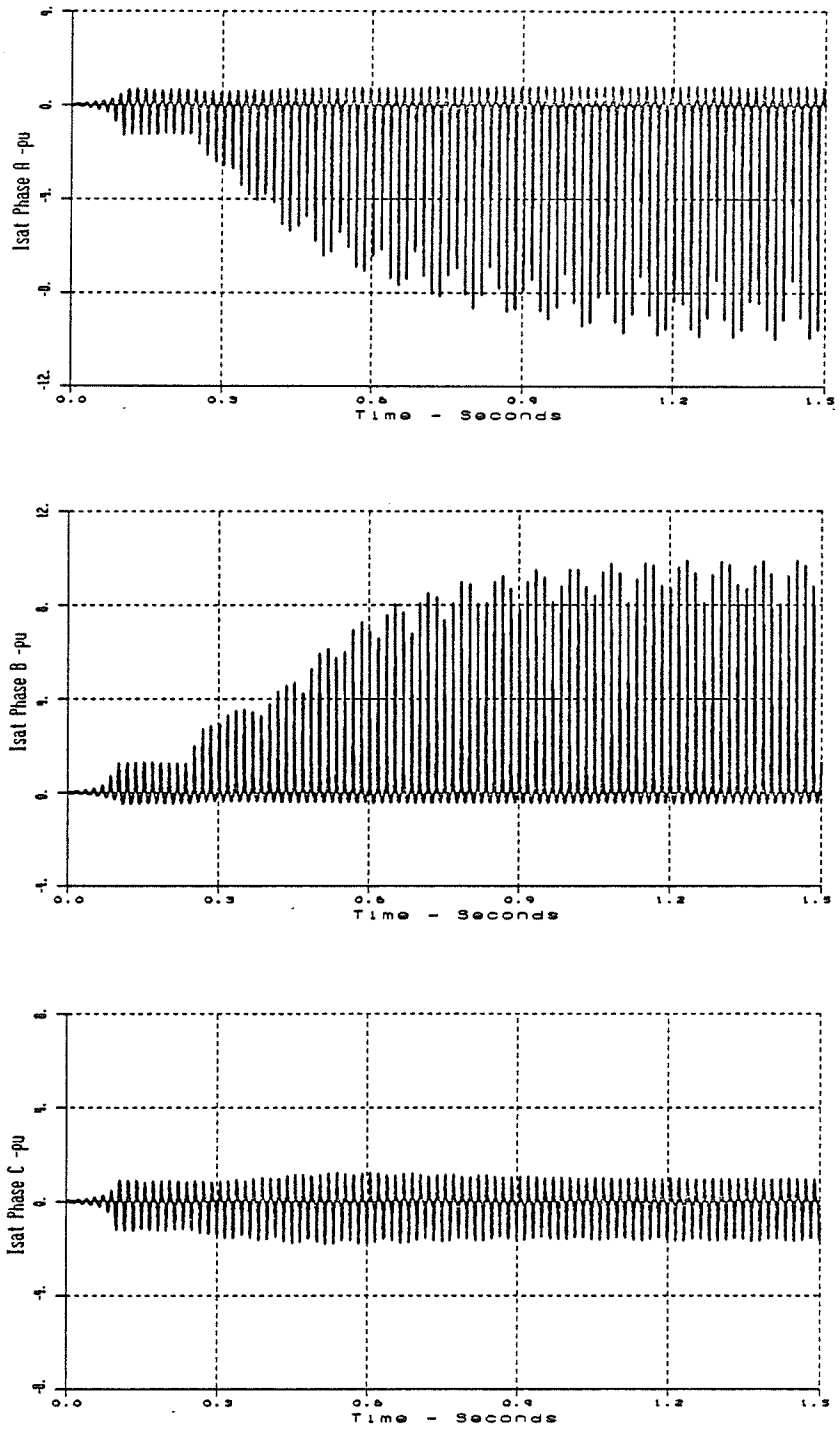

Figure 4.13 Transformer Saturation Current Waveforms, Control of Positive Sequence 2nd Harmonic Component of TCR Line Current, Alpha = 0°, Source: 2nd Harmonic Voltage 30% @ -30°

4.5 TCR Performance using Firing Angle Modulation to Control the Positive Sequence DC Component of the TCR Line Current

The measured real and imaginary dc phasor components of the positive sequence TCR line current were input to the TCR firing angle modulation controller to generate a modulation signal to cancel the dc component. The controller settings that were applied are listed in Table 3.5.

The steady state harmonic phasor components of some SVC variables and the modulation parameters obtained from the EMTDC simulations are presented in Table 4.6 for the cases without transformer saturation modelled, and in Table 4.7 for the cases with transformer saturation modelled. Nominal TCR firing angles of 0°, 20°, 30° and 45° were considered. The system voltage at the point of SVC connection contained a second harmonic voltage component of 30% at -30° phase displacement relative to the fundamental.

The firing angle modulation controller successfully cancelled the dc component from the positive sequence of the TCR line current in all cases, with and without transformer saturation modelled. Firing angle limits were only encountered in the cases with the nominal TCR firing angle at 0°. In this case the TCR var absorption was reduced to 83.6% of the "no modulation" case.

Modulation of the firing angle to control the positive sequence dc component of the TCR line current also decreased the corresponding second harmonic component by approximately 12% (alpha = 0°) to 41% (alpha = 45°) relative to the "no modulation" case.

Figure 4.14 shows the measured dc component of the positive sequence TCR line current and the modulation controller output for the case of alpha = 30° and transformer saturation modelled. The dc component (0.067 pu @ -132°) was reduced to zero in about 300 ms after the controller was turned on. The controller output of -0.045 + j0.246 radians corresponds to a modulation peak of 14.4° and a modulation phase of 100.3°. The corresponding firing angle modulation in each phase was:

$$\Delta ab = -2.6°, \quad \Delta bc = -11.0° \text{ and } \Delta ca = 13.5°$$

Figure 4.15 shows the effect of the modulation of the TCR firing angle on the 60 Hz and second harmonic components of the TCR line current. The 60 Hz component is decreased by 3.0% from 0.392 pu @ -122° to 0.380 pu @ -120°. The second harmonic component is decreased by 30% from 0.140 pu @ -135° to 0.098 pu @ -152°.

Figure 4.16 shows the steady state TCR waveforms for the case alpha = 30° and transformer saturation modelled. Reduction of the dc component did not reduce the TCR line voltage maximum peak magnitude of 1.3 p.u. due to the presence of the infinite second harmonic source. Each thyristor firing pulse was controlled by the modulation signal such that the TCR phase currents waveforms appear more symmetrical with respect to the zero current axis. A dc component is not evident in the TCR line current waveforms plotted in Figure 4.17.

Figure 4.18 shows the SVC transformer saturation current waveforms at a TCR firing angle of 30°. The firing angle modulation only marginally increased the peak values of the saturation current as compared to Figure 4.6, the "no modulation" case at alpha = 30°. Comparison of the dominant harmonic components of the transformer saturation current for the "no modulation" cases (Table 4.3) versus the "dc modulation" cases (Table 4.7) shows that the harmonic component magnitudes of the saturation current increased due to the modulation. The dc component increase ranged from 107% (alpha = 45°) to 134% (alpha = 0°) of the "no modulation" transformer saturation current component. Similarly, the 60 Hz component increase ranged from 105% (alpha = 45°) to 117% (alpha = 0°), and the second harmonic

component increase ranged from 108% (alpha = 45°) to 124% (alpha = 0°). The increase was the largest at alpha = 0°, and is attributed to distortion of the TCR line voltage waveforms due to the one-sided modulation. Figure 4.19 shows the SVC transformer saturation current waveforms at alpha = 0°, with the dc component of TCR controlled as a comparison to Figure 4.7, the "no modulation" case at alpha = 0°.

Comparison of Tables 4.6 and 4.7 indicates that the modelling of transformer saturation did not significantly alter the steady state results relative to the "no saturation" cases.

Table 4.6 Positive Sequence SVC Variables with Control of the Positive Sequence DC Component of TCR Line Current, Transformer Saturation Not Modelled, Source 2nd Harmonic Voltage 30% @ -30°

Firing Angle	alpha = 0°	alpha = 20°	alpha = 30°	alpha = 45°
Variable	pu /-°	pu /-°	pu /-°	pu /-°
TCR Line Current				
DC Comp. **	0.002/-107°	0.0008/-128°	0.001/ 61°	0.001/-132°
60 Hz Comp.	0.777/-119°	0.550/ -119°	0.379/-120°	0.185/-119°
120 Hz Comp.	0.154/-152°	0.127/ -151°	0.098/-152°	0.059/-150°
Xfmr Primary Line Current				
DC Comp.	0.002/ -76°	0.0008/ -94°	0.001/ 87°	0.001/-127°
60 Hz Comp.	0.214/ -82°	0.040/ 48°	0.215/ 83°	0.421/ 86°
120 Hz Comp.	0.273/ 54°	0.310/ 54°	0.349/ 54°	0.402/ 54°
Xfmr Saturation Current				
DC Comp.	-	-	-	-
60 Hz Comp.	-	-	-	-
120 Hz Comp.	-	-	-	-
Primary Line Voltage				
DC Comp.	0.0005/ 75°	0.0005/ 75°	0.0005/ 76°	0.0005/ 75°
60 Hz Comp.	0.999 / 0°	0.999 / 0°	0.999 / 0°	0.999 / 0°
120 Hz Comp.	0.300 /-31°	0.300 /-31°	0.300 /-31°	0.300 /-31°
Secondary Line Voltage				
DC Comp.	0.0005/ 64°	0.0004/ 66°	0.0005/ 67°	0.0004/ 78°
60 Hz Comp.	0.977 / 0°	1.003 / 0°	1.023 / 0°	1.045 /- 1°
120 Hz Comp.	0.359 /-32°	0.367 /-32°	0.375 /-32°	0.387 /-32°
TCR 60 Hz Absorption Mvar (% No Mod. Case)	227.7 (83.6)	165.5 (98)	116.3 (96.6)	58.0 (91.8)
Modulation				
Peak/Phase	24.4°/73.4°	13.6°/88.1°	14.5°/100.8°	17.1°/118.1°
Δ ab	7.0°	0.5°	- 2.7°	- 8.0°
Δ bc	-23.7°	-12.0°	-11.0°	- 9.0°
Δ ca	16.7°	11.6°	13.7°	17.1°

Table 4.7 Positive Sequence SVC Variables with Control of the Positive Sequence DC Component of TCR Line Current, Transformer Saturation Modelled, Source 2nd Harmonic Voltage 30% @ -30°

Firing Angle	alpha = 0°	alpha = 20°	alpha = 30°	alpha = 45°
Variable	pu /-°	pu /-°	pu /-°	pu /-°
TCR Line Current				
DC Comp. **	0.002/- 95°	0.0007/-49°	0.0008/ 3°	0.0008/-142°
60 Hz Comp.	0.774/-119°	0.548/-119°	0.380/-120°	0.187 /-119°
120 Hz Comp.	0.153/-152°	0.125/-152°	0.098/-152°	0.059 /-150°
Xfmr Primary Line Current				
DC Comp.	0.006/-54°	0.006/-39°	0.007/-38°	0.0096/-54°
60 Hz Comp.	0.231/-82°	0.031/ 14°	0.183/ 81°	0.379/ 85°
120 Hz Comp.	0.263/ 53°	0.294/ 54°	0.325/ 54°	0.370/ 54°
Xfmr Saturation Current				
DC Comp.	0.160/136°	0.236/138°	0.314/136°	0.432/131°
60 Hz Comp.	0.835/ 98°	1.062/ 98°	1.297/ 98°	1.673/ 97°
120 Hz Comp.	0.440/ 61°	0.615/ 61°	0.798/ 61°	1.094/ 62°
Primary Line Voltage				
DC Comp.	0.0005/ 75°	0.0005/ 75°	0.0005/ 76°	0.0005/ 75°
60 Hz Comp.	0.999 / 0°	0.999 / 0°	0.999 / 0°	0.999 / 0°
120 Hz Comp.	0.300 /-31°	0.300 /-31°	0.300 /-31°	0.300 /-31°
Secondary Line Voltage				
DC Comp.	0.0005/ 76°	0.0005/ 68°	0.0005/ 62°	0.0005/ 77°
60 Hz Comp.	0.975 / 0°	1.00 / 0°	1.019 / 0°	1.041 /- 1°
120 Hz Comp.	0.357 /-32°	0.363 /-32°	0.370 /-32°	0.380 /-32°
TCR 60 Hz Absorption Mvar (% No Mod. Case)	226.4 (83.6)	164.4 (97.8)	116.2 (97.1)	58.4 (92.7)
Modulation				
Peak/Phase	24.4°/72.9°	13.7°/87.6°	14.4°/100.3°	16.5°/118.2°
Δ ab	7.2°	0.6°	- 2.6°	- 7.8°
Δ bc	-23.8°	-12.1°	-11.0°	- 8.7°
Δ ca	16.6°	11.6°	13.5°	16.5°

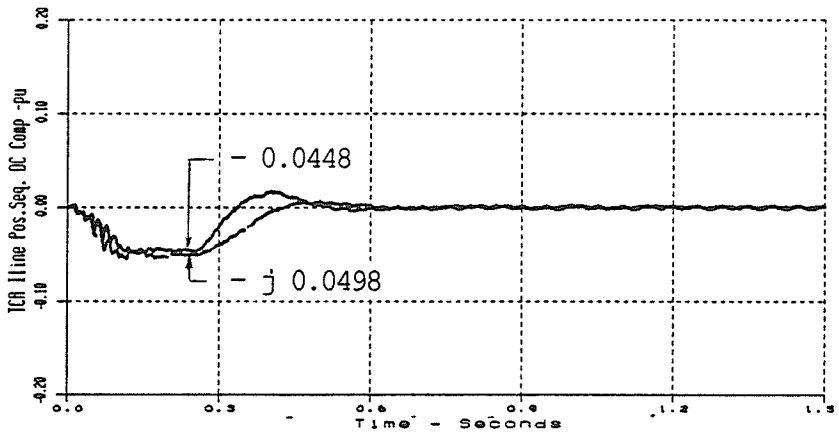

a) Real/Imaginary DC Components - pu

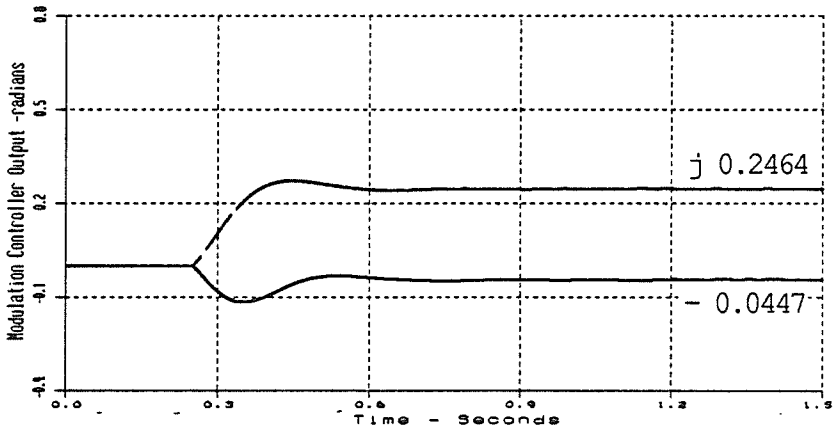

b) Real/Imaginary Modulation Controller Components - radians

Figure 4.14 Control of the Positive Sequence DC Component of TCR Line Current, Alpha = 30°, Transformer Saturation Modelled, Source: 2nd Harmonic Voltage 30% @ -30°

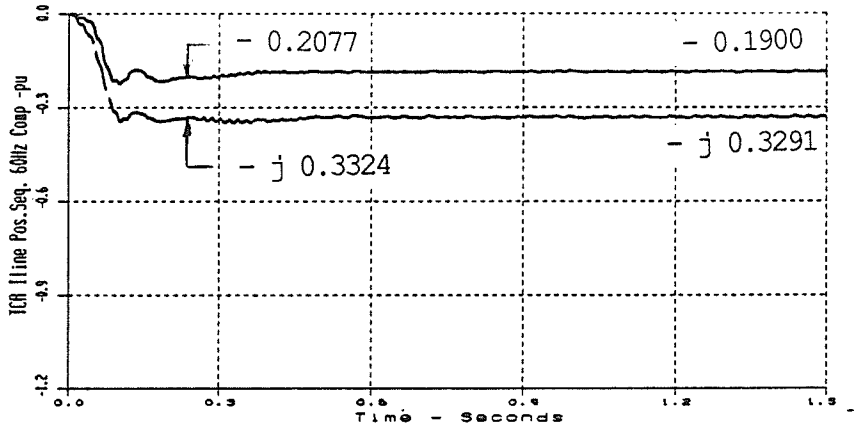

a) Real/Imaginary 60 Hz Components - pu

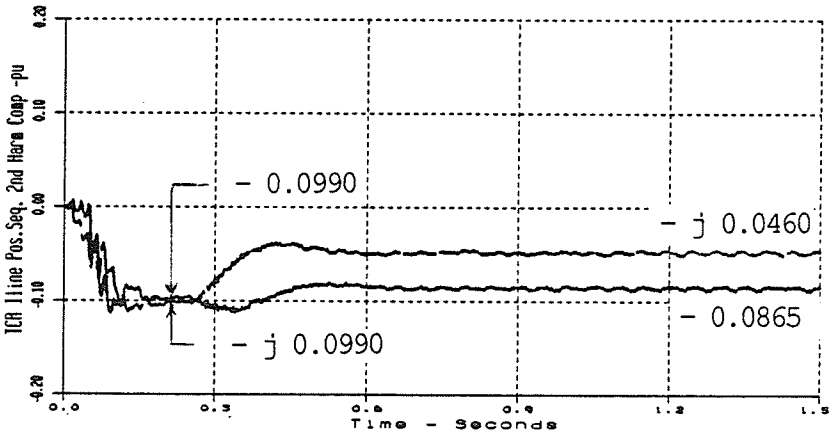

b) Real/Imaginary 2nd Harmonic Components - pu

Figure 4.15 Effect of Control of the Positive Sequence DC Component of TCR Line Current on the 60 HZ and 2nd Harmonic Components, Alpha = 30°, Transformer Saturation Modelled, Source: 2nd Harmonic Voltage 30% @ -30°

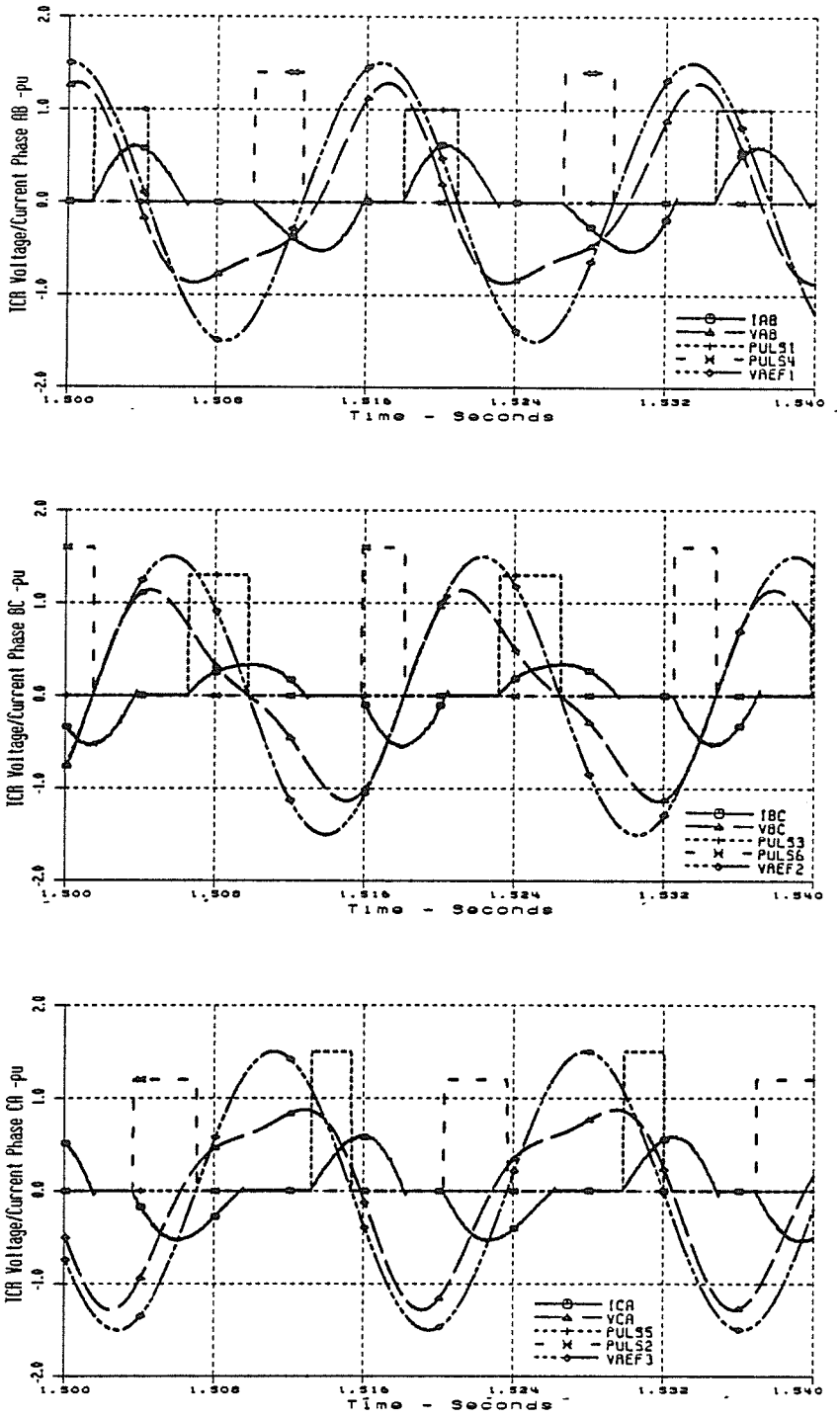

Figure 4.16 TCR Waveforms, Control of the Positive Sequence DC Component of TCR Line Current, Alpha = 30°, Transformer Saturation Modelled, Source: 2nd Harmonic Voltage 30% @ -30°

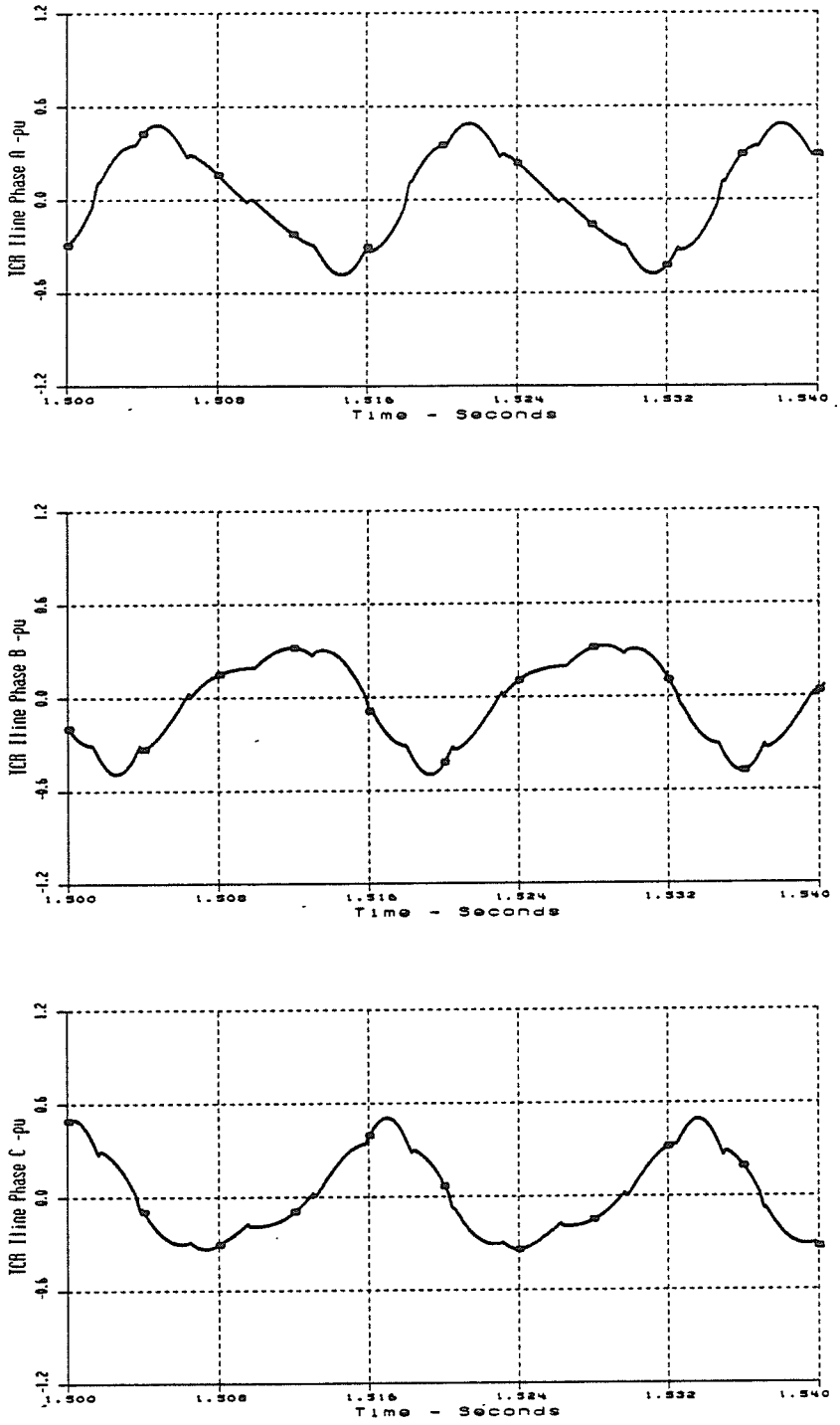

Figure 4.17 TCR Line Current Waveforms, Control of the Positive Sequence DC Component of TCR Line Current, Alpha = 30°, Transformer Saturation Modelled, Source: 2nd Harmonic Voltage 30% @ -30°

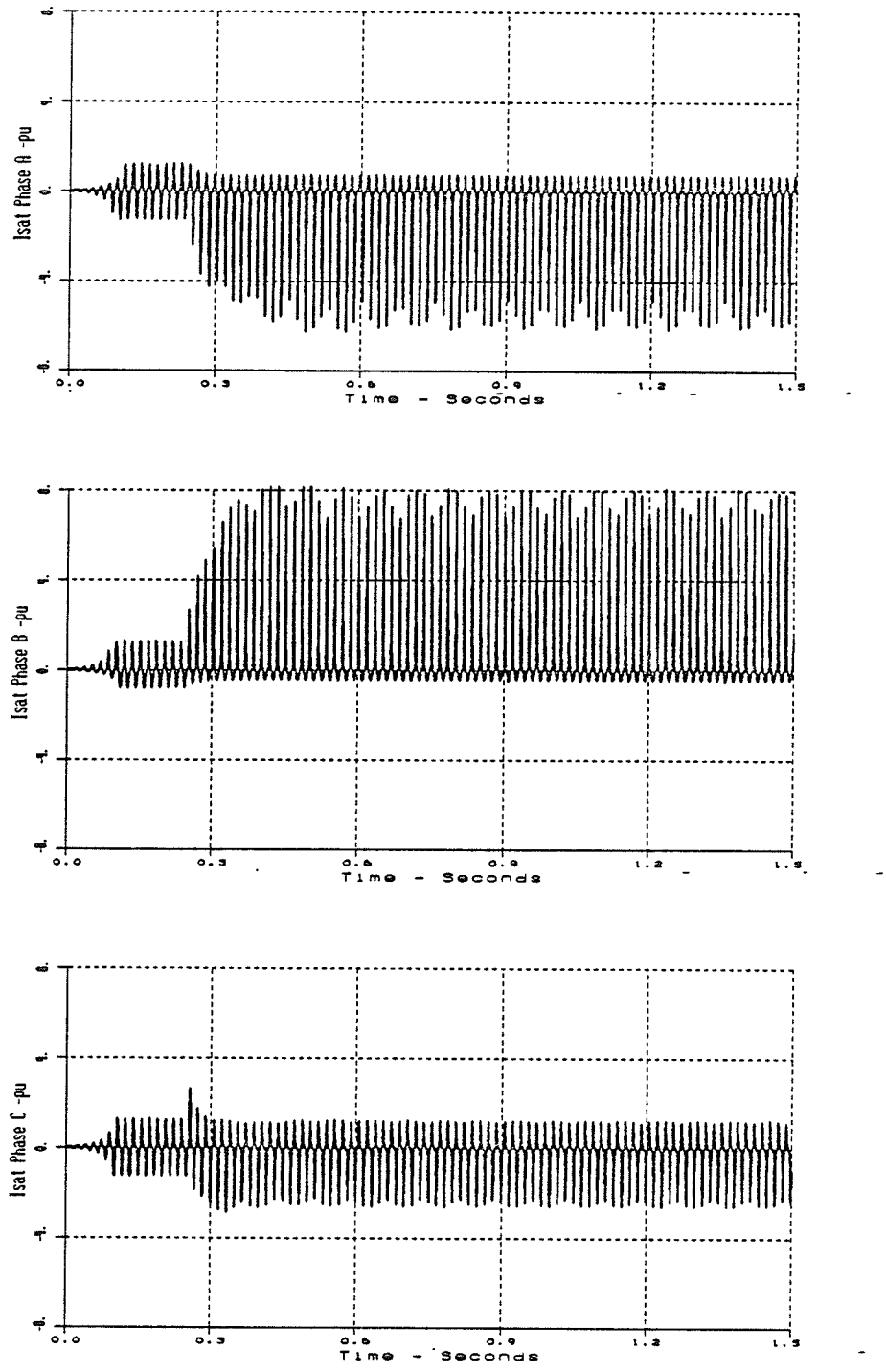

Figure 4.18 Transformer Saturation Current Waveforms, Control of the Positive Sequence DC Component of TCR Line Current, Alpha = 30°, Source: 2nd Harmonic Voltage 30% @ -30°

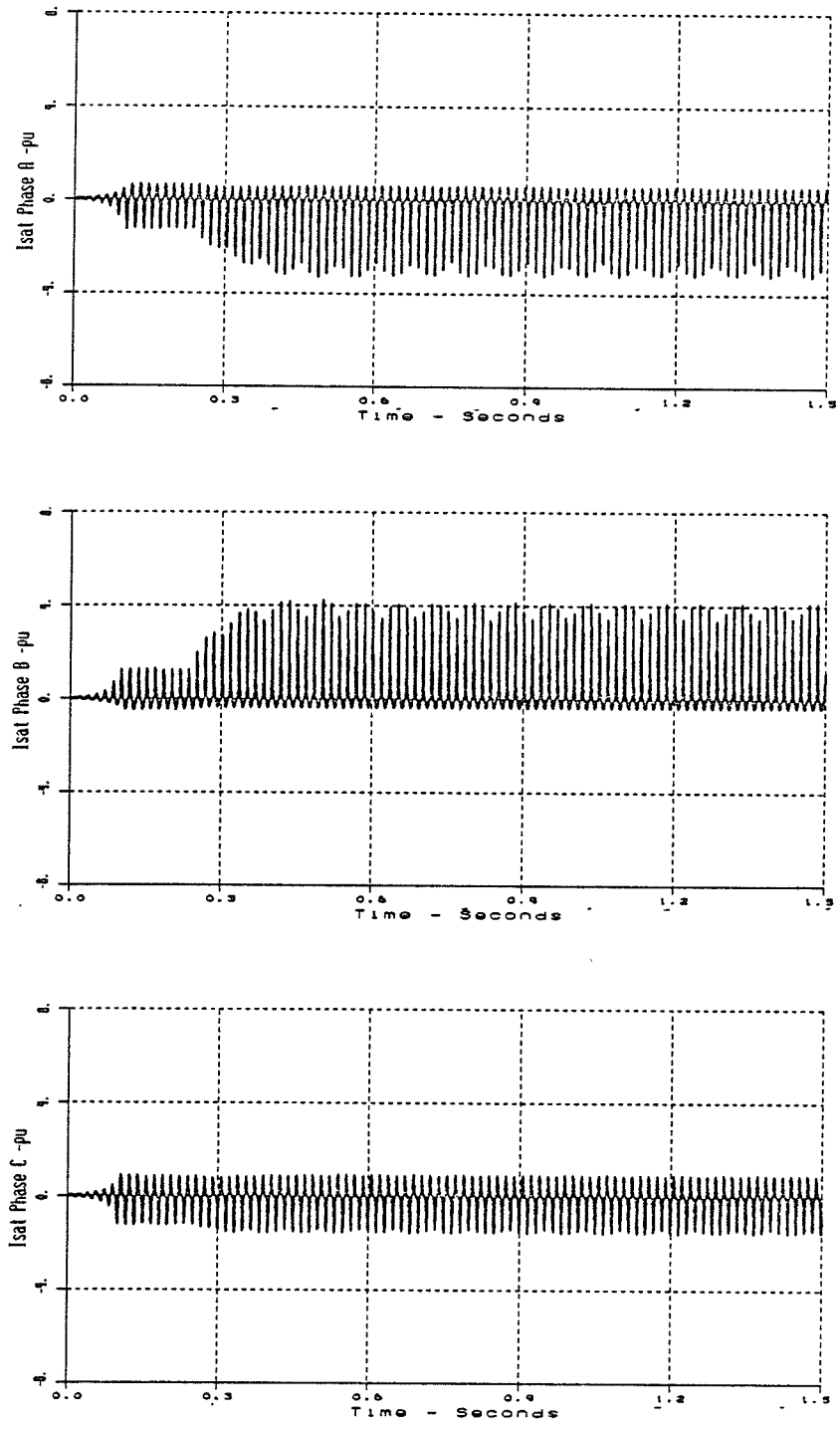

Figure 4.19 Transformer Saturation Current Waveforms, Control of the Positive Sequence DC Component of TCR Line Current, Alpha = 0°, Source: 2nd Harmonic Voltage 30% @ -30°

4.6 Summary and Conclusions

Sinusoidal modulation of the TCR firing angle was successfully applied to eliminate the dc component from the positive sequence of the TCR line current in all cases.

Sinusoidal modulation of the TCR firing angle was also successfully applied to eliminate the second harmonic component from the positive sequence of the TCR line current, except in the case where the TCR firing angle was 0°. In this case the modulation signal required by the controller to cancel the second harmonic component exceeded 90°, resulting in firing of only one of the antiparallel thyristor pairs in a phase. The modulation controller reduced the magnitude but did not entirely eliminate the second harmonic component.

When firing angle limits were encountered, the fundamental frequency TCR loading was reduced by the firing angle modulation. The reduction was as high as 50% for second harmonic component control, and about 20% for the dc component control. The reduction associated with the second harmonic modulation was likely only higher in this case because of the larger magnitude of second harmonic present for the situation under study. This type of reduction is unaccept-

able in practical situations as it could result in voltage instability. A control strategy would have to be designed such that the operating point of the TCR that is estabished by the fundamental frequency voltage controller allow for a reasonable modulation range during times when the system is susceptible to resonance conditions. Modulation angle limits would also have to be applied.

Elimination of the dc component from the positive sequence of the TCR line current also reduced the second harmonic component by about 12% to 41% (with increasing firing angle).

Elimination of the second harmonic component from the positive sequence of the TCR line current, on the other hand, caused the dc component to approximately double in magnitude.

Firing angle modulation caused the peak magnitude of the transformer saturation current to increase. The increase was quite moderate in the case of the dc component control, even when firing angle limitations where encountered. The increase was quite large in the case of second harmonic component control, especially when firing angle limits were encountered.

Complete control of the second harmonic component may not always be feasible due to a strong interaction with the transformer saturation. Modulation angle limits would have to be applied to avoid severely reducing the fundamental frequency TCR current.

CHAPTER FIVE

PERFORMANCE OF AN SVC CONNECTED TO A STRONG AC NETWORK WHICH IS IN SECOND HARMONIC PARALLEL RESONANCE AT THE POINT OF SVC COUPLING.

5.1 Study Network

The performance of the TCR with sinusoidal firing angle modulation was evaluated with the SVC connected to an ac network characterized by a second harmonic parallel resonant condition at the point of SVC coupling. The single line diagram of the study network is shown in Figure 5.1, and the detailed three phase EMTDC simulation circuit is shown in Figure 2.2.

The rating of the SVC and the rating of the SVC step-up transformer were the same as used in Chapter 4.

The equivalent system parameters were chosen such that a second harmonic parallel resonance existed between the equivalent Thevenin reactance of the system and the equivalent shunt connected capacitive reactance. The Thevenin

reactance was chosen such that the three phase short circuit capacity of the system was approximately:

$$Ssc = \frac{(kV)^2}{Zs} = \frac{(120\ kV)^2}{3.0\ ohm} = 4\ 800\ MVA \qquad (5.1)$$

For a second harmonic parallel resonance to exist, the equivalent shunt capacitance rating is given by:

$$Scap = \frac{Ssc}{n^2} = 1\ 200\ Mvar \qquad (5.2)$$

where n is the harmonic number. The effective short circuit capacity at the point of SVC coupling was approximately:

$$Ssce = 3\ 600\ MVA \qquad (5.3)$$

The system damping angle is given by:

$$\phi = \tan^{-1} \frac{w_o\ Ls}{(\ Rs\ )} = \tan^{-1} \frac{3.0}{0.26} = 85° \qquad (5.4)$$

The system compensation ratio, defined for the SVC as:

$$SCR = \frac{Ssce}{Qsvc} = \frac{3600}{480} = 7.50. \qquad (5.5)$$

Considering the TCR alone the SCR is:

$$SCR = \frac{Ssce}{Qtcr} = 12.00. \qquad (5.6)$$

The TCR performance was evaluated at nominal firing angles of 0°, 20°, 30° and 45°. The study system fundamental frequency steady state conditions for each TCR firing angle are shown in Figure 5.2. The fundamental frequency Thevenin voltage source magnitude was adjusted to maintain 1.0 pu voltage at the point of coupling of the SVC to the high voltage system.

Table 5.1 shows the computed variation with frequency in the magnitudes of the fundamental and second harmonic impedances as observed from the point of SVC coupling to the high voltage system for TCR firing angles of 0°, 20°, 30° and 45°. The system is resonant at 120 Hz. Connection of the SVC shifts the resonant point to 115 Hz with the TCR firing angle = 0°. The resonant frequency and the second harmonic impedance decrease with increasing TCR firing angle. The system behaves capacitively at the second harmonic.

The solid line in Figure 5.3 shows the variation in system impedance with frequency as observed at the point of SVC

coupling to the system with the SVC connected and a firing angle of 0°. Clearly a parallel resonance exists near the second harmonic at 115 Hz. The dashed line, which represents the system impedance variation with frequency when the TCR reactor is not connected, is resonant at 110 Hz. The second harmonic impedance is 28.2 ohms.

Table 5.1 Study System Impedance Magnitude versus Frequency as Observed from the Point of SVC Coupling to the AC System

TCR Firing Angle	0°	20°	30°	45°
Frequency	Impedance Magnitude (Ohms)			
60 Hz	3.89	4.02	4.09	4.17
Resonant Point (- Hz)	102.60 (115)	98.02 (113)	95.84 (112)	92.83 (111)
120 Hz	50.65	38.76	34.88	31.06

The effective impedance of the TCR, given by:

$$Ztcr = \frac{\pi \; Xr \; n}{2 \; (\; \pi - \alpha o) + \sin 2 \; \alpha o)} \qquad 90° \leq \alpha o \leq 180, \quad (5.7)$$

was used to compute the apparent fundamental frequency TCR reactance at each firing angle. The variable Xr is the reactance of the TCR reactor and n is the harmonic number. Second harmonic current injection into the network at the point of SVC coupling can produce large second harmonic

voltages due to the high impedance. The voltage amplification due to the parallel resonance will become smaller as the TCR firing angle increases. A second harmonic voltage with a magnitude of 3.0% at -30° relative to the fundamental was superimposed on the fundamental source to provide the current injection required to excite the resonant condition.

5.2 Per unit System

The TCR reactor rating was used to define the per unit base quantities which are defined in Table 4.1. The per unit base used for the transformer saturation current was the rated winding magnetizing current.

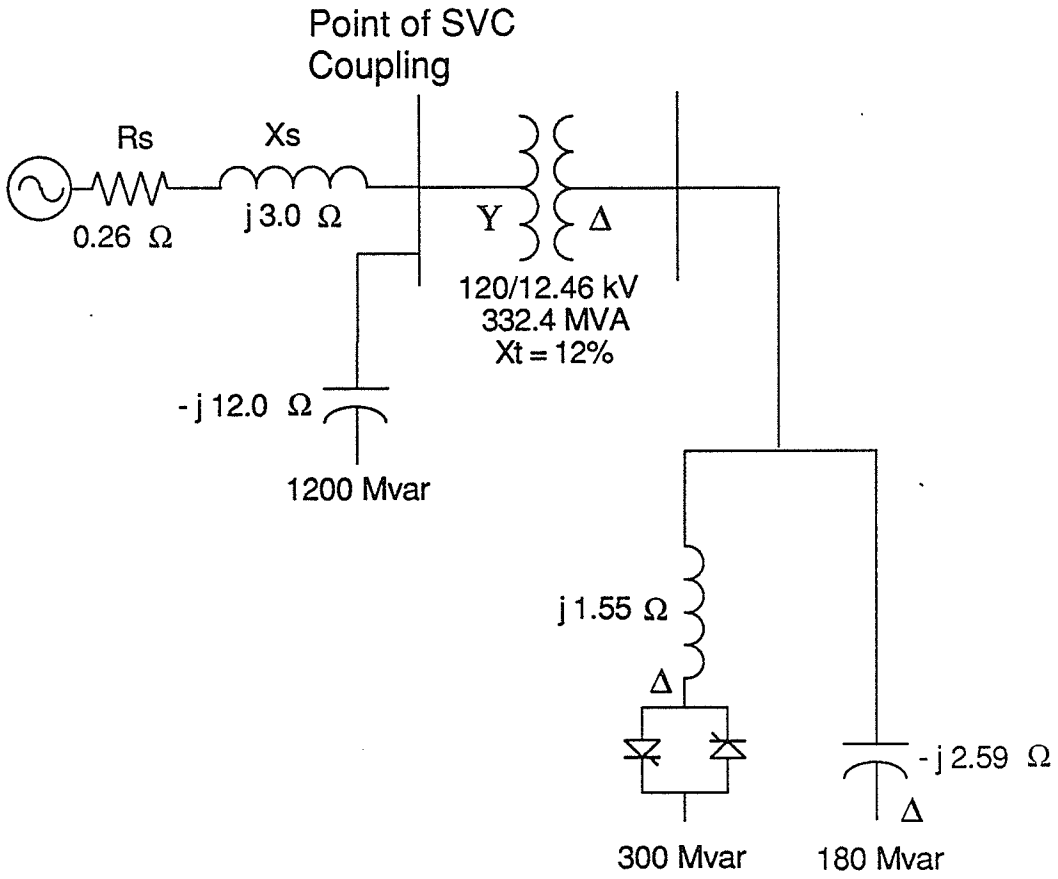

Figure 5.1 Study Network Single Line Diagram , System in Second Harmonic Parallel Resonance at the Point of SVC Coupling.

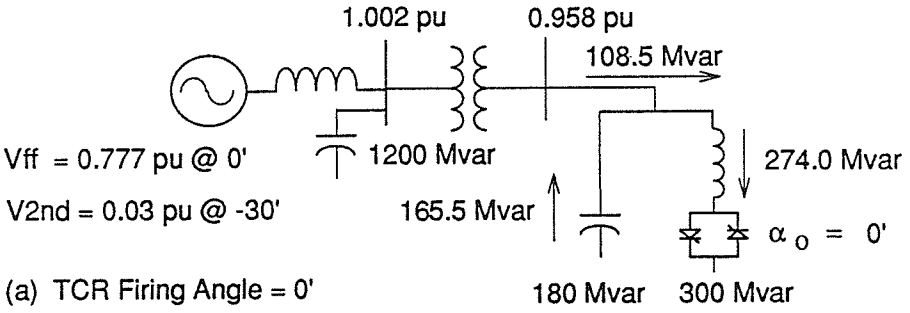

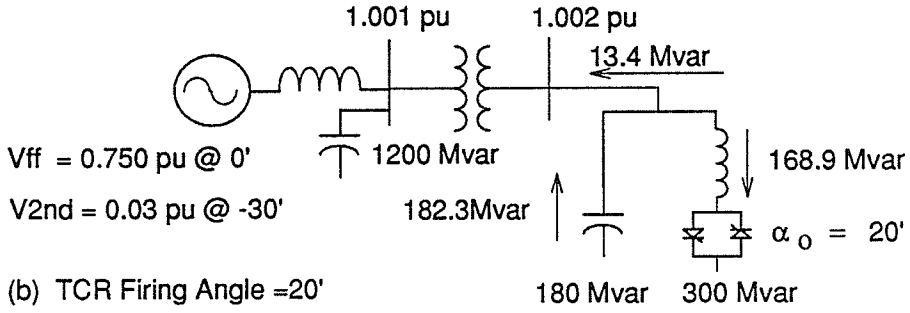

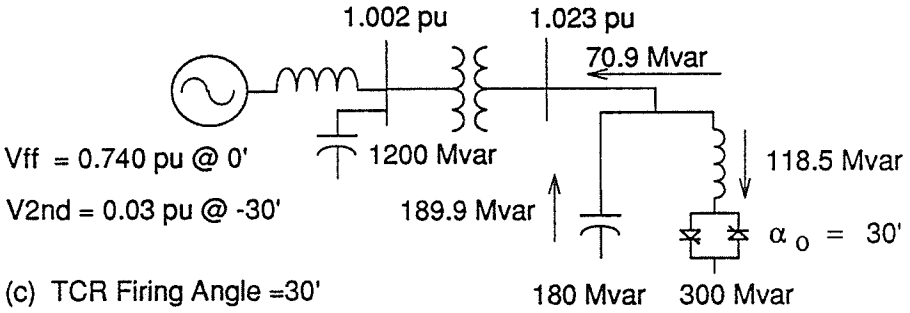

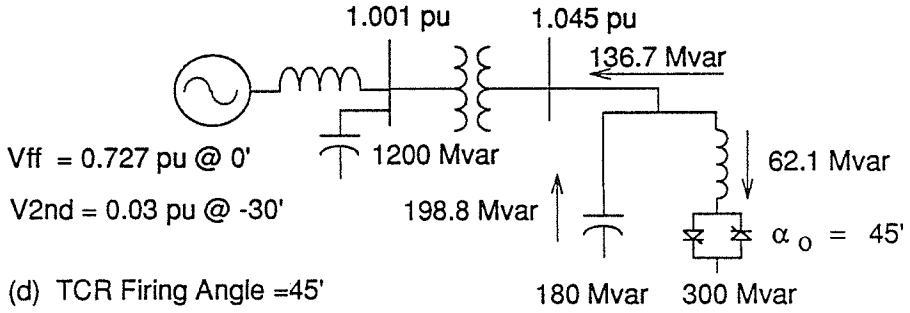

Figure 5.2 Study System Steady State Conditions

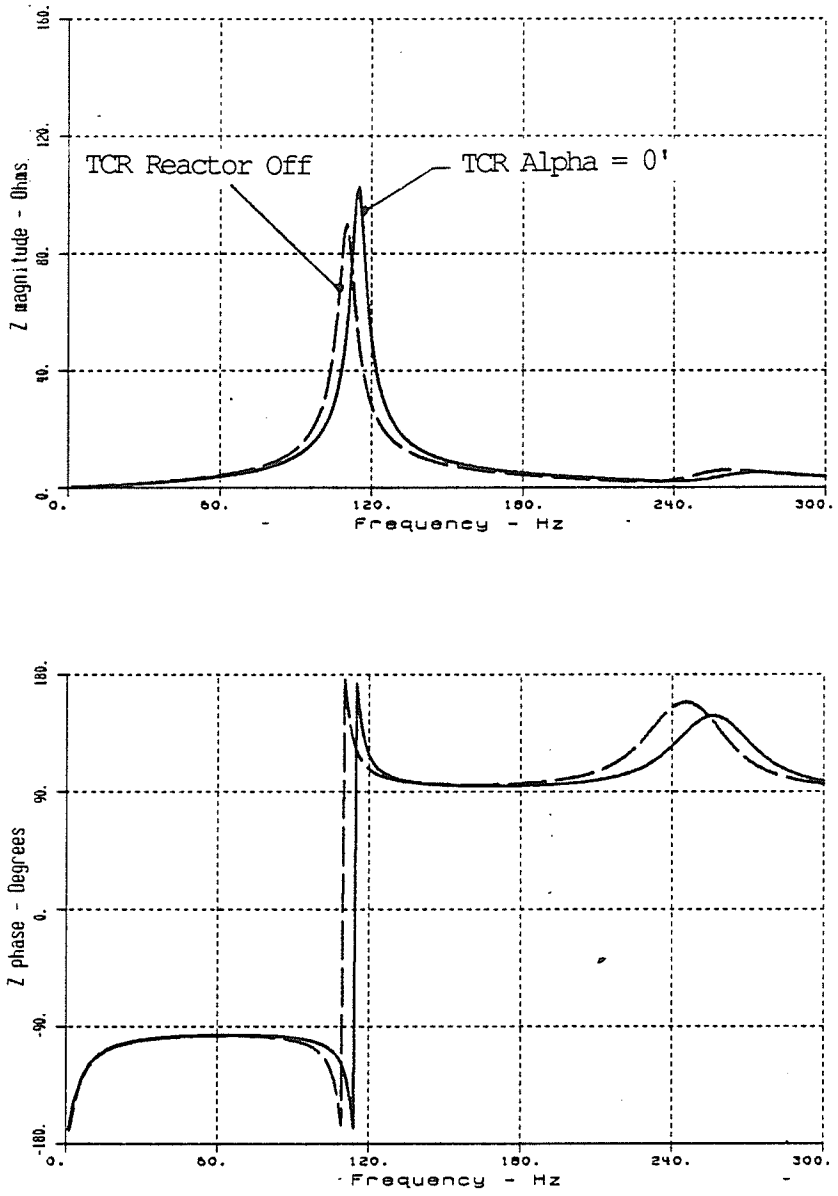

Figure 5.3 System Impedance vs. Frequency at the Point of SVC Coupling to the Network

5.3 TCR Performance with Equidistant Firing

The steady state positive sequence harmonic phasor components of some SVC variables are listed in Table 5.2 for equidistant firing of the TCR at 0°, 20°, 30° and 45°. A second harmonic parallel resonant condition exists between the equivalent system Thevenin reactance and the equivalent system shunt reactance at the point of SVC coupling to the 120 kV network.

The second harmonic source voltage of 3% @ -30° relative to the fundamental Thevenin source voltage was amplified by a factor of 8.4 at alpha = 0°, 7.6 at alpha = 20°, 6.9 at alpha = 30° and 5.9 at alpha = 45°. This second harmonic voltage amplification resulted in second harmonic voltage components ranging from 21.9% to 29.5% across the TCR terminals. This large second harmonic voltage caused severe distortion of the fundamental frequency TCR commutating voltage as was observed in Chapters 3 and 4. Unlike the previous chapters, the magnitude and phase displacement of the second harmonic voltage is now a function of the second harmonic impedance.

The dc component of the positive sequence TCR line current varied from 6.7% to 16.4% relative to the fundamental component over the TCR firing range, while the second harmonic

component varied from 15.3% to 32.8%. The TCR fundamental frequency current, terminal voltage and absorption are comparable to the results in Table 4.3 where a 30% second harmonic voltage was applied.

Figure 5.4 shows the steady state TCR waveforms for the case of alpha = 30°. The second harmonic voltage component of the secondary line voltage was displaced by -178° relative to the fundamental, resulting in a different voltage waveform distortion pattern as compared to Figure 4.3 (-30° displacement). The equidistant TCR firing, due to the non-equidistant voltage waveform zero crossings, resulted in the TCR phase current being unsymmetrical relative to the zero current axis. The TCR line current waveforms plotted in Figure 5.5 clearly contain a dc component.

The measured real and imaginary parts of the dc, 60 Hz and 120 Hz components of the positive sequence TCR line current are shown in Figure 5.6 for TCR firing at 30°. The measured components agree closely with the Fourier analysis results listed in Table 5.2.

Figure 5.7 shows the SVC transformer saturation current waveforms for TCR equidistant firing at 30°. The currents are clearly non-symmetrical. A peak saturation current of

about 3.0 pu (6% of rated transformer winding current) was observed.

Table 5.2 Positive Sequence SVC Variables with Equidistant Firing of the TCR, Transformer Saturation Modelled, SVC Connected to 2nd Harmonic Parallel Resonant Network, Source 2nd Harmonic Voltage: 3% @ -30°

Firing Angle	Alpha = 0°	Alpha = 20°	Alpha = 30°	Alpha = 45°
Variable	pu /-°	pu /-°	pu /-°	pu /-°
TCR Line Current				
DC Comp.	0.064/ 58°	0.058/ 23°	0.049/ 8°	0.031/- 2°
60 Hz Comp.	0.953/-121°	0.562/-122°	0.386/-123°	0.189/-123°
120 Hz Comp.	0.146/ 59°	0.123/ 71°	0.099/ 81°	0.062/ 93°
Xfmr Primary Line Current				
DC Comp.	0.061/ 88°	0.056/ 55°	0.047/ 41°	0.030/ 34°
60 Hz Comp.	0.415/-88°	0.023/- 3°	0.187/ 82°	0.392/ 85°
120 Hz Comp.	0.200/-98°	0.195/-100°	0.198/-103°	0.205/-105°
Xfmr Saturation Current				
DC Comp.	0.083/-79°	0.109/- 81°	0.132/- 82°	0.163/- 80°
60 Hz Comp.	0.632/ 96°	0.781/ 96°	0.894/ 96°	1.042/ 95°
120 Hz Comp.	0.257/-89°	0.320/- 87°	0.365/- 86°	0.421/- 89°
Primary Line Voltage				
DC Comp.	0.0005/- 87°	0.0005/- 98°	0.0005/ 137°	0.0008/ 123°
60 Hz Comp.	1.002 /- 2°	1.001 /- 2°	1.002 /- 2°	1.001 /- 2°
120 Hz Comp.	0.252 / 179°	0.228 /-177°	0.206 /-175°	0.176 /-177°
120 Hz Amplification	8.40	7.60	6.87	5.87
Secondary Line Voltage				
DC Comp.	0.0009/- 93°	0.0009/-113°	0.0007/ 165°	0.0007/ 144°
60 Hz Comp.	0.958 /- 2°	1.002 /- 2°	1.023 /- 2°	1.045 /- 3°
120 Hz Comp.	0.295 /-178°	0.269 /-179°	0.247 /-178°	0.219 /-179°
TCR 60 Hz Absorption Mvar	273.9	168.9	118.5	62.1

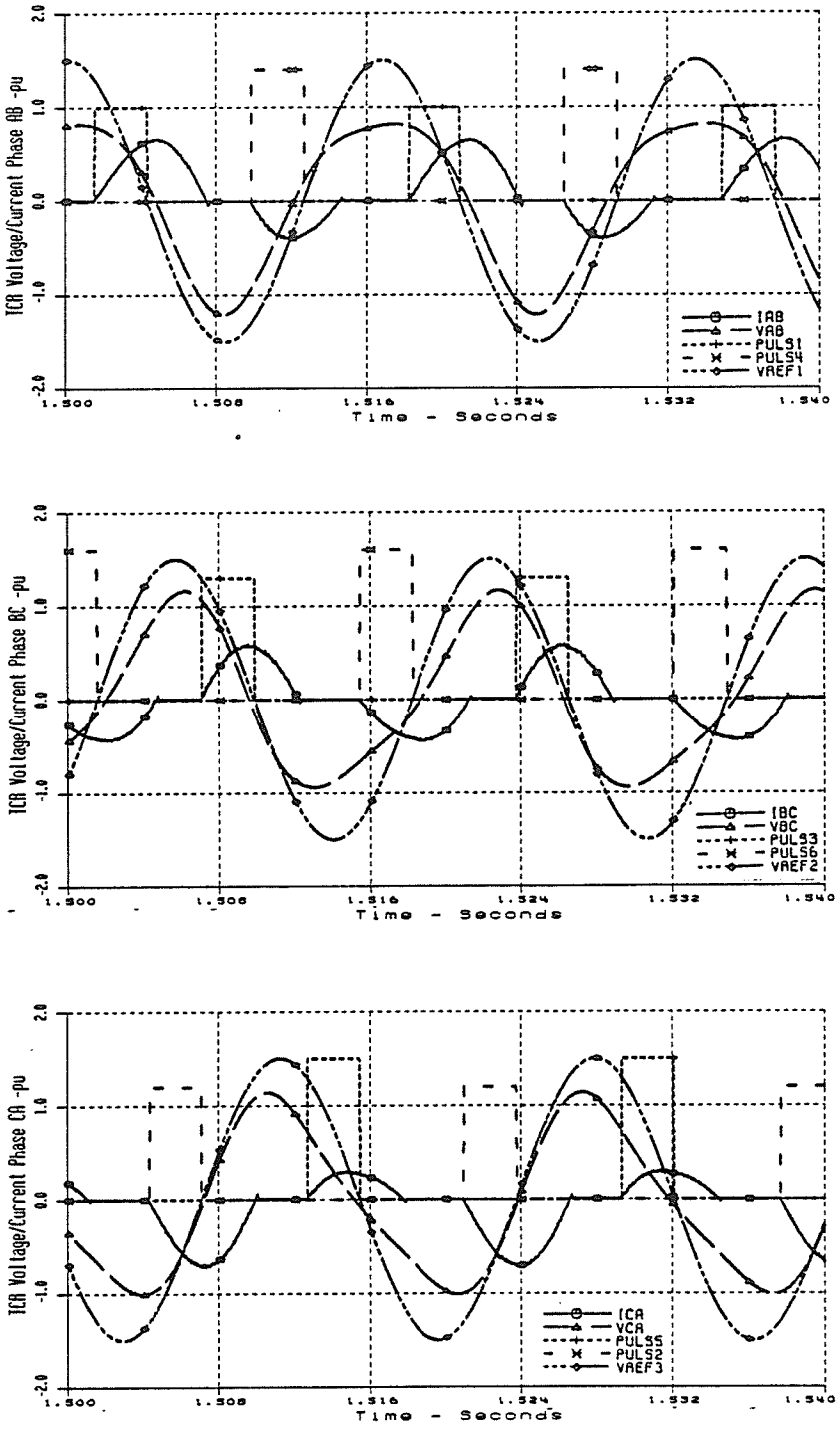

Figure 5.4 TCR Waveforms with Equidistant Firing, Alpha = 30°, 2nd Harmonic Parallel Resonant Network, Source 2nd Harmonic Voltage: 3% @ -30°

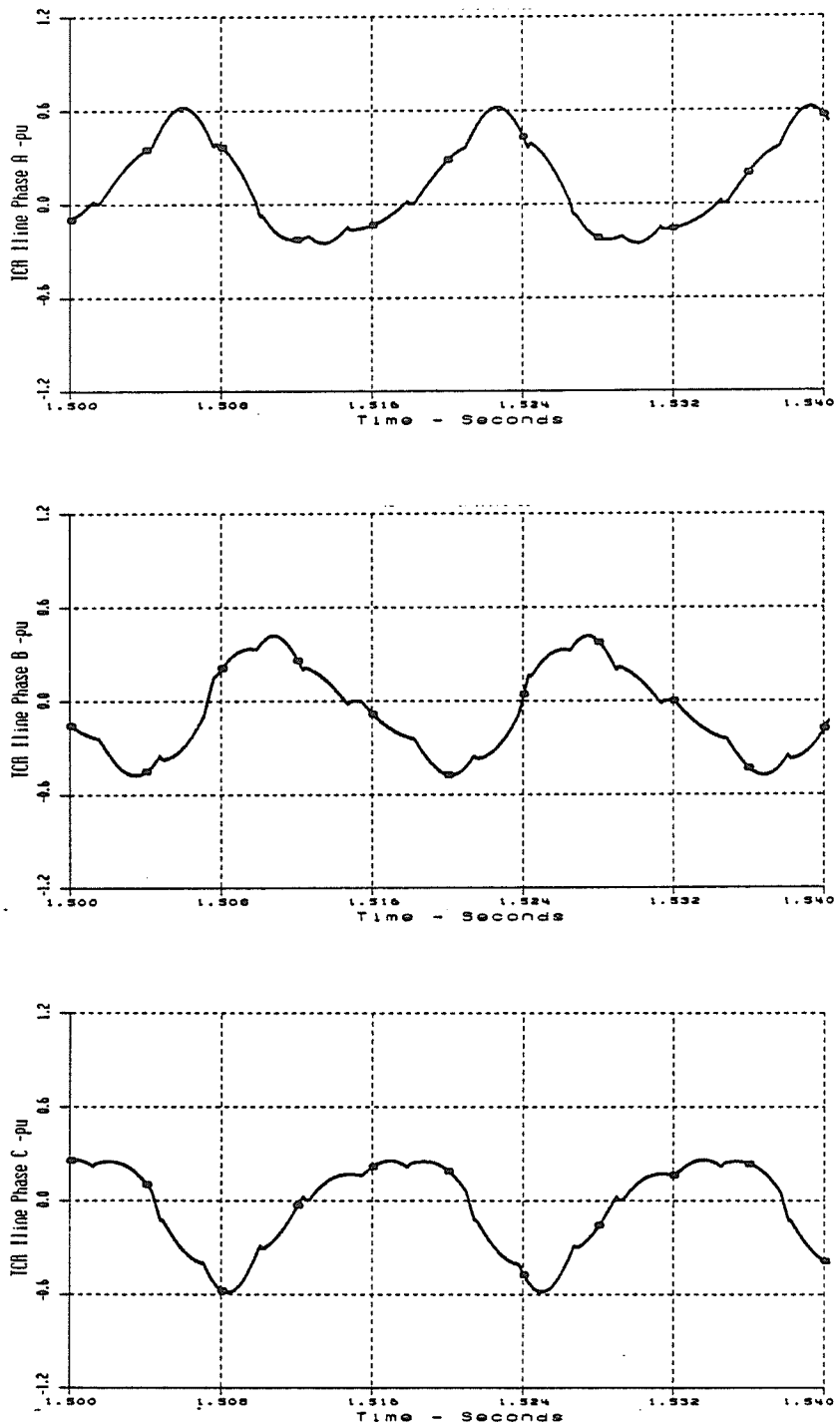

Figure 5.5 TCR Line Current Waveforms with Equidistant Firing, Alpha = 30°, 2nd Harmonic Parallel Resonant Network, Source 2nd Harmonic Voltage: 3% @ -30°

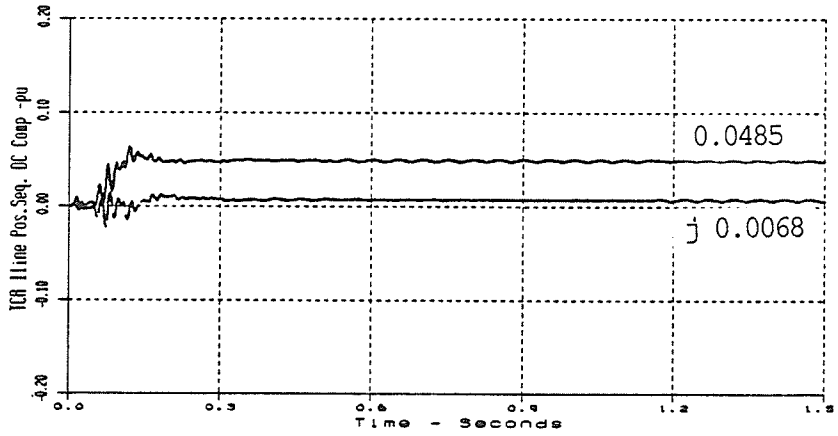

a) Real/Imaginary DC Components - pu

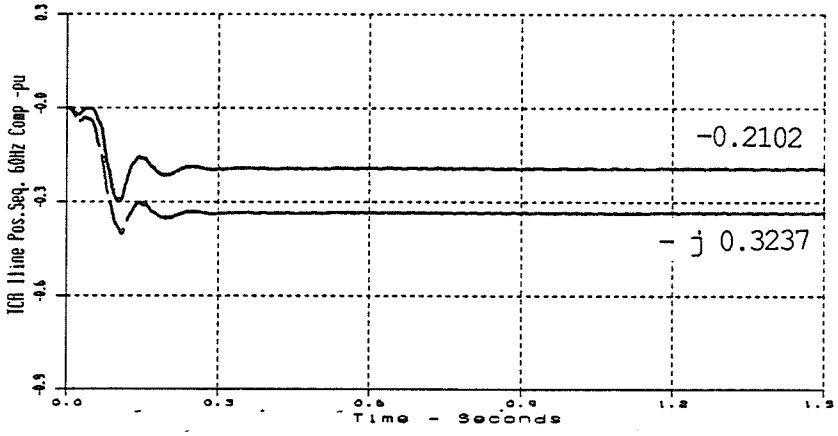

b) Real/Imaginary 60 Hz Components - pu

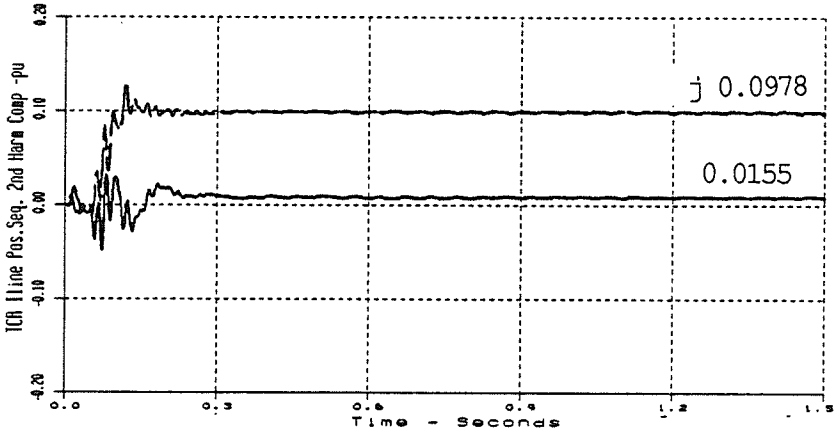

c) Real/Imaginary 2nd Harmonic Components - pu

Figure 5.6 Positive Sequence Phasor Components of TCR Line Current with Equidistant TCR Firing, Alpha = 30°, 2nd Harmonic Parallel Resonant Network, Source 2nd Harmonic Voltage: 3% @ -30°

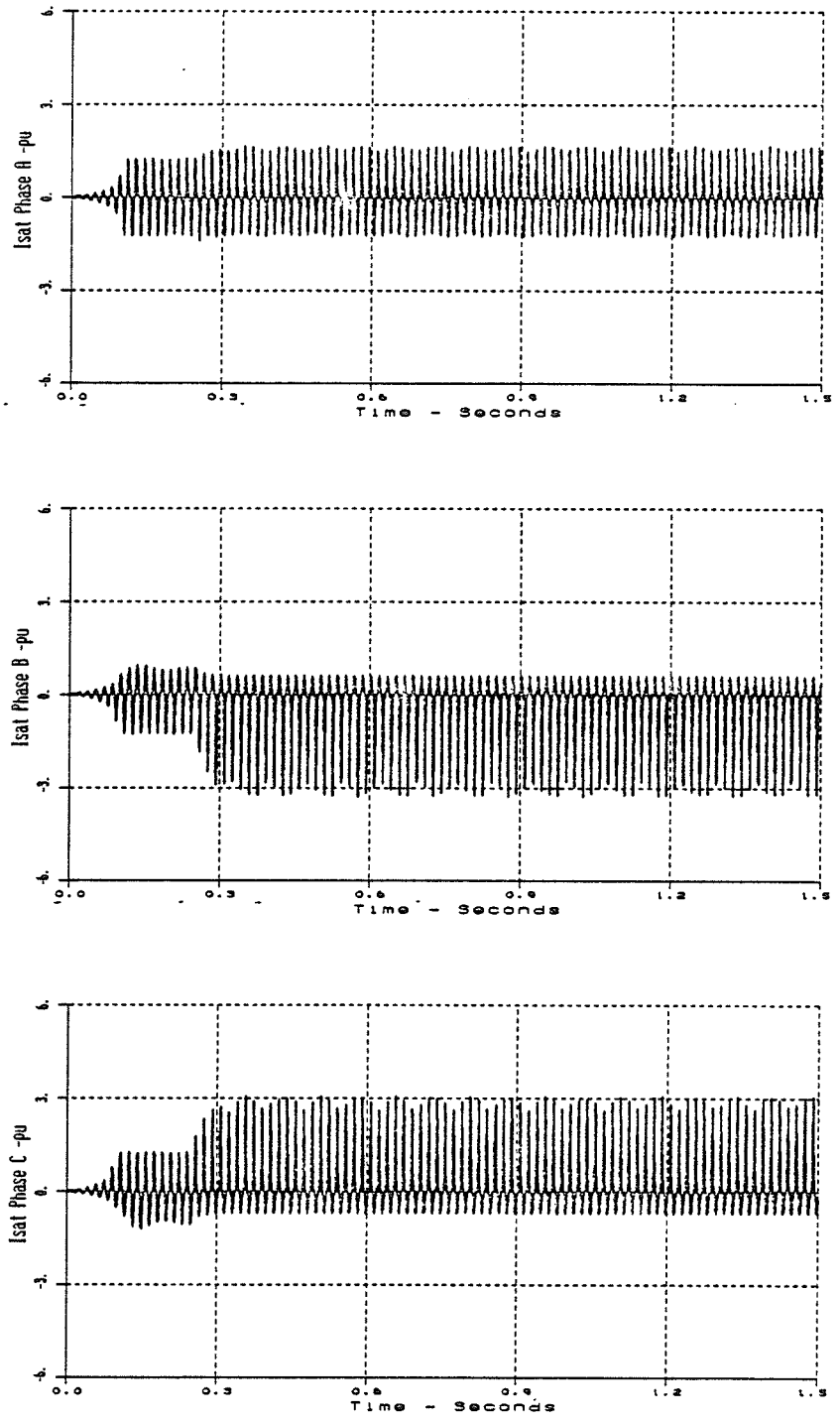

Figure 5.7 Transformer Saturation Current Waveforms with Equidistant TCR Firing, Alpha = 30°, 2nd Harmonic Parallel Resonant Network, Source 2nd Harmonic Voltage: 3% @ -30°

5.4 TCR Performance Using Firing Angle Modulation to Control the Positive Sequence Second Harmonic Phasor Component of the TCR Line Current

The measured real and imaginary second harmonic phasor components of the positive sequence TCR line current were input to the TCR firing angle modulation controller to generate a modulation signal to cancel the second harmonic component. The controller settings that were applied are listed in Table 3.3

The steady state positive sequence harmonic phasor components of some SVC variables and the modulation parameters are presented in Table 5.3 for nominal TCR firing angles of 0°, 20°, 30° and 45°.

Sinusoidal modulation of the TCR firing angle successfully eliminated the second harmonic component from the positive sequence of the TCR line current for all the nominal TCR firing angles considered.

Firing angle limits were encountered at nominal TCR firing angles of 0° and 20°. Clearly at alpha = 0°, the modulation is one sided as limits are encountered for any modulation magnitude and phase. The modulation magnitude required at

alpha = 0° was almost double that required at alpha = 20° although the second harmonic component of the TCR line current was only 19% larger.

Furthermore, the one sided modulation at alpha = 0° reduced the 60 Hz TCR loading to 73% of the no modulation case. The TCR loading at other firing angles was not significantly changed by the modulation.

Modulation of the TCR firing clearly caused some interaction with the system. The second harmonic voltage amplification was reduced by 43% at alpha = 0°, 38% at alpha = 20°, 31% at alpha = 30° and by 19% at alpha = 45° relative to the "no modulation" cases in Table 5.2. With a system compensation ratio of 12.0, the TCR would not be expected to influence the system resonance significantly. However, some reduction in the positive sequence second harmonic voltage was obtained. Since the second harmonic component of the TCR line current is reduced to zero by the firing angle modulation the TCR reactor impedance can be considered infinite. Consequently, the system resonant frequency is shifted away from 120 Hz towards the dashed line in Figure 5.3. This shift in resonant frequency lowers the system impedance at the second harmonic, which results in a lower second harmonic voltage component at the point of SVC coupling to the system.

Figures 5.8 and 5.9 respectively show the TCR waveforms and the TCR line current waveforms for the case of alpha = 30°. The TCR firing is noted to be non-equidistant.

The elimination of the second harmonic component increased the dc component by 84% at 0°, 96.6% at 20° and 24.5% at 30° relative to the "no modulation" case values (Table 5.2). At alpha = 45°, the dc component is reduced by 26%.
Figure 5.10 shows the measured positive sequence dc and 60 Hz components of the TCR line current for TCR firing at 30°. The magnitude of the dc component is increased from 0.049 pu @ 8° (no modulation value) to 0.061 pu @ -113° by the modulation controller action. The 60 Hz component is not changed by the modulation.

Figure 5.11 shows the measured positive sequence second harmonic component of TCR line current and the modulation controller output for TCR firing at 30°. The second harmonic is reduced from 0.099 pu @ 81° to zero in about 300 ms including settling time. The modulation controller output corresponds to a modulation peak of 18.6° and a modulation phase of -83.3°. The response of the controller was very stable and similar at all the TCR firing angles examined.

Figure 5.12 shows the SVC transformer saturation current waveforms for the nominal TCR firing angle of 30°. The modulation controller was activiated at 0.40s, and caused the transformer saturation current to increase initially. However, as the modulation reduced the second harmonic voltage distortion due to the parallel resonance, the peak saturation current was reduced. The envelope of the saturation current (phase B) settled out at 3.0 pu or 6% of the rated transformer current. Comparison of the steady state phasor components of saturation current listed in Tables 5.2 and 5.3 illustrates that the firing angle modulation caused a reduction in the transformer saturation current components except at the TCR firing angle of 0°. Comparison of Figures 5.7 and 5.12 also illustrates this result.

Table 5.3 Positive Sequence SVC Variables With TCR Firing Angle Modultion Control of the Positive Sequence 2nd Harmonic Component of TCR Line Current, Transformation Saturation Modelled, 2nd Harmonic Parallel Resonant Network, Source 2nd Harmonic Voltage: 3% @ -30°

Firing Angle / Variable	Alpha = 0° pu /-°	Alpha = 20° pu /-°	Alpha = 30° pu /-°	Alpha = 45° pu /-°
TCR Line Current				
DC Comp.	0.118 /-105°	0.114 /-111°	0.061/-113°	0.023/ -112°
60 Hz Comp.	0.652 /-121°	0.541 /-121°	0.385/-121°	0.185/ -121°
120 Hz Comp. *	0.0007/-147°	0.0005/-148°	0.0019/-59°	0.0015/-146°
Xfmr Primary Line Current				
DC Comp.	0.111/- 76°	0.106/- 81°	0.056/- 84°	0.019/- 86°
60 Hz Comp.	0.086/- 70°	0.038/ 37°	0.192/ 80°	0.399/ 84°
120 Hz Comp.	0.221/-107°	0.221/-107°	0.222/-106°	0.221/-107°
Xfmr Saturation Current				
DC Comp.	0.118/- 68°	0.088/- 66°	0.105/- 66°	0.143/- 71°
60 Hz Comp.	0.844/ 96°	0.739/ 96°	0.832/ 95°	1.000/ 95°
120 Hz Comp.	0.297/-100°	0.236/-101°	0.280/-101°	0.367/-100°
Primary Line Voltage				
DC Comp.	0.0004/ 111°	0.0003/ 92°	0.0001/ 119°	0.00006/ 98°
60 Hz Comp.	1.030 /- 2°	1.003/- 2°	1.004/- 2°	1.002 /- 2°
120 Hz Comp.	0.143 / 168°	0.141/ 168°	0.143/ 168°	0.143 / 168°
120 Hz Amplification	4.77	4.70	4.77	4.77
Secondary Line Voltage				
DC Comp.	0.0012/105°	0.0011/ 92°	0.0005/101°	0.0008/100°
60 Hz Comp.	1.022/- 2°	1.006/- 2°	1.025/- 2°	1.046/- 3°
120 Hz Comp.	0.191/ 166°	0.189/ 166°	0.191/ 166°	0.191/ 167°
TCR 60 Hz Absorption Mvar (% No Modulation Case)	199.9 (73.0)	163.3 (96.7)	118.4 (99.9)	58.1 (93.5)
Modulation Peak/Phase	50.9/-100.3°	26.7/-92.4°	18.6/-83.3°	14.3/-66.9°
Δ ab	- 9.1°	- 1.1°	2.2°	5.6°
Δ bc	47.9°	23.6°	14.9°	8.6°
Δ ca	-38.8°	-22.5°	-17.1°	-14.2°

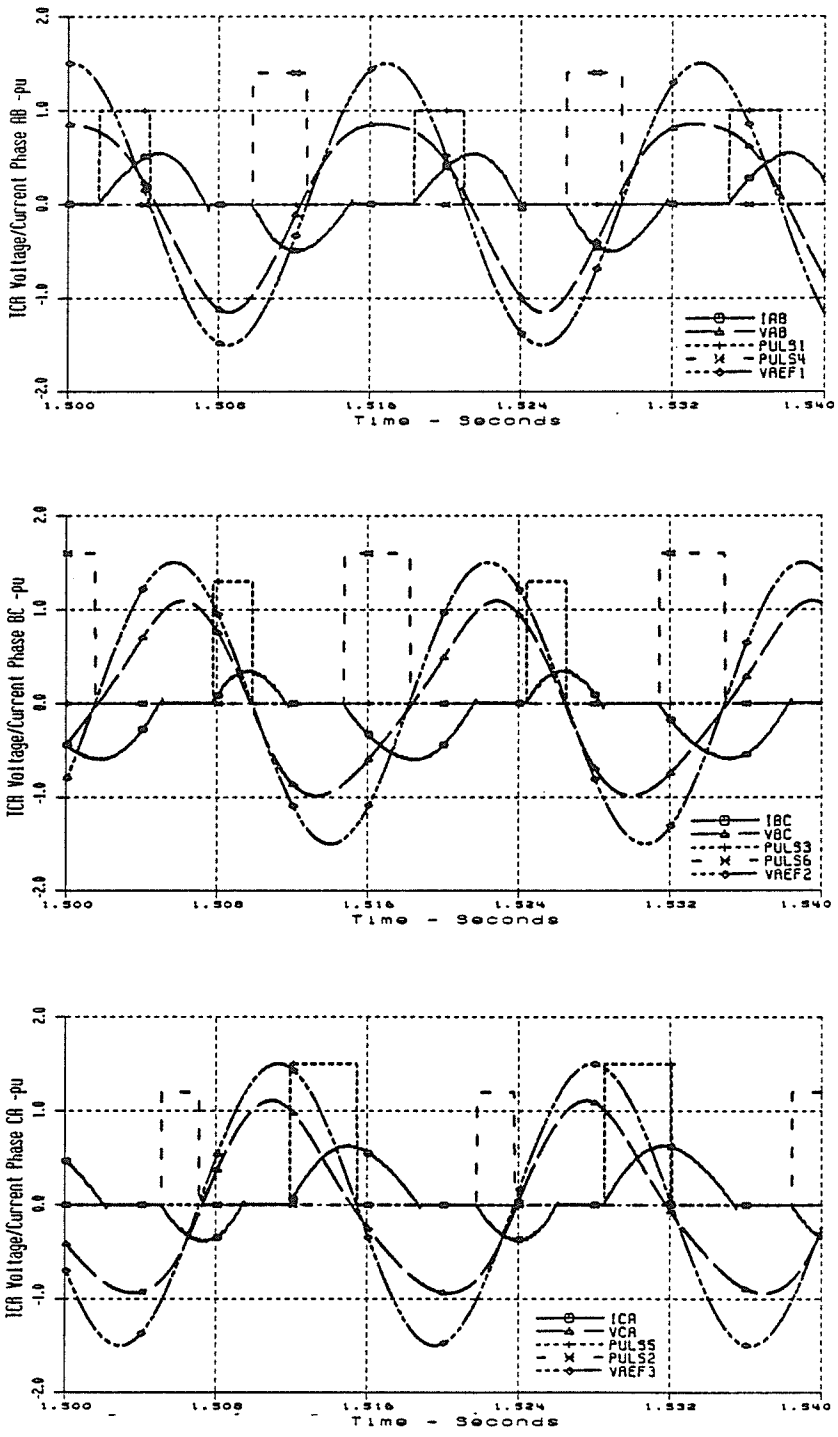

Figure 5.8 TCR Waveforms, Control of Positive Sequence 2nd Harmonic Component of TCR Line Current, Alpha = 30°, 2nd Harmonic Parallel Resonant Network, Source 2nd Harmonic Voltage: 3% @ - 30°

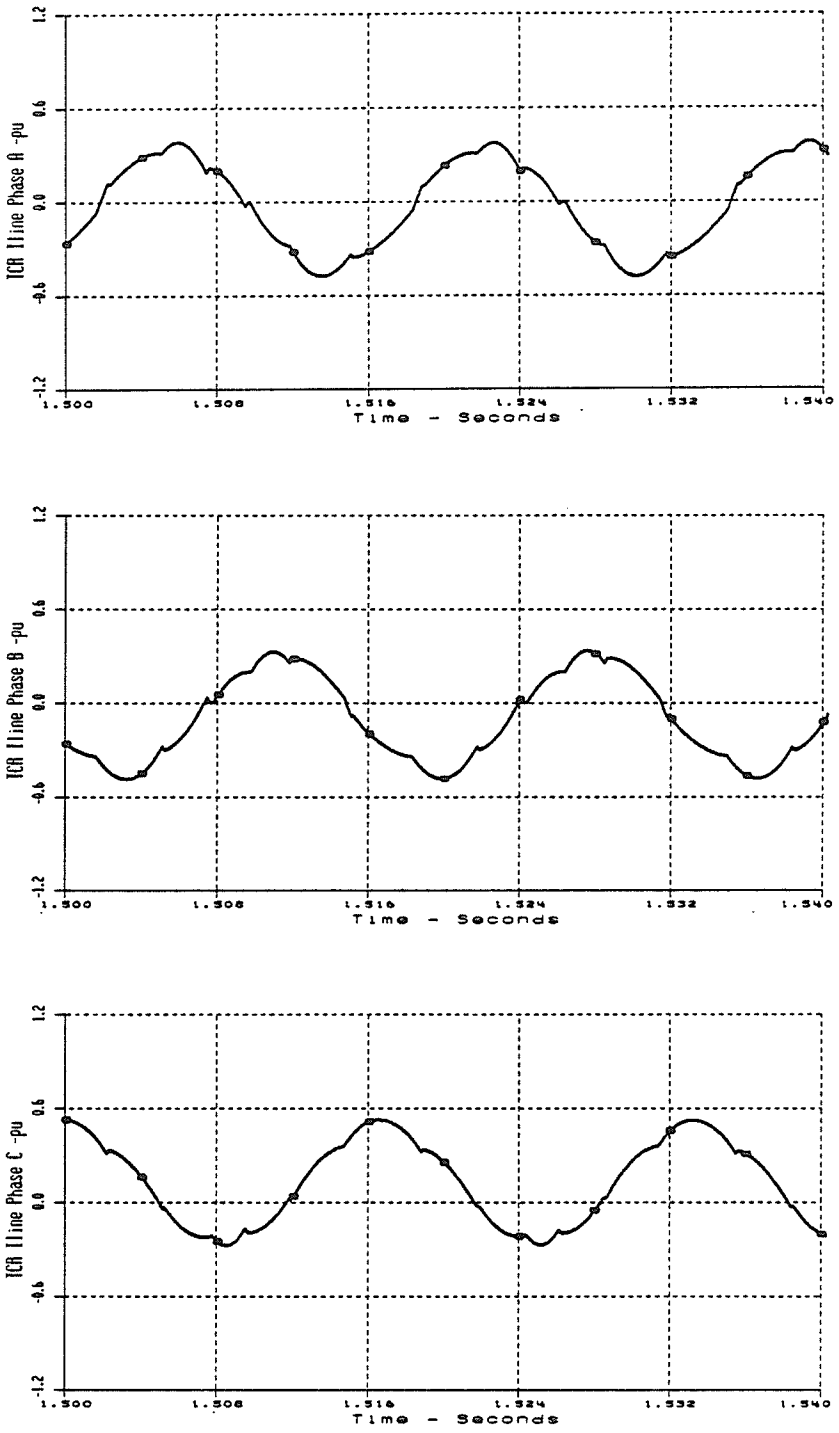

Figure 5.9 TCR Line Current Waveforms, Control of Positive Sequence 2nd Harmonic Component of TCR Line Current, Alpha = 30°, 2nd Harmonic Parallel Resonant Network, Source 2nd Harmonic Voltage: 3% @ -30°

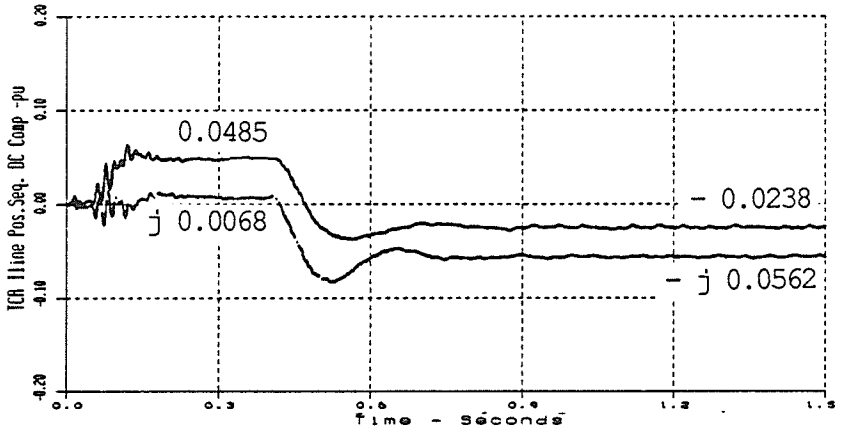

a) Real/Imaginary DC Components - pu

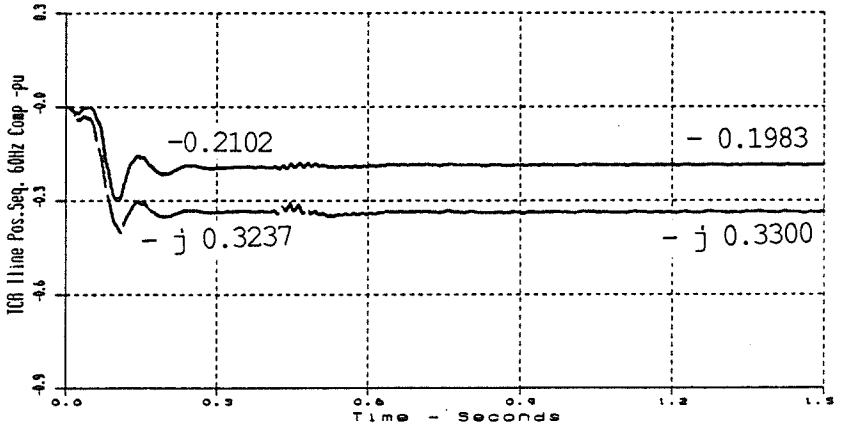

b) Real/Imaginary 60 Hz Components - pu

Figure 5.10 Effect of Control of the Positive Sequence 2nd Harmonic Component of TCR Line Current on the DC and 60 Hz Components, Alpha = 30°, 2nd Harmonic Parallel Resonant Network, Source 2nd Harmonic Voltage: 3% @ -30°

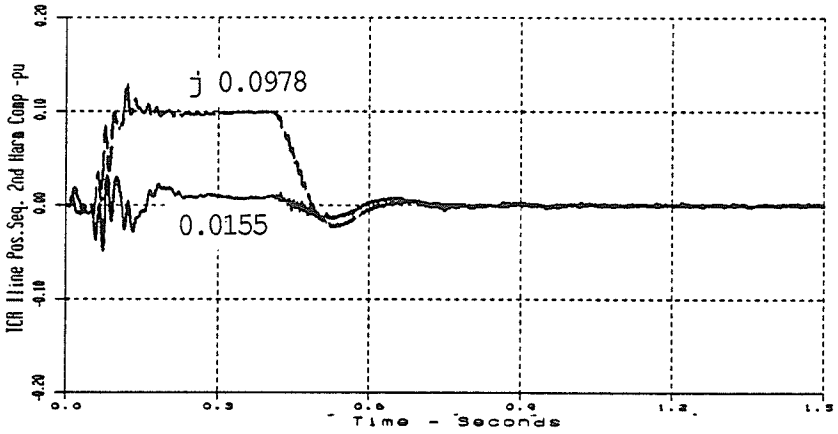

a) Real/Imaginary 2nd Harmonic Components - pu

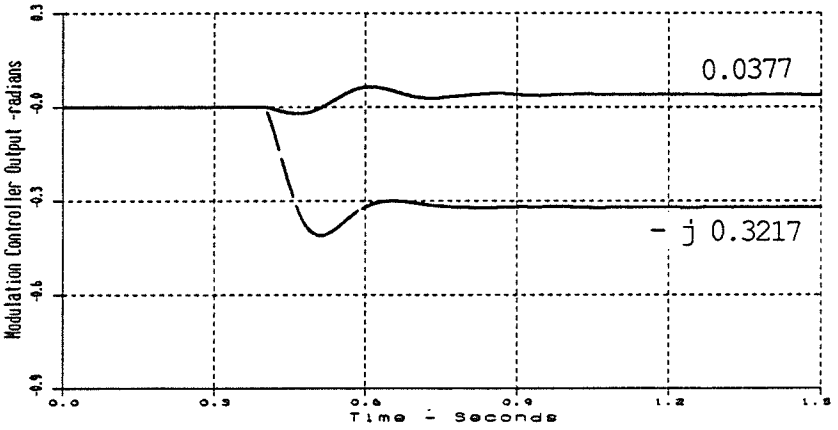

b) Real/Imaginary Modulation Controller Components - radians

Figure 5.11 Control of Positive Sequence 2nd Harmonic Component of TCR Line Current, Alpha = 30°, 2nd Harmonic Parallel Resonant Network, Source 2nd Harmonic Voltage: 3% @ -30°

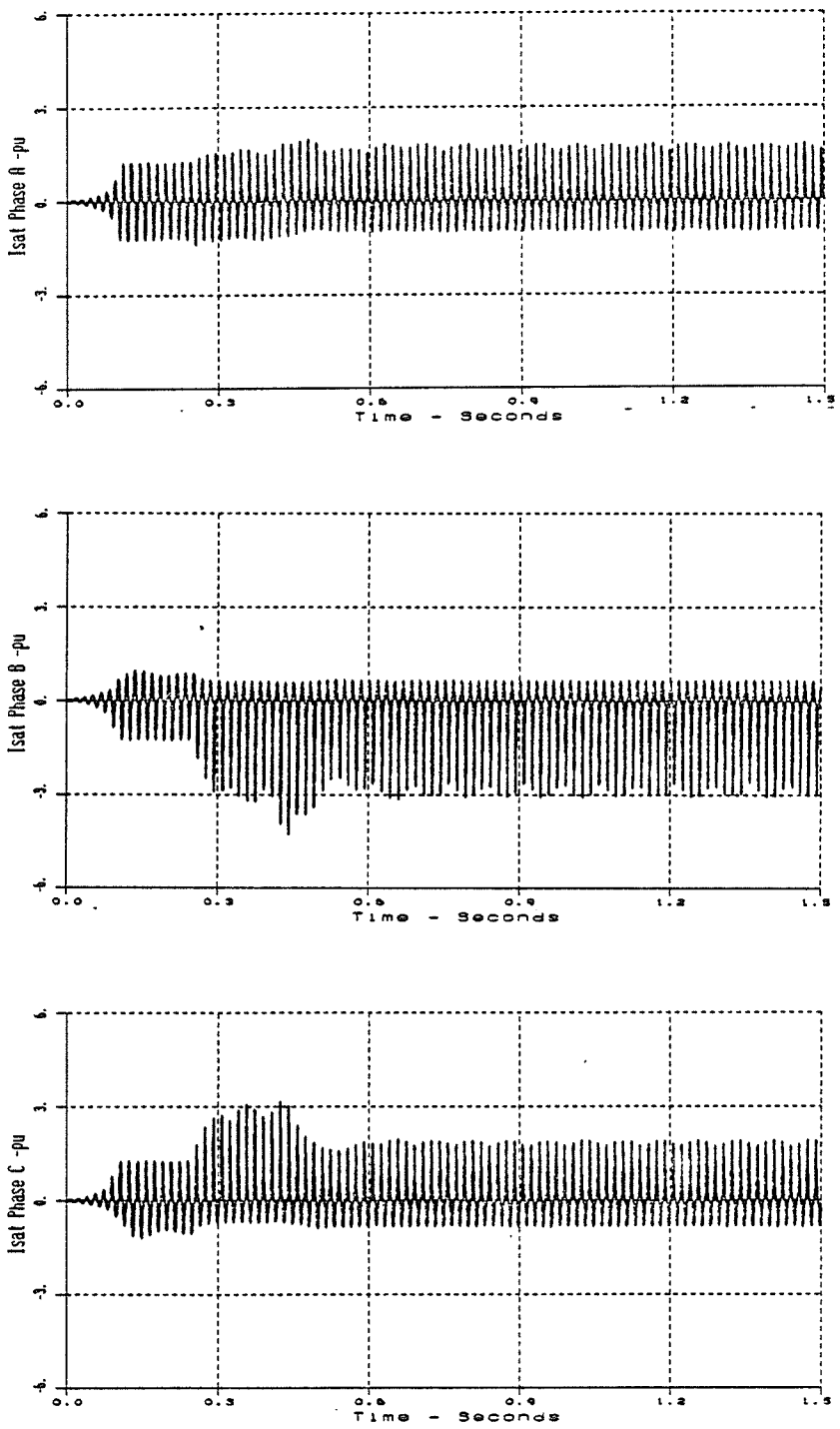

Figure 5.12 Transformer Saturation Current Waveforms, Control of Positive Sequence 2nd Harmonic Component of TCR Line Current, Alpha = 30°, 2nd Harmonic Parallel Resonant Network, Source 2nd Harmonic Voltage: 3% @ -30°

5.5 TCR Performance Using Firing Angle Modulation to Control the Positive Sequence DC Phasor Component of the TCR Line Current

The measured real and imaginary dc phasor components of the positive sequence TCR line current were input to the TCR firing angle modulation controller. The modulation signal was used to generate a dc component of the TCR line current, equal in magnitude to the measured input but 180° out of phase, so as to cancel the dc component. The controller settings that were applied are listed in Table 3.5.

The steady state harmonic phasor components of some SVC variables and the modulation parameters are listed in Table 5.4 for nominal TCR firing angles of 0°, 20°, 30° and 45°.

Sinusodial modulation of the TCR firing angle successfully eliminated the dc component from the positive sequence TCR line current at all nominal firing angles considered. Firing angle limits were only encountered at the nominal firing angle of 0°, where clearly, the modulation was one sided. The one sided dc modulation reduced the TCR loading at alpha = 0° to 91% of the "no modulation" case.

Modulation of the TCR firing angle resulted in only a 4.1% to 7.9% reduction in the second harmonic voltage amplification over the range TCR firing angle.

Figure 5.13 shows the TCR waveforms for the case of alpha = 30°. The TCR firing of each phase is modulated to eliminate the dc component in the TCR line current shown in Figure 5.14.

Elimination of the dc component from the TCR line current also reduced the second harmonic component. The second harmonic component was reduced by 16.4% at alpha = 0°, 26.8% at alpha = 20°, 37.4% at alpha = 30° and 51.6% at alpha = 45° relative to the "no modulation" case. Figure 5.15 shows the effect of the firing angle modulation on the 60 Hz and second harmonic components of the positive sequence TCR line current for the case where the nominal TCR firing angle was 30%.

Figure 5.16 shows the measured positive sequence dc component of TCR line current at alpha = 30°, and the modulation controller output. The dc component was reduced to zero in about 500 ms (including settling time) after the controller was activated. The modulation controller output corresponds to a modulation peak of 9.1° at a modulation

phase of -49.6°. The controller response was found to be stable and similar at all TCR firing angles examined.

Figure 5.17 shows the SVC transformer saturation current for the case where alpha = 30°. The modulation did not change the saturation current appreciably, as can be observed by comparison of Figures 5.7 and 5.17.

Comparison of the sequence components in Tables 5.2 and 5.4 indicates an increase in the saturation current components at the TCR firing angle of 0°. This is likely the effect of one-sided modulation due to TCR firing angle limits being encountered.

Table 5.4 Positive Sequence SVC Variables With TCR Firing Angle Modultion Control of the Positive Sequence DC Component of the TCR Line Current, Transformer Saturation Modelled, 2nd Harmonic Parallel Resonant Network, Source 2nd Harmonic Voltage: 3% @ -30°

Firing Angle	Alpha = 0°	Alpha = 20°	Alpha = 30°	Alpha = 45°
Variable	pu /-°	pu /-°	pu /-°	pu /-°
TCR Line Current				
DC Comp. *	0.0011/-123°	0.0014/- 17°	0.0010/-105°	0.0003/ 117°
60 Hz Comp.	0.848/-121°	0.561/-121°	0.385/-122°	0.185/-121°
120 Hz Comp.	0.122/ 58°	0.090/ 55°	0.062/ 52°	0.032/ 51°
Xfmr Primary Line Current				
DC Comp.	0.0003/-169°	0.0018/ 77°	0.0014/134°	0.0037/120°
60 Hz Comp.	0.299/-86°	0.028/ 1°	0.189/ 80°	0.398/ 84°
120 Hz Comp.	0.203/-99°	0.207/-101°	0.214/-103°	0.216/-104°
Xfmr Saturation Current				
DC Comp.	0.106/-78°	0.107/- 74°	0.133/- 73°	0.166/- 75°
60 Hz Comp.	0.715/ 96°	0.770/ 96°	0.890/ 95°	1.050/ 95°
120 Hz Comp.	0.300/-90°	0.035/- 94°	0.359/- 95°	0.425/- 97°
Primary Line Voltage				
DC Comp.	0.0003/-77°	0.0002/-58°	0.0002/-83°	0.0005/ 97°
60 Hz Comp.	1.012/- 2°	1.001/- 2°	1.003/- 2°	1.002 /- 2°
120 Hz Comp.	0.234/ 178°	0.210/ 175°	0.192/ 173°	0.169 / 171°
120 Hz Amplification	7.80	7.00	6.40	5.63
Secondary Line Voltage				
DC Comp.	0.0002/-81°	0.0002/-45°	0.0002/-88°	0.0005/ 97°
60 Hz Comp.	0.981/- 2°	1.001/- 2°	1.024/- 2°	1.046/- 3°
120 Hz Comp.	0.278/-176°	0.255/ 174°	0.239/ 171°	0.215/ 169°
TCR 60 Hz Absorption Mvar (% No Modulation Case)	249.6 (91.1)	168.5 (99.7)	118.3 (99.8)	58.1 (93.5)
Modulation Peak/Phase	17.6/86.3°	9.0/-61.4°	9.1/-49.6°	10.1/-37.9°
Δ ab	1.1°	4.3°	5.9°	8.0°
Δ bc	14.7°	4.7°	3.1°	1.4°
Δ ca	-15.8°	-9.0°	-9.0°	-9.4°

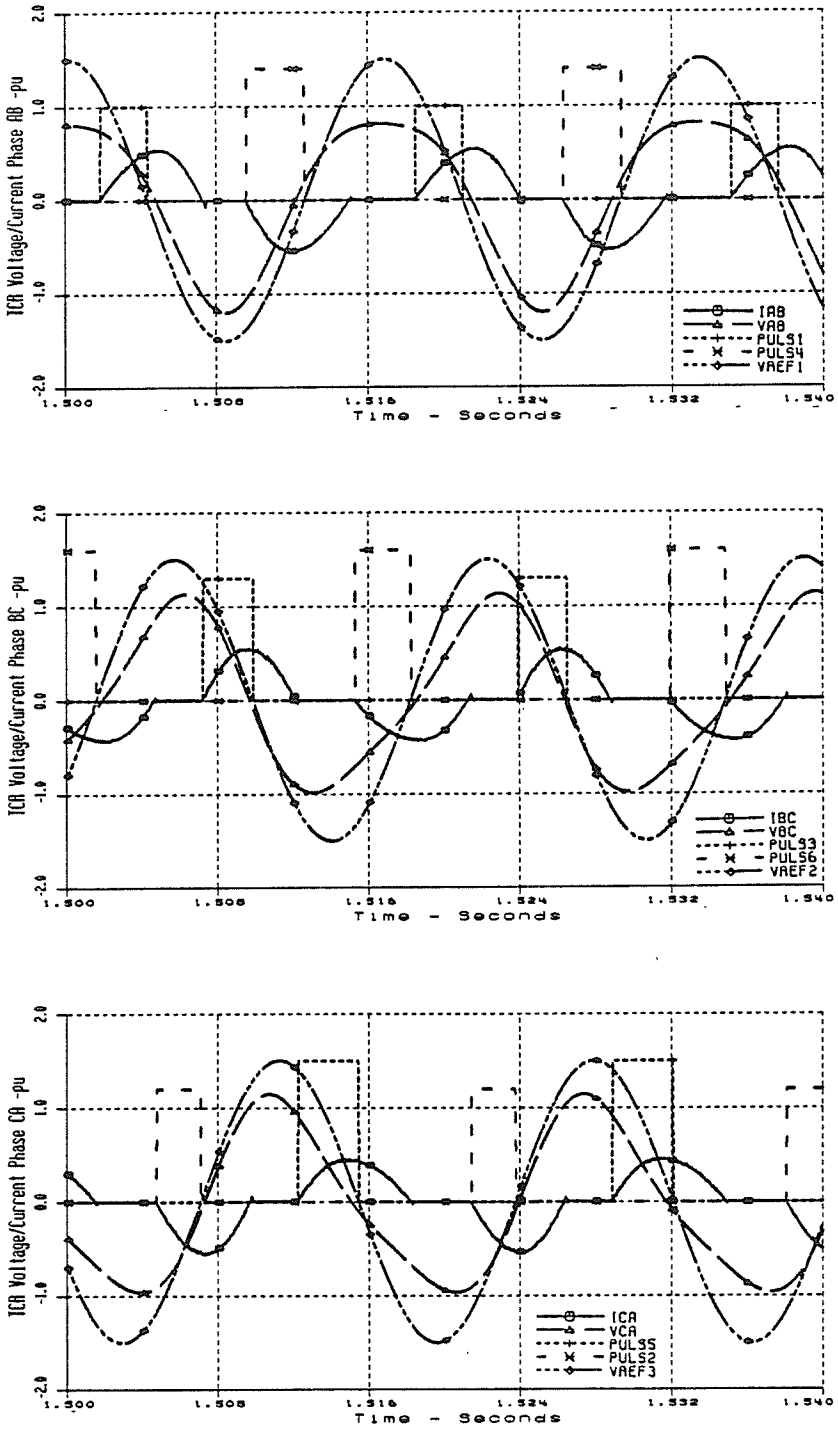

Figure 5.13 TCR Waveforms, Control of Positive Sequence DC Component of TCR Line Current, Alpha = 30°, 2nd Harmonic Parallel Resonant Network, Source 2nd Harmonic Voltage: 3% @ -30°

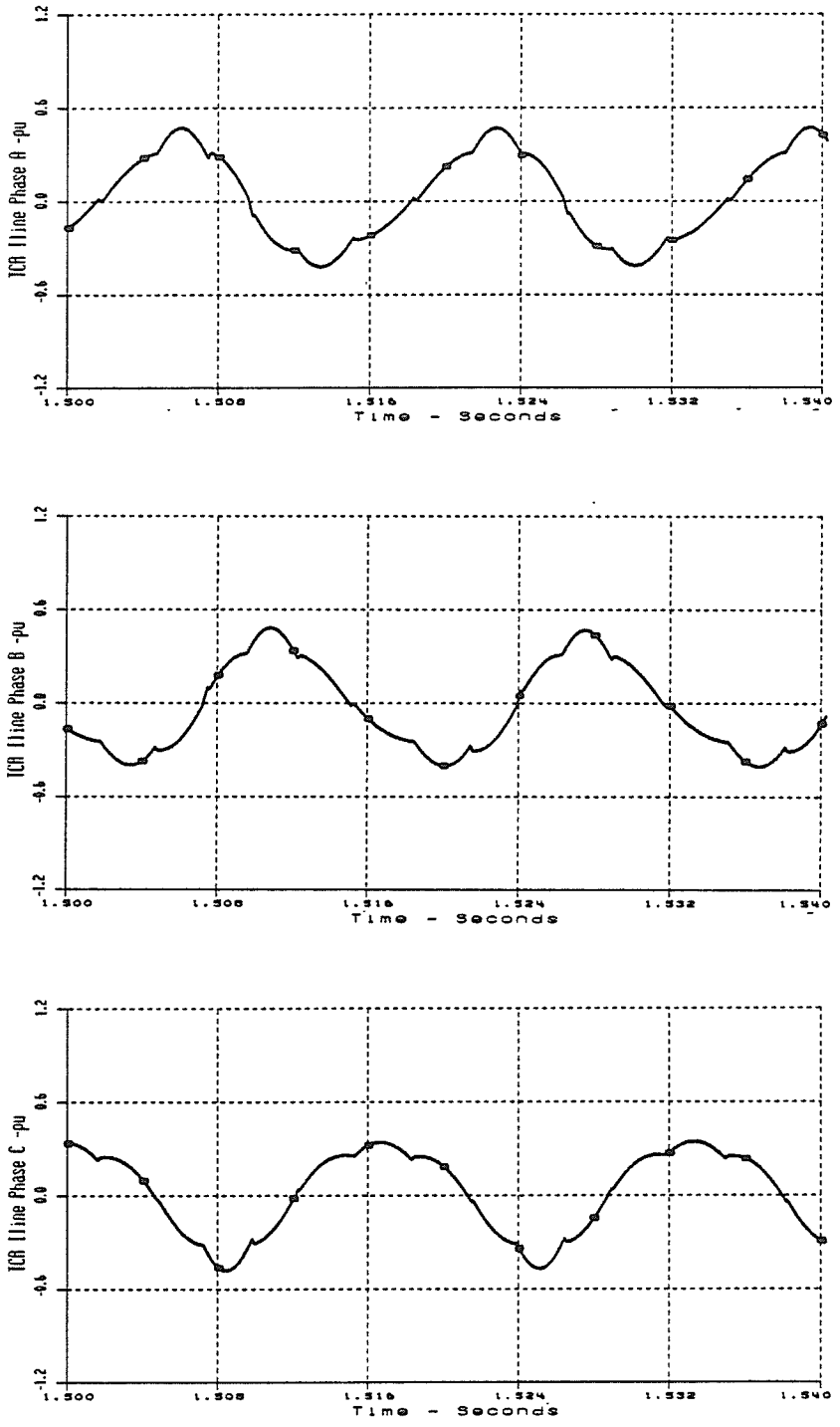

Figure 5.14 TCR Line Current Waveforms, Control of Positive Sequence DC Component of TCR Line Current, Alpha = 30°, 2nd Harmonic Parallel Resonant Network, Source 2nd Harmonic Voltage: 3% @ -30°

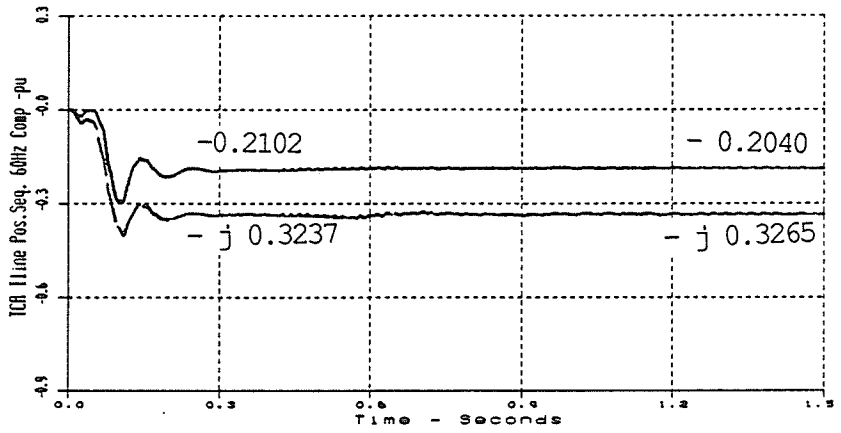

a) Real/Imaginary 60 Hz Components - pu

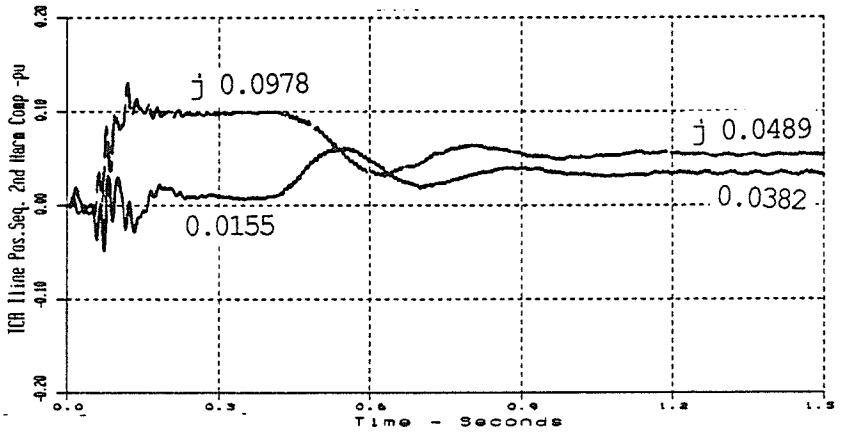

b) Real/Imaginary 2nd Harmonic Components - pu

Figure 5.15 Effect of Control of the Positive Sequence DC Component of TCR Line Current on the 60 Hz and 120 Hz Components, Alpha = 30°, 2nd Harmonic Resonant Network, Source 2nd Harmonic Voltage: 3% @ -30°

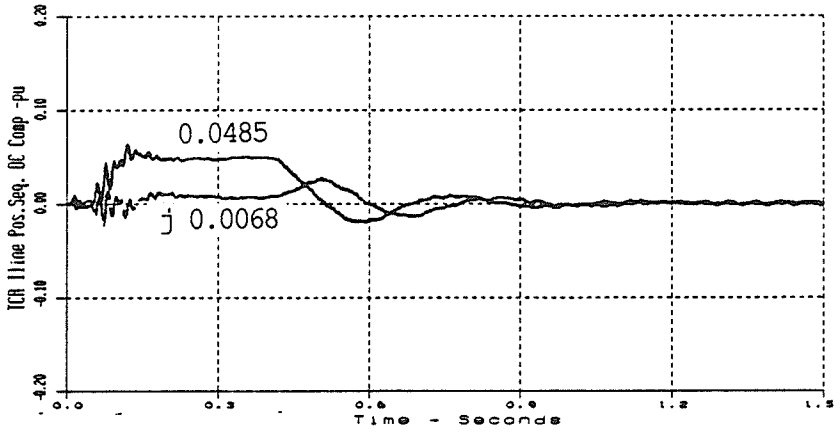

a) Real/Imaginary DC Components - pu

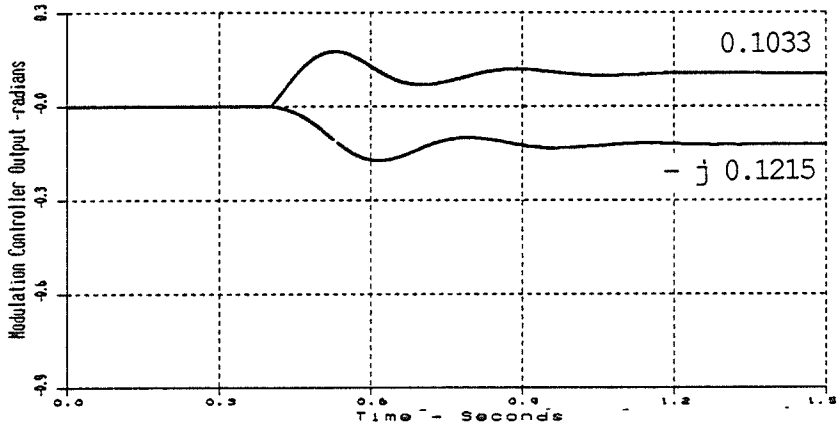

b) Real/Imaginary Modulation Controller Components - radians

Figure 5.16 Control of Positive Sequence DC Component of TCR Line Current, Alpha = 30°, 2nd Harmonic Parallel Resonant Network, Source 2nd Harmonic Voltage: 3% @ -30°

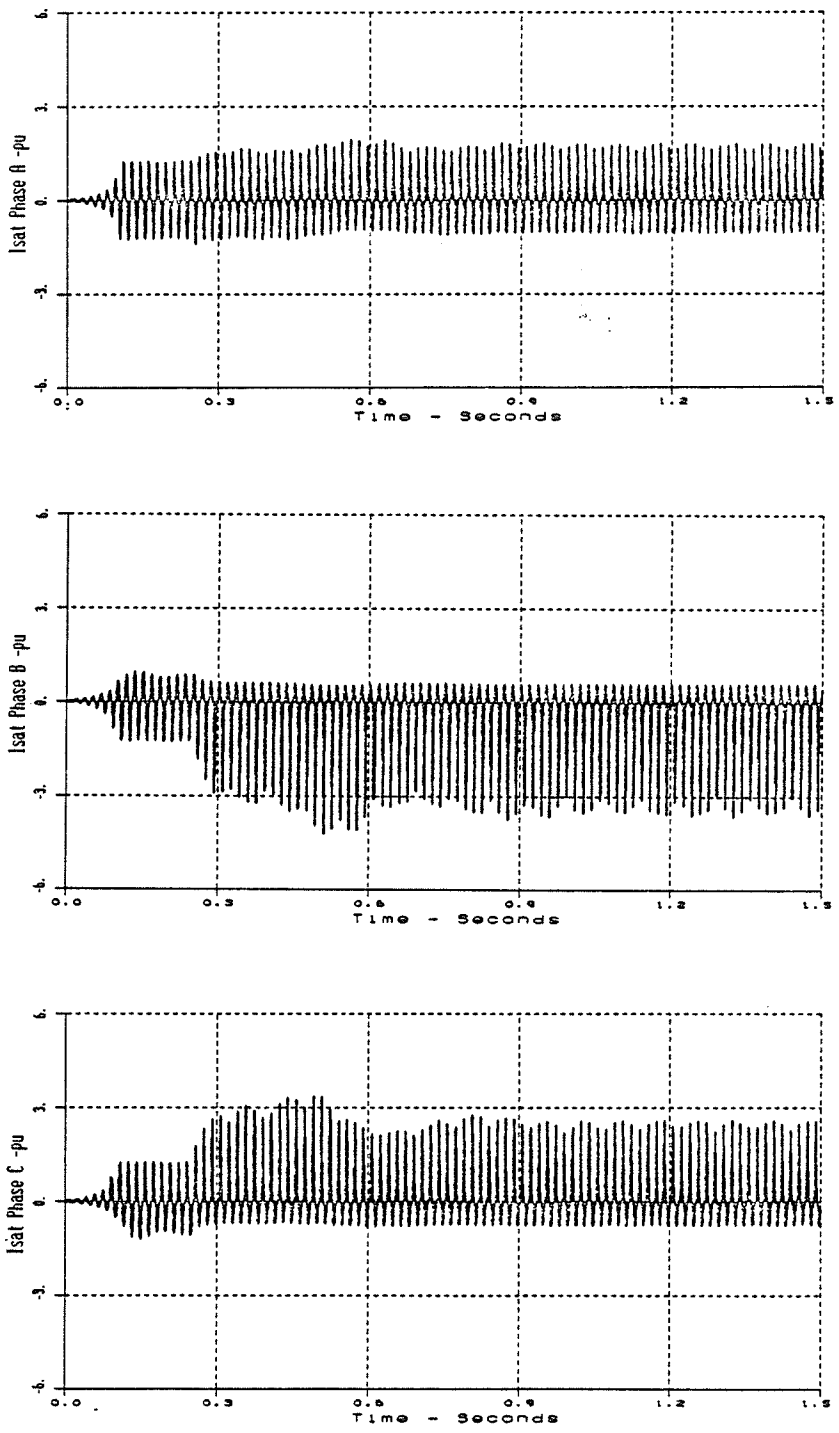

Figure 5.17 Transformer Saturation Current Waveforms, Control of Positive Sequence DC Component of TCR Line Current, Alpha = 30°, 2nd Harmonic Parallel Resonant Network, Source 2nd Harmonic Voltage: 3% @ -30°

5.6 Firing Angle Modulation Using Other Control Parameters

The performance of the TCR sinusoidal firing angle modulation controller was examined using the positive sequence TCR line current as the control parameter.

The positive sequence SVC transformer primary line current or the positive sequence SVC transformer secondary line current were also input to the modulation controller to determine if the parallel resonance condition at the point of SVC compling could be damped.

The modulation controller could not eliminate the second harmonic component from the positive sequence of the primary or secondary transformer line current. In the system under study, the second harmonic component of either of the above currents was of sufficient magnitude such that the TCR was unable to generate the required second harmonic component magnitude to cancel the input variable, even with the maximum modulation as limited by TCR firing angle limits.

This result is expected. It has been demonstrated [4 - Figure 5] that modulation of the TCR firing angle with a modulation magnitude of 30 degrees produces a second harmonic component of about 10% in the positive sequence TCR line current. Modulation magnitudes much in excess of 30°

would result in the modulation being limited by firing angle limits, which in turn would result in a reduction in the positive sequence 60 Hz TCR line current. It is unlikely that second harmonic component magnitudes in excess of 15% could be cancelled by modulation of the TCR firing angle.

The modulation controller successfully eliminated the dc component from either the primary or secondary positive sequence line current. However, modulation using either of these variables as the control parameter was not as effective in damping the second harmonic resonance as was the modulation using the dc component of the TCR line current as the control parameter.

5.7 Summary and Conclusions

Sinusoidal modulation of the TCR firing angle was successfully applied to eliminate the dc component or the second harmonic component from the positive sequence of the TCR line current. However, the modulation did not eliminate the parallel resonant condition existing at the point of SVC coupling to the ac system. Some reduction of the positive sequence second harmonic voltage was observed with either the dc or the second harmonic component of the positive sequence TCR line current as the controlled parameter. Control of the second harmonic component resulted in a larger reduction in the second harmonic voltage at the point of SVC coupling as the modulation effectively reduced the second harmonic impedance.

The TCR line current was the preferred control parameter for the study system since the second harmonic component magnitude of the positive sequence of the SVC transformer primary line current or secondary line current was larger than the maximum second harmonic components that could be generated by the TCR with maximum firing angle modulation.

When firing angle limits were encountered, the fundamental frequency TCR loading was reduced by the firing angle modulation. A reduction of about 10% was observed with the dc

component of the TCR line current as the control parameter. A reduction of about 27% was observed with the second harmonic component as the control parameter.

Elimination of the dc component from the positive sequence of the TCR line current, in general also reduced the second harmonic component by between 15% and 50% of the "no modulation" valves.

Elimination of the second harmonic component, on the other hand, caused the dc component to increase by as much as 96% with the TCR line current as the controlled parameter.

Control of the second harmonic component of TCR line current via firing angle modulation caused the SVC transformer saturation current to increase. The second harmonic modulation generally caused an increase in the dc component of TCR phase current, which caused an increase in the level of transformer saturation. The increase in transformer saturation was not excessive, however, since the damping of the resonance reduced the second harmonic voltage distortion and the peak overvoltages across the transformer windings.

The dc component modulation control only minimally increased the transformer saturation level when firing angle limits were encounted.

Modulation angle limits and a voltage control strategy are required to prevent the controller from forcing the TCR to operate in the region where firing angle limits are encountered, especially if the second harmonic component is to be controlled. This would limit the possibility of driving the SVC transformer into severe saturation.

The modulation controller response was found to be very stable, even with the SVC coupled to a network in parallel resonance at the second harmonic.

CHAPTER SIX

PERFORMANCE OF AN SVC CONNECTED TO A STRONG AC NETWORK WITH A SECOND HARMONIC PARALLEL RESONANCE BETWEEN THE NETWORK AND THE SVC FIXED CAPACITOR

6.1 Study Network

The performance of the TCR with sinusoidal firing angle modulation was evaluated with the SVC connected to an ac network characterized by a second harmonic parallel resonant condition between the network and the fixed capacitor of the SVC as observed from the point of connection of the SVC to the high voltage system. The single line diagram of the study network is shown in Figure 6.1, and the detailed three phase EMTDC simulation circuit is shown in Figure 2.2.

The rating of the SVC and the rating of the SVC step-up transformer were the same as used in Chapter 4.

The equivalent system parameters were chosen such that a second harmonic parallel resonance existed between the equivalent Thevenin reactance of the system, the equivalent system shunt connected capacitive reactance and the combination of the SVC transformer in series with the SVC fixed

capacitor. The three phase short circuit capacity of the system was approximately:

$$Ssc = \frac{(kV)^2}{Zs} = \frac{(120\ kV)^2}{2.5\ ohm} = 5\ 760\ MVA \qquad (6.1)$$

The effective short circuit capacity at the point of SVC coupling was approximately.

$$Ssce = Ssc - Scap = 4\ 560\ MW \qquad (6.2)$$

where Scap = 1200 Mvar, the equivalent system shunt capacitance.

The system damping angle was assumed to be 85°.

The TCR performance was evaluated at nominal firing angles of 0°, 20°, 30° and 45°. The study system fundamental frequency steady state conditions for each TCR firing angle are shown in Figure 6.2. The fundamental frequency Thevenin voltage source magnitude was adjusted to maintain 1.0 pu voltage at the point of coupling of the SVC to the high voltage system.

Table 6.1 shows the computed variation with frequency in the magnitudes of the fundamental and second harmonic impedances as observed from the point of SVC coupling to the high voltage system for TCR firing angles of 0°, 20°, 30° and 45°. As the TCR firing angle increases from 0°, the resonant frequency moves from 125 Hz towards 120 Hz. Also the magnitude of the second harmonic impedance increases with firing angle.

The solid line in Figure 6.3 shows the variation in system impedance with frequency as observed at the point of SVC coupling to the system with the SVC connected and a TCR firing angle of 0°. A parallel resonance exists near the second harmonic at 125 Hz and the system behaves inductively at the second harmonic. The dashed line, which represents the system impedance variation with frequency when the TCR reactor is not connected, shows that the system and SVC fixed capacitor are resonant at 120 Hz.

Table 6.1 Study System Impedance Magnitude versus Frequency as Observed from the Point of SVC Coupling to the AC System

TCR Firing Angle	0°	20°	30°	45°
Frequency	Impedance Magnitude (Ohms)			
60 Hz	3.89	4.02	4.09	4.17
120 Hz	49.76	65.14	72.99	80.45
Resonant Point (- Hz)	94.47 (125)	89.80 (123)	87.43 (122)	84.72 (121)

Second harmonic current injection into the network at the point of SVC coupling can produce large second harmonic voltages due to the high impedance. The second harmonic voltage amplification will be larger as the TCR firing angle increases. A second harmonic voltage with a magnitude of 2.0% at -30° relative to the fundamental was superimposed on the fundamental source to provide the current injection required to excite the resonant condition.

6.2 Per unit System

The TCR reactor rating was used to define the per unit base quantities which are defined in Table 4.1. The per unit base used for the transformer saturation current was the rated winding magnetizing current.

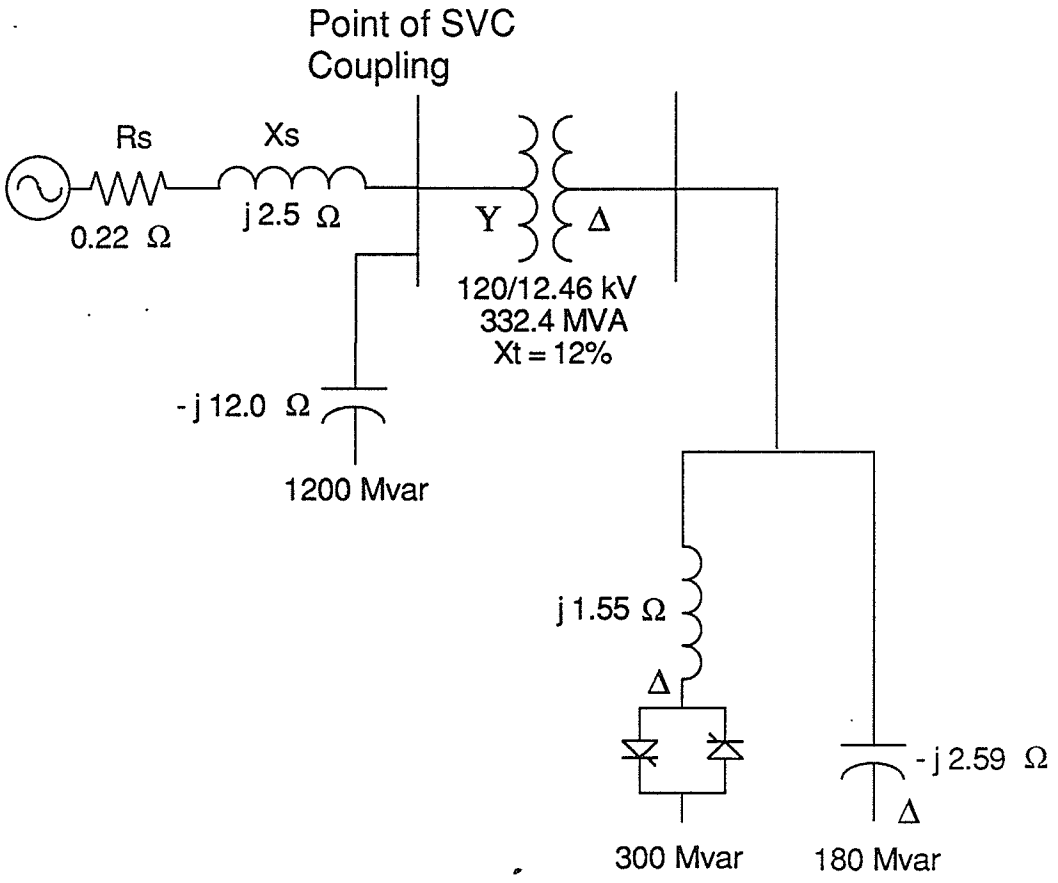

Figure 6.1 Study Network Single Line Diagram,
System and SVC FC in Second Harmonic Parallel
Resonance at the Point of SVC Coupling.

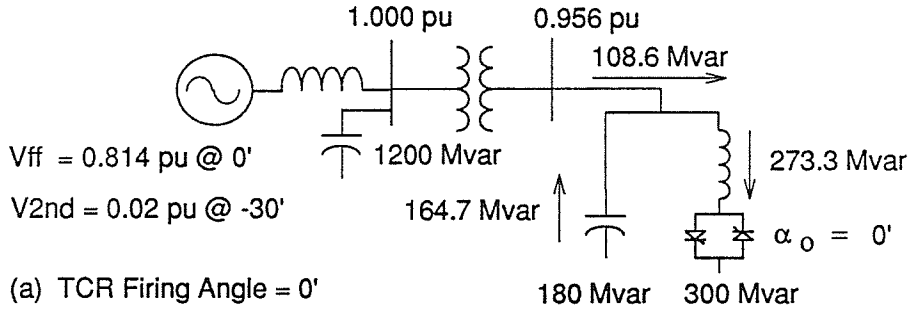

(a) TCR Firing Angle = 0'

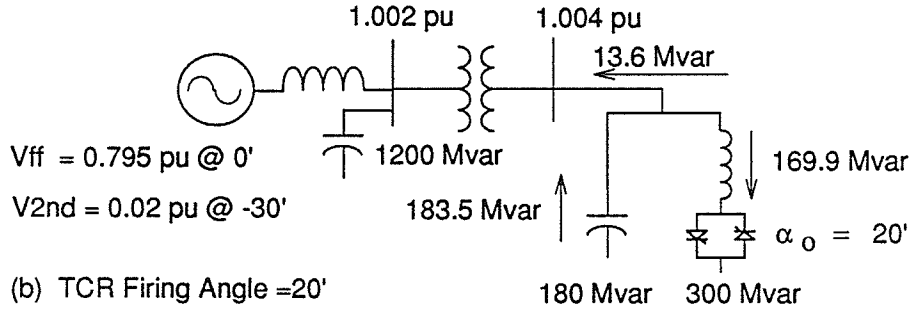

(b) TCR Firing Angle =20'

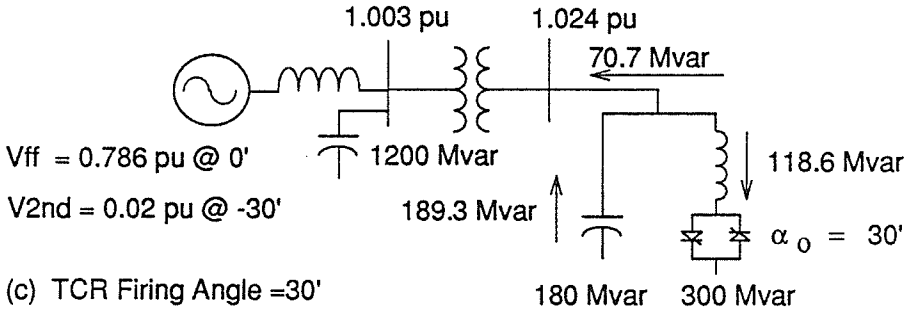

(c) TCR Firing Angle =30'

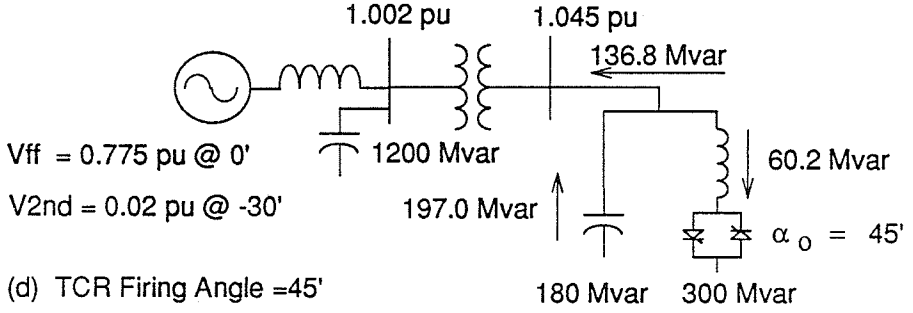

(d) TCR Firing Angle =45'

Figure 6.2 Study System Steady State Conditions

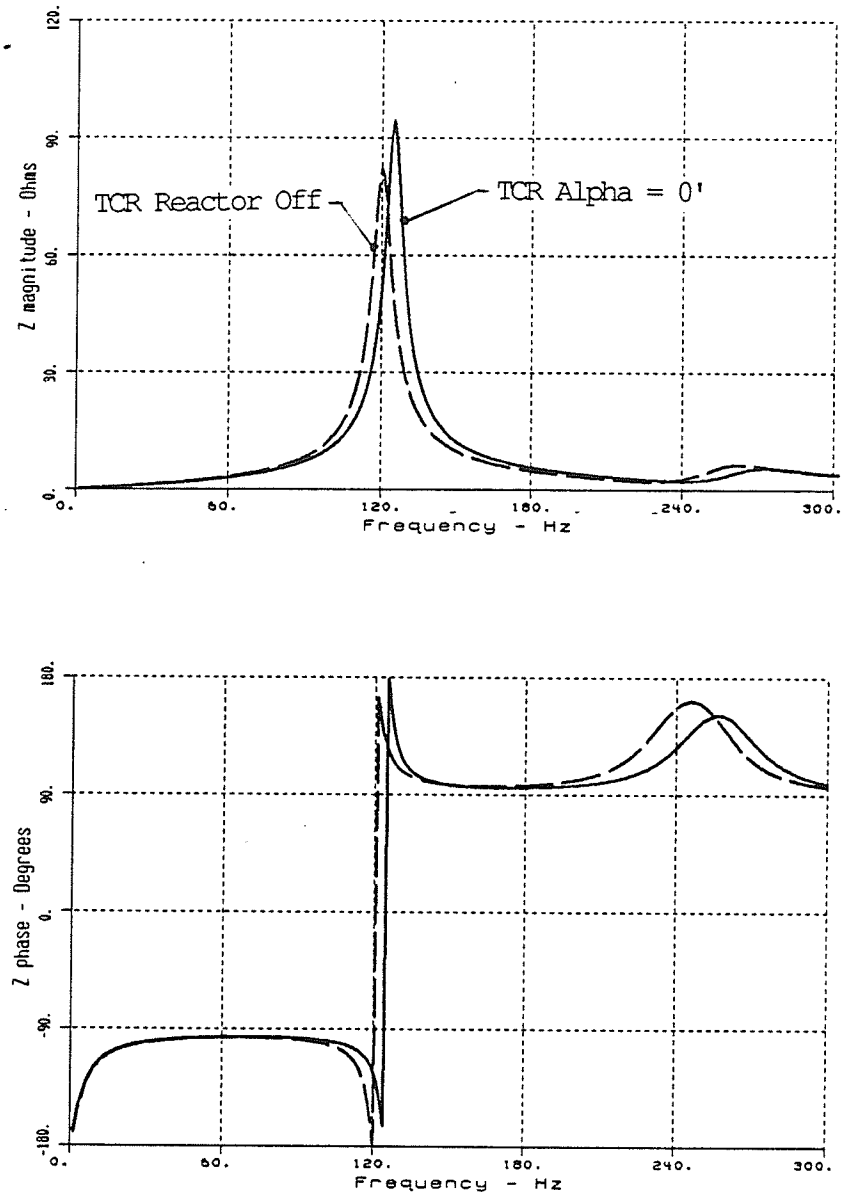

Figure 6.3 System Impedance vs. Frequency at the Point of SVC Coupling to the Network

6.3 TCR Performance with Equidistant Firing

The steady state positive sequence harmonic phasor components of some SVC variables are listed in Table 6.2 for equidistant firing of the TCR at 0°, 20°, 30° and 45°. A second harmonic parallel resonant condition exists between the equivalent system Thevenin reactance, the equivalent system shunt reactance and the SVC fixed capacitor at the point of SVC coupling to the 120 kV network.

The second harmonic source voltage of 2% @ -30° relative to the fundamental Thevenin source voltage was amplified by a factor of 9.65 at alpha = 0°, 9.55 at alpha = 20°, 9.60 at alpha = 30° and 10.35 at alpha = 45°. This second harmonic voltage amplification resulted in second harmonic voltage components ranging from 22.7% to 25.7% across the TCR terminals.

The dc component of the positive sequence TCR line current varied from 5.5% to 17.7% relative to the fundamental component over the TCR firing range, while the second harmonic component varied from 11.8% to 37.5%.

Figure 6.4 shows the steady state TCR waveforms for the case of alpha = 30°. The second harmonic voltage component of the secondary line voltage was displaced by -76° relative to

the fundamental, resulting in a different voltage waveform distortion pattern as compared to Figure 4.3 (-30° displacement). The TCR phase current waveforms, and the line current waveforms plotted in Figure 6.5, clearly contain a dc component.

The measured real and imaginary parts of the dc, 60 Hz and 120 Hz components of the positive sequence TCR line current are shown in Figure 6.6 for TCR firing at 30°.

Figure 6.7 shows the SVC transformer saturation current waveforms for TCR equidistant firing at 30°. The currents are clearly non-symmetrical. A peak saturation current of about 3.0 pu (6% of rated transformer winding current) was obtained on phase A of the SVC transformer.

Table 6.2 Positive Sequence SVC Variables with Equidistant Firing of the TCR, Transformer Saturation Modelled, SVC FC in 2nd Harmonic Parallel Resonance with System, Source 2nd Harmonic Voltage: 2% @ -30°

Firing Angle	Alpha = 0°	Alpha = 20°	Alpha = 30°	Alpha = 45°
Variable	pu /-°	pu /-°	pu /-°	pu /-°
TCR Line Current				
DC Comp.	0.052/- 61°	0.049/- 86°	0.046/- 93°	0.034/- 94°
60 Hz Comp.	0.953/-121°	0.564/-121°	0.386/-122°	0.192/-124°
120 Hz Comp.	0.112/ 179°	0.103/-179°	0.093/-177°	0.072/-174°
Xfmr Primary Line Current				
DC Comp.	0.050/- 31°	0.048/- 55°	0.044/- 61°	0.036/- 57°
60 Hz Comp.	0.414/- 87°	0.024/- 1°	0.188/ 82°	0.388/ 86°
120 Hz Comp.	0.154/ 23°	0.164/ 10°	0.186/ 0°	0.240/- 11°
Xfmr Saturation Current				
DC Comp.	0.054/ 161°	0.084/ 169°	0.118/ 176°	0.212/-173°
60 Hz Comp.	0.568/ 96°	0.732/ 96°	0.865/ 96°	1.144/ 96°
120 Hz Comp.	0.175/ 31°	0.251/ 24°	0.329/ 16°	0.540/ 4°
Primary Line Voltage				
DC Comp.	0.0002/-143°	0.0002/-171°	0.0001/ 178°	0.0002/-150°
60 Hz Comp.	1.000 /- 2°	1.002 /- 2°	1.003 /- 2°	1.002 /- 2°
120 Hz Comp.	0.193 /- 60°	0.191 /- 66°	0.192 /- 73°	0.207 /- 84°
120 Hz Amplification	9.65	9.55	9.60	10.35
Secondary Line Voltage				
DC Comp.	0.0004/ 164°	0.0004/ 141°	0.0004/ 134°	0.0002/ 143°
60 Hz Comp.	0.956 /- 2°	1.004 /- 2°	1.024 /- 2°	1.045 /- 2°
120 Hz Comp.	0.227 /- 61°	0.225 /- 69°	0.231 /- 76°	0.257 /- 88°
TCR 60 Hz Absorption Mvar	273.3	169.9	118.6	60.2

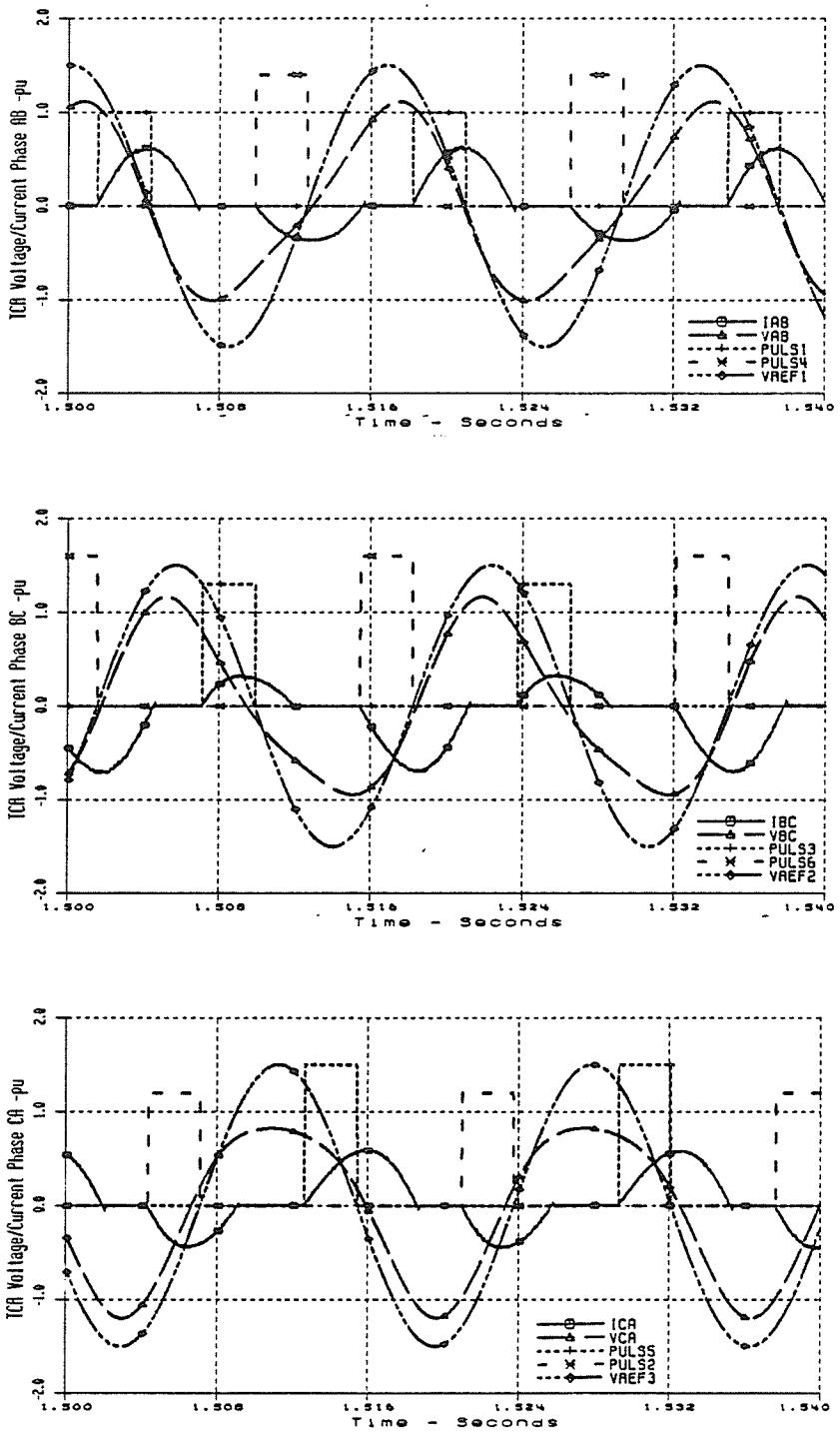

Figure 6.4 TCR Waveforms with Equidistant Firing, Alpha = 30°, System and SVC FC in 2nd Harmonic Parallel Resonance, Source 2nd Harmonic Voltage: 2% @ -30°

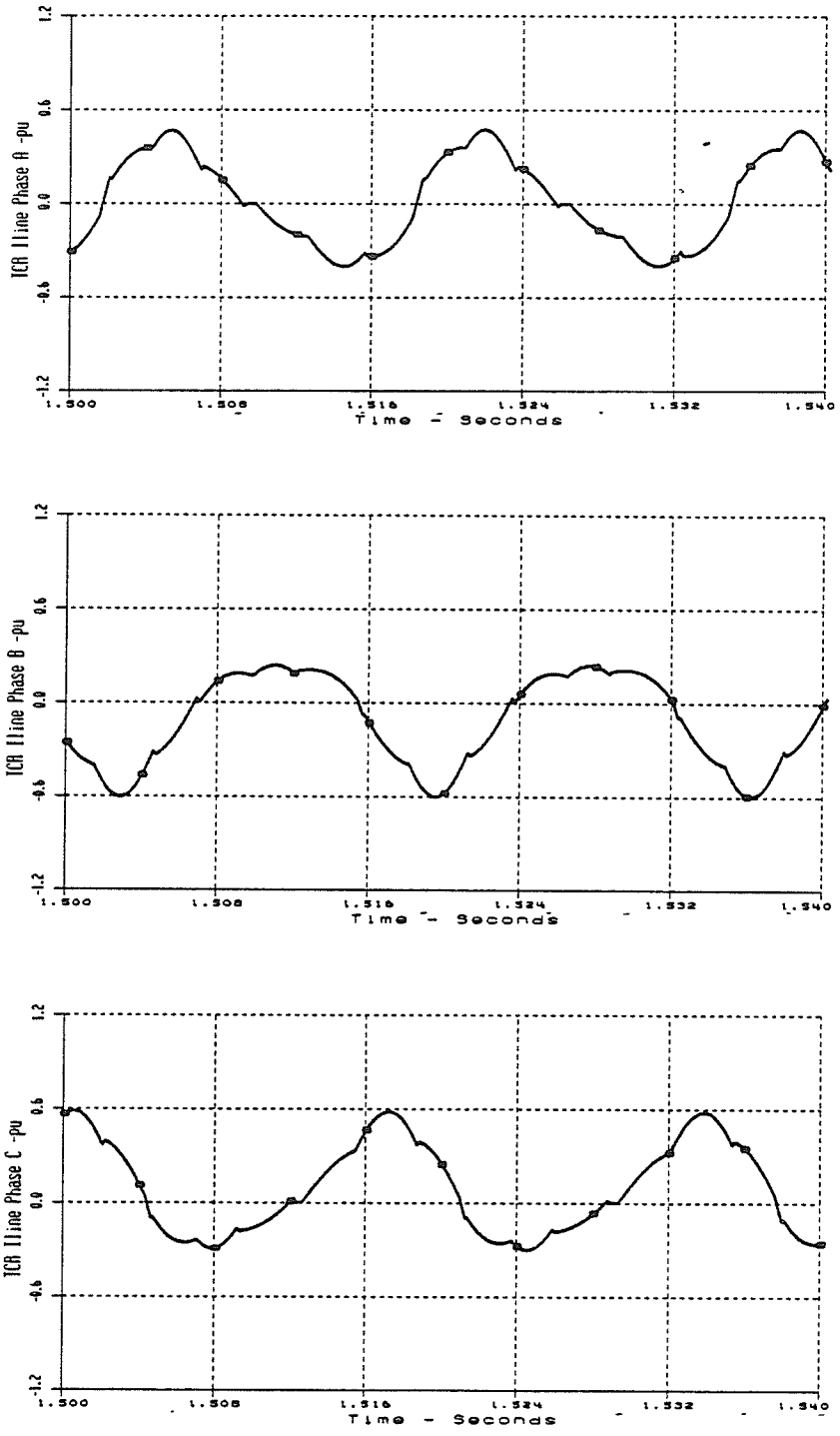

Figure 6.5 TCR Line Current Waveforms with Equidistant Firing, Alpha = 30°, System and SVC FC in 2nd Harmonic Parallel Resonance, Source 2nd Harmonic Voltage: 2% @ -30°

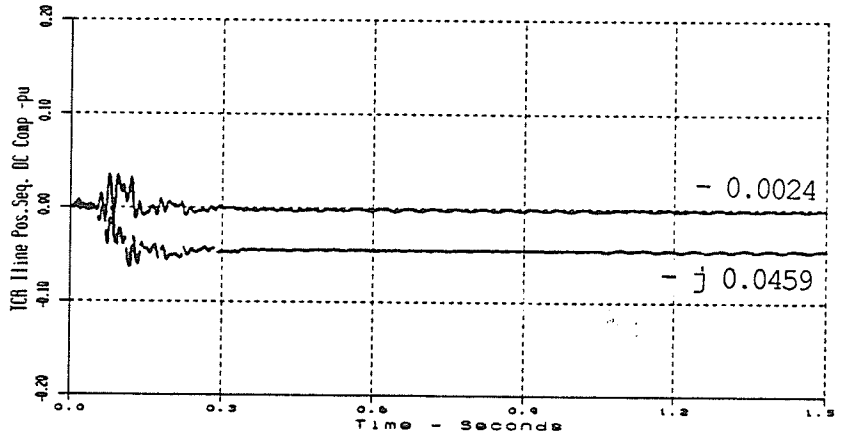

a) Real/Imaginary DC Components - pu

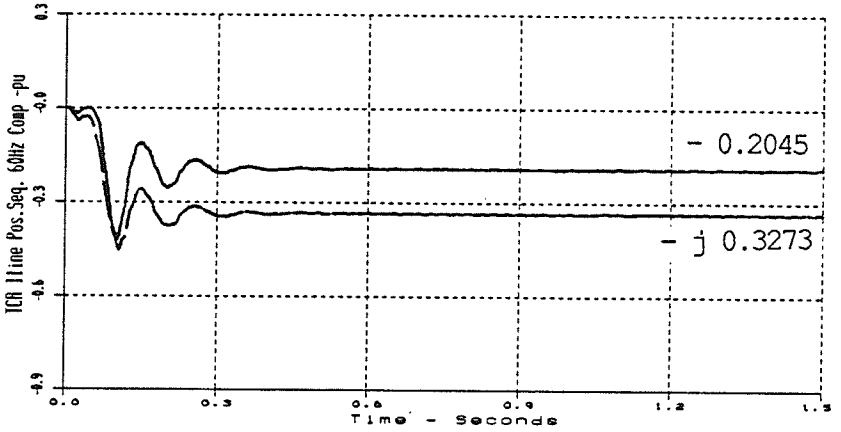

b) Real/Imaginary 60 Hz Components - pu

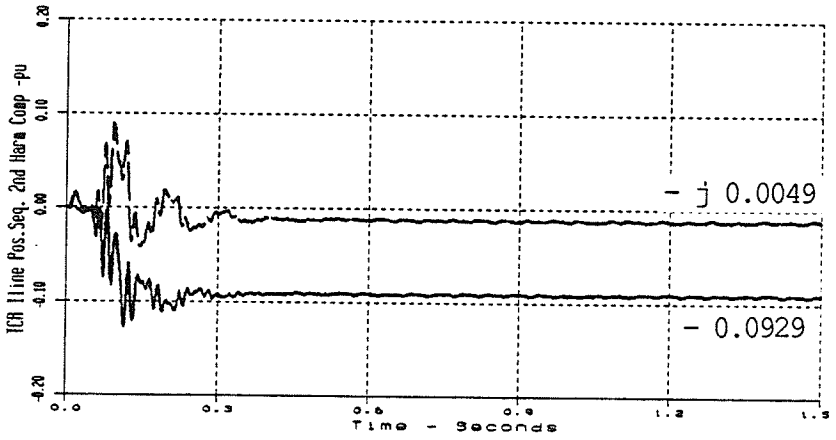

c) Real/Imaginary 2nd Harmonic Components - pu

Figure 6.6 Positive Sequence Phasor Components of TCR Line Current with Equidistant TCR Firing, Alpha = 30°, System and SVC FC in 2nd Harmonic Parallel Resonance, Source 2nd Harmonic Voltage: 2% @ -30°

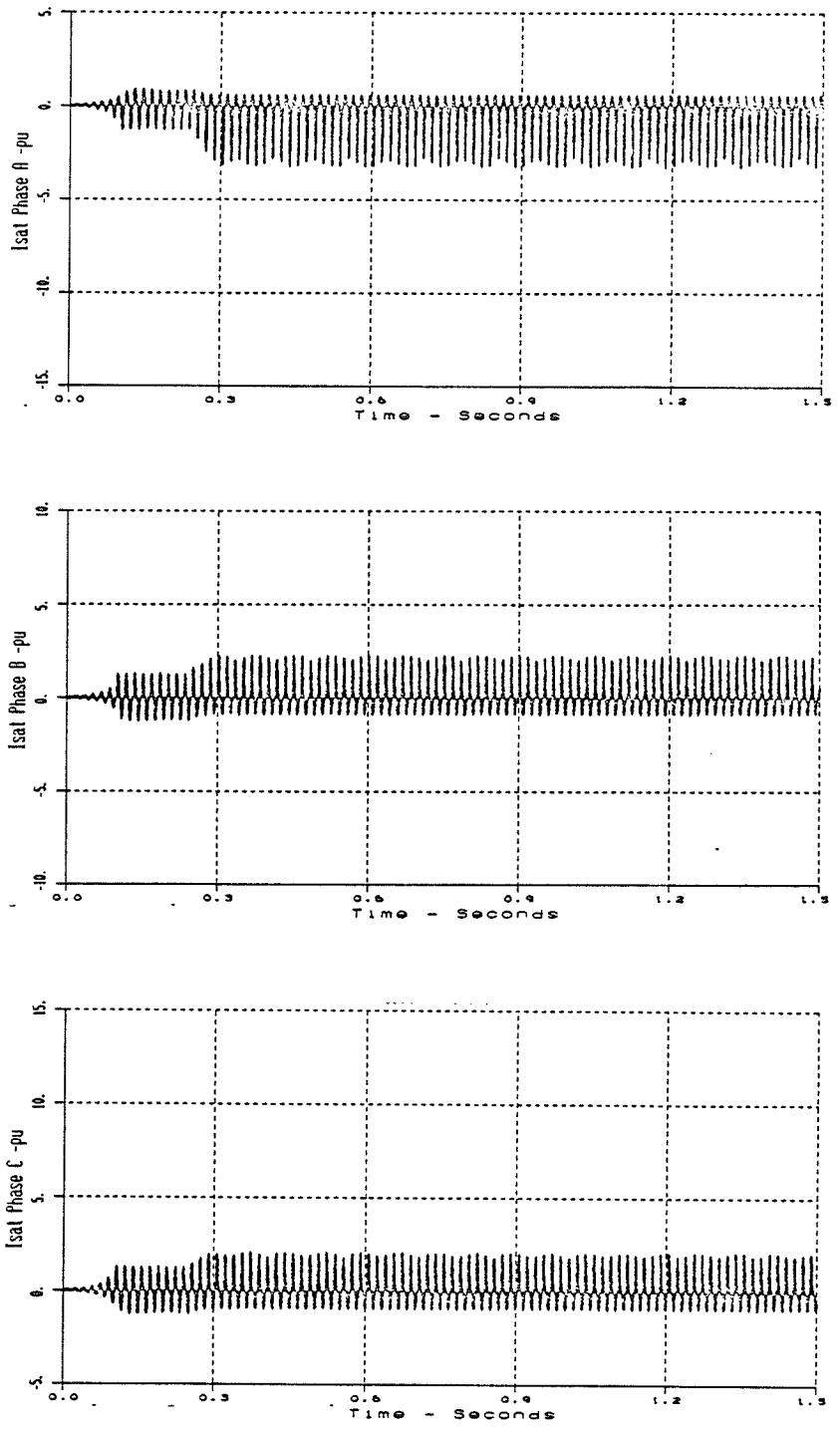

Figure 6.7 Transformer Saturation Current Waveforms with Equidistant TCR Firing, Alpha = 30°, System and SVC FC in 2nd Harmonic Parallel Resonance, Source 2nd Harmonic Voltage: 2% @ -30°

6.4 TCR Performance Using Firing Angle Modulation to Control the Positive Sequence Second Harmonic Phasor Component of the TCR Line Current

The measured real and imaginary second harmonic phasor components of the positive sequence TCR line current were input to the TCR firing angle modulation controller to generate a modulation signal to cancel the second harmonic component. The controller settings that were applied are listed in Table 3.3

The steady state positive sequence harmonic phasor components of some SVC variables and the modulation parameters are presented in Table 6.3 for nominal TCR firing angles of 0°, 20°, 30° and 45°.

Sinusoidal modulation of the TCR firing angle successfully eliminated the second harmonic component from the positive sequence of the TCR line current for all the nominal TCR firing angles considered. However, the parallel resonance at the high voltage system bus was not damped. In fact, the firing angle modulation caused an increase in the second harmonic voltage component. This result can be anticipated by examination of Figure 6.3. Since the second harmonic component of TCR line current is reduced to zero by the firing angle modulation the TCR reactor impedance appears

infinite at the second harmonic. The system resonant point is shifted towards 120 Hz (the dashed line in Figure 6.3), resulting in a higher second harmonic impedance. The second harmonic current flowing through this impedance in part increases the second harmonic voltage component.

Firing angle limits are encountered at nominal TCR firing angles of 0°, 20° and 30°. Figures 6.8 and 6.9 respectively show the TCR waveforms and the TCR line current waveforms for the case of alpha = 30°. The modulation results in one sided modulation on two phases. The voltage and current waveforms are severely distorted. The TCR phase and line current waveforms contain a large dc component. This dc component causes extensive saturation of the transformer. The transformer saturation current contains a large second harmonic component which enhances the second harmonic voltage distortion.

The elimination of the second harmonic component increased the dc component by 223% at 0°, 192% at 20°, 189% at 30° and 100% at 45° relative to the "no modulation" case values (Table 6.2). Figure 6.10 shows the measured positive sequence dc and 60 Hz components of the TCR line current for TCR firing at 30°. The magnitude of the dc component is increased from 0.046 pu @ -93° (no modulation value) to 0.133 pu @ 159° by the modulation controller action. The 60 Hz component is not changed by the modulation even though

firing angle limits were encountered. However, the one sided modulation at alpha = 0° and 20° reduced the 60 Hz TCR loading to 49.5% and 76.5% of the respective "no modulation" case values.

Figure 6.11 shows the measured positive sequence second harmonic component of TCR line current and the modulation controller output for TCR firing at 30°. The second harmonic is reduced from 0.093 pu @ -177° to zero in about 600 ms. The modulation controller output corresponds to a modulation peak of 57.9° and a modulation phase of -2.2°. The response of the controller was not optimized, but was very stable and similar at all the TCR firing angles examined.

Figure 6.12 shows the SVC transformer saturation current waveforms for the nominal TCR firing angle of 30°. The modulation controller was activiated at 0.40s, and clearly caused the transformer saturation current to increase. This increase is related to the increase in the dc component of the TCR phase current (Figure 6.8), which enhances saturation of the transformer. The envelope of the saturation current (phase C) reached 15.0 pu or 30% of the rated transformer current. Comparison of the steady state phasor components of saturation current listed in Tables 6.2 and 6.3 illustrates that the firing angle modulation caused a large increase in the transformer saturation current components.

Comparison of Figures 6.7 and 6.12 also illustrates this result.

Table 6.3 Positive Sequence SVC Variables With TCR Firing Angle Modultion Control of the Positive Sequence 2nd Harmonic Component of TCR Line Current, Transformation Saturation Modelled, SVC FC in 2nd Harmonic Parallel Resonance with System, Source 2nd Harmonic Voltage: 2% @ -30°

Firing Angle	Alpha = 0°	Alpha = 20°	Alpha = 30°	Alpha = 45°
Variable	pu /-°	pu /-°	pu /-°	pu /-°
TCR Line Current				
DC Comp.	0.141 / 154°	0.138 / 156°	0.133 / 159°	0.068 / 159°
60 Hz Comp.	0.430 /-121°	0.422 /-121°	0.383 /-121°	0.210 /-121°
120 Hz Comp. *	0.0025/-119°	0.0045/-166°	0.0011/-128°	0.0018/- 73°
Xfmr Primary Line Current				
DC Comp.	0.122/-179°	0.122/-177°	0.116/-173°	0.053 /-175°
60 Hz Comp.	0.129/ 72°	0.132/ 74°	0.167/ 76°	0.346 / 83°
120 Hz Comp.	0.474/- 15°	0.481/- 17°	0.501/- 17°	0.492 /- 18°
Xfmr Saturation Current				
DC Comp.	0.722/-156°	0.592/-152°	0.579/-151°	0.593 /-158°
60 Hz Comp.	2.386/ 96°	1.968/ 97°	1.949/ 96°	2.042 / 96°
120 Hz Comp.	1.750/- 9°	1.432/- 13°	1.421/- 14°	1.466 /- 11°
Primary Line Voltage				
DC Comp.	0.0006/- 14°	0.0007/- 12°	0.0005/- 7°	0.0003/ 98°
60 Hz Comp.	1.035 /- 2°	1.011 /- 2°	1.001 /- 2°	1.998 /- 2°
120 Hz Comp.	0.327 /-100°	0.328 /-102°	0.339 /-106°	0.332 /-103°
120 Hz Amplification	16.35	16.4	16.95	16.60
Secondary Line Voltage				
DC Comp.	0.0015/ 1°	0.0016/ 1°	0.0014/ 7°	0.0007/- 8°
60 Hz Comp.	1.049 /- 2°	1.026 /- 2°	1.020 /- 2°	1.037 /- 2°
120 Hz Comp.	0.430 /-101°	0.433 /-103°	0.447 /-104°	0.439 /-104°
TCR 60 Hz Absorption Mvar (% No Modulation Case)	135.3 (49.5)	129.9 (76.5)	117.2 (98.8)	65.3 (108.5)
Modulation Peak/Phase	106.7/-1.1 °	67.9/-1.4°	57.9/-2.2°	35.5/-14.1°
Δ ab	106.7°	67.9°	57.8°	34.4°
Δ bc	-55.1°	-32.5°	-27.0°	-26.7°
Δ ca	-51.6°	-35.4°	-30.8°	- 9.7°

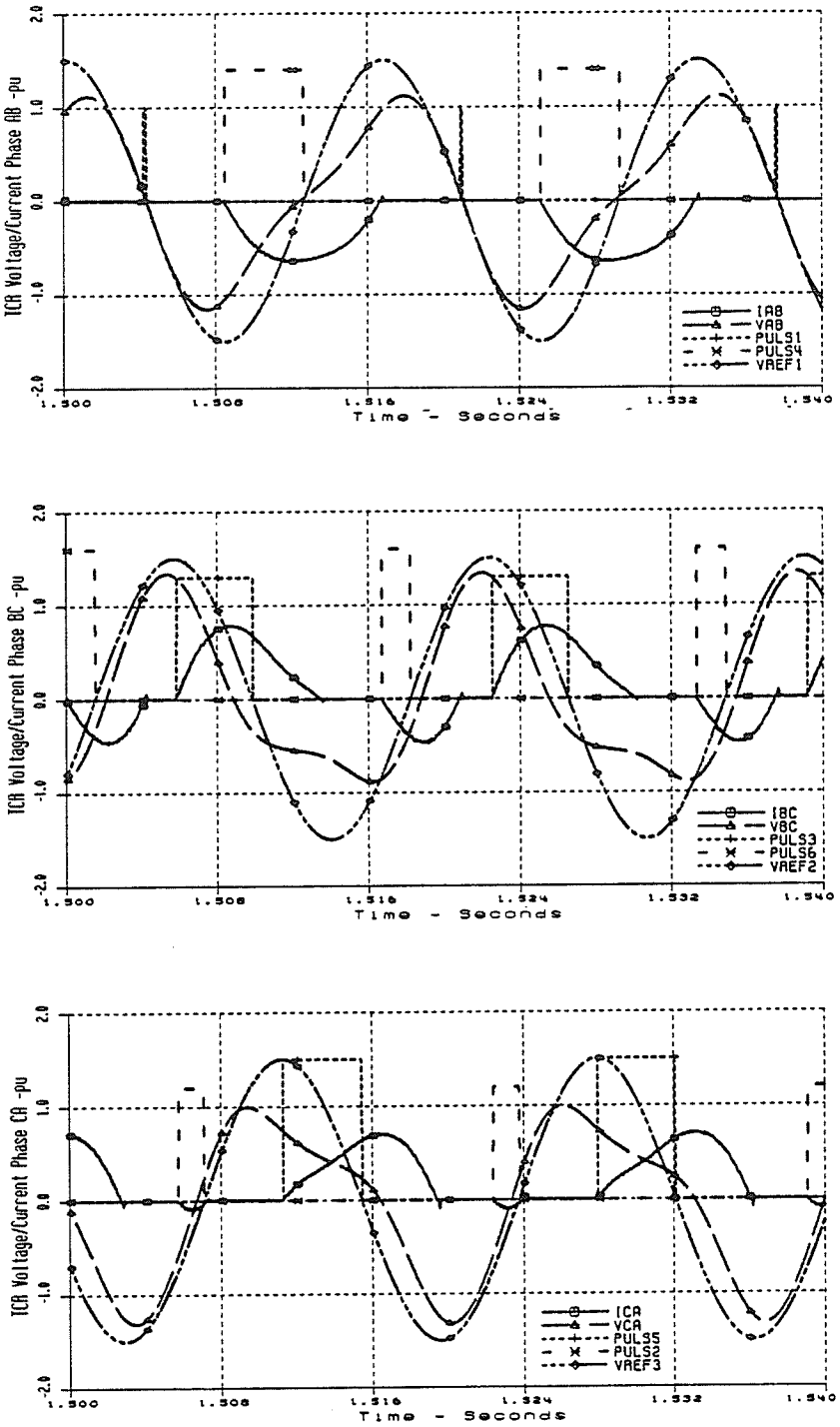

Figure 6.8 TCR Waveforms, Control of Positive Sequence 2nd Harmonic Component of TCR Line Current, Alpha = 30°, System and SVC FC in 2nd Harmonic Parallel Resonance, Source 2nd Harmonic Voltage: 2% @ - 30°

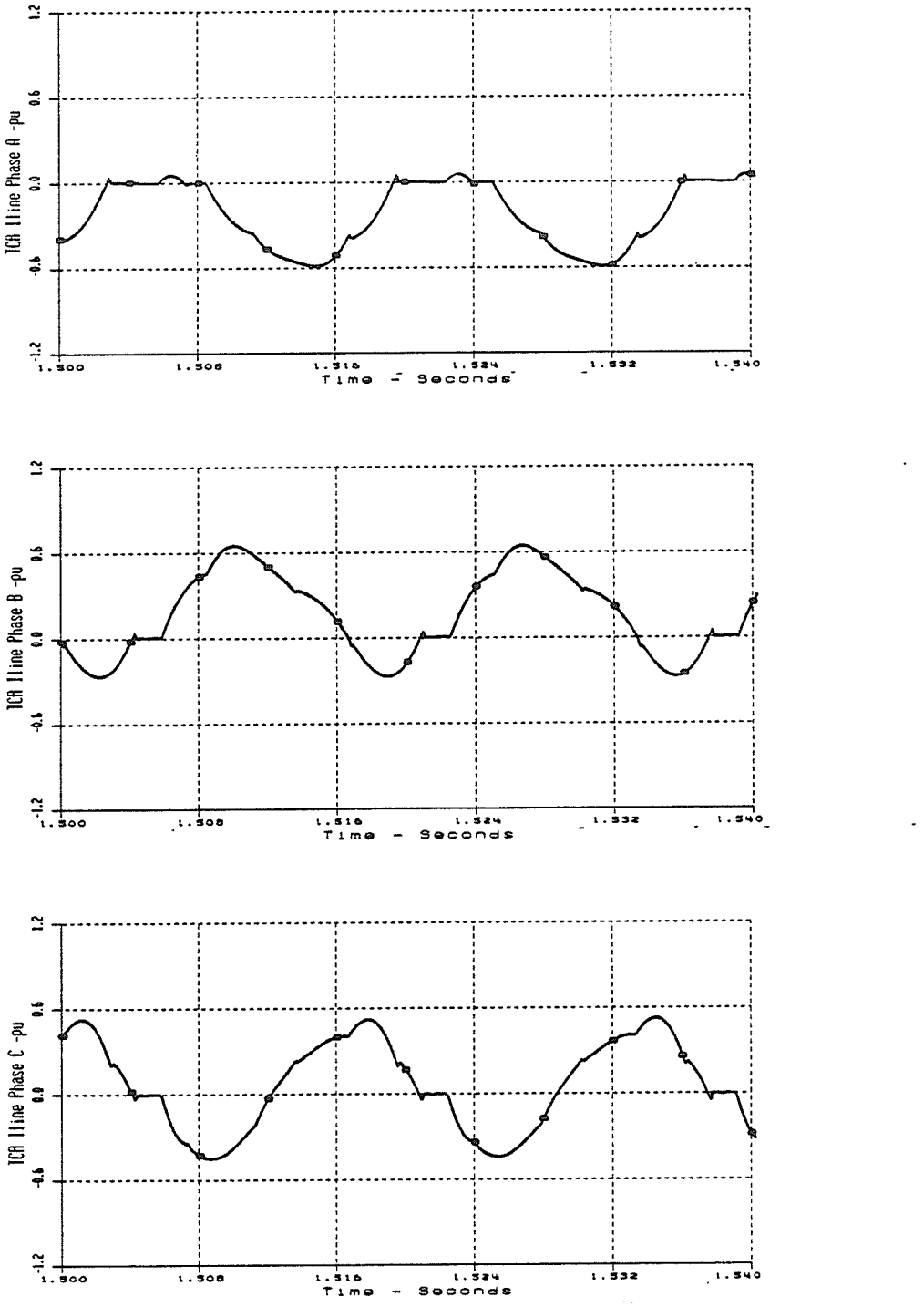

Figure 6.9 TCR Line Current Waveforms, Control of Positive Sequence 2nd Harmonic Component of TCR Line Current, Alpha = 30°, System and SVC FC in 2nd Harmonic Parallel Resonance, Source 2nd Harmonic Voltage: 2% @ -30°

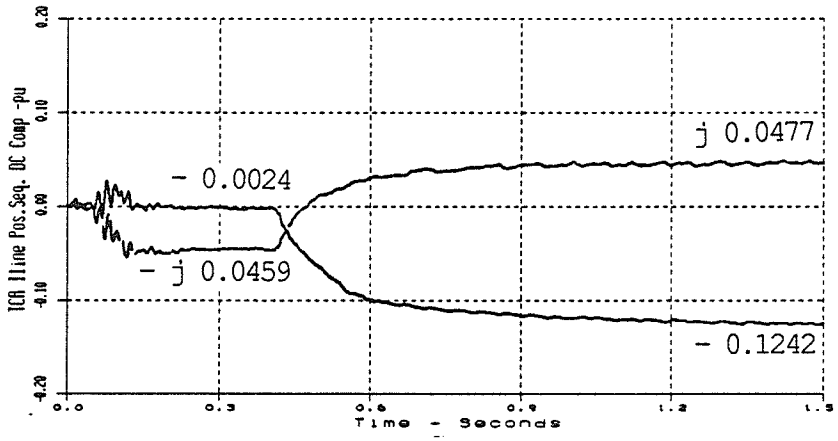

a) Real/Imaginary DC Components - pu

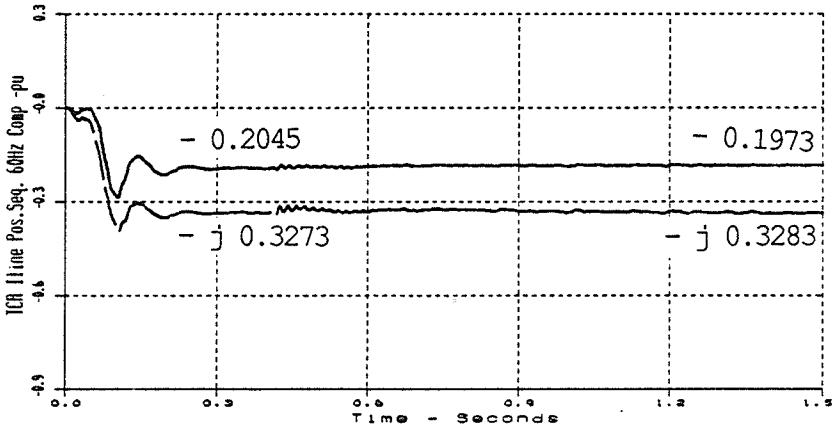

b) Real/Imaginary 60 Hz Components - pu

Figure 6.10 Effect of Control of the Positive Sequence 2nd Harmonic Component of TCR Line Current on the DC and 60 Hz Components, Alpha = 30°, System and SVC FC in 2nd Harmonic Parallel Resonance, Source 2nd Harmonic Voltage: 2% @ -30°

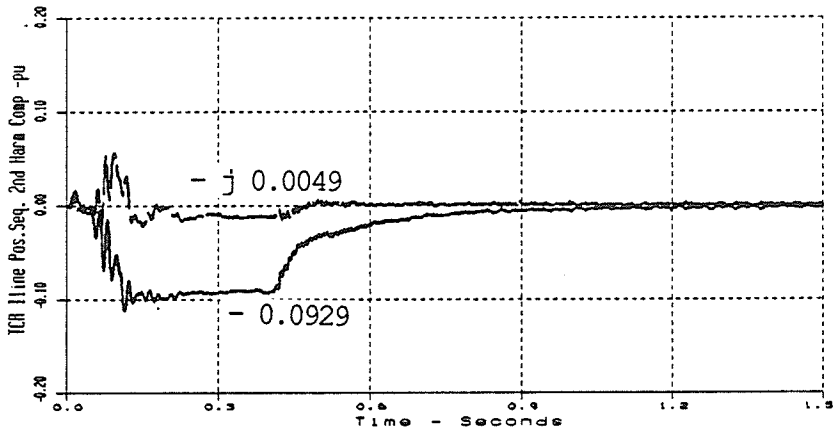

a) Real/Imaginary 2nd Harmonic Components - pu

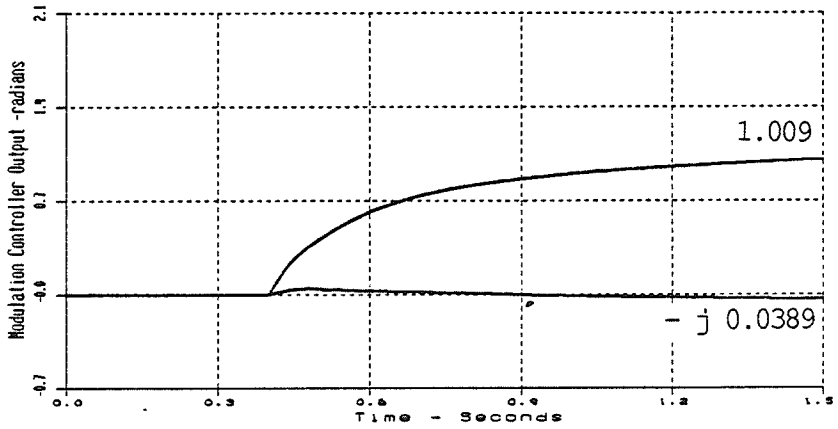

b) Real/Imaginary Modulation Controller Components - radians

Figure 6.11 Control of Positive Sequence 2nd Harmonic Component of TCR Line Current, Alpha = 30°, System and SVC FC in 2nd Harmonic Parallel Resonance, Source 2nd Harmonic Voltage: 2% @ -30°

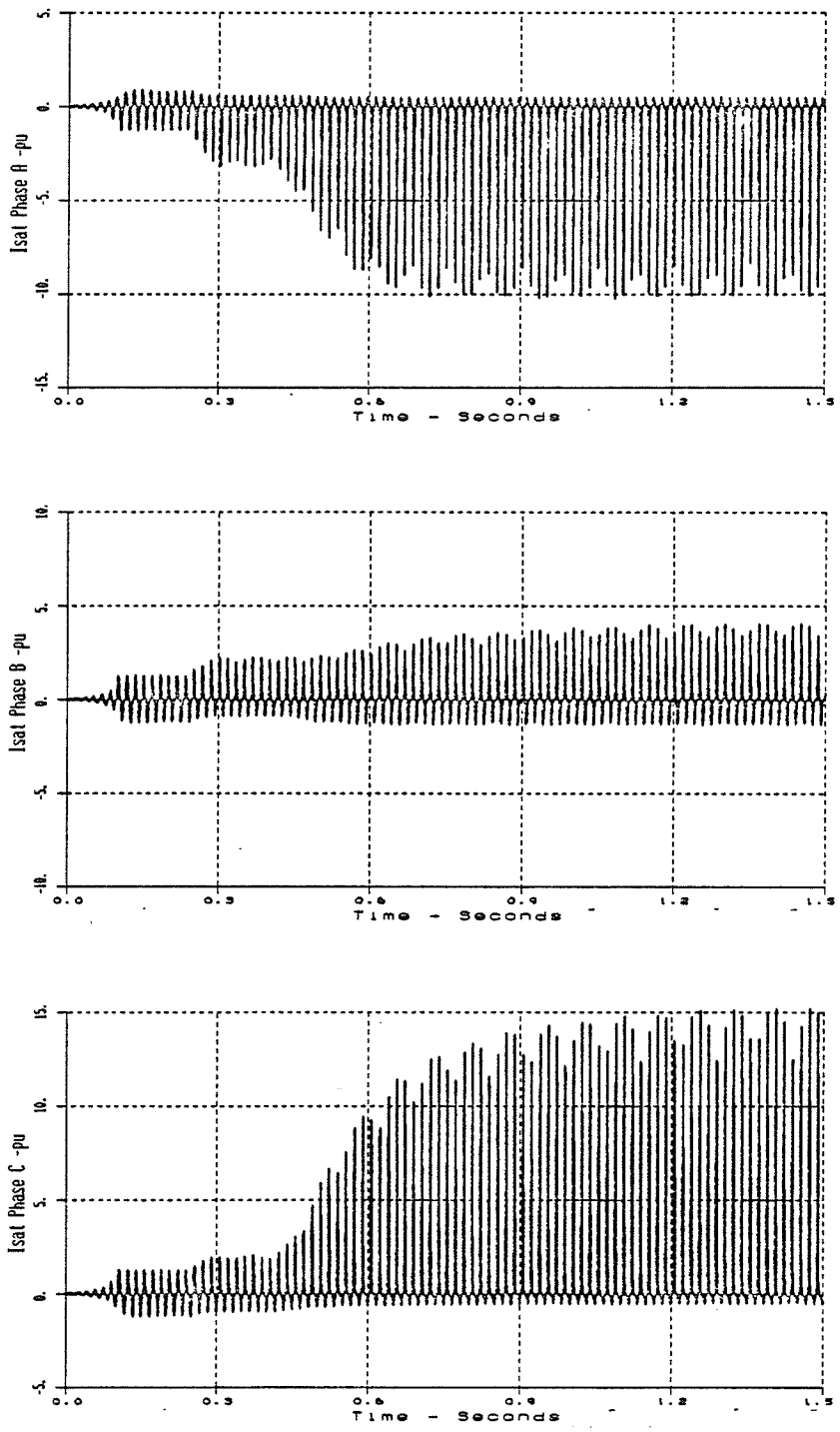

Figure 6.12 Transformer Saturation Current Waveforms, Control of Positive Sequence 2nd Harmonic Component of TCR Line Current, Alpha = 30°, System and SVC FC in 2nd Harmonic Parallel Resonance, Source 2nd Harmonic Voltage: 2% @ -30°

6.5 TCR Performance Using Firing Angle Modulation to Control the Positive Sequence DC Phasor Component of the TCR Line Current

The measured real and imaginary dc phasor components of the positive sequence TCR line current were input to the TCR firing angle modulation controller. The modulation signal was used to generate a dc component of the TCR line current, equal in magnitude to the measured input but 180° out of phase, so as to cancel the dc component. The controller settings that were applied are listed in Table 3.5.

The steady state harmonic phasor components of some SVC variables and the modulation parameters are listed in Table 6.4 for nominal TCR firing angles of 0°, 20°, 30° and 45°.

Sinusodial modulation of the TCR firing angle successfully eliminated the dc component from the positive sequence TCR line current at all nominal firing angles considered.

However, the second harmonic parallel resonance at the point of SVC coupling to the system was not damped. Modulation of the TCR firing angle resulted in a 6.2% to 39% increase in the second harmonic voltage amplification over the range of the TCR firing angle.

Firing angle limits were only encountered at the nominal firing angle of 0°, where clearly, the modulation was one sided. The one sided dc modulation reduced the TCR loading at alpha = 0° to 91.6% of the "no modulation" case.

Figure 6.13 shows the TCR waveforms for the case of alpha = 30°. The TCR firing of each phase is modulated to eliminate the dc component in the TCR phase current, and the TCR line current shown in Figure 6.14.

Elimination of the dc component from the TCR line current also reduced the second harmonic component. The second harmonic component was reduced by only 2.7% at alpha = 0°, 4.9% at alpha = 20°, 9.6% at alpha = 30° and 25.0% at alpha = 45° relative to the "no modulation" case. Figure 6.15 shows the effect of the firing angle modulation on the 60 Hz and second harmonic components of the positive sequence TCR line current for the case where the nominal TCR firing angle was 30°. The 60 Hz component was not changed by the modulation.

Figure 6.16 shows the measured positive sequence dc component of TCR line current at alpha = 30°, and the modulation controller output. The dc component was reduced to zero in about 200 ms (including settling time) after the controller was activated. The modulation controller output

corresponds to a modulation peak of 12.2° at a modulation phase of 62.7°. The controller response was found to be stable and similar at all TCR firing angles examined.

Figure 6.17 shows the SVC transformer saturation current for the case where alpha = 30°. The modulation did not change the saturation current appreciably, as can be observed by comparison of Figures 6.7 and 6.17.

Comparison of the sequence components in Tables 6.2 and 6.4 indicates a small increase in the saturation current components. The modulation caused a small increase in the peak to peak transformer secondary voltage, thereby increasing the saturation current.

Table 6.4 Positive Sequence SVC Variables With TCR Firing Angle Modultion Control of the Positive Sequence DC Component of the TCR Line Current, Transformer Saturation Modelled, SVC FC in 2nd Harmonic Parallel Resonance with System, Source 2nd Harmonic Voltage: 2% @ -30°

Firing Angle	Alpha = 0°	Alpha = 20°	Alpha = 30°	Alpha = 45°
Variable	pu /-°	pu /-°	pu /-°	pu /-°
TCR Line Current				
DC Comp. *	0.0014/ 26°	0.0015/- 90°	0.0006/-117°	0.0013/- 1°
60 Hz Comp.	0.857 /-121°	0.561 /-121°	0.385 /-121°	0.181 /-121°
120 Hz Comp.	0.109 / 178°	0.098 / 172°	0.084 / 167°	0.054 / 158°
Xfmr Primary Line Current				
DC Comp.	0.002 / 26°	0.0031/- 23°	0.0045/- 8°	0.0096/ 5°
60 Hz Comp.	0.310 /- 86°	0.028 / 0°	0.185 / 80°	0.388 / 84°
120 Hz Comp.	0.176 / 21°	0.228 / 16°	0.279 / 11°	0.356 / 2°
Xfmr Saturation Current				
DC Comp.	0.079 / 163°	0.130 / 169°	0.222 / 173°	0.429 / 179°
60 Hz Comp.	0.646 / 96°	0.825 / 96°	1.090 / 96°	1.653 / 95°
120 Hz Comp.	0.231 / 29°	0.363 / 24°	0.581 / 19°	1.059 / 10°
Primary Line Voltage				
DC Comp.	0.0002/- 93°	0.0002/-102°	0.0002/-112°	0.0004/ 94°
60 Hz Comp.	1.007 /- 2°	1.002 /- 2°	1.003 /- 2°	1.001 /- 2°
120 Hz Comp.	0.205 /- 62°	0.231 /- 68°	0.254 /- 73°	0.288 /- 83°
120 Hz Amplification	10.25	11.55	12.7	14.4
Secondary Line Voltage				
DC Comp.	0.0002/- 86°	0.0002/-100°	0.0002/-131°	0.0004/ 97°
60 Hz Comp.	0.974 /- 2°	1.004 /- 2°	1.024 /- 2°	1.044 /- 3°
120 Hz Comp.	0.243 /- 64°	0.280 /- 69°	0.315 /- 74°	0.365 /- 84°
TCR 60 Hz Absorption Mvar (% No Modulation Case)	250.4 (91.6)	169.0 (99.5)	118.3 (99.7)	56.7 (94.2)
Modulation Peak/Phase	15.6/27.3°	9.8/54.5°	12.2/62.7°	16.0/68.2°
Δ ab	13.8°	5.7°	5.6°	5.9°
Δ bc	-13.1°	-9.8°	-12.2°	-15.8°
Δ ca	0.7°	4.1°	6.6°	9.9°

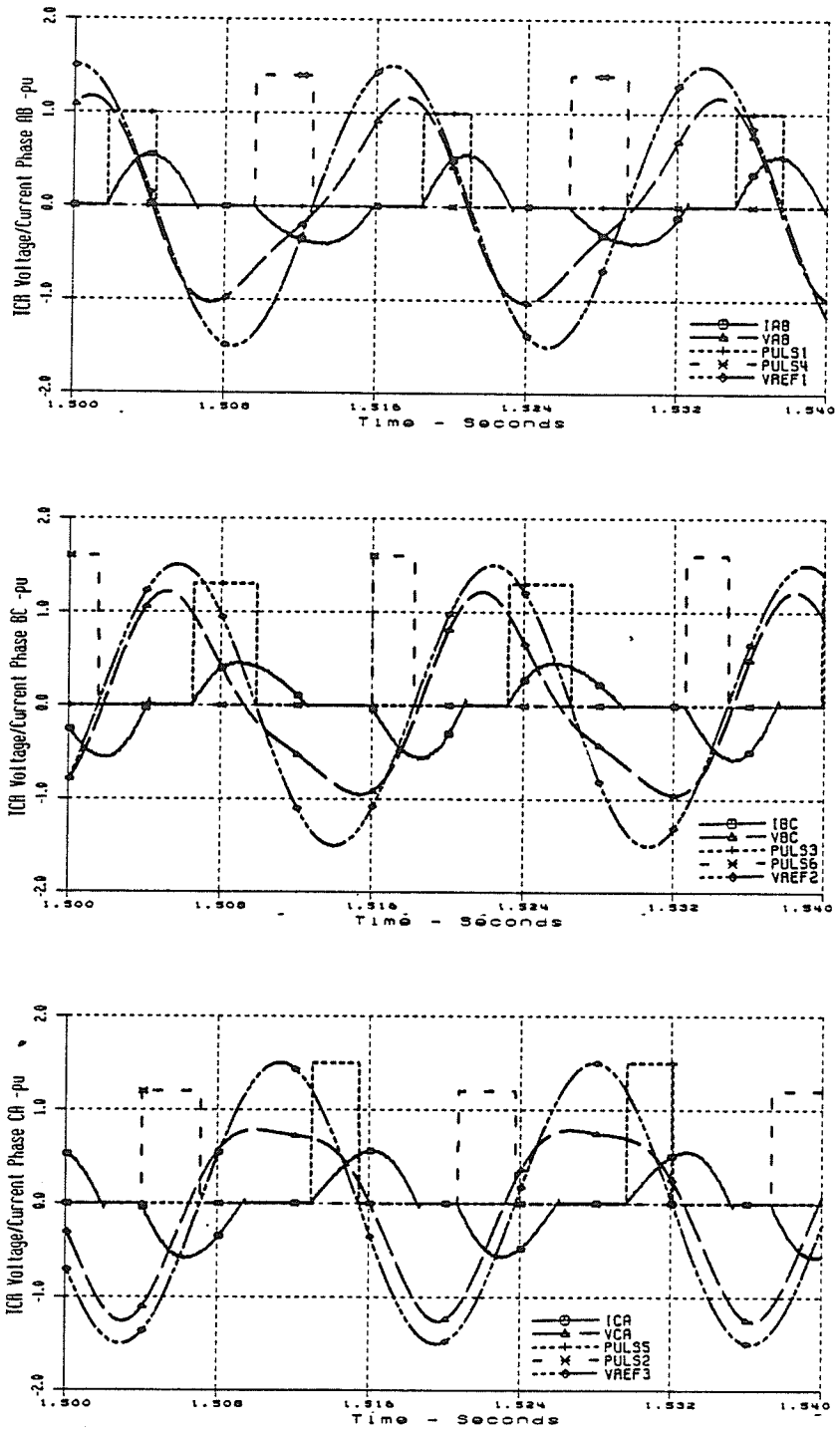

Figure 6.13 TCR Waveforms, Control of Positive Sequence DC Component of TCR Line Current, Alpha = 30°, System and SVC FC in 2nd Harmonic Parallel Resonance, Source 2nd Harmonic Voltage: 2% @ -30°

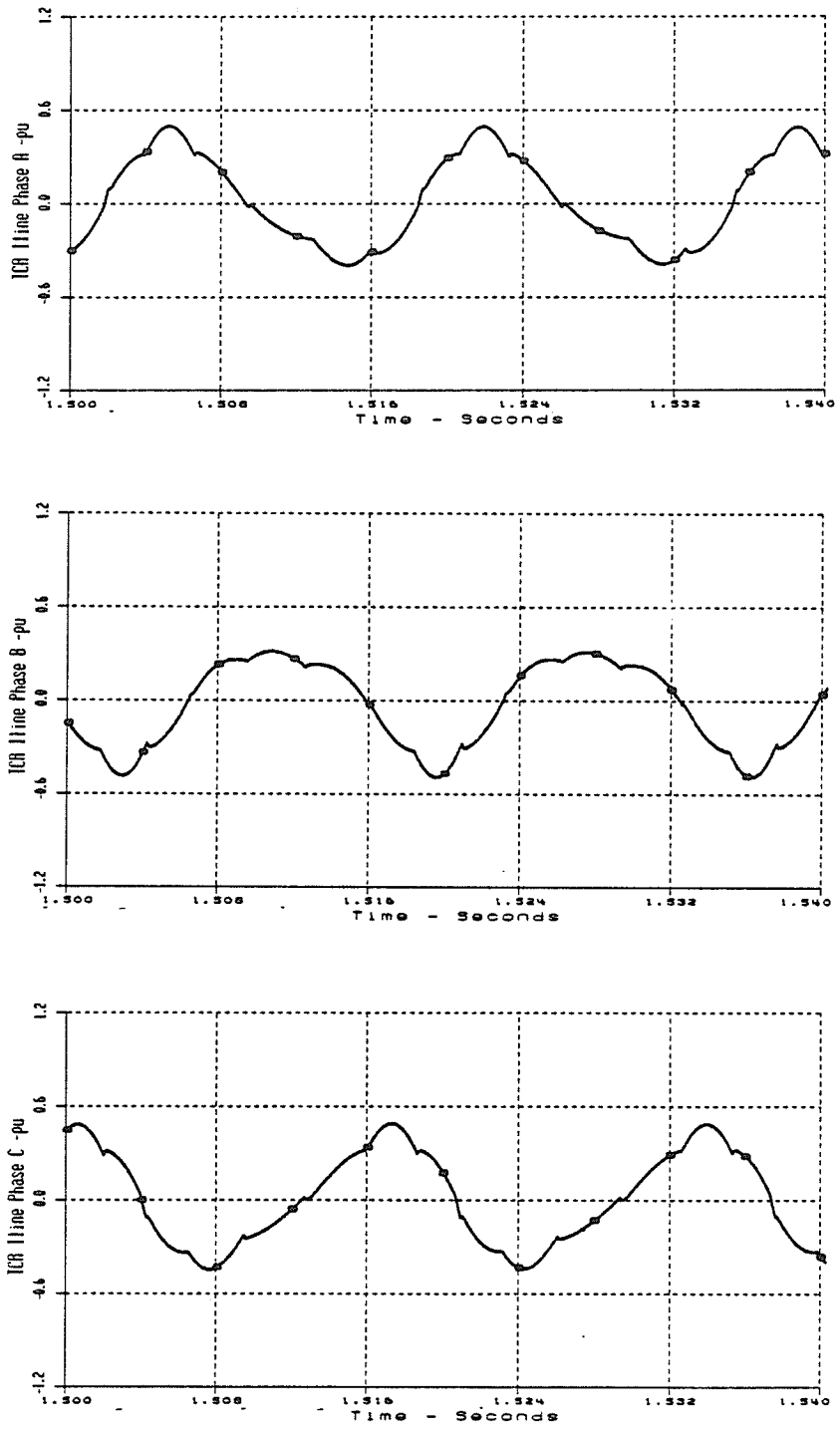

Figure 6.14 TCR Line Current Waveforms, Control of Positive Sequence DC Component of TCR Line Current, Alpha = 30°, System and SVC FC in 2nd Harmonic Parallel Resonance, Source 2nd Harmonic Voltage: 2% @ -30°

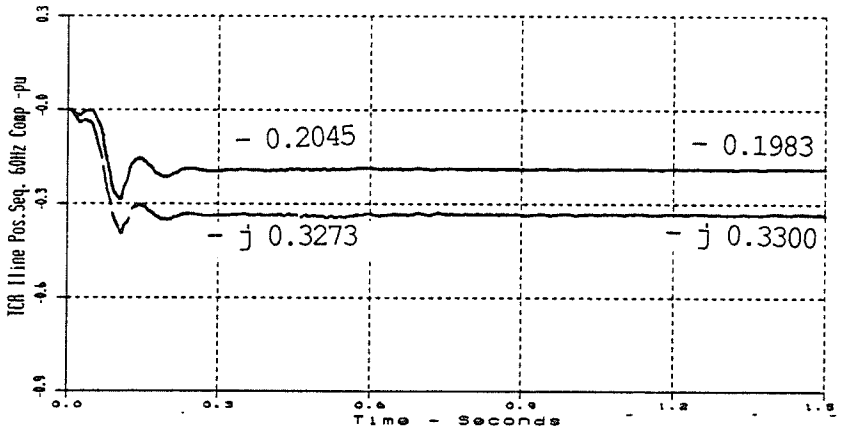

a) Real/Imaginary 60 Hz Components - pu

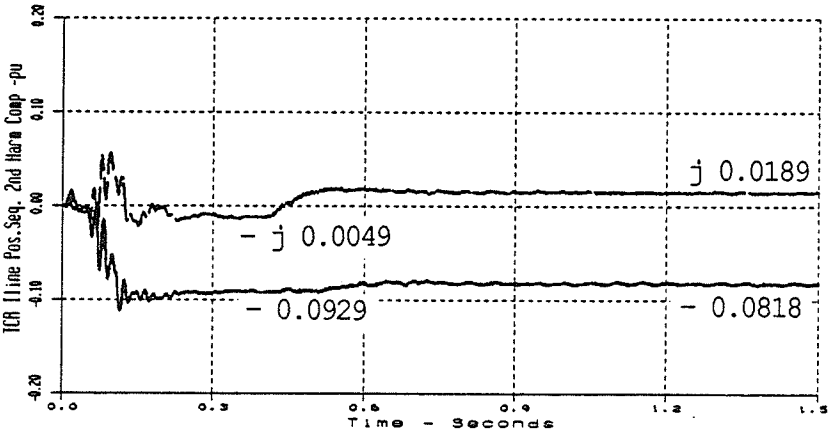

b) Real/Imaginary 2nd Harmonic Components - pu

Figure 6.15 Effect of Control of the Positive Sequence DC Component of TCR Line Current on the 60 Hz and 120 Hz Components, Alpha = 30°, System and SVC FC in 2nd Harmonic Resonance, Source 2nd Harmonic Voltage: 2% @ -30°

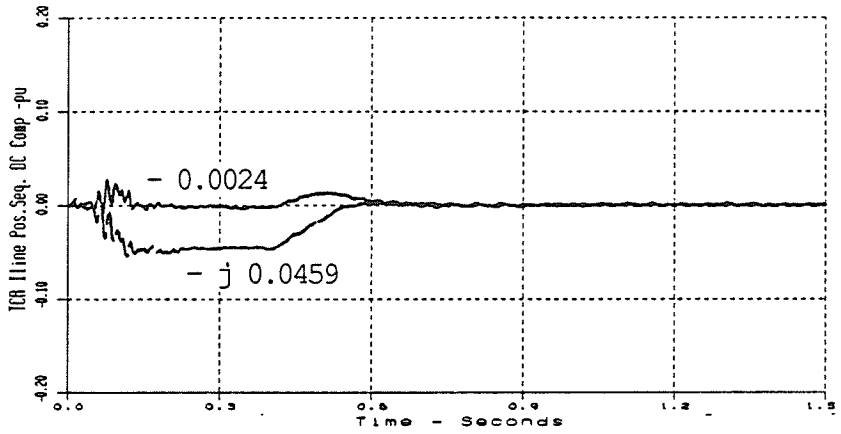

a) Real/Imaginary DC Components - pu

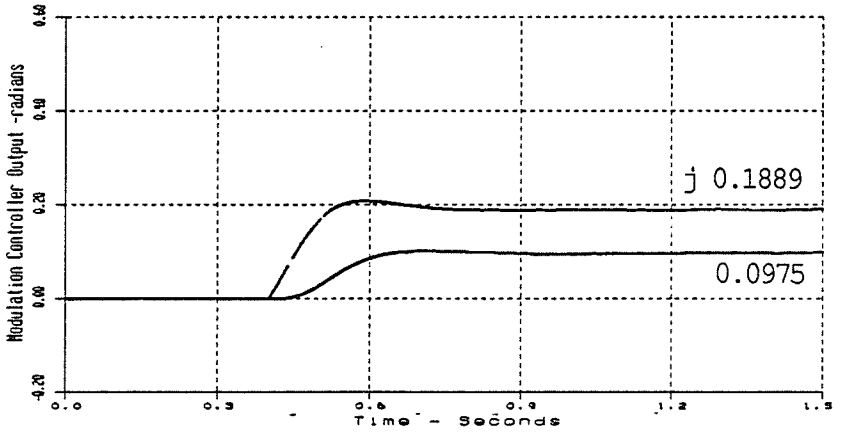

b) Real/Imaginary Modulation Controller Components - radians

Figure 6.16 Control of Positive Sequence DC Component of TCR Line Current, Alpha = 30°, System and SVC FC in 2nd Harmonic Parallel Resonance, Source 2nd Harmonic Voltage: 2% @ -30°

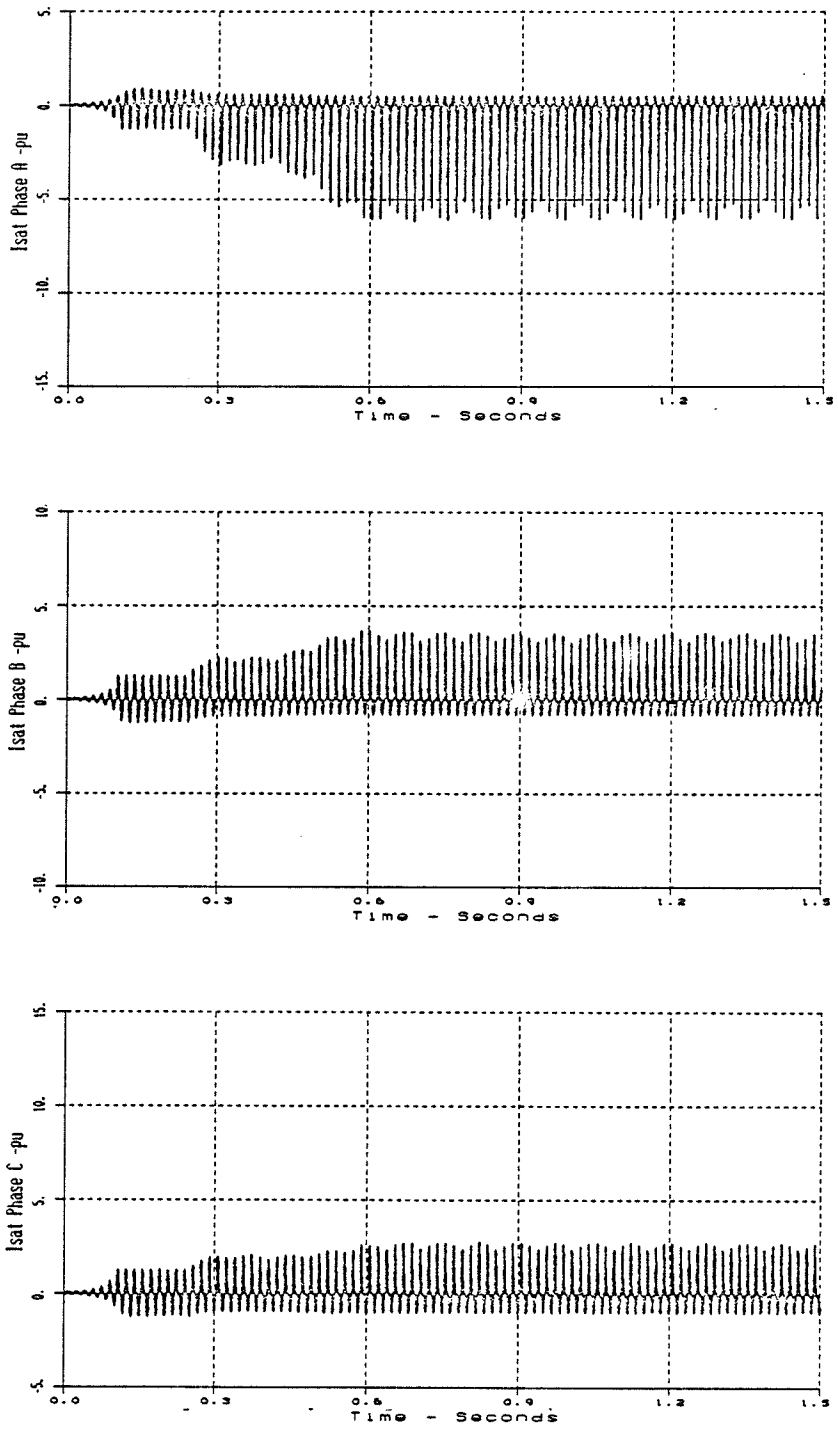

Figure 6.17 Transformer Saturation Current Waveforms, Control of Positive Sequence DC Component of TCR Line Current, Alpha = 30°, System and SVC FC in 2nd Harmonic Parallel Resonance, Source 2nd Harmonic Voltage: 2% @ -30°

6.6 Summary and Conclusions

Sinusoidal modulation of the TCR firing angle was successfully applied to eliminate the dc component or the second harmonic component from the positive sequence of the TCR line current. However, the modulation did not eliminate the parallel resonant condition existing at the point of SVC coupling to the ac system. An increase in the positive sequence second harmonic voltage at the point of SVC coupling was observed with either the dc or the second harmonic component of the positive sequence TCR line current used as the modulation control parameter.

Control of the second harmonic component of the TCR line current increased the second harmonic impedance of the study system as observed from the point of SVC coupling to the system. This increased the second harmonic component of the positive sequence system voltage. Furthermore, considerable modulation was required to cancel the second harmonic component of the TCR line current. The large modulation signals caused extensive SVC transformer saturation due to the dc component in the TCR phase current waveforms, which further aggravated the voltage distortion.

For the system investigated in this chapter, control of the dc component of the TCR line may be more beneficial in that the saturation of the SVC transformer is minimized. However, even control of the dc component aggravated the voltage distortion due to the parallel resonance.

When firing angle limits were encountered, the fundamental frequency TCR loading was reduced by the firing angle modulation. A reduction of about 10% was observed with the dc component of the TCR line current as the control parameter. A reduction of up to 50% was observed with the second harmonic component as the control parameter.

Elimination of the dc component from the positive sequence of the TCR line current, in general also reduced the second harmonic component by between 2.7% and 25% of the "no modulation" valves.

Elimination of the second harmonic component, on the other hand, caused the dc component to increase by as much as 223% with the TCR line current as the controlled parameter.

Control of the second harmonic component of TCR line current via firing angle modulation caused the SVC transformer saturation current to increase. The second harmonic modula-

tion generally caused an increase in the dc component of TCR phase current, which caused an increase in the level of transformer saturation.

The dc component modulation control only minimally increased the transformer saturation level when firing angle limits were encounted.

Modulation angle limits and a voltage control strategy are required to prevent the controller from forcing the TCR to operate in the region where firing angle limits are encountered, especially if the second harmonic component is to be controlled. This would limit the possibility of driving the SVC transformer into severe saturation.

The modulation controller response was found to be very stable.

CHAPTER SEVEN

PERFORMANCE OF AN SVC CONNECTED TO A WEAK AC NETWORK WITH A SECOND HARMONIC PARALLEL RESONANCE BETWEEN THE NETWORK AND THE SVC

7.1 Study Network

The performance of the TCR with sinusoidal firing angle modulation was evaluated with the SVC connected to an ac network characterized by a second harmonic parallel resonant condition between the network and the SVC (fixed capacitor plus TCR with alpha = 0°) as observed from the point of SVC coupling to the network. The single line diagram of the study network is shown in Figure 7.1, and the detailed three phase EMTDC simulation circuit is shown in Figure 2.2.

The rating of the SVC and the rating of the SVC step-up transformer were the same as used in Chapter 4.

The equivalent system parameters were chosen such that a second harmonic parallel resonance existed between the equivalent Thevenin reactance of the system the equivalent shunt connected capacitive reactance and the SVC. The three

phase short circuit capacity of the system was approximately:

$$Ssc = \frac{(kV)^2}{Zs} = \frac{(120\ kV)^2}{13.16\ ohm} = 1\ 094\ MVA \qquad (7.1)$$

The effective short circuit capacity at the point of SVC coupling was approximately:

$$Ssce = Ssc - Scap = 944\ MVA \qquad (7.2)$$

where Scap = 150 Mvar, the equivalent system shunt capacitance. The system damping angle was assumed to be 85°.

The system compensation ratio, defined for the SVC as:

$$SCR = \frac{Ssce}{Qsvc} = \frac{944}{480} = 1.97. \qquad (7.3)$$

Considering the TCR alone the SCR is:

$$SCR = \frac{Ssce}{Qtcr} = 3.15. \qquad (7.4)$$

The TCR performance was evaluated at nominal firing angles of 0°, 20°, 30° and 45°. The study system fundamental frequency steady state conditions for each TCR firing angle are shown in Figure 7.2. The fundamental frequency Thevenin voltage source magnitude was adjusted to maintain 1.0 pu voltage at the point of coupling of the SVC to the high voltage system.

Table 7.1 shows the computed variation with frequency in the magnitudes of the fundamental and second harmonic impedances as observed from the point of SVC coupling to the high voltage system for TCR firing angles of 0°, 20°, 30° and 45°. As the firing angle increases the resonant frequency shifts below 120 Hz, and the magnitude of the second harmonic impedance decreases with firing angle.

The solid line in Figure 7.3 shows the variation in system impedance with frequency as observed at the point of SVC coupling to the system with the SVC connected and a TCR firing angle of 0°. Clearly a parallel resonance exists at the second harmonic. The system impedance behaves capacitively at the second harmonic when alpha is greater than 0°. The dashed line, which represents the system impedance variation with frequency when the TCR reactor is not connected, shows that the system is resonant at 103 Hz without the TCR reactor.

Table 7.1 Study System Impedance Magnitude versus Frequency as Observed from the Point of SVC Coupling to the AC System				
TCR Firing Angle	0°	20°	30°	45°
Frequency	Impedance Magnitude (Ohms)			
60 Hz	13.6	15.4	16.4	17.8
Resonant Point (- Hz)	266.0 (120)	256.1 (113)	249.7 (110)	240.6 (106)
120 Hz	266.0	130.4	96.1	72.0

A second harmonic current injection into the network at the point of SVC coupling can produce large second harmonic voltages due to the high impedance. The voltage amplification will be smaller as the TCR firing angle increases. A second harmonic voltage with a magnitude of 3.0% at -30° relative to the fundamental was superimposed on the fundamental source to provide the current injection required to excite the resonant condition.

7.2 Per unit System

The TCR reactor rating was used to define the per unit base quantities which are defined in Table 4.1. The per unit base used for the transformer saturation current was the rated winding magnetizing current.

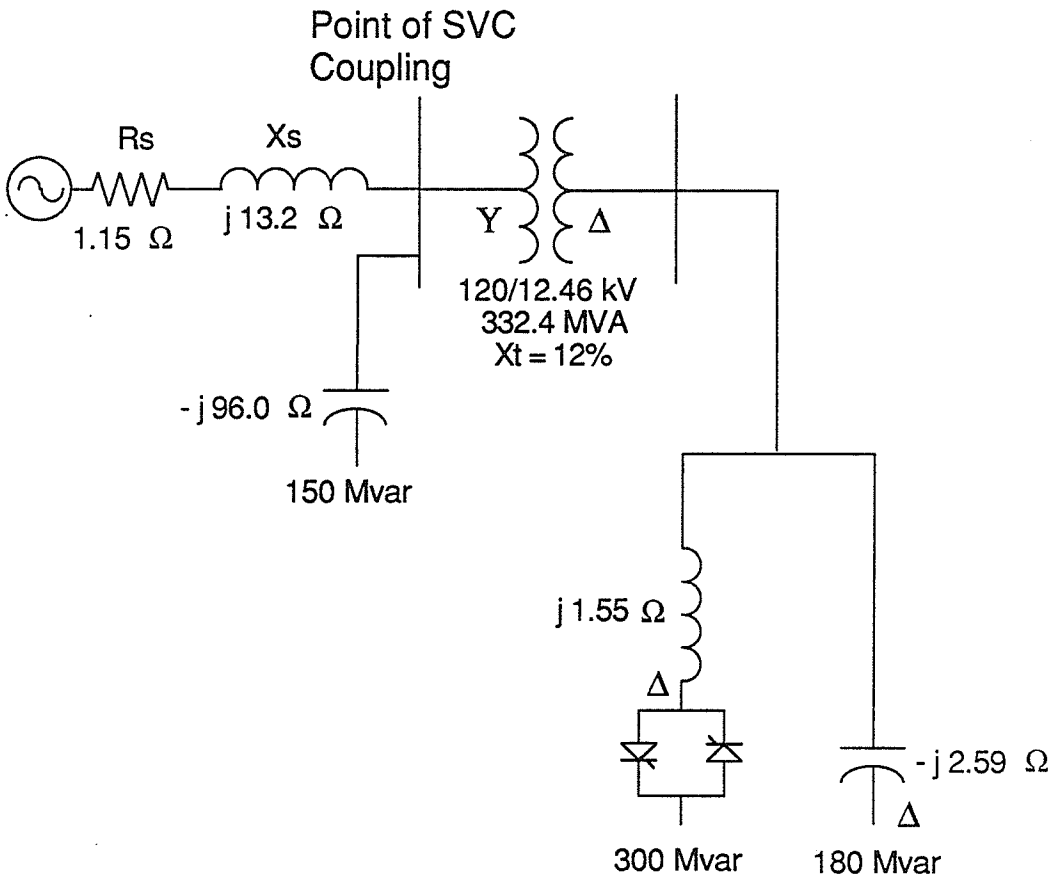

Figure7.1 Study Network Single Line Diagram,
System and SVC in Second Harmonic Parallel
Resonance at the Point of SVC Coupling.

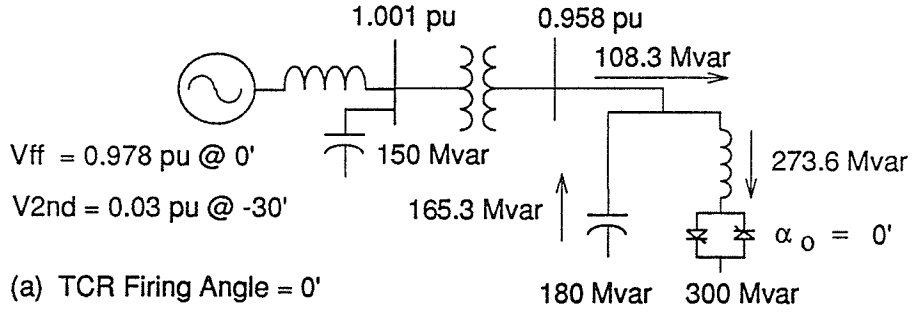

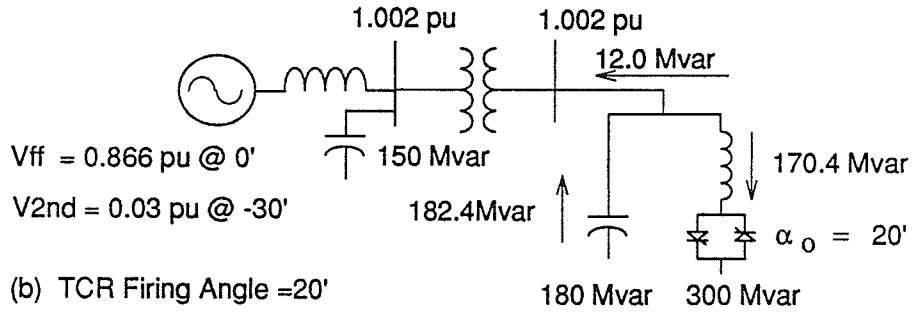

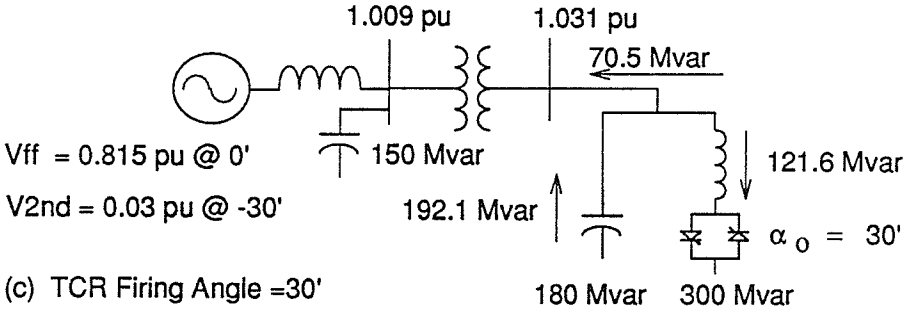

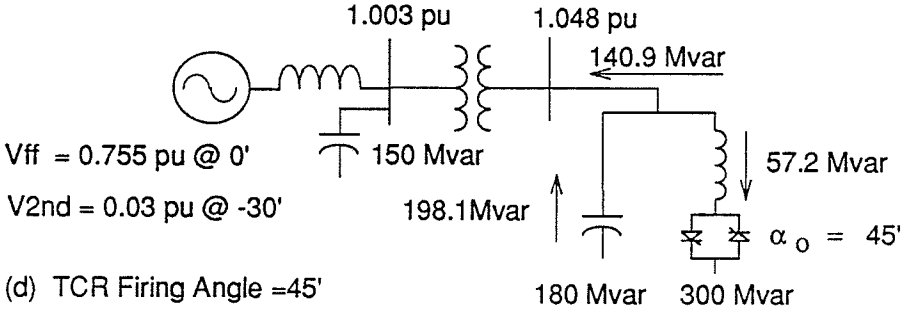

Figure 7.2 Study System Steady State Conditions

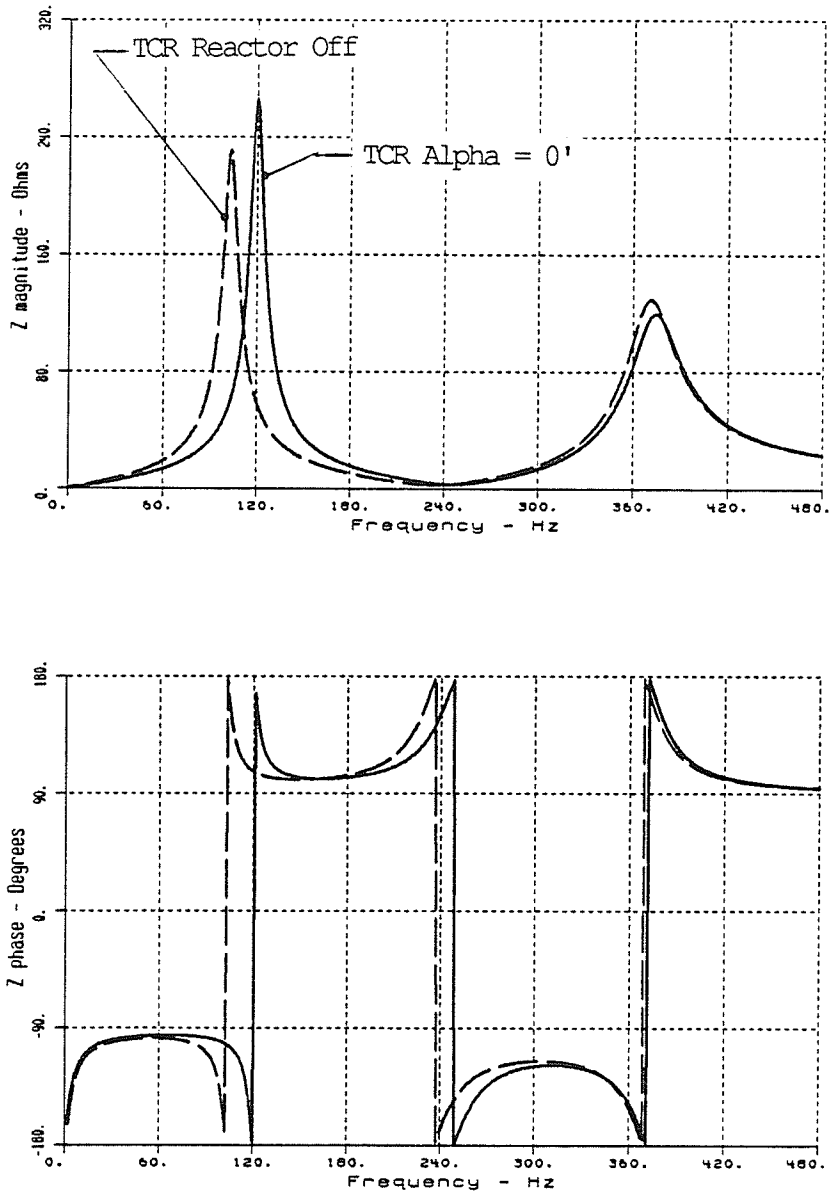

Figure 7.3 System Impedance vs. Frequency at the Point of SVC Coupling to the Network

7.3 TCR Performance with Equidistant Firing

The steady state positive sequence harmonic phasor components of some SVC variables are listed in Table 7.2 for equidistant firing of the TCR at 0°, 20°, 30° and 45°. A second harmonic parallel resonant condition exists between the equivalent system Thevenin reactance, the equivalent system shunt capacitance and the SVC at the point of SVC coupling to the 120 kV network.

The second harmonic source voltage of 3% @ -30° relative to the fundamental Thevenin source voltage was amplified by a factor of 9.83 at alpha = 0°, 6.53 at alpha = 20°, 4.93 at alpha = 30° and 3.47 at alpha = 45°. This second harmonic voltage amplification resulted in second harmonic voltage components ranging from 13.0% to 34.5% across the TCR terminals. The reduction in voltage amplification is due to the reduction in the magnitude of the second harmonic impedance with firing angle as shown in Table 7.1.

The dc component of the positive sequence TCR line current only varied from 7.6% to 9.9% relative to the fundamental component over the TCR firing range, while the second harmonic component varied from 18.3% to 20.3%.

Figure 7.4 shows the steady state TCR waveforms for the case of alpha = 20°. The TCR line current waveforms are plotted in Figure 7.5.

The measured real and imaginary parts of the dc, 60 Hz and 120 Hz components of the positive sequence TCR line current are shown in Figure 7.6 for TCR firing at 20°.

Figure 7.7 shows the SVC transformer saturation current waveforms for TCR equidistant firing at 20°. The currents are clearly non-symmetrical due to the voltage waveform distortion caused by the second harmonic voltage component. A peak saturation current of about 2.5 pu (5% of rated transformer winding current) was observed.

Table 7.2 Positive Sequence SVC Variables with Equidistant Firing of the TCR, Transformer Saturation Modelled, SVC and Network in 2nd Harmonic Parallel Resonance, Source 2nd Harmonic Voltage: 3% @ -30°

Firing Angle	Alpha = 0°	Alpha = 20°	Alpha = 30°	Alpha = 45°
Variable	pu /-°	pu /-°	pu /-°	pu /-°
TCR Line Current				
DC Comp.	0.072 /- 7°	0.053 /- 34°	0.036 /- 33°	0.018 /- 26°
60 Hz Comp.	0.952 /-120°	0.567 /-121°	0.393 /-122°	0.182 /-123°
120 Hz Comp.	0.173 / 134°	0.107 / 128°	0.072 / 123°	0.037 / 116°
Xfmr Primary Line Current				
DC Comp.	0.045 / 24°	0.033 /- 3°	0.027 / 0°	0.011 / 10°
60 Hz Comp.	0.415 /- 87°	0.024 /- 12°	0.186 / 81°	0.405 / 84°
120 Hz Comp.	0.232 /- 23°	0.168 /- 44°	0.141 /- 60°	0.123 /- 82°
Xfmr Saturation Current				
DC Comp.	0.094 /-154°	0.085 /-132°	0.086 /-118°	0.075 /-101°
60 Hz Comp.	0.665 / 96°	0.737 / 96°	0.827 / 96°	0.870 / 95°
120 Hz Comp.	0.303 /- 14°	0.254 /- 33°	0.243 /- 47°	0.203 /- 67°
Primary Line Voltage				
DC Comp.	0.0010/-140°	0.0009/-167°	0.0007/-150°	0.0005/-124°
60 Hz Comp.	1.001 /- 1°	1.002 /- 2°	1.009 /- 2°	1.003 /- 3°
120 Hz Comp.	0.295 /-105°	0.196 /-120°	0.148 /-133°	0.104 /-155°
120 Hz Amplification	9.83	6.53	4.93	3.47
Secondary Line Voltage				
DC Comp.	0.0014/-144°	0.0013/-172°	0.0009/-154°	0.0006/-131°
60 Hz Comp.	0.958 /- 1°	1.002 /- 2°	1.031 /- 2°	1.048 /- 3°
120 Hz Comp.	0.345 /-107°	0.232 /-122°	0.177 /-136°	0.130 /-158°
TCR 60 Hz Absorption Mvar	273.6	170.4	121.6	57.2

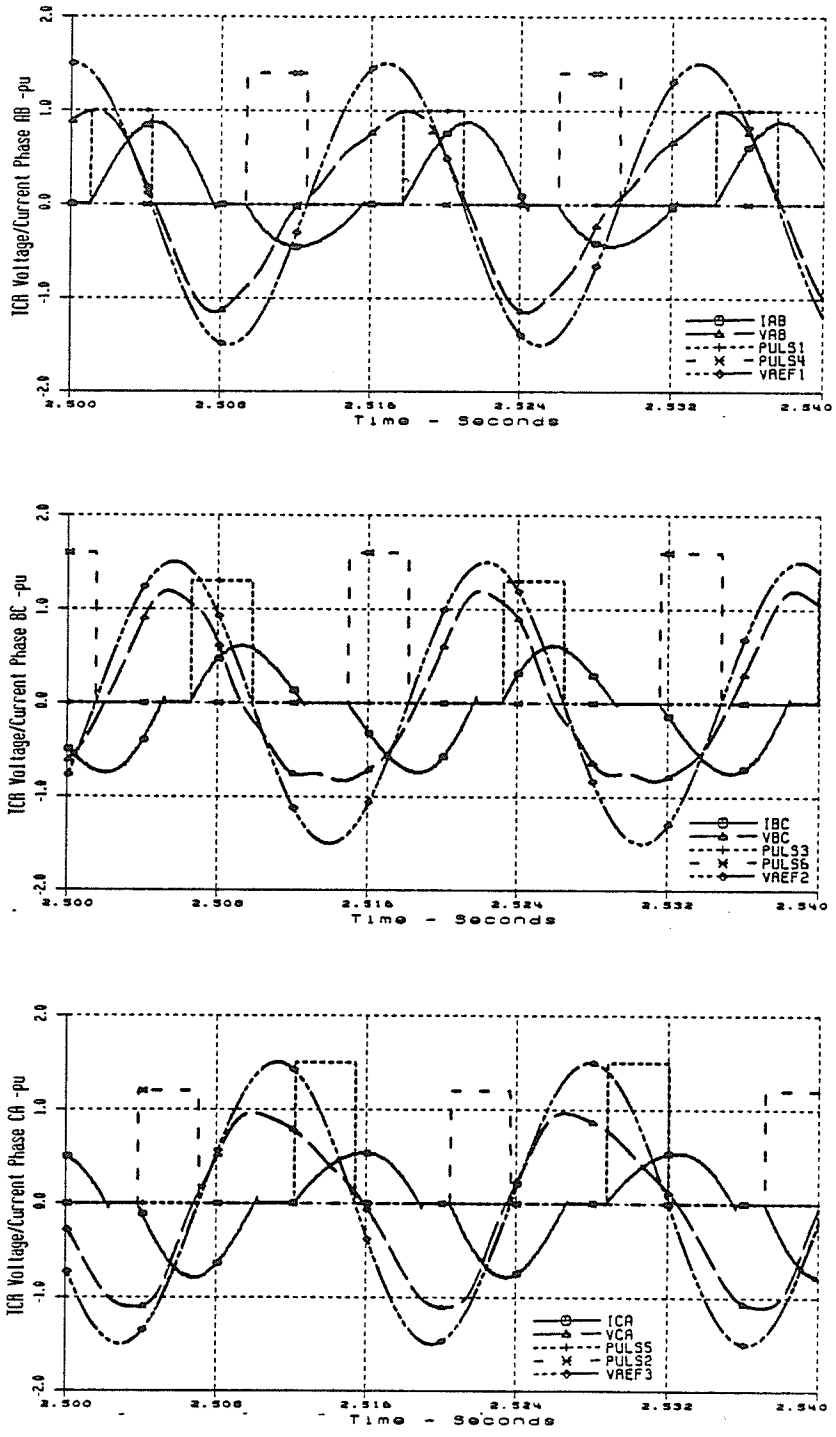

Figure 7.4 TCR Waveforms with Equidistant Firing, Alpha = 20°, System and SVC in 2nd Harmonic Parallel Resonance, Source 2nd Harmonic Voltage: 3% @ -30°

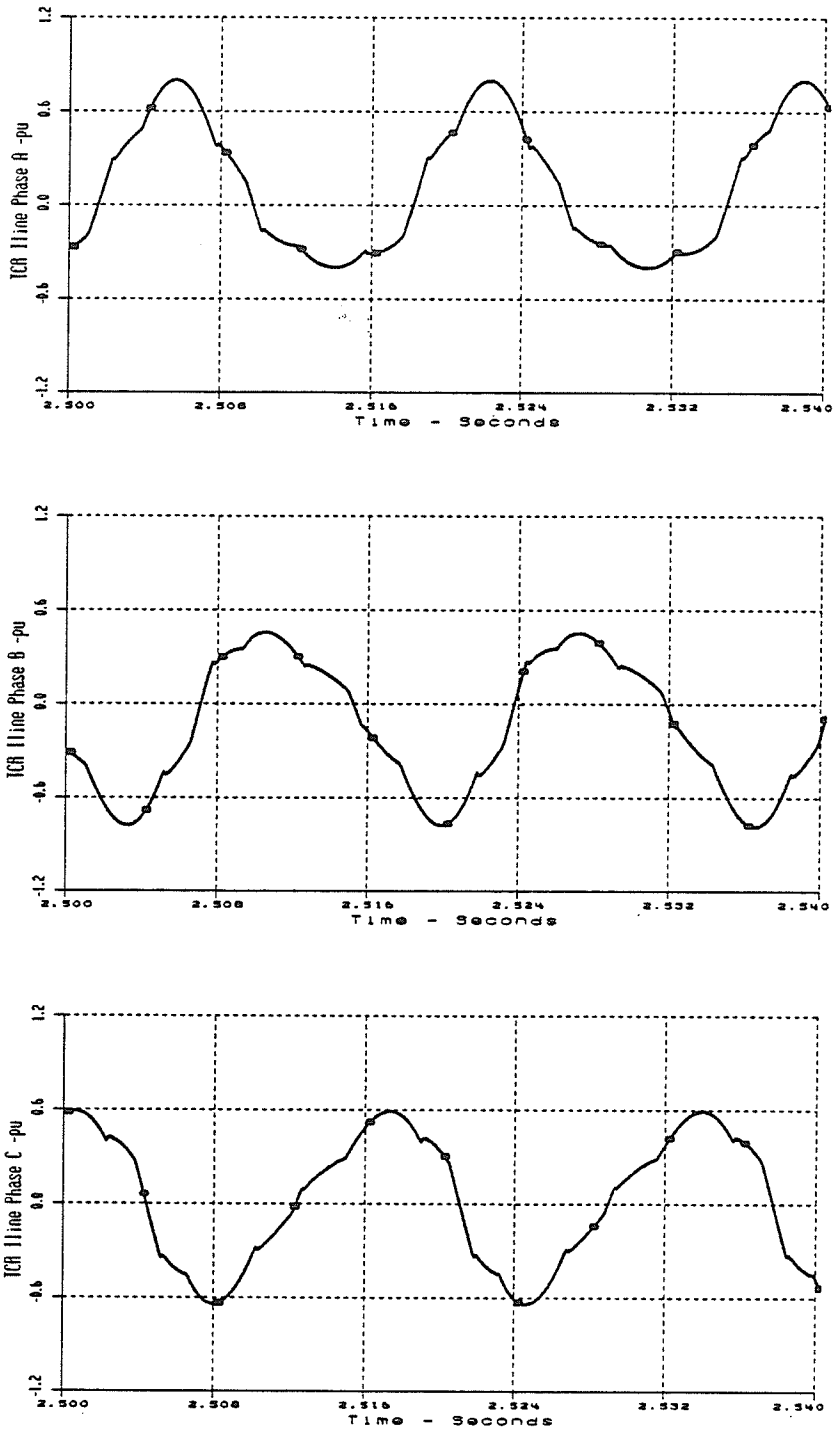

Figure 7.5 TCR Line Current Waveforms with Equidistant Firing, Alpha = 20°, System and SVC in 2nd Harmonic Parallel Resonance, Source 2nd Harmonic Voltage: 3% @ -30°

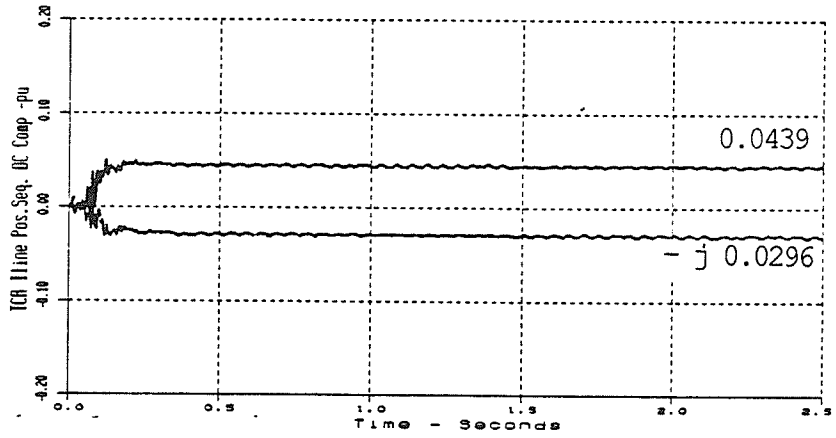

a) Real/Imaginary DC Components - pu

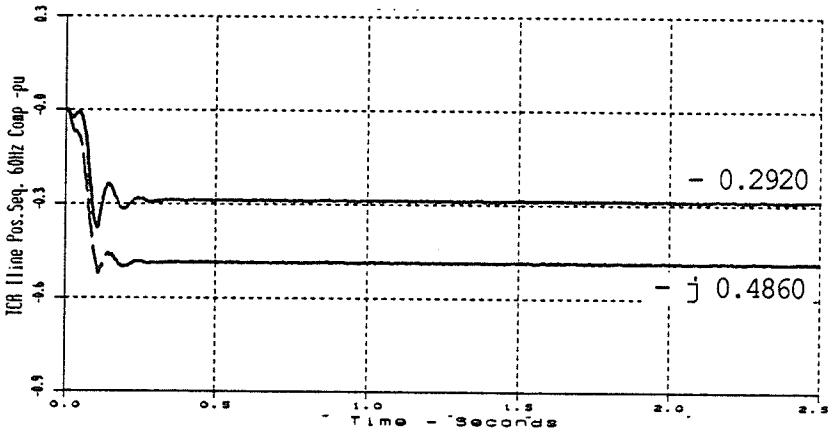

b) Real/Imaginary 60 Hz Components - pu

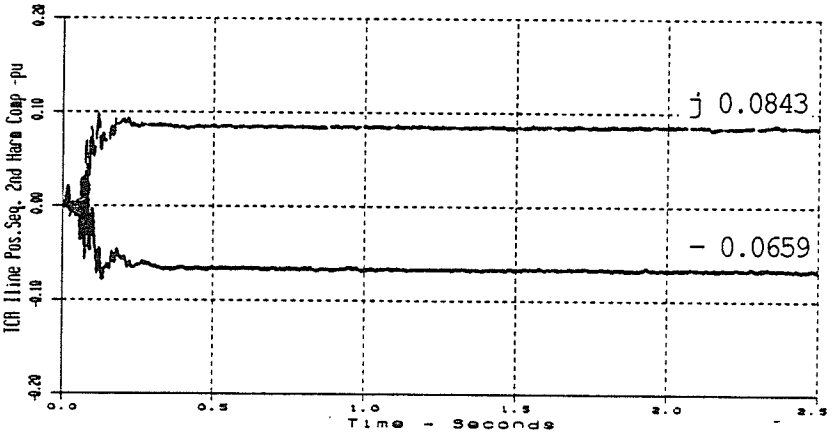

c) Real/Imaginary 2nd Harmonic Components - pu

Figure 7.6 Positive Sequence Phasor Components of TCR Line Current with Equidistant TCR Firing, Alpha = 20°, System and SVC in 2nd Harmonic Parallel Resonance, Source 2nd Harmonic Voltage: 3% @ -30°

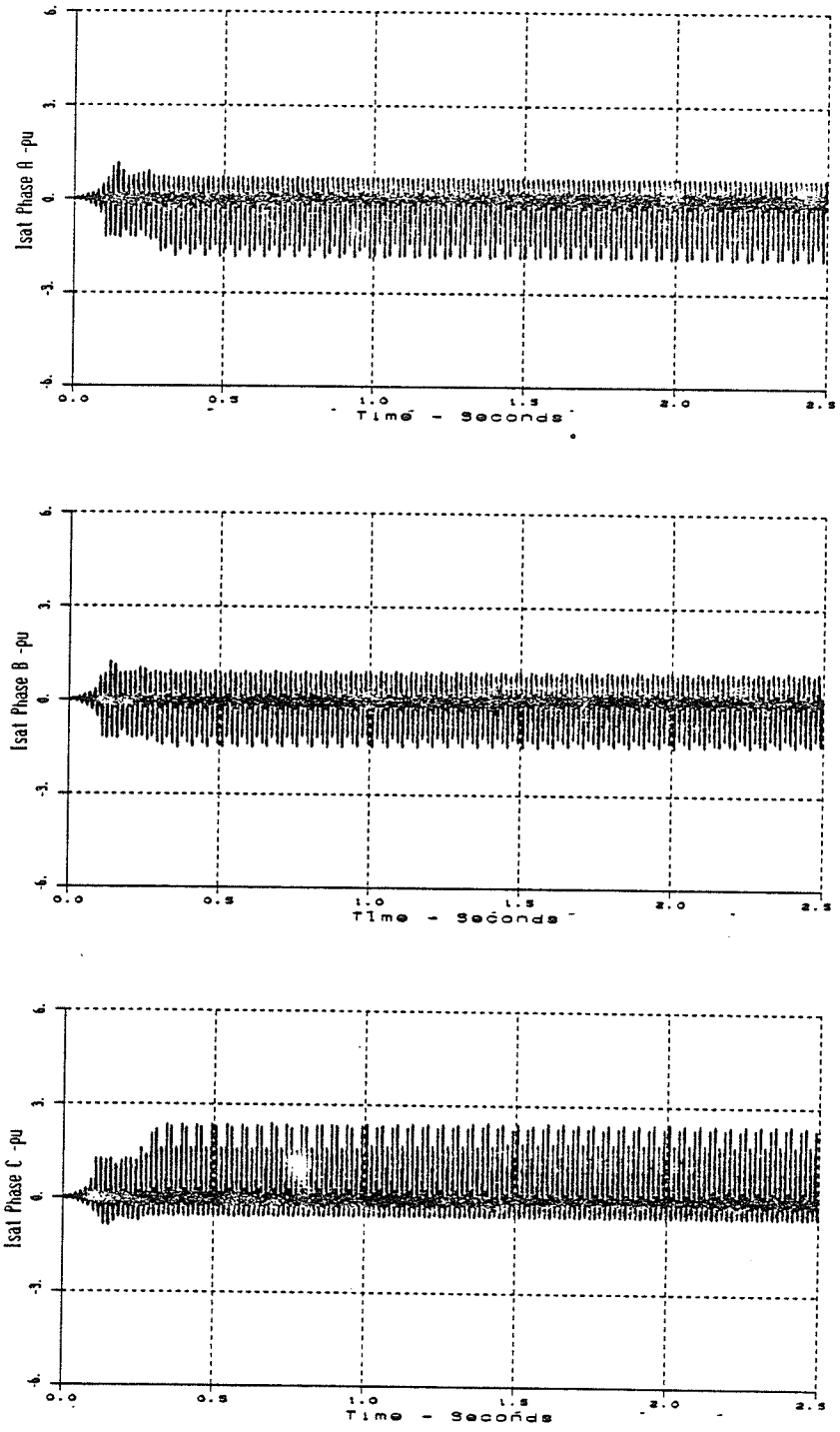

Figure 7.7 Transformer Saturation Current Waveforms with Equidistant TCR Firing, Alpha = 20°, System and SVC in 2nd Harmonic Parallel Resonance, Source 2nd Harmonic Voltage: 3% @ -30°

7.4 TCR Performance Using Firing Angle Modulation to Control the Positive Sequence Second Harmonic Phasor Component of the TCR Line Current

The measured real and imaginary second harmonic phasor components of the positive sequence TCR line current were input to the TCR firing angle modulation controller to generate a modulation signal to cancel the second harmonic component. The controller settings that were applied are listed in Table 3.3 with the exception that the integral gain was reduced from -90 to -15 rad/pu-s.

The steady state positive sequence harmonic phasor components of some SVC variables and the modulation parameters are presented in Table 7.3 for nominal TCR firing angles of 0°, 20°, 30° and 45°.

Sinusoidal modulation of the TCR firing angle successfully eliminated the second harmonic component from the positive sequence of the TCR line current for all the nominal TCR firing angles considered. The modulation also damped the second harmonic parallel resonance. The second harmonic voltage amplification was reduced to 26% at alpha = 0°, 39% at alpha = 20°, 51% at alpha = 30° and 72% at alpha = 45° of the "no modulation" values. The damping of the second harmonic resonance by the modulation can be explained by consideration of Figure 7.3. Cancellation of the second

harmonic component of TCR line current makes the TCR reactance appear infinite at 120 Hz since no second harmonic current can flow. That is, the system resonant frequency is shifted toward the dashed curve in Figure 7.3, thereby reducing the second harmonic impedance from that of the "no modulation" cases.

Firing angle limits were encountered at nominal TCR firing angles of 0°. Clearly at alpha = 0°, the modulation is one sided as limits are encountered for any modulation magnitude and phase. The one sided modulation at alpha = 0° reduced the 60 Hz TCR loading to 89% of the "no modulation" case. The TCR loading at other firing angles was not significantly changed by the modulation.

Figures 7.8 and 7.9 respectively show the TCR waveforms and the TCR line current waveforms for the case of alpha = 20°. Some voltage waveform distortion exists at the voltage peak but otherwise the waveforms are nearly symmetrical relative to the zero voltage axis.

The elimination of the second harmonic component increased the dc component by 50% at 0°, but only 13% at 20° relative to the "no modulation" values (Table 7.2). At alpha = 30° and 45°, the dc component is reduced by 17% and 44% respec-

tively. Figure 7.10 shows the measured positive sequence dc and 60 Hz components of the TCR line current for TCR firing at 20°. The magnitude of the dc component is increased from 0.053 pu @ -34° (no modulation value) to 0.060 pu @ -109° by the modulation controller action. The 60 Hz component is only marginally reduced by the modulation.

Figure 7.11 shows the measured positive sequence second harmonic component of TCR line current and the modulation controller output for TCR firing at 20°. The second harmonic is reduced from 0.107 pu @ 128° to zero in about 400 ms. The modulation controller output corresponds to a modulation peak of 12.9° and a modulation phase of -92.2°. The response of the controller was very stable and similar at all the TCR firing angles examined. However, with the TCR reactor contributing to the parallel resonance, the integral gains had to be reduced from -90 to -15 rad/pu-s. Otherwise, the response would be considerably underdamped relative to the cases in the previous chapters.

Figure 7.12 shows the SVC transformer saturation current waveforms for the nominal TCR firing angle of 20°. The modulation controller was activiated at 0.40s. The transformer saturation current did not change significantly as the modulation reduced the voltage waveform distortion caused by the second harmonic parallel resonance. Com-

parison of the steady state phasor components of saturation current listed in Tables 7.2 and 7.3 illustrates that the firing angle modulation caused a reduction in the transformer saturation current components except at the TCR firing angle of 0° where the "one sided" modulation increased the dc component of TCR phase current. Comparison of Figures 7.7 and 7.12 also illustrates this result.

Table 7.3 Positive Sequence SVC Variables With TCR Firing Angle Modultion Control of the Positive Sequence 2nd Harmonic Component of TCR Line Current, Transformation Saturation Modelled, SVC and Network in 2nd Harmonic Parallel Resonance, Source 2nd Harmonic Voltage: 3% @ -30°

Firing Angle	Alpha = 0°	Alpha = 20°	Alpha = 30°	Alpha = 45°
Variable	pu /-°	pu /-°	pu /-°	pu /-°
TCR Line Current				
DC Comp.	0.106/-105°	0.060/-109°	0.030 /-111°	0.010°/-113
60 Hz Comp.	0.767/-121°	0.554/-121°	0.390 /-121°	0.180°/-122
120 Hz Comp. *	0.002/-146°	0.002/ 40°	0.001 /- 12°	0.0007/ 59°
Xfmr Primary Line Current				
DC Comp.	0.073/- 73°	0.039/- 82°	0.023 /- 87°	0.006 /- 95°
60 Hz Comp.	0.183/- 81°	0.032/ 27°	0.191 / 80°	0.409 / 84°
120 Hz Comp.	0.115/-107°	0.114/-107°	0.114 /-107°	0.115 /-107°
Xfmr Saturation Current				
DC Comp.	0.158/- 69°	0.054/- 71°	0.160 /- 70°	0.061 /- 71°
60 Hz Comp.	1.033/ 95°	0.690/ 96°	0.781 / 96°	0.853 / 95°
120 Hz Comp.	0.325/-103°	0.132/-100°	0.149 /-100°	0.160 /- 99°
Primary Line Voltage				
DC Comp.	0.0022/ 100°	0.0007/ 93°	0.0003/ 95°	0.0001/-101°
60 Hz Comp.	1.074 /- 2°	1.008/- 2°	1.011 /- 2°	1.003 /- 3°
120 Hz Comp.	0.076 / 168°	0.075/ 168°	0.075 / 166°	0.075 / 168°
120 Hz Amplification	2.53	2.50	2.50	2.50
Secondary Line Voltage				
DC Comp.	0.0029/ 102°	0.0012/ 92°	0.0005/ 95°	0.0001/-163°
60 Hz Comp.	1.056 /- 2°	1.010 /- 2°	1.032 / - 2°	1.049 /- 3°
120 Hz Comp.	0.101 / 167°	0.100 / 166°	0.100 / 165°	0.100 / 166°
TCR 60 Hz Absorption Mvar (% No Modulation Case)	243.0 (88.8)	167.9 (98.5)	120.7 (99.3)	56.6 (99.0)
Modulation Peak/Phase	36.0/-102.5°	12.9/-92.2°	9.4/-82.8°	7.0/-64.3°
Δ ab	- 7.8°	- 0.5°	1.2°	3.0°
Δ bc	34.3°	11.4°	7.4°	3.9°
Δ ca	-26.5°	-10.9°	-8.6°	-6.9°

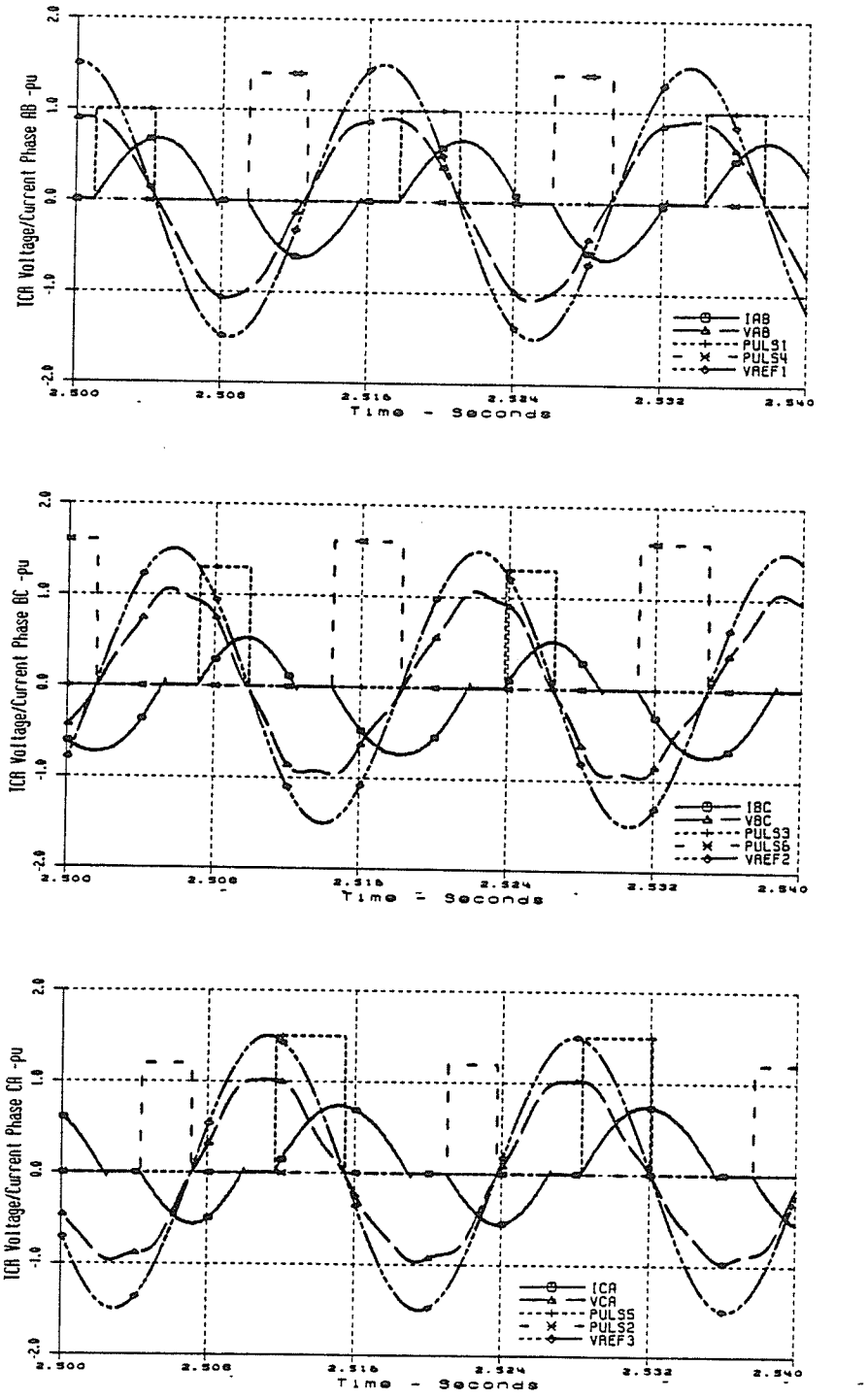

Figure 7.8 TCR Waveforms, Control of Positive Sequence 2nd Harmonic Component of TCR Line Current, Alpha = 20°, System and SVC in 2nd Harmonic Parallel Resonance, Source 2nd Harmonic Voltage: 3% @ - 30°

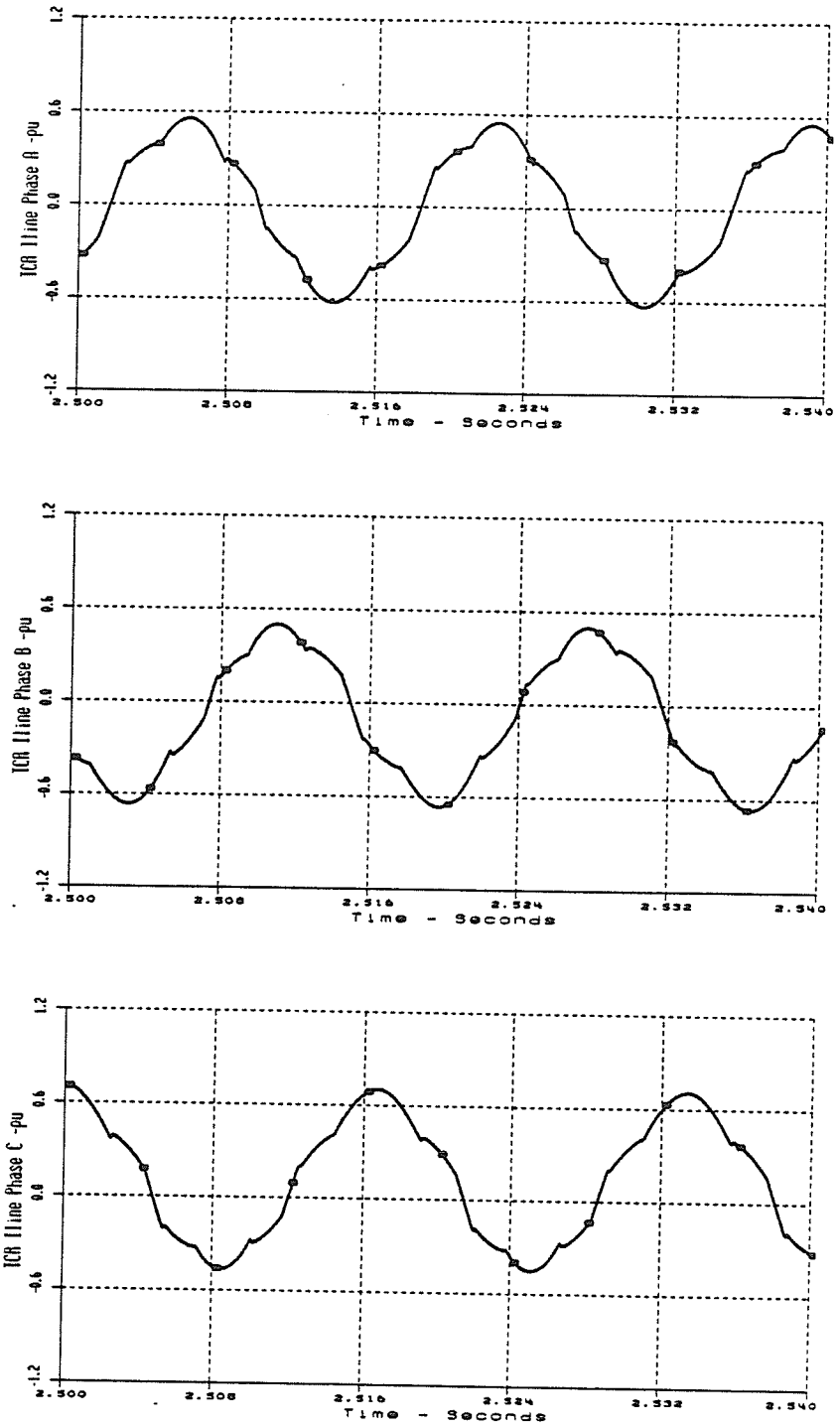

Figure 7.9 TCR Line Current Waveforms, Control of Positive Sequence 2nd Harmonic Component of TCR Line Current, Alpha = 20°, System and SVC in 2nd Harmonic Parallel Resonance, Source 2nd Harmonic Voltage: 3% @ -30°

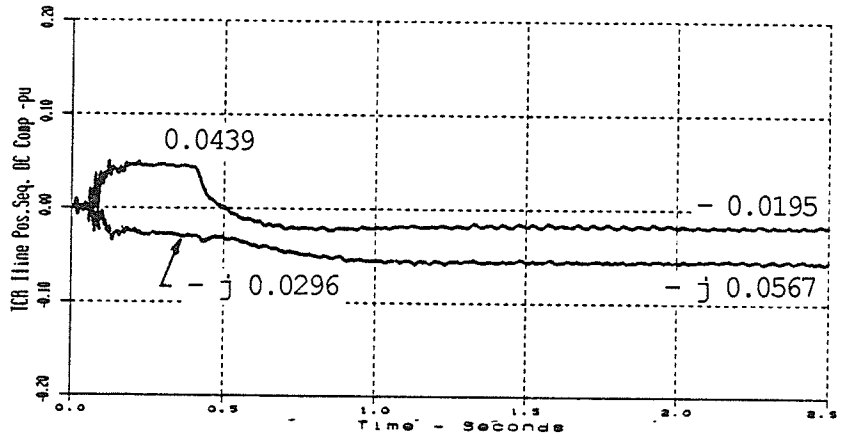

a) Real/Imaginary DC Components - pu

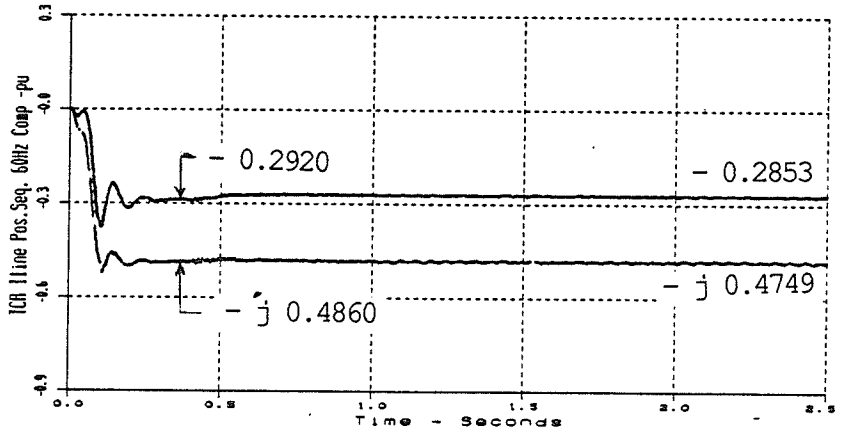

b) Real/Imaginary 60 Hz Components - pu

Figure 7.10 Effect of Control of the Positive Sequence 2nd Harmonic Component of TCR Line Current on the DC and 60 Hz Components, Alpha = 20°, System and SVC in 2nd Harmonic Parallel Resonance, Source 2nd Harmonic Voltage: 3% @ -30°

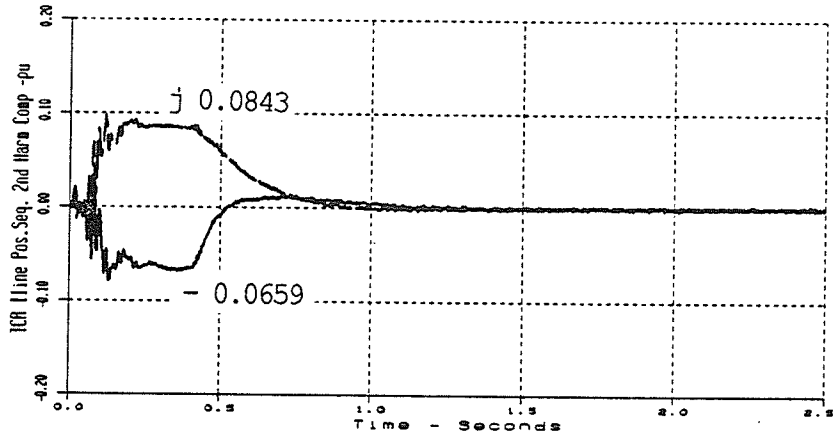

a) Real/Imaginary 2nd Harmonic Components - pu

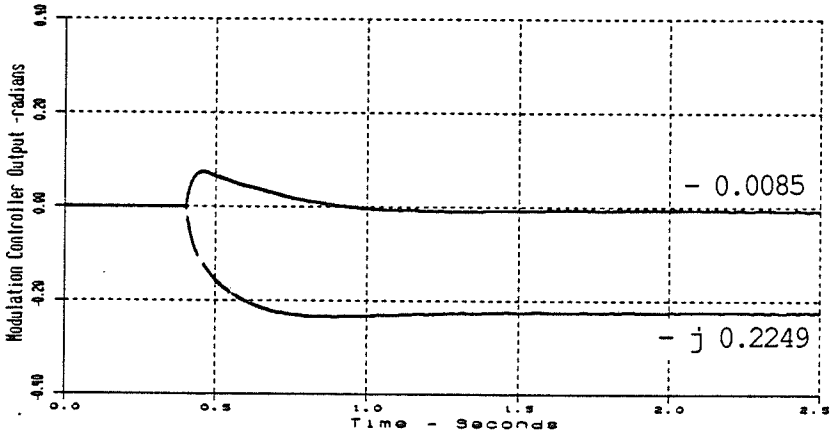

b) Real/Imaginary Modulation Controller Components - radians

Figure 7.11 Control of Positive Sequence 2nd Harmonic Component of TCR Line Current, Alpha = 20°, System and SVC in 2nd Harmonic Parallel Resonance, Source 2nd Harmonic Voltage: 3% @ -30°

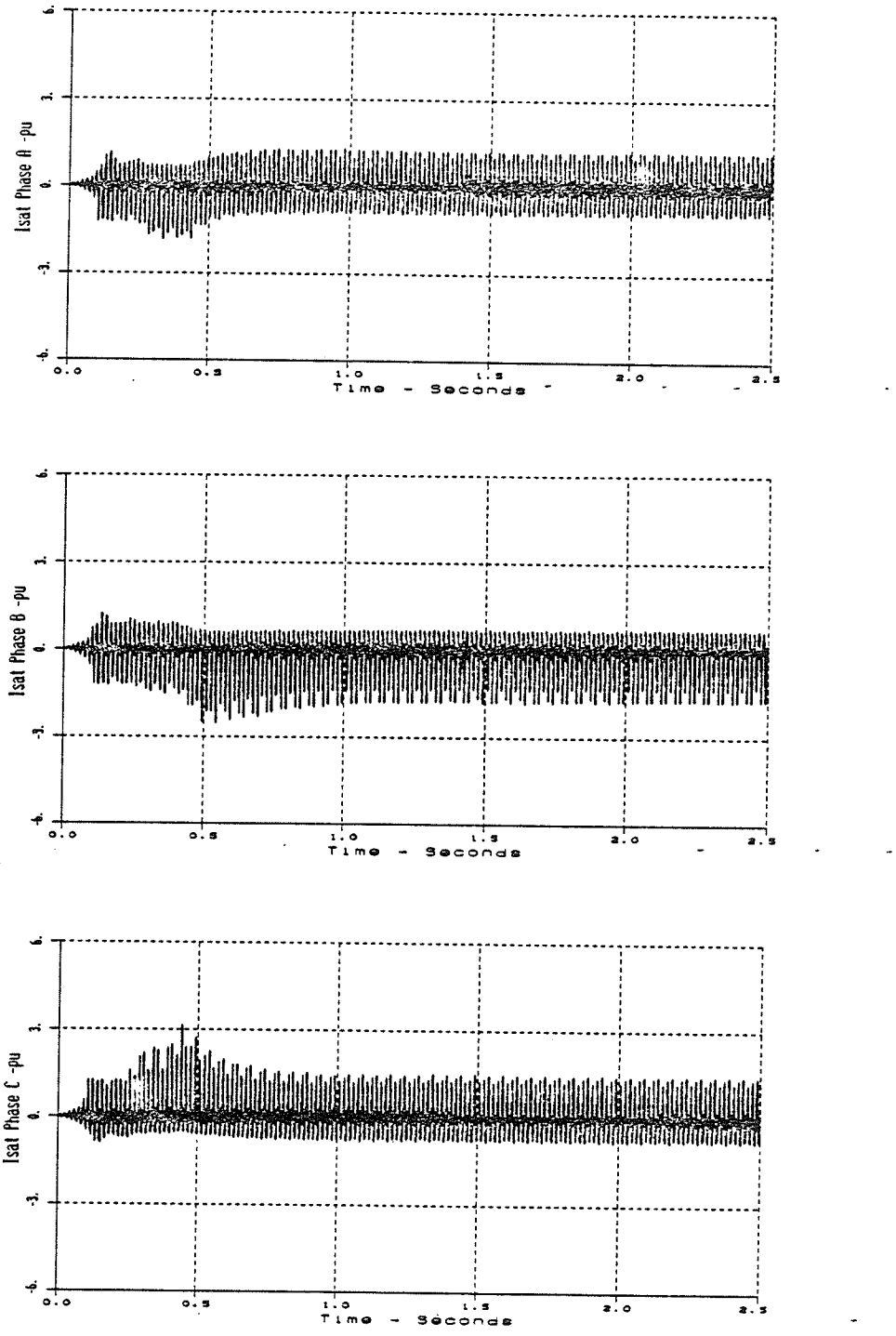

Figure 7.12 Transformer Saturation Current Waveforms, Control of Positive Sequence 2nd Harmonic Component of TCR Line Current, Alpha = 20°, System and SVC in 2nd Harmonic Parallel Resonance, Source 2nd Harmonic Voltage: 3% @ -30°

7.5 TCR Performance Using Firing Angle Modulation to Control the Positive Sequence DC Phasor Component of the TCR Line Current

The measured real and imaginary dc phasor components of the positive sequence TCR line current were input to the TCR firing angle modulation controller. The modulation signal was used to generate a dc component of the TCR line current, equal in magnitude to the measured input but 180° out of phase, so as to cancel the dc component. The controller settings that were applied are listed in Table 3.5, except that the integral gain was reduced from 60 rad/pu-s to 25 rad/pu-s.

The steady state harmonic phasor components of some SVC variables and the modulation parameters are listed in Table 7.4 for nominal TCR firing angles of 0°, 20°, 30° and 45°.

Sinusoidal modulation of the TCR firing angle successfully eliminated the dc component from the positive sequence TCR line current at all nominal firing angles considered.

However, the second harmonic parallel resonance was not damped. Modulation of the TCR firing angle with the positive sequence dc component of the TCR line current as the

control parameter resulted in an increase in the second harmonic voltage amplification for TCR firing angles of 20° and 30°.

Firing angle limits were only encountered at the nominal firing angle of 0°, where clearly, the modulation was one sided. The one sided dc modulation reduced the TCR loading at alpha = 0° to 93.7% of the "no modulation" case.

Figure 7.13 shows the TCR waveforms for the case of alpha = 20°. The TCR firing of each phase is modulated to eliminate the dc component in the TCR line current shown in Figure 7.14.

Elimination of the dc component from the TCR line current also reduced the second harmonic component. The second harmonic component was reduced by 12.7% at alpha = 0°, 7.5% at alpha = 20°, 27.8% at alpha = 30° and 48.6% at alpha = 45° relative to the "no modulation" case. Figure 7.15 shows the effect of the firing angle modulation on the 60 Hz and second harmonic components of the positive sequence TCR line current for the case where the nominal TCR firing angle was 20%. There was only a small reduction in the 60 Hz TCR line current.

Figure 7.16 shows the measured positive sequence dc component of TCR line current at alpha = 20°, and the modulation controller output. The dc component was reduced to zero in about 1.20s (including settling time) after the controller was activated. The modulation controller output corresponds to a modulation peak of 10.1° at a modulation phase of -32.6°. The controller response was found to be stable but became increasely underdamped with increasing firing angle. The magnitude of the integral gain was reduced from 60 to 25 rad/pu-s to achieve the response shown.

Figure 7.17 shows the SVC transformer saturation current for the case where alpha = 20°. The modulation increased the saturation current somewhat compared to the "no modulation", case shown in Figure 7.7.

Comparison of the sequence components in Tables 7.2 and 7.4 also indicates an increase in the saturation current components at all TCR firing angles.

Table 7.4 Positive Sequence SVC Variables With TCR Firing Angle Modulation Control of the Positive Sequence DC Component of the TCR Line Current, Transformer Saturation Modelled, SVC and Network in 2nd Harmonic Parallel Resonance, Source 2nd Harmonic Voltage: 3% @ -30°

Firing Angle / Variable	Alpha = 0° pu /-°	Alpha = 20° pu /-°	Alpha = 30° pu /-°	Alpha = 45° pu /-°
TCR Line Current DC Comp. * 60 Hz Comp. 120 Hz Comp.	0.002/- 65° 0.847/-121° 0.151/ 117°	0.001/ 73° 0.558/-121° 0.099/ 82°	0.002/- 61° 0.390/-122° 0.052/ 68°	0.001/- 51° 0.182/-122° 0.019/ 60°
Xfmr Primary Line Current DC Comp. 60 Hz Comp. 120 Hz Comp.	0.002/- 9° 0.293/- 85° 0.248/- 41°	0.003/ 149° 0.027/ 5° 0.227/- 74°	0.002/-161° 0.186/ 80° 0.175/- 90°	0.001/ 84° 0.406/ 84° 0.136/-100°
Xfmr Saturation Current DC Comp. 60 Hz Comp. 120 Hz Comp.	0.317/-134° 1.228/ 96° 0.760/- 34°	0.148/-102° 0.867/ 96° 0.398/- 67°	0.100/- 87° 0.818/ 95° 0.271/- 82°	0.079/- 78° 0.878/ 95° 0.212/- 92°
Primary Line Voltage DC Comp. 60 Hz Comp. 120 Hz Comp. 120 Hz Amplification	0.0004/ 80° 1.039/- 1° 0.295/-124° 9.83	0.0005/109° 1.002/- 2° 0.232/-158° 7.73	0.0003/-55° 1.002/- 2° 0.158/-173° 5.27	0.0003/-80° 1.003 /- 3° 0.104 /171° 3.47
Secondary Line Voltage DC Comp. 60 Hz Comp. 120 Hz Comp.	0.0003/ 75° 1.009/- 1° 0.349/-125°	0.0005/120° 1.004/- 2° 0.281/-170°	0.0003/-47° 1.023/- 2° 0.196/-175°	0.0004/-80° 1.048/- 3° 0.133/ 174°
TCR 60 Hz Absorption Mvar (% No Modulation Case)	256.4 (93.7)	168.1 (98.7)	119.7 (98.4)	57.2 (100)
Modulation Peak/Phase Δ ab Δ bc Δ ca	20.8/-30.6° 17.9° 0.2° -18.1°	10.1/-32.6° 8.5° 0.5° -9.0°	7.9/-38.1° 6.2° 1.1° -7.3°	6.1/-34.7° 5.0° 0.5° -5.5°

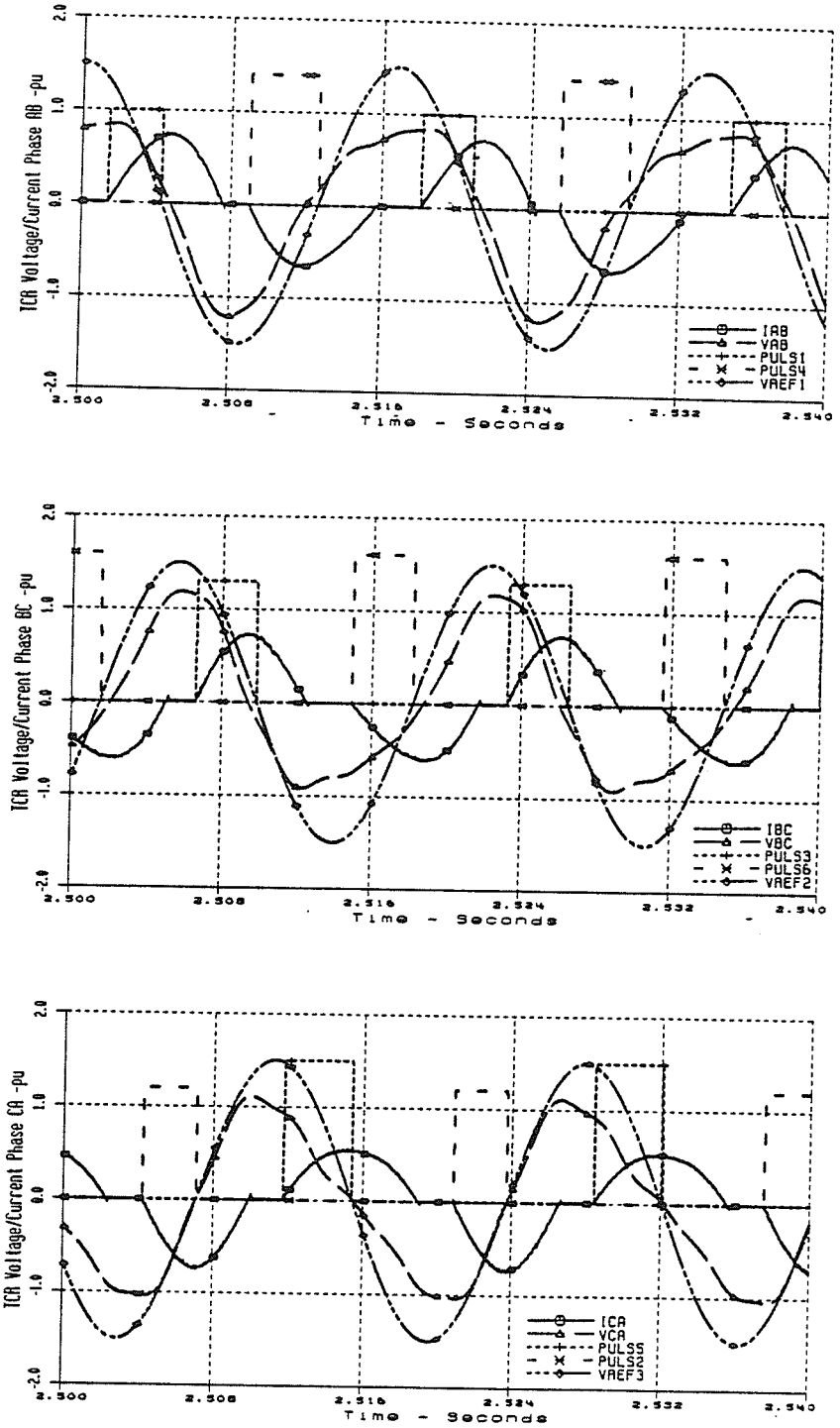

Figure 7.13 TCR Waveforms, Control of Positive Sequence DC Component of TCR Line Current, Alpha = 20°, System and SVC in 2nd Harmonic Parallel Resonance, Source 2nd Harmonic Voltage: 3% @ -30°

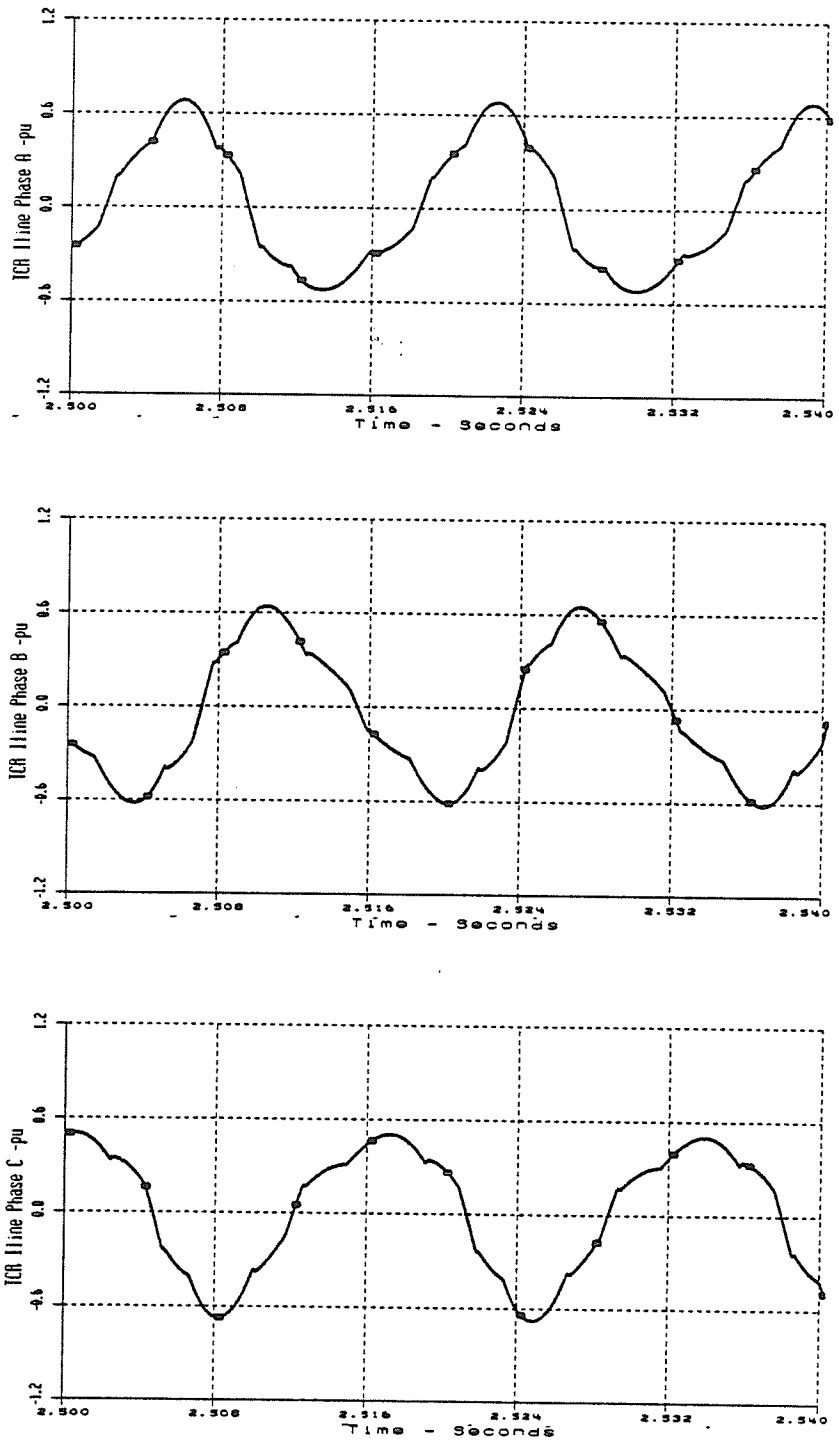

Figure 7.14 TCR Line Current Waveforms, Control of Positive Sequence DC Component of TCR Line Current, Alpha = 20°, System and SVC in 2nd Harmonic Parallel Resonance, Source 2nd Harmonic Voltage: 3% @ -30°

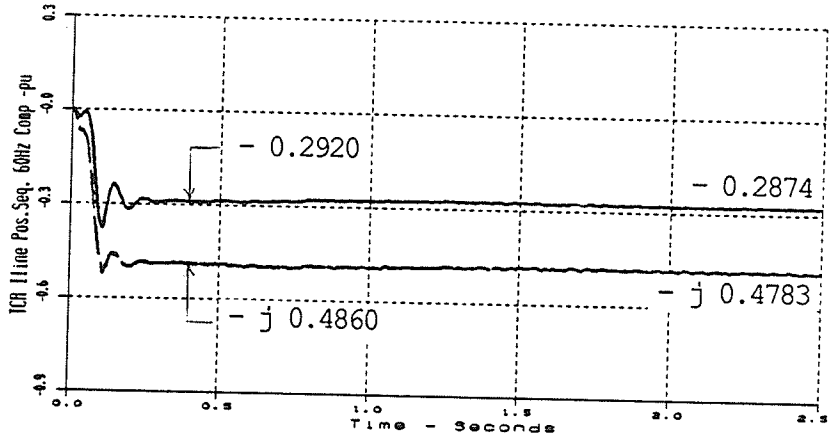

a) Real/Imaginary 60 Hz Components - pu

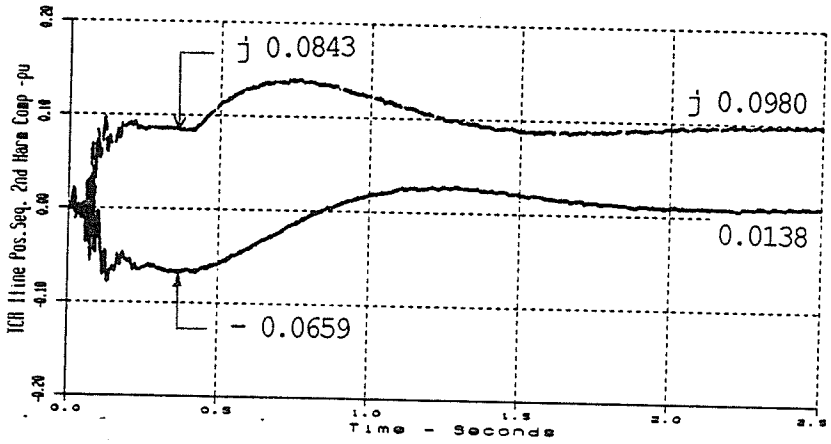

b) Real/Imaginary 2nd Harmonic Components - pu

Figure 7.15 Effect of Control of the Positive Sequence DC Component of TCR Line Current on the 60 Hz and 120 Hz Components, Alpha = 20°, System and SVC in 2nd Harmonic Resonance, Source 2nd Harmonic Voltage: 3% @ -30°

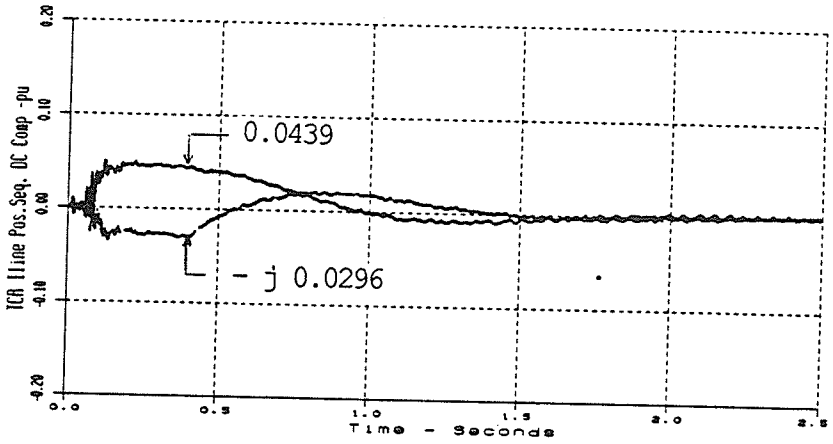

a) Real/Imaginary DC Components - pu

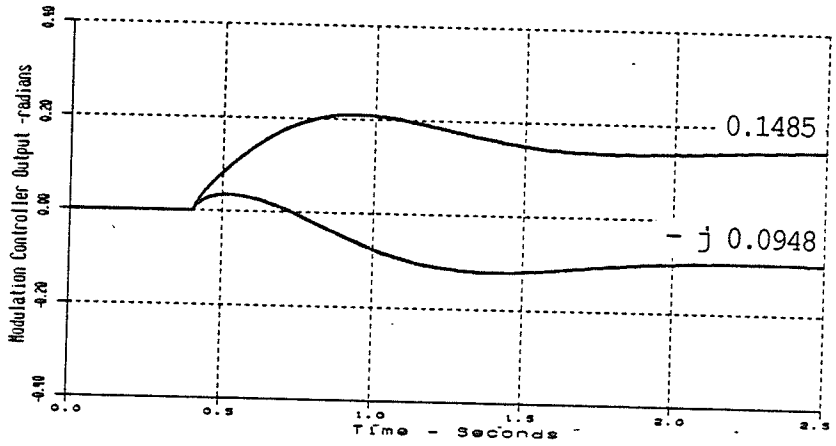

b) Real/Imaginary Modulation Controller Components - radians

Figure 7.16 Control of Positive Sequence DC Component of TCR Line Current, Alpha = 20°, System and SVC in 2nd Harmonic Parallel Resonance, Source 2nd Harmonic Voltage: 3% @ -30°

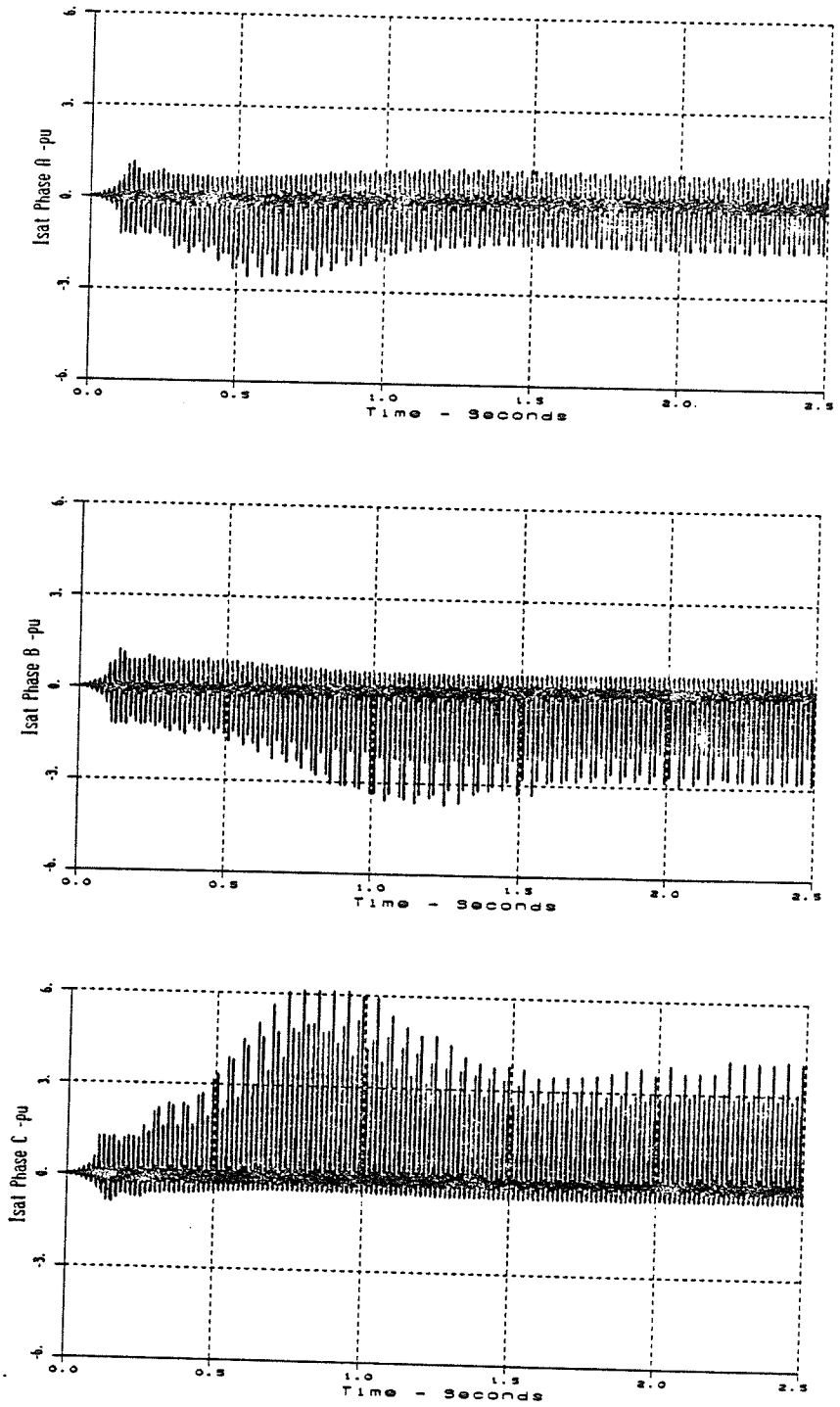

Figure 7.17 Transformer Saturation Current Waveforms, Control of Positive Sequence DC Component of TCR Line Current, Alpha = 20°, System and SVC in 2nd Harmonic Parallel Resonance, Source 2nd Harmonic Voltage: 3% @ -30°

7.6 Summary and Conclusions

Sinusoidal modulation of the TCR firing angle successfully eliminated either the dc component or the second harmonic component from the positive sequence of the TCR line current.

Firing angle modulation control of the second harmonic component also was effective in damping the second harmonic parallel resonance between the network and the SVC (fixed capacitor plus TCR) as it effectively reduced the second harmonic impedance by shifting the system resonant frequency away from 120 Hz.

Firing angle modulation control of the dc component was not effective in damping the second harmonic resonance.

When firing angle limits were encountered, the fundamental frequency TCR loading was reduced by the firing angle modulation. A reduction of about 6% was observed with the dc component of the TCR line current as the control parameter. A reduction of about 11% was observed with the second harmonic component as the control parameter.

Elimination of the dc component from the positive sequence of the TCR line current, in general also reduced the second harmonic component by between 13% and 49% of the "no modulation" valves.

Elimination of the second harmonic component from the TCR line current, caused the dc component to increase by 50% when firing angle limits were encountered (alpha = 0°) but otherwise caused a reduction in the dc component.

Control of the second harmonic component of TCR line current via firing angle modulation did not change the SVC transformer saturation current peak magnitude since the modulation damped the parallel resonance and reduced the voltage waveform distortion.

The dc component modulation control minimally increased the transformer saturation level.

The modulation controller response was stable at reduced integral gain relative to the previous chapters. The controller response was found to be very underdamped when the TCR was contributing to the resonant condition, as opposed to the cases examined where it was not part of the resonance.

CHAPTER EIGHT

GENERAL OBSERVATIONS AND CONCLUSIONS

An SVC can be viewed as a source of harmonic current which can contribute to harmonic instability of a lightly damped power system.

Weak ac systems which interface to a dc link can form a parallel resonance with the ac filters. Similarly a parallel resonance can occur between the ac system and a long EHV transmission line. The resonant frequency of these systems is often of low harmonic order, usually near the second or third harmonic. Harmonic current, flowing through the high parallel resonant impedance, can generate large harmonic voltages, which when superimposed on the fundamental frequency voltage waveforms, can cause severe distortion of these waveforms.

SVC's are often installed at dc converter buses, or at points along an EHV ac transmission line. The TCR of the SVC, when fired equidistantly in the presence of an energizing voltage which is severely distorted by a low order harmonic such as the second harmonic, is known to generate non-characteristic harmonic currents of even order. In the

case of second harmonic voltage distortion, a dc component and the second harmonic component appear as the dominant components in the positive sequence of the TCR line current.

The concept of sinusoidally modulating the TCR firing angle [3] to eliminate an undesired harmonic component from the TCR line current was applied to investigate the feasibility of using the TCR to control or damp harmonic resonant conditions in the ac system. Digital simulation models were developed for the EMTDC program [7] to simulate the operation of a TCR with sinusoidal firing angle modulation control. The models developed included a TCR model with a phase-locked loop firing controller, a measurement system to obtain the phasor value of any desired harmonic component of a time varying signal and a proportional-integral firing angle modulation controller. These models were used to investigate a variety of system conditions where a large positive sequence second harmonic voltage was present at the point of coupling of the SVC to the system. This voltage was generated by a second harmonic parallel resonance between the system equivalent reactance and shunt connected capacitive elements, and in some cases the SVC.

A thorough understanding of the variation of the ac system impedance with frequency at the point of SVC coupling to the

system is required to ensure that the application of firing angle modulation of the TCR to control an undesired low order harmonic resonance is successful. Although it may be possible to sinusoidally modulate the TCR firing angle to successfully cancel the second harmonic component from the TCR line current, the parallel resonance at the point of SVC coupling may not be damped, and in fact can be made worse.

TCR firing angle modulation reduced the system resonant frequency in the systems considered in the study. For example, if a parallel resonance develops in the system, with the SVC connected, such that the resonant frequency is slightly above the second harmonic (the system behaves inductively at 120 Hz), then modulation of the TCR firing angle to control the second harmonic component of the positive sequence TCR line current will shift the resonant frequency towards the second harmonic. The second harmonic impedance will increase and result in a increase in the second harmonic voltage component at the point of resonance if a second harmonic current source exists in the system. On the other hand, if a parallel resonance develops in the system, with the SVC connected, such that the resonant frequency is at or below the second harmonic (the system behave capacitively at 120 Hz in the latter case), then modulation of the TCR firing angle to control the second

harmonic current component will shift the resonant frequency away from and below the second harmonic. The second harmonic impedance will decrease thereby resulting in a reduction in the second harmonic voltage generated at the resonant point in the system. The amount of parallel resonance damping (or enhancement) will depend on the quality factor of the parallel resonant system. Further, if the SVC (fixed capacitor and TCR) is part of the resonant circuit, the modulation will result in a greater amount of damping.

The positive sequence TCR line current was found to be the most suitable control parameter. Sinusoidal modulation (about the nominal firing angle) of the TCR antiparallel thyristor pairs in each TCR phase causes harmonic components of even order to appear in the TCR line current, the dominant harmonics being the dc and second harmonic components. Modulation angles should be limited to a maximum of 30° to 40° in order to avoid excessive "one-sided" modulation due to firing angle limits. Modulation magnitudes of 30° to 40° will generate dc and second harmonic current component magnitudes of between 10% to 15% of the rated positive sequence fundamental TCR line current. Consequently, second harmonic current component magnitudes much in excess of 15% will be reduced in magnitude but not cancelled by the modulation. For the system conditions examined in this study,

the second harmonic component magnitudes of the other control parameters considered, such as the positive sequence primary or secondary line currents of the SVC transformer, were too large to be successfully eliminated. The dc component magnitudes of the transformer primary or secondary line currents were small enough to be successfully controlled; however, control of the dc component of the positive sequence TCR line current was found to be more beneficial as discussed below. Other possible inputs, such as a harmonic component of the positive sequence primary voltage at the point of SVC coupling to the system, are measurable but not necessarily controllable. For example, the source of the harmonic voltage component may be the inrush current of a remote transformer which happens to excite the system parallel resonance. Furthermore, the TCR may not be capable of driving a large enough current magnitude into the harmonic impedance to cancel the voltage component.

The effectiveness of using modulation control of the dc component as compared to modulation control of the second harmonic component of the positive sequence TCR current was examined. Control of the dc component was not effective in damping the parallel resonance. Control of the second harmonic component was effective in damping the parallel resonance under some system conditions, as discussed above.

However, control of the dc component of TCR line current can be beneficial in situations where damping of the parallel resonance can not be achieved bu modulation control of the second harmonic component. The dc component in the TCR line current waveforms that results from equidistant firing of the TCR under conditions where the voltage waveforms are severely distorted (by a large second harmonic voltage generated by a system parallel resonance) causes saturation of the SVC step-up transformer. The transformer saturation current contains a second harmonic component which can further aggravate the parallel resonant condition. Modulation control of the dc component of the TCR line current can limit saturation of the transformer.

Control of the dc component of the positive sequence TCR line current resulted in a decrease in the second harmonic component by as much as 50% depending upon the nominal TCR firing angle and the system being studied.

Control of the positive sequence second harmonic component of TCR line current resulted in an increase in the dc component. Even when damping of the parallel resonance was achieved, the dc component increased by 50% to 100%. The dc component increase was especially pronounced when TCR firing angle limits were encountered by the modulation controller.

The increase in the dc component was not found to be detrimental in the cases where damping of the second harmonic resonance was achieved since the voltage distortion was reduced. Therefore, saturation of the transformer was reduced compared to the "no modulation" case despite an increase in the dc component.

Control of both the dc and second harmonic components simultaneously was not possible as the two components are of opposing phase rotation. The gain of the real part of the modulation controller was of opposite polarity for the dc component input relative to the second harmonic component input.

When the TCR firing angle limits were encountered a larger modulation signal was required to eliminate either the dc or the second harmonic component from the positive sequence of the input current since the modulation becomes "one-sided". Large modulation angles, in conjunction with firing angle limitations resulted in a reduction in the fundamental frequency loading of the TCR. The reduction was about 10% with the dc component as the controlled variable. When modulation control of the second harmonic component resulted in damping of the parallel resonance, the reduction in the 60 Hz component of TCR current was observed to be less than

25%, but when the parallel resonance was not damped, the reduction was as high as 50%. This situation could result in system voltage instability as the reduction in loading is in conflict with the fundamental frequency voltage controller. An SVC control strategy is required to avoid operation with a nominal TCR firing angle near zero degrees. Furthermore, the modulation angle magnitude should be limited to between 30° to 40° to avoid operation of the TCR where firing of only one antiparallel thyristor pair results. Such operation generally causes an increase in the dc component, which in turn enhances saturation of the SVC transformer. The peak transformer saturation current was observed to increase to as high as 30% of rated winding current when large modulation angles resulted in excessive "one-sided" TCR firing. Under such conditions, cancellation of the second harmonic component was not possible. Control of the dc component on the other hand only caused a small increase in the peak transformer saturation current relative to the equidistant TCR firing case.

The firing angle modulation controller response was found to be stable and well damped over the variety of system configurations analyzed. The PI controller integral gain settings were chosen to minimize the controller settling time to a step input. The selected harmonic component was

usually reduced to zero by the controller in less than 500 ms. An exception to this robust performance was observed for the cases where the SVC (fixed capacitor plus TCR) was in parallel resonance with the ac system. The integral gains of the controller had to be reduced to about 25% of the values used throughout the study in order to minimize the settling time to less than 1.5 seconds with the TCR line current as the input parameter. Adaptive gain control may be required to ensure stable operation.

LIST OF REFERENCES

[1] R.M. Mathur (Editor), "Static Compensators for Reactive Power Control", Canadian Electrical Association (CEA), Montreal, Quebec, Canada.

[2] Dr. K. Reichert, Dr. L. Terens, J. Durr, W. Pfyl, "Harmonic Interactions Between Static Var Compensators and the Network; Problems, Analysis and Solutions", Brown, Boveri & Company Limited, Baden, Switzerland. International Symposium on Controlled Reactive Compensation, IREQ, Quebec, September, 1979.

[3] G.B. Mazur, "Control of Power System Harmonics with Firing Angle Modulation of a Thyristor Controlled Reactor", Technical Report TR 86-1, Department of Electrical Engineering, University of Manitoba, Winnipeg, Canada.

[4] G.B. Mazur and R.W. Menzies, "Firing Angle Modulation of a Thyristor Controlled Reactor for the Control of Power System Harmonics", Second International Conference on Harmonics in Power Systems, October 1986; Winnipeg, Manitoba.

[5] P.V. Goosen, R.D. MacFarlane, P. Pesch, P. Sieber, M. Schubert, "FC-TCR Type Static Compensator in ESCOM's 132 kV Network", CIGRE Report 38-09, August 29 - September 6, 1984 Session.

[6] S.T. Ranade, K.H. Voegthe, P.V. Goosen, T. Wess, "Unsymmetrical Control of ESCOM 132 kV and 400 kV Static Compensators", IEEE/PES 1986 Winter Power Meeting, Paper 86 WM 728-3.

[7] D.A. Woodford, A.M. Gole, R.W. Menzies, "Digital Simulation of DC Links and AC Machines", IEEE Transactions, Vol. PAS-102, pp1616-1623, June 1983.

[8] "EMTDC USER's MANUAL", Manitoba HVDC Research Centre, 400-1619 Pembina Highway, Winnipeg, Canada.

[9] "HVDC Back-to-Back Tie, Poste Chateauguay, Hydro-Quebec, Canada", Brown Boveri Publication No. CH-N-22.001.8E.

[10] A.E. Hamad, "Analysis of Power System Stability Enhancement by Static Compensators", IEEE Transactions, Vol. PWRS-1, No. 4, November, 1986.

APPENDICES

APPENDIX A

EMTDC SIMULATION MODEL

A1: EMTDC "DATA" File

A2: EMTDC "DSDYN" File

A3: EMTDC "DSOUT" File

A1: EMTDC "DATA" File

Network Data for Figure 2.2

```
NETWORK DATA FOR TCR FIRING ANGLE MODULATION ANALYSIS - FIGURE 2.2 /
0.000050 2.55000 0.001250 / delt fintime prtstep
1 /                  no. of subsystems
24  /                no.of nodes in ss1, smoothing factor
0.0 /                initial node voltages
1 4   0.0 0.00412     / n1 n2 r=0. l=0.00412h c=0. (300 Mvar Reactor)
2 5   0.0 0.00412     / n1 n2 r=0. l=0.00412h c=0. (300 Mvar Reactor)
3 6   0.0 0.00412     / n1 n2 r=0. l=0.00412h c=0. (300 Mvar Reactor)
4 2   0.025 0.0 0.0 / n1 n2 r=0.025 l=0. c=0. (thyristor Ron)
5 3   0.025 0.0 0.0 / n1 n2 r=0.025 l=0. c=0. (thyristor Ron)
6 1   0.025 0.0 0.0 / n1 n2 r=0.025 l=0. c=0. (thyristor Ron)
2 7   100.0 0.0 0.0 / n1 n2 r=100.0 l=0. c=0. (Rsnubber)
3 8   100.0 0.0 0.0 / n1 n2 r=100.0 l=0. c=0. (Rsnubber)
1 9   100.0 0.0 0.0 / n1 n2 r=100.0 l=0. c=0. (Rsnubber)
4 7   0.0 0.0 1.5 / n1 n2 r=0.0 l=0. c=1.5 (Csnubber)
5 8   0.0 0.0 1.5 / n1 n2 r=0.0 l=0. c=1.5 (Csnubber)
6 9   0.0 0.0 1.5 / n1 n2 r=0.0 l=0. c=1.5 (Csnubber)
1 10 0.010 0.0 0.0 / n1 n2 r=0.010 l=0. c=0. (xfmr sec. resistor)
2 11 0.010 0.0 0.0 / n1 n2 r=0.010 l=0. c=0. (xfmr sec. resistor)
3 12 0.010 0.0 0.0 / n1 n2 r=0.010 l=0. c=0. (xfmr sec. resistor)
-1 0 300.0 0.0 0.0 / n1 n2 r=300.0 l=0. c=0. (stabilizing resistor)
-2 0 300.0 0.0 0.0 / n1 n2 r=300.0 l=0. c=0. (stabilizing resistor)
-3 0 300.0 0.0 0.0 / n1 n2 r=300.0 l=0. c=0. (stabilizing resistor)
-1 0 100.0 0.0 2.5 / n1 n2 r=100.0 l=0. c=2.5 ( RC stabilizing circuit)
-2 0 100.0 0.0 2.5 / n1 n2 r=100.0 l=0. c=2.5 ( RC stabilizing circuit)
-3 0 100.0 0.0 2.5 / n1 n2 r=100.0 l=0. c=2.5 ( RC stabilizing circuit)
10 0 300.0 0.0 0.0 / n1 n2 r=300.0 l=0. c=0. (stabilizing resistor)
11 0 300.0 0.0 0.0 / n1 n2 r=300.0 l=0. c=0. (stabilizing resistor)
12 0 300.0 0.0 0.0 / n1 n2 r=300.0 l=0. c=0. (stabilizing resistor)
1 22  0.10 0.0 0.0 / n1 n2 r=0.10 l=0. c=0. (Rc fixed cap.)
2 23  0.10 0.0 0.0 / n1 n2 r=0.10 l=0. c=0. (Rc fixed cap.)
3 24  0.10 0.0 0.0 / n1 n2 r=0.10 l=0. c=0. (Rc fixed cap.)
1 24  0.0 0.0 512.6 / n1 n2 r=0.0 l=0. c=512.6 (Cfixed cap.- 180 Mvar)
2 22  0.0 0.0 512.6 / n1 n2 r=0.0 l=0. c=512.6 (Cfixed cap.- 180 Mvar)
3 23  0.0 0.0 512.6 / n1 n2 r=0.0 l=0. c=512.6 (Cfixed cap.- 180 Mvar)
16 19  0.0 0.0106 0.0 / n1 n2 r=0. l=0.0106h c=0. (Xs)
17 20  0.0 0.0106 0.0 / n1 n2 r=0. l=0.0106h c=0. (Xs)
18 21  0.0 0.0106 0.0 / n1 n2 r=0. l=0.0106h c=0. (Xs)
13 16  0.01 0.0 0.0 / n1 n2 r=0.01 l=0. c=0. (Rp Xfmr)
14 17  0.01 0.0 0.0 / n1 n2 r=0.01 l=0. c=0. (Rp Xfmr)
15 18  0.01 0.0 0.0 / n1 n2 r=0.01 l=0. c=0. (Rp Xfmr)
16 0  0.0 0.0 165.79 / n1 n2 r=0.0 l=0. c=165.79 (System cap.-600 Mvar)
17 0  0.0 0.0 165.79 / n1 n2 r=0.0 l=0. c=165.79 (System cap.-600 Mvar)
18 0  0.0 0.0 165.79 / n1 n2 r=0.0 l=0. c=165.79 (System cap.-600 Mvar)
999 /                end of ss1 node data
19  0.705 0.0 0. 0. 0. / thevenin branch src r=0.705 l=0.0 c=0. es=0. cs=0.
20  0.705 0.0 0. 0. 0. / thevenin branch src r=0.705 l=0.0 c=0. es=0. cs=0.
21  0.705 0.0 0. 0. 0. / thevenin branch src r=0.705 l=0.0 c=0. es=0. cs=0.
999 /                end of source data
2   /                number of mutually coupled wdgs on one core
13 0    0.00000000    5.7453308     /1 SIDE WNDING
10 2    0.00000000    1.0320570   0.00000000   0.18583840     /2 SIDE WNDING
888 /
14 0 /
11 3 /
888 /
15 0 /
12 1 /
999 /                end of mutually coupled element data
999 /                end of transmission line data
-2.0.2.0   /         min,max screen plot scale
20 /                 no.of channels on screen
77.86E+03  0.0  0.0  2.940E+03 -30.0  146.97E+03  1250.0  0.025  0.001
20.0  60.0  60.0  10.0  0.0  -75.0  +75.0  0.010  0.0040  1.0  0.0083
0.2618  0.1745  0.02  1.00  0  1.00  1.00  0.032
0.00  -2.00 +2.00   +60.00  +1.00   1.00  0.032
0.00  -2.00 +2.00   -60.00  -1.00    0.00  0.00  1
110.8E+06  12460.0  +0.40  1.15  60.0  1.0E-06  0.02  0.00  1
5.0  0 /
999 /                end of data file
U1 PHIF DPHI U2 PHIH Vrefm Roff Ron CTO              /VARS 1-9
ALPHO FREQS FREQR G=7  YO TLO THI TI=2.5 TIF=0.0087 GL TL=0.0083 /VARS 10-20
VSET HYST TDPU=.04 TDDO=.06 CMODE SF GRLF TCRLF              /VARS 21-28
SCRLO SCRLL SCRLU GISCRL GPSCRL GIMGF TCIMGF         /VARS 29-35
SIMGO SIMGL SIMGU GISIMG GPSIMG ARMOD AIMOD MANUAL /VARS36-43
TMVA1.VW.XL.XK.FR.TD.CM.HL.KB                        /VARS TSAT21 44-52
TSTEP ISTEP / ISTEP = 0 OR 1(PLL PHASE STEP AT TIME=TSTEP) 53-54
KB=0 or 1 XFMR SATURATION BLOCKED or FUNCTIONING
-------------------------------------------------------
GPR=-1.GIR=-90.TCR=0.016   FOR 2ND HARMONIC MODULATION
GPI=-1.GII=-90.TCI=0.016   OF TCR LINE CURRENT
-------------------------------------------------------
GPR=+1.GIR=+60.TCR=0.032   FOR DC COMPONENT MODULATION
GPI=-1.GII=-60.TCR=0.032   OF TCR LINE CURRENT
-------------------------------------------------------
```

A2: EMTDC "DSDYN" File

User Defined Dynamics

```
      SUBROUTINE DSDYN
C
      INCLUDE 'EMT.E'
      COMMON /S1/ TIME,DELT,ICH,PRINT,FINTIM
      COMMON /S2/ STOR(5000),NEXC
      COMMON /S4/ VAR(100),CON(100),PGB(25)
C
      REAL CREAL,CIMAG,CDCRL,CDCIM,C2NDRL,C2NDIM
      INTEGER CMODE
C
CC    DEFINE PRINT STEP
C
      IF(TIME.GT.2.49870) PRINT=0.000050
C
CC    DEFINE CONSTANTS
C
      PI=3.141592654    /* PI RADIANS  180'
      TWOPI=6.283185308   /* 2*PI RADIANS 360'
      DEG120=2.094395102   /* 2*PI/3 RADIANS 120'
C
CC    SYSTEM PARAMETERS INPUT
CC
C     U1=VAR(1)            /* FUND. FREQ. VOLTAGE MAGNITUDE (V p-p PH-GRD)
      PHIF=VAR(2)          /* FUND. FREQ. PHASE DISPLACEMENT (DEGREES)
      DPHI=VAR(3)          /* FUND. FREQ. PHASE CHANGE (DEGREES) PLL TESTING
C     U2=VAR(4)            /* 2nd HARM. VOLTAGE MAGNITUDE (V p-p PH-GRD)
      PHIH=VAR(5)          /* 2nd HARM. PHASE DISPLACEMENT (DEGREES)
      VREFM=VAR(6)         /* PLL REFERENCE VOLTAGE MAGNITUDE
C     NOTE: U1 & U2 DEFINED BELOW TO RAMP UP SOURCE
CC
CC    CONVERT DEGREES TO RADIANS
C
      PHIF=PHIF*PI/180.0
      PHIH=PHIH*PI/180.0
      DPHI=DPHI*PI/180.0
C
CCC   STEP CHANGE IN PHASE FOR PLL TESTING
CCC
CCC   TSTEP=VAR(53)        /* TIME OF STEP CHANGE IN PHASE
CCC   ISTEP=VAR(54)        /* ISTEP=0 NORMAL,=1 STEP SOURCE PHASE BY DPHI
CCC   IF(TIME.GT.TSTEP.AND.ISTEP.EQ.1)THEN
CCC   PHIH=DPHI
CCC   END IF
CCC
CCC   DEFINE ANGULAR VELOCITY (RADIANS/SECOND)
C
      FREQS=VAR(11)        /* SYSTEM FREQUENCY (HZ)
      FREQR=VAR(12)        /* PLL REFERENCE FREQUENCY (HZ)
C
CC    RAMP FREQS FOR PLL TESTING (10HZ/SEC)
CC    IF(TIME.GT.TSTEP.AND.ISTEP.EQ.2) THEN
CC    FREQS=FREQS+10.0*DELT
CC    ELSE
CC    FREQS=VAR(11)
CC    END IF
CC    IF(TIME.GE.(TSTEP+1.0)) FREQS=70.0
C
      WS=TWOPI*FREQS /* SYSTEM ANGLULAR VELOCITY (R/S)
      CON(1)=WS
      WR=TWOPI*FREQR     /* PLL REFERENCE ANGULAR VELOCITY (R/S)
C
CC    SOURCE
CC    RAMP UP AC VOLTAGE IN 0.10S
C
      U1RATE=0.00
      IF (TIME.GE.DELT) U1RATE=TIME*10.0
      IF (TIME.GT.0.10) U1RATE=1.0
      U1=U1RATE*VAR(1)
C
      U2RATE=0.00
      IF (TIME.GE.DELT) U2RATE=TIME*10.0
      IF (TIME.GT.0.10) U2RATE=1.0
      U2=U2RATE*VAR(4)
```

```
C
      CALL SRC7(1, 19, 20, 21,U1,U2,WS,PHIF,PHIH,THETA,THETA2)
C
C     MODEL STEP UP TRANSFORMER SATURATION ON SECONDARY WINDING
C     CALL TSAT21(IA,JA,IB,JB,IC,JC,M,TMVA1,VW,XL,XK,FR,TD,CM,HL,KB)
C
C     DEFINE SATURATION PARAMETERS
      TMVA1=VAR(44)        /* WDG RATING (110.8E06)
      VW=VAR(45)           /* VOLTS (12460.0)
      XL=VAR(46)           /* PU XFMR AIR CORE REACTANCE ON XFMR BASE (+0.40)
      XK=VAR(47)           /* PU KNEE VOLTS (1.15 PU)
      FR=VAR(48)           /* RATED FREQUENCY HZ (60.0)
      TD=VAR(49)           /* SEC. INRUSH CURRENT DECAY TIME CONSTANT (1.0E-06)
      CM=VAR(50)           /* PU MAGNETIZING CURRENT AT RATED VOLTS (0.02)
      HL=VAR(51)           /* PU NO LOAD LOSSES (0.0)
      KB=VAR(52)           /* =1 SAT. FUNCTIONING, =0 SAT.COMPUTED-NOT FUNCT'ING
C
      IF(TIME.LT.0.20) XK=-1.15
      CALL TSAT21( 10, 2, 11, 3, 12, 1, 1, TMVA1, VW, XL, XK, FREQS,
     &             TD, CM, HL, KB)
C
C
C  SUBROUTINE R6P120: VALVE GROUP MODEL
C
C  VALVE PARAMETERS
      ROFF=VAR(7)          /* VALVE OFF RESISTANCE (OHMS)
      RON=VAR(8)           /* VALVE ON RESISTANCE (OHMS)
      CTO=VAR(9)           /* VALVE CURRENT TURN OFF LEVEL (PU)
      ALPHO=VAR(10)        /* ORDERED FIRING ANGLE (DEGREES)
      ALPHO=ALPHO*PI/180.0
C  PLL CONTROLLER INPUT
      G=VAR(13)            /* PLL PROPORTIONAL GAIN (RADIANS/DEGREE-SECOND)
      YO=VAR(14)           /* INITIAL O/P OF PLL PROP. CONTROL (RADIANS/SECOND)
      TLO=VAR(15)          /* PLL PI CONTROLLER LOW O/P LIMIT (RADIANS/SECONDS)
      THI=VAR(16)          /* PLL PI CONTROLLER HI O/P LIMIT (RADIANS/SECONDS)
      TI=VAR(17)           /* PLL INTEGRAL GAIN (RADIANS/DEGREES-SECOND**2)
      TIF=VAR(18)          /* PLL INTEGRAL GAIN FOR FREQUENCY CHANGES
      GL=VAR(19)           /* PLL ERROR FILTER GAIN (UNITLESS)
      TL=VAR(20)           /* PLL ERROR FILTER TIME CONSTANT (SECONDS)
      VSET=VAR(21)         /* PLL TIMER PICKUP SETTING (DEGREES)
      HYST=VAR(22)         /* PLL TIMER HYSTERISIS (DEGREES)
      TDPU=VAR(23)         /* PLL TIMER PICKUP TIME DELAY (SECONDS)
      TDDO=VAR(24)         /* PLL TIMER DROP OUT TIME DELAY (SECONDS)
C
C     CALL R6P120(MA,NA,NB,NC,N1T,N1F,N2T,N2F,N3T,N3F,N4T,N4F,
C    &     N5T,N5F,N6T,N6F,KV,KB,ROFF,RON,CTO,ALPHO,VREFM,FREQS,
C    &     WR,G,TI,TIF,YO,TLO,THI,GL,TL,VSET,HYST,TDPU,TDDO,RPUL24,
C    &     DELRS,DELST,DELTR)
C
C     BLOCK VALVE FIRING UNTIL PLL SYNCHRONIZES TO BUS VOLTAGE
      KBLK=0
      IF(TIME.GT.DELT) KBLK=1
C
C     NOTE KV=0 FOR WYE-DELTA TRANSFORMER (Vlg -prim in phase with Vll-sec.)
C          KV=1 FOR WYE-WYE TRANSFORMER OR NO TRANSFORMER (Vlg -prim is
C               phase shifted -30' wrt Vll -sec.)
C
      CALL R6P120( 1, 13, 14, 15, 2, 4, 6, 1, 3, 5,
     &     4, 2, 1, 6, 5, 3, 0,KBLK,ROFF,RON,CTO,ALPHO,VREFM,FREQS,
     &     WR,G,TI,TIF,YO,TLO,THI,GL,TL,VSET,HYST,TDPU,TDDO,RPUL24,
     &     DELRS,DELST,DELTR)
C
```

```
C
C     MEASURE POSITIVE SEQUENCE PRIMARY TCR LINE CURRENT FOR USE
C     AS INPUT TO THE FIRING ANGLE PI MODULATION CONTROLLER
C     ------------------------------------------------------------
C
C     TCR LINE CURRENT INPUT TO MODULATION CONTROLLER (PU)
C
        CURRA=(CDC(4,1,1)-CDC(6,3,1))/19658.8
        CURRB=(CDC(5,2,1)-CDC(4,1,1))/19658.8
        CURRC=(CDC(6,3,1)-CDC(5,2,1))/19658.8
C
C     SVC TRANSFORMER PRIMARY LINE CURRENT INPUT TO MODULATION CONTROLLER
C
C       CURRA=CDC(13,16,1)/2041.2
C       CURRB=CDC(14,17,1)/2041.2
C       CURRC=CDC(15,18,1)/2041.2
C
C       CURRA=VDC(16,1)/97.98E3
C       CURRB=VDC(17,1)/97.98E3
C       CURRC=VDC(18,1)/97.98E3
C
C
C    PSEQE & AVGF25 INPUT
       SF=VAR(26)          /* AVGF25 SCALING FACTOR
       DO 1200 IJK=1,3
         NIJK=IJK-1
       CALL PSEQU(CURRA,CURRB,CURRC,NIJK,STOR(51),CALP,CBETA,CPRL,CPIM)
       CALL AVGF25(CPRL,SF,RPUL24,CPREAL)
       CALL AVGF25(CPIM,SF,RPUL24,CPIMG)
C
C      WRITE(1,*) CPREAL,CPIMG,NEXC,NIJK
C
C    NIJK=0 :  RESOLVE DC   COMPONENT IN PHASOR FORM
C    ------------------------------------------------
C    NIJK=1 :  RESOLVE FUNDAMENTAL COMPONENT IN PHASOR FORM
C    ------------------------------------------------------
C    NIJK=2 :  RESOLVE SECOND HARMONIC COMPONENT IN PHASOR FORM
C    ----------------------------------------------------------
       IF(NIJK.EQ.0)THEN
       STOR(199)=CALP
       STOR(200)=CBETA
       STOR(201)=CPRL
       STOR(202)=CPIM
       STOR(203)=0.5*CPREAL
       STOR(204)=0.5*CPIMG
       NEXC=NEXC+6
       END IF
       IF(NIJK.EQ.1)THEN
       STOR(255)=CALP
       STOR(256)=CBETA
       STOR(257)=CPRL
       STOR(258)=CPIM
       STOR(259)=CPREAL
       STOR(260)=CPIMG
       NEXC=NEXC+6
       END IF
       IF(NIJK.EQ.2)THEN
       STOR(311)=CALP
       STOR(312)=CBETA
       STOR(313)=CPRL
       STOR(314)=CPIM
       STOR(315)=CPREAL
       STOR(316)=CPIMG
       NEXC=NEXC+6
       END IF
 1200  CONTINUE
C
```

```
C    PCNTR20 PARAMETERS
       GRLF=VAR(27)        /* CREAL INPUT FILTER GAIN (1.0)
       TCRLF=VAR(28)       /* CREAL INPUT FILTER TIME CONSTANT (0.016)
       SCRLO=VAR(29)       /* INITIAL VALUE CREAL,REAL PART OF CONT. O/P (0.0)
       SCRLL=VAR(30)       /* LOWER LIMIT OF CREAL (-1.00)
       SCRLU=VAR(31)       /* UPPER LIMIT OF CREAL (+1.00)
       GIMGF=VAR(34)       /* CIMG INPUT FILTER GAIN (1.00)
       TCIMGF=VAR(35)      /* CIMG INPUT FILTER TIME CONSTANT (0.016)
       SIMGO=VAR(36)       /* INITIAL VALUE CIMAG,IMAG PART OF CONT. O/P (0.0)
       SIMGL=VAR(37)       /* LOWER LIMIT OF CIMAG (-1.00)
       SIMGU=VAR(38)       /* UPPER LIMIT OF CIMAG (+1.00)
       GISCRL=VAR(32)      /* INTEGRAL GAIN OF REAL PART OF CONTROLLER
       GPSCRL=VAR(33)      /* PROP. GAIN OF REAL PART OF CONTROLLER
       GISIMG=VAR(39)      /* INTEGRAL GAIN OF IMAG PART OF CONTROLLER
       GPSIMG=VAR(40)      /* PROP. GAIN OF IMAG PART OF CONTROLLER
       ARMOD=VAR(41)       /* MANUAL I/P REAL PART OF ANGLE MODULATION(RADIANS)
       AIMOD=VAR(42)       /* MANUAL I/P IMAG PART OF ANGLE MODULATION(RADIANS)
       MANUAL=VAR(43)      /* SELECT MANUAL CONTROL =2,AUTO CONTROL =0
C
C      IF(TIME.LE.0.20) THEN
C        ARMOD=0.0
C        AIMOD=0.0
C      ELSE
C        ARMOD=VAR(41)
C        AIMOD=VAR(42)
C      END IF
C
C      TO CONTROL THE +VE SEQ. DC COMPONENT OF LINE CURRENT,INPUT
C      ----------------------------------------------------------
C      STOR(203)=CPREAL AND STOR(204)=CPIMG TO PCTR20.TO CONTROL
C      ----------------------------------------------------------
C       THE +VE SEQ. 2ND HARMONIC,INPUT STOR(315)=CPREAL AND
C       ----------------------------------------------------
C       STOR(316)=CPIMG TO PCTR20
C       -------------------------
       CMODE=VAR(25)
C      DC MODULATION CONTROL  CMODE=VAR(25)=0
       IF (CMODE.EQ.0) THEN
          CREAL=STOR(203)
          CIMAG=STOR(204)
C      2ND HARMONIC CONTROL  CMODE=VAR(25)=2
       ELSE IF (CMODE.EQ.2) THEN
          CREAL=STOR(315)
          CIMAG=STOR(316)
       ELSE
          CREAL=0.0
          CIMAG=0.0
       END IF
       IF (TIME.LT.0.40) THEN
          CREAL=0.0
          CIMAG=0.0
       END IF
C
       CALL PCTR20(CREAL,CIMAG,STOR(51),GRLF,TCRLF,SCRLO,SCRLL,
     & SCRLU,GISCRL,GPSCRL,GIMGF,TCIMGF,SIMGO,SIMGL,SIMGU,GISIMG,
     & GPSIMG,ALPMOD,CRL1,CIMG1,ARMOD,AIMOD,MANUAL,CRLINT,CIMGIN,
     & DELRS,DELST,DELTR)
C
       RETURN
       END
```

A3: EMTDC "DSOUT" File

User Specified Output

```
      SUBROUTINE DSOUT
C
      INCLUDE 'EMT.E'
      COMMON /S1/ TIME,DELT,ICH,PRINT,FINTIM
      COMMON /S2/ STOR(5000),NEXC
      COMMON /S4/ VAR(100),CON(100),PGB(25)
C
C   PGB3 - PGB7 ARE ADDITIONAL OUTPUT ARRAYS TO THE PGB ARRAY
      DIMENSION PGB3(10),PGB4(10),PGB5(10),PGB6(10),PGB7(10)
C
      PGB(1)=(VDC(4,1)-VDC(2,1))*GDC(2,4,1)/11350.0   /* IAB -PU TCR PHASE
      PGB(2)=STOR(48)/97.98E3                 /* URSK1 -PU LINE-LINE
      PGB(3)=STOR(79)                         /* PULS(1)
      PGB(4)=STOR(80)                         /* PULS(4)
      PGB(5)=STOR(41)/97.98E3                 /* PLL VREF1 -PU
C
      PGB(6)=(VDC(5,1)-VDC(3,1))*GDC(3,5,1)/11350.0   /* IBC -PU TCR PHASE
      PGB(7)=STOR(49)/97.98E3                 /* USTK1 -PU LINE-LINE
      PGB(8)=STOR(81)                         /* PULS(3)
      PGB(9)=STOR(82)                         /* PULS(6)
      PGB(10)=STOR(42)/97.98E3                /* PLL VREF2 -PU
C
      PGB(11)=(VDC(6,1)-VDC(1,1))*GDC(1,6,1)/11350.0   /* ICA -PU TCR PHASE
      PGB(12)=STOR(50)/97.98E3                /* UTRK1 -PU LINE-LINE
      PGB(13)=STOR(83)                        /* PULS(5)
      PGB(14)=STOR(84)                        /* PULS(2)
      PGB(15)=STOR(43)/97.98E3                /* PLL VREF3 -PU
C
      PGB(16)=STOR(199)                       /* CALP DC COMP Ialpha(t)-PU
      PGB(17)=STOR(200)                       /* CBETA DC COMP Ibeta(t)-PU
      PGB(18)=STOR(31)*180.0/3.14159          /* PLL ERROR -UNFILTR'D -DEG
      PGB(19)=STOR(32)*180.0/3.14159          /* PLL ERROR - FILTERED -DEG
      PGB(20)=STOR(94)                        /* LAST VALVE TO FIRE
C
C   OPENING FILE - USE CON(91) AS A MEMORY
C   FORTRAN 77 FILE OPENING PROCEDURE
      A1=FINTIM-TIME
      IF (A1.LE.CON(91)) GO TO 20
C
C   OUTPUT WILL BE PRINTED IN  "O.TCR3","O.TCR4","O.TCR5","O.TCR6","O.TCR7"
      OPEN(UNIT=9,FILE='O.TCR3',STATUS='UNKNOWN',FORM='FORMATTED')
      OPEN(UNIT=10,FILE='O.TCR4',STATUS='UNKNOWN',FORM='FORMATTED')
      OPEN(UNIT=11,FILE='O.TCR5',STATUS='UNKNOWN',FORM='FORMATTED')
      OPEN(UNIT=12,FILE='O.TCR6',STATUS='UNKNOWN',FORM='FORMATTED')
      OPEN(UNIT=13,FILE='O.TCR7',STATUS='UNKNOWN',FORM='FORMATTED')
   20 CON(91)=A1
C
C   USE CON(92) TO DEFINE PRINT STEP
      IF (TIME.GE.CON(92)) THEN
      CON(92)=TIME+PRINT
C
C   TO LOAD UP THE PRT ARRAY WITH USER SPECIFIED STATEMENTS
C   O.TCR3
C
      PGB3(1)=CDC(4,1,1)/11350.0      /* TCR IAB (pu) PHASE
      PGB3(2)=CCIN(10,1)/251.5        /* PH A Isat (pu)
      PGB3(3)=(CDC(4,1,1)-CDC(6,3,1))/19658.8   /* IA TCR Line (pu)
      PGB3(4)=CDC(13,16,1)/2041.2     /* Ia xfmr prim (pu)
      PGB3(5)=-CS(19,1)/2041.2        /* Isrc Phase A (pu)
      PGB3(6)=VDC(13,1)/97.98E3       /* VA Xfmr Prim (pu)
      PGB3(7)=(VDC(1,1)-VDC(2,1))/17621.1    /* Vab Sec. volts (pu)
      PGB3(8)=STOR(203)               /* CPREAL DC COMP.- AVGF O/P
      PGB3(9)=STOR(204)               /* CPIMG DC. COMP.- AVGF O/P
      PGB3(10)=STOR(46)               /* RPUL1 PLL REF. PULSE (1/CY)
C
C   O.TCR4
C
      PGB4(1)=CDC(5,2,1)/11350.0      /* TCR IBC (pu)
      PGB4(2)=CCIN(11,1)/251.5        /* PH B Isat (pu)
      PGB4(3)=(CDC(5,2,1)-CDC(4,1,1))/19658.8   /* IB TCR Line (pu)
      PGB4(4)=CDC(14,17,1)/2041.2     /* Ib xfmr prim (pu)
      PGB4(5)=-CS(20,1)/2041.2        /* Isrc Phase B (pu)
      PGB4(6)=VDC(14,1)/97.98E3       /* VB Xfmr Prim (pu)
      PGB4(7)=(VDC(2,1)-VDC(3,1))/17621.1    /* Vbc Sec. volts (pu)
      PGB4(8)=STOR(259)               /* CPREAL FUND. COMP. - AVGF O/P
      PGB4(9)=STOR(260)               /* CPIMG FUND. COMP.  - AVGF O/P
      PGB4(10)=STOR(46)               /* RPUL1 PLL REF. PULSE (1/CY)
C
```

```
C    O.TCR5
C
       PGB5(1)=CDC(6,3,1)/11350.0      /* TCR ITR (pu)
       PGB5(2)=CCIN(12,1)/251.5        /* Ph C Isat (pu)
       PGB5(3)=(CDC(6,3,1)-CDC(5,2,1))/19658.8   /* IC TCR Line (pu)
       PGB5(4)=CDC(15,18,1)/2041.2     /* Ic xfmr prim(pu)
       PGB5(5)=-CS(21,1)/2041.2        /* Isrc Phase C (pu)
       PGB5(6)=VDC(15,1)/97.98E3       /* VC Xfmr Prim (pu)
       PGB5(7)=(VDC(3,1)-VDC(1,1))/17621.1    /* Vca Sec. volts (pu)
       PGB5(8)=STOR(315)               /* CPREAL 2ND HARM.- AVGF O/P
       PGB5(9)=STOR(316)               /* CPIMG 2ND HARM. - AVGF O/P
       PGB5(10)=STOR(46)               /* RPUL1 PLL REF. PULSE (1/CY)
C
C
C    O.TCR6
C
       PGB6(1)=STOR(327)                 /* CPRL1 - PI CONT. REAL O/P
       PGB6(2)=STOR(328)                 /* CIMG1 - PI CONT. IMAG O/P
       PGB6(3)=STOR(329)*180.0/3.14159   /* DELTA (DEG) - MODULATION PHASE
       PGB6(4)=STOR(330)*180.0/3.14159   /* PKDEL (DEG) - MODULATION MAG.
       PGB6(5)=STOR(331)*180.0/3.14159   /* DELRS (DEG) = PKDEL*COS(DELTA)
       PGB6(6)=STOR(332)*180.0/3.14159   /* DELST (DEG) = PKDEL*COS(DELTA+120')
       PGB6(7)=STOR(333)*180.0/3.14159   /* DELTR (DEG) = PKDEL*COS(DELTA+240')
       PGB6(8)=STOR(334)                 /* CRL11 = CRL1*COS(THETR-166')
       PGB6(9)=STOR(335)                 /* CIMG11= CIMG1*-1.0*SIN(THETR-166')
       PGB6(10)=STOR(336)                /* ALPMOD = CRL11 + CIMG11
C
C      O.TCR7
C
       PGB7(1)=STOR(1)/97.98E3         /* VA SRC FF -PU
       PGB7(2)=STOR(2)/97.98E3         /* VB SRC FF -PU
       PGB7(3)=STOR(3)/97.98E3         /* VC SRC FF -PU
       PGB7(4)=STOR(18)/46.74          /* FYA A -PU
       PGB7(5)=STOR(20)/46.74          /* FYA B -PU
       PGB7(6)=STOR(22)/46.74          /* FYA C -PU
       PGB7(7)=STOR(4)/97.98E3         /* VA SRC 2ND HARM -PU
       PGB7(8)=STOR(5)/97.98E3         /* VB SRC 2ND HARM -PU
       PGB7(9)=STOR(6)/97.98E3         /* VC SRC 2ND HARM -PU
       PGB7(10)=STOR(46)               /* PLL REF PULSE(1/CY)
C
C
       WRITE(9,40) TIME,(PGB3(I),I=1,10)
       WRITE(10,40) TIME,(PGB4(I),I=1,10)
       WRITE(11,40) TIME,(PGB5(I),I=1,10)
       WRITE(12,40) TIME,(PGB6(I),I=1,10)
       WRITE(13,40) TIME,(PGB7(I),I=1,10)
   40  FORMAT(F8.5,10(1X,G11.4))
C
       END IF
C
C    FORTRAN 77 CLOSING PROCEDURE
C
       IF (TIME.GE.FINTIM) THEN
       CLOSE(UNIT=9)
       CLOSE(UNIT=10)
       CLOSE(UNIT=11)
       CLOSE(UNIT=12)
       CLOSE(UNIT=13)
       CON(91)=0.0
       END IF
C
         RETURN
         END
```

APPENDIX B

EMTDC USER WRITTEN MODEL SOURCE CODE

B1: Subroutine SRC7 - Voltage Source Model

B2.1: Subroutine R6P120 - TCR Model

B2.2: Subroutine TIMD5 - TCR Model Time Delay Relay

B3: Subroutine PSEQU - Phasor Measurement

B4: Subroutine AVGF25 - Averaging Filter

B5: Subroutine PCTR20 - Firing Angle Modulation Controller

B6: Subroutine FOURIER.FOR - Fourier Analysis

B1: Subroutine SRC7 - Voltage Source Model

```
      SUBROUTINE SRC7(MA,NA,NB,NC,U1,U2,WS,PHIF,PHIH,THETA,THETA2)
C
CCC   SUBROUTINE TO CREATE A 3 PHASE VOLTAGE SOURCE FOR THEVENIN SOURCE
CCC
CCC
CCC   THE ARGUMENT CONSISTS OF:
CCC      MA         = SUB SYSTEM NUMBER.
CCC      NA,NB,NC   = NODE NUMBERS OF THEVENIN SOURCES
CCC                   (ANTI-CLOCKWISE VOLTAGE ROTATION ASSUMED)
CCC            U1   = PEAK PHASE TO GROUND VOLTS (KV)
CCC            U2   = 2ND HARM. PEAK PHASE TO GROUND VOLTS (KV)
CCC            WS   = FUNDAMENTAL FREQUENCY (RADIANS/SECOND)
CCC          PHIF   = FUND. FREQ. PHASE DISPLACEMENT (RADIANS)
CCC          PHIH   = 2ND HARMONIC PHASE DISPLACEMENT wrt FUND. FREQ.
CCC         THETA   = FUND. FREQ. ANGULAR POSITION (RADIANS)
CCC        THETA2   = 2ND HARM ANGULAR POSITION (RADIANS)(+VE FOR ANTI-CLOCKWISE)
CCC
CCC         OUTPUT:
CCC          FORMULATES ES(NA,MA),ES(NB,MA),ES(NC,MA)
CCC          COSINE FUNCTION CHOSEN WITH FUND. FREQ. PHASE LAG PHIF
CCC          SUCH THAT PH-PH VOLTAGE ACROSS TCR IS SQRT(3)*U1*COS(THETA)
CCC          WHERE THETA=(WS*DELT-PHIH) FOR PROPER REFERENCE TO PLL
CCC          SOURCE U1*SIN(THETR) WHERE THETR-THETA=90'
CCC          2ND HARMONIC OF MAGNITUDE U2 AND PHASE DISPLACEMENT PHIH
CCC           i.e. THETA2=2.0*(THETA-PHIH)
C
      INCLUDE 'EMT.E'
      COMMON /S1/TIME,DELT,ICH,PRINT,FINTIM
      COMMON /S2/STOR(5000),NEXC
      COMMON /S4/ VAR(100),CON(100),PGB(25)
C
CCC   AC STAR SOURCE DEFINITION
CCC
C     DEFINE MODULUS TWOPI
      PI=3.141592654          /* PI RADIANS = 180'
      TWOPI=6.283185308       /* 2*PI RADIANS = 360'
      DEG120=2.094395102      /* 2*PI/3 RADIANS = 120'
C
      IF (TIME.GE.DELT) THEN
C
CCC   DEFINE SYSTEM ANGULAR POSITION EACH TIME STEP
C
      ANG=STOR(NEXC+7)+WS*DELT
      IF (ANG.GE.TWOPI) ANG=ANG-TWOPI
      STOR(NEXC+7)=ANG
      THETA=ANG+PHIF
      IF (THETA.GE.TWOPI) THETA=THETA-TWOPI
      THETA2=2.0*THETA+PHIH
      IF (THETA2.GE.TWOPI) THETA2=THETA2-TWOPI
C
C     DEFINE FUNDAMENTAL FREQUENCY SOURCE
        STOR(NEXC+1)=U1*COS(THETA)
        STOR(NEXC+2)=U1*COS(THETA-2.094395103)
        STOR(NEXC+3)=-1.0*(STOR(NEXC+1)+STOR(NEXC+2))
C     DEFINE 2ND HARMONIC SOURCE
        STOR(NEXC+4)=U2*COS(THETA2)
        STOR(NEXC+5)=U2*COS(THETA2-2.094395103)
        STOR(NEXC+6)=-1.0*(STOR(NEXC+4)+STOR(NEXC+5))
C     DEFINE FUND.FREQ. PLUS 2ND HARM. SOURCE
        ES(NA,MA)=STOR(NEXC+1)+STOR(NEXC+4)
        ES(NB,MA)=STOR(NEXC+2)+STOR(NEXC+5)
        ES(NC,MA)=-1.0*(ES(NA,MA)+ES(NB,MA))
C
      ELSE
C
CCC   INITIALIZE VARIABLES IF TIME LESS THAN DELT
C
        ANG=0.0
        THETA=ANG+PHIF
        IF (THETA.GE.TWOPI) THETA=THETA-TWOPI
        THETA2=2.0*THETA+PHIH
        IF (THETA2.GE.TWOPI) THETA2=THETA2-TWOPI
C
        DO 10 I=1,7
   10   STOR(NEXC+I)=0.0
        ES(NA,MA)=STOR(NEXC+1)+STOR(NEXC+4)
        ES(NB,MA)=STOR(NEXC+2)+STOR(NEXC+5)
        ES(NC,MA)=-1.0*(ES(NA,MA)+ES(NB,MA))
      END IF
C
      NEXC=NEXC+7
C
      RETURN
      END
```

B2.1: Subroutine R6P120 - TCR Model

```
      SUBROUTINE R6P120(MA,NA,NB,NC,N1T,N1F,N2T,N2F,N3T,N3F,N4T,N4F,
     &     N5T,N5F,N6T,N6F,KV,KB,ROFF,RON,CTO,ALPHO,VREFM,FREQS,
     &     WR,G,TI,TIF,YO,TLO,THI,GL,TL,VSET,HYST,TDPU,TDDO,RPUL24,
     &     DELRS,DELST,DELTR)
C
C    SUBROUTINE TO MODEL A SIX PULSE THYRISTOR CONTROLLED REACTOR
C    R. W. MAZUR    87 07 23
C    CURRENT RUNNING VERSION LAST UPDATE NOV.16/88
C
C      INPUTS :
C   MA         = SUB-SYSTEM NUMBER
C   NA,NB,NC   = MAIN CIRCUIT COMMUTATING BUS NUMBERS
C   NIT,NIF    = "TO" NODE AND "FROM" NODE FOR 1ST VALVE TO FIRE
C                CURRENT DIRECTION +VE TOWARDS "TO" NODE
C   KV         = 0 PULSE FIRING IN SYNC WITH VOLTS ON NODE NA ETC
C              = 1 PULSE FIRING IS 30 DEG IN PHASE ADVANCE OF NA
C   KB         = 0 BLOCK, =1 DEBLOCK
C   ROFF       = EQUIV VALVE OFF RESISTANCE IN OHMS
C   RON        = EQUIV VALVE RESISTANCE WHEN "ON"
C   CTO        = THYRISTOR TURN OFF CURRENT IN K-AMPS (USE ABOUT 2% RATED ID)
C                (IF CTO = 0.0, THEN TURN-OFF CURRENT AUTOMATICALLY SET)
C   ALPHO      = ALPHA ORDER IN RADIANS
C   VREFM      = PPL REFERENCE VOLTAGE MAGNITUDE (KV PH-GRD P-P)
C   FREQS      = SYTEM FREQ (HZ)
C   WR         = PLL BASE FREQUENCY (RADIANS/SECOND)
C   G          = PLL PROPORTIONAL GAIN (RADIANS/DEGREE-SECOND)
C   TI,TIF     = PLL INTEGRAL GAIN (RADIANS/DEGREE-SECOND**2)
C                TIF IS GAIN USED FOR FREQUENCY CHANGES
C   YO         = INITIAL OUTPUT OF PI CONTROLLER (RADIANS/SECOND)
C   TLO,THI    = PLL PI-CONTROLLER LOW & HIGH LIMITS (RADIANS/SECOND)
C   GL,TL      = PLL ERROR FILTER GAIN [UNITLESS] AND TIME LAG (SECONDS)
C   VSET,HYST= PLL TIMER PICKUP SETTING & HYSTERSIS (DEGREES)
C                TIMER ACTIVES INTEGRAL GAIN CHANGE
C   TDPU,TDDO= PLL TIMER PICKUP AND DROPOUT DELAY (SECONDS)
C   DELRS, DELST, DELTR = FIRING ANGLE MODULATION FOR EACH VALVE (RADIANS)
C    OUTPUTS :
C   E1,E       = PLL PHASE ERROR, UNFILTERED AND FILTERED
C   EINT       = OUTPUT OF CONTROLLER,INTEGRAL TERM (RADIANS/SECONDS)
C   DELW       = PLL CONTROLLER FREQUENCY OUTPUT INCREMENT (RADIANS/SECONDS)
C   YT         = PLL TIMER OUTPUT STATE, 1= TIF IS ACTIVE
C   OMEGR      = PLL FREQUENCY= WR + DELW (RADIANS/SECONDS)
C   THETR,THETRL = PLL PHASE POSITION (RADIANS)
C                THETRL IS PREVIOUS TIME STEP VALUE
C   VREF1, VREF2, VREF3 = PLL REFERENCE VOLTAGES
C   RPUL1      = PLL REFERENCE PULSE , ONE PER FUND. FREQ. CYCLE
C   RPUL24     = PLL REFERENCE PULSE, 24 PER FUND. FREQ. CYCLE
C      ------------------------------------------------------------
C
       INCLUDE 'EMT.E'
       COMMON /S1/TIME,DELT,ICH,PRINT,FINTIM
       COMMON /S2/STOR(5000),NEXC
       COMMON /S4/VAR(100),CON(100),PGB(25)
       DIMENSION JTO(6),JFR(6),UMN(6),XSING(6),POLR(6),ER(6)
       DIMENSION V(6),PULS(6),ALPH(6)
       REAL INTGL3,E,E1,EINT,DELW,DELRS,DELST,DELTR,
     1      THETR,THETRL,OMEGR,RPUL1,RPUL24
C
C      DEFINE CONSTANTS
C
       PI=3.141592654        /* PI RADIANS = 180'
       TWOPI=6.283185308     /* 2*PI RADIANS = 360'
       DEG120=2.094395102    /* 2*PI/3 RADIANS = 120'
C
C      DEFINE CONSTANTS TO PHASE ADVANCE AC COMMUTATING BUS VOLTAGE
C      BY ONE TIME STEP IF TCR IS IN SEPARATE SUBSYSTEM.
C           CPHASE - MULTIPLIER IN PHASE WITH VOLTAGE
C           CORTHG - MULTIPLIER IN QUADRATURE WITH VOLTAGE
C
       A1=TWOPI*FREQS*DELT
       CPHASE=1.0-A1*A1
       CORTHG=0.577350*A1
C
```

```
C      INITIALIZE VARIABLES
C
       IF (TIME.GE.DELT) THEN
C
CC      *** NEXC=0 ***
CC      E1 IS THE MEASURED PLL PHASE ERROR WRT. THE SYSTEM VOLTAGES
CC      ------------------------------------------------------------
CC      THE ERROR IS FILTERED WITH A FIRST ORDER FILTER
C       ----------------------------------------------
       E =REALP2(GL,TL,E1)
C      *** NEXC=2 ***
C      STOR E1 & E : PLL INPUT ERROR - UNFILTERED & FILTERED
       STOR(NEXC+1)=E1
       STOR(NEXC+2)=E
       NEXC=NEXC+2
C      *** NEXC=4 ***
C
CC     PLL PI-CONTROLLER MODEL
CC     -----------------------
C
       EINT=INTGL3(YO,TLO,THI,TI,E)
C      *** NEXC=7 ***
       DELW =G*E  + EINT
       IF(DELW .GT.THI) DELW =THI
       IF(DELW .LT.TLO) DELW =TLO
C
CC     STOR EINT & DELW : PLL CONTROLLER INTEGRAL & FREQUENCY INCREMENT OUTPUT
C
       STOR(NEXC+1)=EINT
       STOR(NEXC+2)=DELW
C      GENERATE ANGULAR FREQ. &  POSITION ( RECTANGULAR INTEGRATION)
C      ------------------------------------------------------------
       OMEGR=WR+DELW
       THETR=STOR(NEXC+16)+OMEGR*DELT
       IF(THETR.GE.TWOPI) THETR=THETR-TWOPI
C
C      STOR OMEGR : PLL FREQUENCY (RADIANS/SECOND)
       STOR(NEXC+3)=OMEGR
C
CC      GENERATE REFERENCE VOLTAGES OF PLL
C       ---------------------------------
       VREF1=VREFM*SIN(THETR)
       VREF2=VREFM*SIN(THETR-DEG120)
       VREF3=-1.0*(VREF1+VREF2)
       VREF6P=1.0*SIN(6.0*THETR)
C
CC      OUTPUT REFERENCE PULSE EVERY PLL FUNDAMENTAL FREQ. CYCLE
CC      -------------------------------------------------------
C       PULSE COMES AT +VE CROSSING AND HAS DURATION DELT
C       ------------------------------------------------
       V1K1=SIGN(1.00,VREF1)
       V1K= STOR(NEXC+4)
       STOR(NEXC+4)=V1K1
       IF((V1K1-V1K).GT. 0.00)THEN
        RPUL1=1.50
       ELSE
        RPUL1=0.0
       END IF
C  EXTEND DURATION OF PLL REFERENCE FIRING PULSE
       IF (RPUL1.GT.0.50)THEN
       TEXD=TIME+16*DELT
       END IF
       IF (TIME.LT.TEXD)THEN
       RPUL1=1.4999
       ELSE
       RPUL1=0.0
       END IF
C      GENERATE SAMPLING PULSE 24 TIMES A FUND. FREQ. CYCLE
CC     ----------------------------------------------------
C      PULSE DURATION IS DELT
C      ----------------------
       VREF24=1.0*SIN(24.0*THETR)
       V24K=STOR(NEXC+5)
       V24K1=SIGN(1.00,VREF24)
       STOR(NEXC+5)=V24K1
       IF((V24K1-V24K).LT. 0.00) THEN
        RPUL24=1.00
       ELSE
        RPUL24=0.0
       END IF
C
```

```
C       STOR VREF1,VREF2,VREF3,VREF6P,VREF24,RPUL1,RPUL24
        STOR(NEXC+6)=VREF1
        STOR(NEXC+7)=VREF2
        STOR(NEXC+8)=VREF3
        STOR(NEXC+9)=VREF6P
        STOR(NEXC+10)=VREF24
        STOR(NEXC+11)=RPUL1
        STOR(NEXC+12)=RPUL24
C
C       PREPARE FOR MEASURING ZERO CROSSINGS
C       ------------------------------------
C      RECALL LAST TIMESTEP SYSTEM VOLTAGES AND PUT PRESENT ONES IN ARRAY
C      & RECALL LAST TIMESTEP ANGULAR POSITION AND SAVE AS THETRL.
C      ------------------------------------------------------------------
        URPK=STOR(NEXC+13)
        USPK=STOR(NEXC+14)
        UTPK=STOR(NEXC+15)
        THETRL=STOR(NEXC+16)
C
C   TO DETERMINE FIRING PULSE SYNCHRONIZATION (ACW ROTATION 1 2 3)
        IF (KV.NE.0) GO TO 190
C     PULSE FIRING IN SYNCHRONISM WITH PRIMARY L-G VOLTS
C     KV=0   TCR WITH STAR/DELTA TRANSFORMER
C
        URPK1=VDC(NA,MA)
        USPK1=VDC(NB,MA)
        UTPK1=VDC(NC,MA)
C
        UMN(1)=URPK1
        UMN(3)=USPK1
        UMN(5)=UTPK1
        GO TO 193
  190 IF (KV.NE.1) GO TO 193
C     PULSE FIRING 30 DEGREES IN ADVANCE OF PRIMARY L-G VOLTS
C     KV=1   TCR WITH STAR/STAR TRANSFORMER
C
        URPK1=VDC(NA,MA)-VDC(NB,MA)
        USPK1=VDC(NB,MA)-VDC(NC,MA)
        UTPK1=VDC(NC,MA)-VDC(NA,MA)
C
        UMN(1)=URPK1
        UMN(3)=USPK1
        UMN(5)=UTPK1
  193 CONTINUE
C
C    PLACE PREVIOUS REF. BUS VOLTAGES IN ARRAY UMN(I)
C
        UMN(2)=URPK
        UMN(4)=USPK
        UMN(6)=UTPK
C
C      THE FOLLOWING LINE IS NEEDED BECAUSE THETR IS MODULO 2*PI
C      WHEN THETR = 360.0', THETR=THETR-TWOPI=0.0' & THETRL=359.99
C      AS AN EXAMPLE, SO THETR-THETRL=359.99' AND THE CROSSING
C      INTERPOLATION DOES NOT MAKE SENSE.
C      ----------------------------------------------------------
        IF(THETRL.GT.THETR)THETRL=THETRL-TWOPI
C
C      LOOKING FOR VOLTAGE ZERO CROSSING NOW
C      -------------------------------------
        DO 10   J=1,5,2
        POLR(J)=SIGN(1.0,UMN(J))
        POLR(J+1)=SIGN(1.0,UMN(J+1))
        IF(ABS(POLR(J)-POLR(J+1)).GT.0.10) THEN
C
C      AVOID POSSIBLE DIVISION BY ZERO
C      -------------------------------
        DIFF=UMN(J)-UMN(J+1)
        IF(ABS(DIFF).LT.1.0E-06)THEN
        DIFF=1.0E-06
        END IF
C
```

```
C      FIND & SAVE +VE ZERO CROSSING
C      -----------------------------
       IF(UMN(J) .GE. 0.00 .AND. UMN(J+1).LT.0.00)THEN
       XSING(J)=(UMN(J)*THETRL-UMN(J+1)*THETR)/DIFF
       ER(J)=(J-1.0)*PI/3.0-XSING(J)
       IF(ABS(ER(J)).GT.(PI+0.018)) THEN
          IF(ER(J).GE.0.00) THEN
           ER(J)=ER(J)-TWOPI
          ELSE
           ER(J)=ER(J)+TWOPI
          END IF
       END IF
C
C      FIND & SAVE -VE ZERO CROSSING
C      -----------------------------
       ELSE IF(UMN(J).LT.0.00 .AND. UMN(J+1).GE.0.00)THEN
       XSING(J+1)=(UMN(J)*THETRL-UMN(J+1)*THETR)/DIFF
       ANGL=(J+2.0)*PI/3.0
       IF(ANGL.GE.TWOPI)THEN
         ANGL=ANGL-TWOPI
       END IF
       ER(J+1)=ANGL-XSING(J+1)
       IF(ABS(ER(J+1)).GT.(PI+0.018))THEN
            IF(ER(J+1).GE.0.00) THEN
             ER(J+1)=ER(J+1)-TWOPI
            ELSE
             ER(J+1)=ER(J+1)+TWOPI
            END IF
       END IF
       END IF
       END IF
C
  10   CONTINUE
C
C      FIND TOTAL ERROR
C      ----------------
       E1=0.0
       DO 20 J=1,6
  20   E1=E1+ER(J)
C
C
C      WRITE TO STOR THIS TIMESTEP VOLTAGES & PLL ANGULAR POSITION
C      -----------------------------------------------------------
       STOR(NEXC+13)=URPK1
       STOR(NEXC+14)=USPK1
       STOR(NEXC+15)=UTPK1
       STOR(NEXC+16)=THETR
       NEXC=NEXC+16
C      **** NEXC=23 ****
C
C      CHECK IF PLL INTEGRAL GAIN SHOULD BE INCREASED
C      ----------------------------------------------
       VIN=ABS(E)
       YT= TIMD5(VIN,VSET,TDPU,TDDO,HYST)
C      **** NEXC=28 ****
C
       IF(YT.GT.0.5)THEN
        TI=TIF
C       WRITE(1,*) YT,TIF
       ELSE
        TI=TI
       END IF
C 199 FORMAT('YT = ',I3,1F10.5)
C
C      SAVE LAST TIME STEPS VOLTAGES & ANGULAR POSTION
C
       STOR(NEXC+1)=URPK
       STOR(NEXC+2)=USPK
       STOR(NEXC+3)=UTPK
       STOR(NEXC+4)=THETRL
       NEXC=NEXC+4
C      *** NEXC=32 ***
```

```
C
C      STOR ZERO XSING ANGLES (RADIANS)
C
       DO 11 J=1,5,2
       STOR(NEXC+J)=XSING(J)
   11  STOR(NEXC+J+1)=XSING(J+1)
       NEXC=NEXC+6
C      *** NEXC=38 ***
C
C     STOR XSING PLL - SYSTEM XSING ANGLE ERRORS
C
       DO 12 J=1,5,2
       STOR(NEXC+J)=ER(J)
   12  STOR(NEXC+J+1)=ER(J+1)
       NEXC=NEXC+6
C     *** NEXC=44 ***
C
C      CALCULATE FIRING ANGLES FOR SINUSOIDAL MODULATION
C      -------------------------------------------------
       ALPH(1)=ALPHO+DELRS
       ALPH(4)=ALPHO-DELRS
       ALPH(3)=ALPHO+DELST
       ALPH(6)=ALPHO-DELST
       ALPH(5)=ALPHO+DELTR
       ALPH(2)=ALPHO-DELTR
C
C      APPLY ALPHA LIMITS (0.0.LE.ALPHA.LE.90.0)
C      -----------------------------------------
       DO 25 J=1,6
       IF(ALPH(J).LT.0.0) ALPH(J) =0.0
       IF(ALPH(J) .GT.(PI/2.0)) ALPH(J) =PI/2.0
   25  CONTINUE
C
C      STOR FIRING ANGLES (RADIANS)
       STOR(NEXC+1)=ALPH(1)
       STOR(NEXC+2)=ALPH(4)
       STOR(NEXC+3)=ALPH(3)
       STOR(NEXC+4)=ALPH(6)
       STOR(NEXC+5)=ALPH(5)
       STOR(NEXC+6)=ALPH(2)
       NEXC=NEXC+6
C      **** NEXC=50 ***
C
C      OUTPUT FIRING PULSES
C      --------------------
C      RS-PHASE
C      --------
       IF(THETR.GE.(ALPH(1)  +PI/2.) .AND. THETR.LT.PI)THEN
        PULS(1)=1.00
       ELSE
        PULS(1)=0.00
       END IF
       IF(THETR.GE.(ALPH(4)  +3.*PI/2.) .AND. THETR.LT.TWOPI)THEN
        PULS(4)=1.4
       ELSE
        PULS(4)=0.00
       END IF
C      ST-PHASE
C      --------
       IF(THETR.GE.(ALPH(3)  +7.*PI/6.) .AND.
     +    THETR.LT.(5.*PI/3.))THEN
        PULS(3)=1.30
       ELSE
        PULS(3)=0.00
       END IF
       IF(THETR.GE.(ALPH(6)  +PI/6.) .AND. THETR.LT.DEG120)THEN
        PULS(6)=1.60
       ELSE
        PULS(6)=0.00
       END IF
C      TR-PHASE
C      --------
       IF(THETR.GE.(ALPH(2)  +5.*PI/6.) .AND.
     +    THETR.LT.(4.*PI/3.))THEN
        PULS(2)=1.20
       ELSE
        PULS(2)=0.00
       END IF
       IF(THETR.LT.PI/3.0.AND.THETR.GE.(ALPH(5)-PI/6.0))THEN
        PULS(5)=1.50
       ELSE IF( THETR.GE. (ALPH(5)+11.0*PI/6.0)) THEN
        PULS(5)=1.5
       ELSE
        PULS(5)=0.0
       END IF
C
```

```
C     WRITE TO STOR THIS TIMESTEP PULS(J)
C
      STOR(NEXC+1)=PULS(1)
      STOR(NEXC+2)=PULS(4)
      STOR(NEXC+3)=PULS(3)
      STOR(NEXC+4)=PULS(6)
      STOR(NEXC+5)=PULS(5)
      STOR(NEXC+6)=PULS(2)
      NEXC=NEXC+6
C     **** NEXC=56 ****
C
      ELSE
C
C     INITIALIZE PLL VARIABLES FOR TIME.LT.DELT
C
C     PARAMETER FOR EXTENDING RPULS(1) DURATION
C
      TEXD=0.0
C
C  TO DETERMINE FIRING PULSE SYNCHRONIZATION (ACW ROTATION 1 2 3)
      IF (KV.NE.0) GO TO 191
C    PULSE FIRING IN SYNCHRONISM WITH PRIMARY L-G VOLTS
C    KV=0   TCR WITH STAR/DELTA TRANSFORMER
C
      URPK1=VDC(NA,MA)
      USPK1=VDC(NB,MA)
      UTPK1=VDC(NC,MA)
C
      UMN(1)=URPK1
      UMN(3)=USPK1
      UMN(5)=UTPK1
      GO TO 194
  191 IF (KV.NE.1) GO TO 194
C    PULSE FIRING 30 DEGREES IN ADVANCE OF PRIMARY L-G VOLTS
C    KV=1   TCR WITH STAR/STAR TRANSFORMER
C
      URPK1=VDC(NA,MA)-VDC(NB,MA)
      USPK1=VDC(NB,MA)-VDC(NC,MA)
      UTPK1=VDC(NC,MA)-VDC(NA,MA)
C
      UMN(1)=URPK1
      UMN(3)=USPK1
      UMN(5)=UTPK1
  194 CONTINUE
C
C   PLACE PREVIOUS REF. BUS VOLTAGES IN ARRAY UMN(I)
C
      UMN(2)=UMN(1)
      UMN(4)=UMN(3)
      UMN(6)=UMN(5)
C
C
      E1=0.00
      E=REALP2(GL,TL,E1)
C     **** NEXC=2 ****
C   INITIALIZE STOR E1 & E : PLL INPUT ERROR - UNFILTERED & FILTERED
      STOR(NEXC+1)=E1
      STOR(NEXC+2)=E
      NEXC=NEXC+2
C     *** NEXC=4 ***
C
      EINT=INTGL3(YO,TLO,THI,TI,E)
C     **** NEXC=7 ****
      DELW =G*E + EINT
      IF(DELW .GT.THI) DELW =THI
      IF(DELW .LT.TLO) DELW =TLO
      OMEGR=DELW+WR
      THETR= 1.570796327
      THETRL=THETR
C
```

```
C      STOR EINT & DELW : PLL CONTROLLER INTEGRAL & FREQUENCY INCREMENT OUTPUT
C      INITIAL VALUES
       STOR(NEXC+1)=EINT
       STOR(NEXC+2)=DELW
C      INITIALIZE STOR OMEGR : PLL FREQUENCY (RADIANS/SECOND)
       STOR(NEXC+3)=OMEGR
C
       VREF1=VREFM*SIN(THETR)
       VREF2=VREFM*SIN(THETR-DEG120)
       VREF3=-1.0*(VREF1+VREF2)
       VREF6P=1.0*SIN(6.0*THETR)
C
       DELRS=0.0
       DELST=0.0
       DELTR=0.0
C
C      REFERENCE PULSE
C      ---------------
       V1K1=SIGN(1.00,VREF1)
       STOR(NEXC+4)=V1K1
       VREF24=1.0*SIN(24.0*THETR)
       V24K1=SIGN(1.00,VREF24)
       STOR(NEXC+5)=V24K1
       RPUL1=0.0
       RPUL24=0.0
C      INITIALIZE STORAGE VREF1,VREF2,VREF3,VREF6P,VREF24,RPUL1,RPUL24
       STOR(NEXC+6)=VREF1
       STOR(NEXC+7)=VREF2
       STOR(NEXC+8)=VREF3
       STOR(NEXC+9)=VREF6P
       STOR(NEXC+10)=VREF24
       STOR(NEXC+11)=RPUL1
       STOR(NEXC+12)=RPUL24
C
C      INITIALIZE STORAGE THIS TIMESTEP VOLTAGES & PLL ANGULAR POSITION
C      ----------------------------------------------------------------
       STOR(NEXC+13)=URPK1
       STOR(NEXC+14)=USPK1
       STOR(NEXC+15)=UTPK1
       STOR(NEXC+16)=THETR
       NEXC=NEXC+16
C      **** NEXC=23 ****
       YT=TIMD5(E,VSET,TDPU,TDDO,HYST)
C      **** NEXC=28 ****
C      INITIALIZE STORAGE LAST TIME STEPS VOLTAGES & ANGULAR POSTION
C
       STOR(NEXC+1)=URPK1
       STOR(NEXC+2)=USPK1
       STOR(NEXC+3)=UTPK1
       STOR(NEXC+4)=THETRL
       NEXC=NEXC+4
C      *** NEXC=32 ***
C
       DO 40 J=1,5,2
       POLR(J)=SIGN(1.0,UMN(J))
    40 POLR(J+1)=SIGN(1.0,UMN(J+1))
       DO 30 J=1,6
       PULS(J)=0.00
       ER(J)=0.0
       ALPH(J)=0.00
    30 XSING(J)=0.00
C
C      INITIALIZE STORAGE ZERO XSING ANGLES (RADIANS)
C
       DO 13 J=1,5,2
       STOR(NEXC+J)=XSING(J)
    13 STOR(NEXC+J+1)=XSING(J+1)
       NEXC=NEXC+6
C      *** NEXC=38 ***
C
C     INITIALIZE STORAGE PLL ZERO XSING - SYSTEM ZERO XSING ANGLE ERRORS
C
       DO 14 J=1,5,2
       STOR(NEXC+J)=ER(J)
    14 STOR(NEXC+J+1)=ER(J+1)
       NEXC=NEXC+6
C     *** NEXC=44 ***
```

```
C      INITIALIZE STORAGE FIRING ANGLES (RADIANS)
       STOR(NEXC+1)=ALPH(1)
       STOR(NEXC+2)=ALPH(4)
       STOR(NEXC+3)=ALPH(3)
       STOR(NEXC+4)=ALPH(6)
       STOR(NEXC+5)=ALPH(5)
       STOR(NEXC+6)=ALPH(2)
       NEXC=NEXC+6
C      **** NEXC=50 ***
C
C      INITIALIZE STOR FOR PULS(J)
C
       STOR(NEXC+1)=PULS(1)
       STOR(NEXC+2)=PULS(4)
       STOR(NEXC+3)=PULS(3)
       STOR(NEXC+4)=PULS(6)
       STOR(NEXC+5)=PULS(5)
       STOR(NEXC+6)=PULS(2)
       NEXC=NEXC+6
C      **** NEXC=56 ****
C
       END IF
C
C      INITIALIZE PARAMETERS FOR VALVE FIRING/BLOCKING
C
C
       IF (TIME.GE.DELT) GO TO 9
       DO 1 I=1,64
         STOR(NEXC+I)=0.0
     1 CONTINUE
       STOR(NEXC+10)=1.001
     9 CONTINUE
C
       IF (TIME.GE.DELT) GO TO 15
C
       STOR(NEXC+2)=DELT
C
C    VALVE GROUP PARAMETERS  -  RON & ROFF
       STOR(NEXC+4)=1.0/ROFF
       STOR(NEXC+5)=1.0/RON
C
C     TO SET CURRENT TURN OFF LEVEL FOR THYRISTOR (DEFAULT=.001KA)
       STOR(NEXC+7)=CTO
       IF (CTO.LT.0.001) STOR(NEXC+7)=0.001
       STOR(NEXC+8)=3.0*STOR(NEXC+7)
       STOR(NEXC+9)=20.0*STOR(NEXC+7)
C
C   TURN ALL VALVES OFF INITIALLY
       DO 3 I=1,6
         N3=NEXC+10+I
         STOR(N3)=STOR(NEXC+4)
     3 CONTINUE
C
    15 CONTINUE
C
C   SAVE CURRENT VALUE OF TIME
       STOR(NEXC+1)=TIME
C   VALVE FIRING, ALPHA & GAMMA MEASUREMENT
       DO 333 I=1,6
         NZ=NEXC+28+I
         NY=NEXC+22+I
         NCTO=NEXC+40+I
         NVG=NEXC+46+I
         N3=NEXC+10+I
         A1=STOR(N3)
         IF (STOR(NZ).GT.STOR(NCTO)) GO TO 334
C      RWM  -COULD COMMENT OUT NEXT 3 LINES
         A0=STOR(NZ)+STOR(NZ)-STOR(NY)
         IF (A0.GT.STOR(NEXC+7)) GO TO 334
         IF (STOR(NY).GT.STOR(NEXC+9)) GO TO 334
         GO TO 332
C
```

```
C
C  TO SWITCH VALVE ON
C
  334   CONTINUE
        IF(KB.LE.0) GO TO 333
        J=1
        IF (I.EQ.2) J=4
        IF (I.EQ.3) J=3
        IF (I.EQ.4) J=6
        IF (I.EQ.5) J=5
        IF (I.EQ.6) J=2
        IF (PULS(J).LT.0.2) GO TO 333
        A2=STOR(NVG)
        STOR(NVG)=ABS(A1-STOR(NEXC+5))
C       RWM  COULD BE COMMEMTED OUT
        IF (A2.GE.1.0E-06) GO TO 333
        STOR(N3)=STOR(NEXC+5)
        IF (STOR(NVG).LT.1.0E-03) GO TO 333
C
C    DETERMINE WHICH VALVE FIRED LAST
        NV=1
        IF (I.EQ.2) NV=4
        IF (I.EQ.3) NV=3
        IF (I.EQ.4) NV=6
        IF (I.EQ.5) NV=5
        IF (I.EQ.6) NV=2
        STOR(NEXC+10)=NV+0.01
C
C       SETTING ICH=MA (SUBSYSTEM NO.) SIGNALS MAIN PGM TO INVERT 'G' MATRIX
        ICH=MA
        GO TO 333
C       TURN VALVE OFF & TIMING OF GAMMA
C
  332   A2=STOR(NVG)
        STOR(NVG)=ABS(A1-STOR(NEXC+4))
C       RWM -COMMENT OUT NEXT LINE
        IF (A2.GE.1.0E-06) GO TO 333
        STOR(N3)=STOR(NEXC+4)
        IF (STOR(NVG).LT.1.0E-03) GO TO 333
C       TIME VALVE LAST TURNED OFF N2=35-40
        N2=NEXC+34+I
        STOR(N2)=STOR(NEXC+1)
C
C       SETTING ICH=MA (SUBSYSTEM NO.) SIGNALS MAIN PGM TO INVERT 'G' MATRIX
        ICH=MA
C  ****** TO COUNT NO. OF VALVES CONDUCTING ******
        NCON=0
        NV1=NEXC+11
        NV2=NEXC+16
        G2=1.1*STOR(NEXC+4)
        DO 3330 K=NV1,NV2
          IF (STOR(K).LT.G2) GO TO 3330
          NCON=NCON+1
3330   CONTINUE
  333 CONTINUE
C
C ** INTERFACE BETWEEN SUBSYTEM AND CONTROLLER
C    SETTING UP NODES OF VALVES
      JTO(1)=N1T
      JTO(6)=N2T
      JTO(3)=N3T
      JTO(2)=N4T
      JTO(5)=N5T
      JTO(4)=N6T
C
      JFR(1)=N1F
      JFR(6)=N2F
      JFR(3)=N3F
      JFR(2)=N4F
      JFR(5)=N5F
      JFR(4)=N6F
C
```

```
C     TO DETERMINE VOLTS ACROSS VALVES
      DO 305 I=1,6
        J1=JTO(I)
        K1=JFR(I)
        N=NEXC+28+I
        K=NEXC+16+I
        L=NEXC+10+I
        I1=0
        IF (J1.EQ.0) GO TO 301
        IF (K1.EQ.0) GO TO 302
        V(I)=VDC(K1,MA)-VDC(J1,MA)
        GO TO 303
  301   I1=J1+K1
        V(I)=VDC(K1,MA)
        GO TO 303
  302   I1=J1+K1
        V(I)=-VDC(J1,MA)
  303   IF (TIME.GE.DELT) GO TO 305
        IF (J1.LT.0) GO TO 183
        IF (K1.LT.0) GO TO 183
        IF (I1.EQ.0) GO TO 309
        IF (ABS(GDCS(I1,MA)).LT.1.0E-10) GO TO 183
        GO TO 305
  309   IF (ABS(GDC(J1,K1,MA)).LT.1.0E-10) GO TO 183
        GO TO 305
C
C     ERROR MESSAGES
  183   WRITE(1,184) J1,K1,MA
  184   FORMAT('VALVE BETWEEN NODES',I3,' AND',I3,'IN SUB SYSTEM',I3)
        WRITE(1,185)
  185   FORMAT('IS NOT CORRECTLY ENTERED. CHECK DATA & ARGUMENT')
        CLOSE(UNIT=5)
        CLOSE(UNIT=6)
      STOP
C
  305 CONTINUE
      DO 300 I=1,6
        J1=JTO(I)
        K1=JFR(I)
        N=NEXC+28+I
        K=NEXC+16+I
        L=NEXC+10+I
        NCTO=NEXC+40+I
        NY=NEXC+22+I
        I1=J1+K1
        IF (K1.EQ.0) GO TO 306
        IF (J1.EQ.0) GO TO 306
C     RESET CONDUCTANCES TO ZERO
        GDC(J1,K1,MA)=0.0
        GDC(K1,J1,MA)=0.0
        GO TO 307
  306   GDCS(I1,MA)=0.0
C
C    CURRENT THROUGH EACH VALVE  STOR(N)   N = 29 TO 34
  307   STOR(NY)=STOR(N)
        STOR(N)=STOR(L)*V(I)
        IF (STOR(N).GE.0.0) GO TO 308
        IF (STOR(NY).GE.0.0) GO TO 308
        STOR(NCTO)=0.0
        GO TO 300
  308   IF (STOR(N).LE.STOR(NEXC+8)) GO TO 300
        IF (STOR(NY).LE.STOR(NEXC+8)) GO TO 300
        STOR(NCTO)=STOR(NEXC+8)
  300 CONTINUE
C
C     TO SET UP INTERFACE TO SUBSYSTEM, IE THROUGH GDC AND CCDC
      DO 320 I=1,6
        J1=JTO(I)
        K1=JFR(I)
        K=NEXC+16+I
        L=NEXC+10+I
C
        IF (J1.EQ.0) GO TO 311
        IF (K1.EQ.0) GO TO 311
        GDC(J1,K1,MA)=GDC(J1,K1,MA)+STOR(L)
        GDC(K1,J1,MA)=GDC(J1,K1,MA)
        GO TO 320
C
  311   I1=J1+K1
        GDCS(I1,MA)=GDCS(I1,MA)+STOR(L)
  320 CONTINUE
      NEXC=NEXC+64
C     *** NEXC=120 ****
C
      RETURN
      END
C     ~~~~~~~~~~~~~~~~~~~~~~~~~~~~~~~~~~~~~~~~~~~~~~~~~~~~~~~~~~~~~~~~~~~~~~~~~~~~~~~~
```

B2.2: Subroutine TIMD5 - TCR Model Time Delay Relay

```
      FUNCTION TIMD5(VIN,VSET,TDPU,TDDO,HYST)
C     ~~~~~~~~~~~~~~~~~~~~~~~~~~~~~~~~~~~~~~~
C     -----------------------------------------------
      INCLUDE 'EMT.E'
      COMMON /S1/TIME,DELT,ICH,PRINT,FINTIM
      COMMON /S2/STOR(5000),NEXC
C
C
C     TIME DELAY ON PICK-UP,RETRIGGERABLE  &  ON DROPOUT,RETRIGGERABLE
C     ---------------------------------------------------------------
C     WHEN INPUT "VIN" EXCEEDS SETPOINT "VSET" FOR TIME = "TDPU",
C     -----------------------------------------------------------
C     THEN OUTPUT GOES TO LOGIC 1 (HI) FROM LOGIC 0 (LOW)
C     ---------------------------------------------------
C     IF OUTPUT GOES HI IT REMAINS HI FOR TIME= TDDO
C     ----------------------------------------------
C
      IF (TIME.GE.DELT)THEN
      TIMD5=STOR(NEXC+1)
      ICNT1=STOR(NEXC+2)
      ICNT2=STOR(NEXC+3)
C
      IF(TIMD5.LT.0.222)THEN
C
      IF(VIN.GE.VSET)THEN
C
        IF(ICNT1.LT.1 )THEN
        STOR(NEXC+4)=TIME+TDPU
        ICNT1=2
        END IF
      ELSE
C
      STOR(NEXC+4)=4000.
      ICNT1=0
      END IF
C
      IF(TIME.GE.STOR(NEXC+4)) THEN
      ICNT1=0
      TIMD5=1.0000
       END IF
C
      ELSE
C
      IF(VIN.LE.(VSET-HYST))THEN
       IF(ICNT2.LT.1)THEN
       STOR(NEXC+5)=TIME+TDDO
       ICNT2=3
       END IF
       ELSE
       ICNT2=0
       STOR(NEXC+5)=5000.
       END IF
      IF(TIME.GE.STOR(NEXC+5))THEN
      ICNT2=0
      TIMD5=0.0000
      END IF
      END IF
      ELSE
C
      ICNT1=0
      ICNT2=0
      TIMD5=0.00000
      STOR(NEXC+4)=TDPU
      STOR(NEXC+5)=TDDO
C
      END IF
C
      STOR(NEXC+1)=TIMD5
      STOR(NEXC+2)=ICNT1
      STOR(NEXC+3)=ICNT2
      NEXC=NEXC+5
      RETURN
      END
```

B3: Subroutine PSEQU - Phasor Measurement

```
      SUBROUTINE PSEQU(CURRA,CURRB,CURRC,N,THETR,CALP,CBETA,
     &                 CPREAL,CPIMG)
C     ~~~~~~~~~~~~~~~~~~~~~~~~~~~~~~~~~~~~~~~~~~~~~~~~~~~~~~~~~~~~~~~~
C     --------------------------------------------------------
C     THIS SUBROUTINE CALCULATES THE POSITIVE SEQUENCE COMPONENTS
C     ----------------------------------------------------------
C     OF ANY SPECIFIED 3 PHASE SET OF CURRENTS.THE MEASUREMENT IS
C     ----------------------------------------------------------
C     INSTANTANEOUS AND OUTPUTS THE REAL & IMAGINARY TERMS OF
C     ------------------------------------------------------
C     THE SPECIFIED HARMONIC COMPONENT. THE ALPHA/BETA TRANSFORMATION
C     -------------------------------------------------------------
C     IS USED AND THE ALPHA/BETA- SYM. COMPONENT TRANSFORMATION IS USED
C     ---------------------------------------------------------------
      INCLUDE 'EMT.E'
      COMMON /S1/ TIME,DELT,ICH,PRINT,FINTIM
      COMMON /S2/ STOR(5000),NEXC
C
      REAL CURRA,CURRB,CURRC,CALP,CBETA,CPREAL,CPIMG,THETR,CO,SI
      INTEGER N
C
C     INPUTS :
C        CURRA,B,C: CURRENTS TO BE TRANSFORMED (PU)
C        N  :  HARMONIC COMPONENT OF CURRENT RESOLVED INTO PHASOR
C     OUTPUTS :
C        CALP,CBETA: TIME-VARYING I-alpha AND I-beta
C        CPREAL,CPIMG: REAL & IMAGINARY PART OF POSITIVE SEQUENCE PHASOR
C        ------------------------------------------------------------
C        CO=COS(N*W*T)     SI=SIN(N*W*T)
C        ------------------------------
C
C
C     DEFINE CONSTANTS
C
      PI=3.141592654    /* PI RADIANS  180'
      TWOPI=6.283185308    /* 2*PI RADIANS 360'
      DEG120=2.094395102    /* 2*PI/3 RADIANS 120'
C
      CALP=0.666667*CURRA-0.333333*CURRB-0.333333*CURRC
      CBETA=0.577350*(CURRB-CURRC)
C
      CO=COS(N*(THETR-PI/2.))
      SI=SIN(N*(THETR-PI/2.))
C
C  NOTE PI/2=1.570796 IS PHASE POSITION OF PLL WRT PHASOR REF COORDINATE SYS
      CPREAL=CALP*CO +CBETA*SI
      CPIMG=-CALP*SI +CBETA*CO
C
      RETURN
      END
C     ~~~~~~~~~~~~~~~~~~~~~~~~~~~~~~~~~~~~~~~~~~~~~~~~~~~~~~~~~~~~~~~
```

B4: Subroutine AVGF25 - Averaging Filter

```
      SUBROUTINE AVGF25(SIGIN,SF,RPULS,SIGOUT)
C     ~~~~~~~~~~~~~~~~~~~~~~~~~~~~~~~~~~~~~~~~~~~~~~~~~~~~~~~~~~~~~~~~~~~~
C
C     ---------------------------------------------------------------
      COMMON /S1/ TIME,DELT,ICH,PRINT,FINTIM
      COMMON /S2/ STOR(5000),NEXC
C     ~~~~~~~~~~~~~~~~~~~~~~~~~~~~~~~~~~~~~~~~~~~~~~~~~~~~~~~~~~~~~~~~~~~~
C     SIGIN : INPUT SIGNAL FOR FILTERING
C     SF    : SCALE FACTOR (FOURNUM RMS O/P VS. PSEQ P-P O/P IS SQRT(6))
C     RPULS : SAMPLING PULSE FROM PLL-24 SAMPLES PER FUND. PERIOD
C     SIGOUT: FILTERED OUTPUT SIGNAL
C     ----------------------------------
C
      REAL SIGIN,SF,RPULS,SIGOUT
C
C     IF(TIME.GE.1.95975)THEN
C     WRITE(1,230) SIGIN,SF,RPULS
C     END IF
C 230 FORMAT(' SIGIN =',G11.3,' SF =',G11.3,' RPULS =',G11.3)
C
      IF(TIME.GT.0.0)THEN
      IF(RPULS .GT. 0.10) THEN
      DO 10  J=1,23
      N=25-J
      M=24-J
10    STOR(NEXC+N)=STOR(NEXC+M)
      STOR(NEXC+1)=SIGIN
      SIGOUT=0.0
      DO 20  J=1,24
20    SIGOUT=SIGOUT+STOR(NEXC+J)
      SIGOUT=SIGOUT*SF/24.0
      STOR(NEXC+25)=SIGOUT
      ELSE
      SIGOUT=STOR(NEXC+25)
C
C     IF(TIME.GE.1.96975)THEN
C     WRITE(1,237)   SIGOUT,NEXC,STOR(NEXC+25)
C     END IF
C 237 FORMAT(' SIGOUT =',G11.3,' NEXC =',I4,' STOR(NEXC+25) =',G11.3)
      END IF
      ELSE
      DO 30 J=1,25
30    STOR(NEXC+J)=0.00
      SIGOUT=0.0
      DO 40 J=1,24
40    SIGOUT=SIGOUT+STOR(NEXC+J)
      SIGOUT=SIGOUT*SF/24.0
C
C     WRITE(1,*) SIGOUT,(STOR(J),J=36,60)
C
      END IF
C
C     IF(TIME.GE.1.96975)THEN
C     WRITE(1,*) (STOR(NEXC+J),J=1,25),NEXC,SIGOUT
C     END IF
C
      NEXC=NEXC+25
      RETURN
      END
C     ~~~~~~~~~~~~~~~~~~~~~~~~~~~~~~~~~~~~~~~~~~~~~~~~~~~~~~~~~~~~~~~~~~~~
```

B5: Subroutine PCTR20 - Firing Angle Modulation Controller

```
C     ~~~~~~~~~~~~~~~~~~~~~~~~~~~~~~~~~~~~~~~~~~~~~~~~~~~~~~~~~~~~~~~~~~~~~~~~~~~~
      SUBROUTINE PCTR20(CPREAL,CPIMG,THETR,GRLF,TCRLF,SCRLO,SCRLL,
     & SCRLU,GISCRL,GPSCRL,GIMGF,TCIMGF,SIMGO,SIMGL,SIMGU,GISIMG,
     & GPSIMG,ALPMOD,CRL1,CIMG1,ARMOD,AIMOD,MANUAL,CRLINT,CIMGIN,
     & DELRS,DELST,DELTR)
C     ~~~~~~~~~~~~~~~~~~~~~~~~~~~~~~~~~~~~~~~~~~~~~~~~~~~~~~~~~~~~~~~~~~~~~~~~~~~~
C     ------------------------------------------------------------------
      INCLUDE 'EMT.E'
      COMMON /S1/TIME,DELT,ICH,PRINT,FINTIM
      COMMON /S2/STOR(5000),NEXC
      REAL INTGL3,CPREAL,CPIMG,THETR,DELRS,DELST,DELTR,ALPMOD,
     1     CRLINT,CIMGIN,ARMOD,AIMOD,CRL1,CIMG1,GRLF,TCRLF,
     1     SCRLO,SCRLL,SCRLU,GISCRL,GPSCRL,GIMGF,TCIMGF,
     1     SIMGO,SIMGL,SIMGU,GISIMG,GPSIMG
      INTEGER MANUAL
C
C      PCONTR10  CALCULATES PEAK AND PHASE ANGLE IN DEGREES  FOR THE
C      ---------------------------------------------------------------
C      SINUSOIDAL MODULATION SIGNAL DELALPxy =PEAK * SIN( 0r + PHASE)
C      ---------------------------------------------------------------
C      THE MODULATION  IS SUCH THAT THE POSITIVE SEQUENCE
C      ---------------------------------------------------------------
C      PHASOR(CPREAL + J*CPIMG) OF MEASURED LINE CURRENT IS MADE ZERO
C      ---------------------------------------------------------------
C      INPUTS :
C      CPREAL   : REAL PART OF CURRENT PHASOR
C      CPIMG    : IMAG PART OF CURRENT PHASOR
C      THETR    : PLL PHASE POSITION
C      SCRLO    : INITIAL VALUE OF  CRL1, THE REAL PART CONTROLLER OUTPUT
C      SCRLL    : LOWER LIMIT OF  CRL1
C      SCRLU    : UPPER LIMIT OF  CRL1
C      GISCRL   : INTEGRAL GAIN FOR  CRL1
C      GPSCRL   : PROP.    GAIN FOR  CRL1
C      SIMGO    : INITIAL VALUE OF CIMG1, THE IMG PART CONTROLLER OUTPUT
C      SIMGL    : LOWER LIMIT OF CIMG1
C      SIMGU    : UPPER LIMIT OF CIMG1
C      GISIMG   : INTEGRAL GAIN FOR CIMG1
C      GPSIMG   : PROP.    GAIN FOR CIMG1
C      MANUAL   : MANUAL/AUTO SWITCH    0=AUTO 2=AUTO
C      ARMOD, AIMOD : REAL & IMG PARTS OF MODULATION SIGNAL IN RADIANS
C     OUTPUTS :
C      CRL1     : OUTPUT  FROM REAL PART PI-CONTROLLER
C      CIMG1    : OUTPUT  FROM IMG  PART PI-CONTROLLER
C      CRLINT, CIMGINT : INTEGRAL TERM OF THE RESP. PI CONTR.
C      DELRS, DELST, DELTR : ALPHA MOD SIGNAL FOR EACH OF THE
C                            THYRISTOR PAIRS IN THE 3 PHASES
C      ---------------------------------------------------------
C
C      PI -CONTROLLER MODELS
C      ---------------------
      TISCRL=1.0/GISCRL
      TISIMG=1.0/GISIMG
C     FILTER MEASURED CURRENT
      CRL=REALP2(GRLF,TCRLF,CPREAL)
      CIMG=REALP2(GIMGF,TCIMGF,CPIMG)
C     REMOVE C in Col 1 of next two lines to bypass input filtering.
C     CRL=CPREAL
C     CIMG=CPIMG
      CRLINT=INTGL3(SCRLO,SCRLL,SCRLU,TISCRL,CRL)
      CRL1=GPSCRL*CRL +CRLINT
```

```
      CIMGIN=INTGL3(SIMGO,SIMGL,SIMGU,TISIMG,CIMG)
      CIMG1=GPSIMG*CIMG + CIMGIN
      IF(CRL1 .LT.SCRLL)CRL1 =SCRLL
      IF(CRL1 .GT.SCRLU)CRL1 =SCRLU
      IF(CIMG1.LT.SIMGL)CIMG1=SIMGL
      IF(CIMG1.GT.SIMGU)CIMG1=SIMGU
C
C     MANUAL FEATURE FOR SETTING FIRING ANGLE MODULATION MAG/PHASE
C     ------------------------------------------------------------
      IF(MANUAL.GT. 1)THEN
      CRL1=ARMOD
      CIMG1=AIMOD
      END IF
C
C     FIND MODULATION PEAK AND PHASE FROM REAL & IMG PARTS
C     ----------------------------------------------------
      IF(ABS(CRL1).LE.1.0E-08) CRL1=SIGN(1.0E-08,CRL1)
      DELTA=ATAN2(CIMG1,CRL1)
      PKDEL=SQRT(CRL1**2+CIMG1**2)
C
C     DEFINE MODULATION FOR RS, ST & TR PHASE THYRISTORS
C     SUCH THAT MODULATION IS SINUSOIDAL
C     ----------------------------------------------------
      DELRS=PKDEL*COS(DELTA)
      DELST=PKDEL*COS(DELTA+2.094395)
      DELTR=PKDEL*COS(DELTA+4.188790)
C
C     ACTUALLY GENERATE THE SINUSOIDAL MODULATION SIGNAL
C     ----------------------------------------------------
C
      CRL11=CRL1 * COS(THETR -1.57080)
      CIMG11=CIMG1 * (-1.0*SIN(THETR-1.57080))
      ALPMOD=CRL11 + CIMG11
C
      STOR(NEXC+1)=CRL1
      STOR(NEXC+2)=CIMG1
      STOR(NEXC+3)=DELTA
      STOR(NEXC+4)=PKDEL
      STOR(NEXC+5)=DELRS
      STOR(NEXC+6)=DELST
      STOR(NEXC+7)=DELTR
      STOR(NEXC+8)=CRL11
      STOR(NEXC+9)=CIMG11
      STOR(NEXC+10)=ALPMOD
      NEXC=NEXC+10
C
      RETURN
      END
C     ~~~~~~~~~~~~~~~~~~~~~~~~~~~~~~~~~~~~~~~~~~~~~~~~~~~~~~~~~~~~~~~~~~~~~~~~
```

B6: Subroutine FOURIER.FOR - Fourier Analysis

```
C      THIS PROGRAM DOES A FOURIER ANALYSIS OF SVC MODEL OUTPUT DATA
C      ------------------------------------------------------------
C      IN FILES"0.TCR3"(R PHASE),"0.TCR4"(S PHASE),&"0.TCR5"(T PHASE)
C      ------------------------------------------------------------------------
C      TRAPEZOIDAL RULE IS USED FOR COMPUTING  A(N) & B(N).
C      ---------------------------------------------------
C      SYMETRICAL COMPONENTS OF EACH FREQUENCY ARE THEN CALCULATED
C      ----------------------------------------------------------
C      WITH VALUES REFERENCED TO  R-PHASE .
C      -----------------------------------
C
       COMMON DATA
       DIMENSION SUMA(9),SUMB(9),A(9),B(9),C(9),PHI(9),DATA(6000,11)
       DIMENSION AR(9),BR(9),CR(9),PHIR(9),CDOM(9),CDOA(9)
       DIMENSION AS(9),BS(9),CS(9),PHIS(9),CDPM(9),CDPA(9)
       DIMENSION AT(9),BT(9),CT(9),PHIT(9),CDNM(9),CDNA(9)
       COMPLEX CDO(9),CDP(9),CDN(9),CMPLX
       CHARACTER*72 TITLE1,TITLE2,TITLE3
       CHARACTER*8 FDATA
       CHARACTER*8 FSTAT
       CHARACTER*8 DATA1,DATA2,DATA3
       REAL OMEGA
C
       WRITE(1,3)
 3     FORMAT(' ENTER 3 FILENAMES CONTAINING THE DATA',
      &' TO BE ANALYZED -MAX. 8 CHARACTERS:')
       READ(1,4) DATA1,DATA2,DATA3
 4     FORMAT(3A)
C
       WRITE(1,6)
 6     FORMAT(' ENTER AN UP TO 8 CHARACTER OUTPUT FILE NAME:')
       READ(1,7) FDATA
 7     FORMAT(A)
       WRITE(1,8)
 8     FORMAT(' ENTER AN UP TO CHARACTER STATISTIC O/P FILE NAME:')
       READ(1,7) FSTAT
C
C      IUNIT0 = UNIT NUMBER OPENED TO CREATE OUTPUT FILE 'FDATA'
       IUNIT0=7
C      IUNIT1 = UNIT NUMBER OPENED TO CREATE OUTPUT FILE 'FSTAT'
       IUNIT1=8
C
       OPEN (IUNIT0,FILE=FDATA)
       OPEN (IUNIT1,FILE=FSTAT)
C
C
       WRITE(1,500)
 500   FORMAT(' THIS PROGRAM READS 3 EMTDC OUTPUT FILES AND THEN'/,
      & ' PERFORMS A FOURIER ANALYSIS ON THE SAME USER SPECIFIED'/,
      & ' CHANNEL IN EACH FILE. THE PROGRAM ASSUMES THAT TIME IS'/,
      & ' IN CHANNEL "0" AND DATA TO BE ANALYZED IS IN CHANNELS'/,
      & ' "1" THROUGH "10". THE PROGRAM ALSO REQUIRES'/,
      &' PERIOD MARKERS FROM ONE OF THE CHANNELS - THE PROGRAM LOOKS'/,
      &' FOR A POSITIVE EDGE OF A PULSE TO MARK THE START OF A PERIOD'/,
      &' AND THE EDGE OF A SUBSEQUENT PULSE TO MARK THE END OF A '/,
      &' PERIOD OR AN INTEGRAL NUMBER OF PERIODS.'/,
      &' THE ANALYSIS WILL START AT THE FIRST PERIOD MARKER AFTER THE'/,
      &' START TIME INPUT BY THE USER.'/)
C
C      INPUT USER-SPECIFIED DATA
C
       WRITE(1,501)
 501   FORMAT(' INPUT A 3 LINE TITLE DESCRIBING THE SIGNAL TO BE '/,
      &' ANALYZED (UP TO 72 CHARACTERS) TITLE = :'/)
       READ(1,502)  TITLE1
       READ(1,502)  TITLE2
       READ(1,502)  TITLE3
 502   FORMAT(A)
C
       WRITE(1,503)
 503   FORMAT(' NUMBER OF DATA CHANNELS USED IN EMTDC OUTPUT FILE'/,
      &' (INTEGER FROM "1-10") CHANNELS EQUALS : ')
       READ(1,*) NCHAN
C
```

```
      WRITE(1,504)
 504  FORMAT(' INPUT CHANNEL NUMBER OF DATA TO BE ANALYZED'/,
     &' (INTEGER BETWEEN "1" AND "10"). CHANNEL # EQUALS : ')
      READ(1,*) ICHAN
C
      WRITE(1,505)
 505  FORMAT(' ENTER CHANNEL NUMBER WHICH CONTAINS THE PERIOD MARKERS',/
     &' (INTEGER "1-10")'/,
     & ' CHANNEL NUMBER EQUALS : ')
      READ(1,*) IPERD
C
      WRITE(1,507)
 507  FORMAT(' INPUT NUMBER OF PERIODS OVER WHICH ANALYSIS IS TO'/,
     &' BE CALCULATED. PERIODS EQUALS : ')
      READ(1,*) NPERD
      WRITE(1,508)
 508  FORMAT(' INPUT TIME IN SECONDS AFTER WHICH ANALYSIS IS TO BE',/
     &' CALCULATED. TSTART = : ')
      READ(1,*) TSTART
C
      WRITE(IUNIT0,700)
      WRITE(IUNIT1,700)
 700  FORMAT( ///)
      WRITE(IUNIT0,701)
      WRITE(IUNIT1,701)
 701  FORMAT(' ',6X,'**************************************************',
     &'************************')
C
      WRITE(IUNIT0,702) TITLE1
      WRITE(IUNIT0,702) TITLE2
      WRITE(IUNIT0,702) TITLE3
      WRITE(IUNIT1,702) TITLE1
      WRITE(IUNIT1,702) TITLE2
      WRITE(IUNIT1,702) TITLE3
 702  FORMAT(7X,A72)
C
      WRITE(IUNIT0,703)
      WRITE(IUNIT1,703)
 703  FORMAT(/' ',6X,'**************************************************',
     &'************************')
C
C      A FOURIER ANALYSIS OF EACH PHASE IS CALCULATED IN TURN.
C      -------------------------------------------------------
C      TO DO THIS DATA FROM THE APPROPRIATE DATA FILE IS READ
C      -----------------------------------------------------
C      INTO AN ARRAY.COLUMN 1 IS TIME,COLUMN 2 - 10 CAN CONTAIN
C      --------------------------------------------------------
C      DATA ON WHICH THE PERFORM A FOURIER ANALYSIS, EXCEPT CHNL IPERD
C      ---------------------------------------------------------------
C      CONTAINS DATA USED TO IDENTITY THE DURATION OF A PERIOD.
C      -------------------------------------------------------
C
      M=NCHAN+1
      ICHAN=ICHAN+1
      IPERD=IPERD+1
C
      IPHASE=1
      DO 5 KK=1,3
      IF(IPHASE.EQ.1) OPEN(18,FILE='0.TCR3')
      IF(IPHASE.EQ.2) OPEN(19,FILE='0.TCR4')
      IF(IPHASE.EQ.3) OPEN(20,FILE='0.TCR5')
C
      IF(IPHASE.EQ.1) WRITE(IUNIT0,190)
      IF(IPHASE.EQ.2) WRITE(IUNIT0,191)
      IF(IPHASE.EQ.3) WRITE(IUNIT0,192)
190   FORMAT('       FOURIER COEFFICIENTS OF R-PHASE - PEAK VALUES '/)
191   FORMAT('       FOURIER COEFFICIENTS OF S-PHASE - PEAK VALUES '/)
192   FORMAT('       FOURIER COEFFICIENTS OF T-PHASE - PEAK VALUES '/)
C
C     READ DATA FILE TO AN ARRAY
C     --------------------------
      LINE=0
      IUNIT=IPHASE+17
      DO 10 I=1,6001
      READ(IUNIT,99,END=12) (DATA(I,J),J=1,M)
99    FORMAT(F8.5,10(1X,G11.4))
10    LINE=LINE+1
12    CONTINUE
14    CONTINUE
C
```

```
C      INDENTIFY A DURATION OF ONE PERIOD IN LENGTH AFTER
C      ------------------------------------------------
C      TIME SPECIFIED BY  TSTART. ISTART  AND  ISTOP  IDENTIFY
C      ------------------------------------------------------
C      THE FIRST AND LAST ROWS OF DATA USED FOR THE FOURIER ANALYSIS.
C      ------------------------------------------------------------

       IFLG=0
       LCNT=1
       NPULS= 0
       ISTART=0
       ISTOP=0
       DO 20 I=2,LINE
       IF(DATA(I,1) .GT. TSTART) THEN
       IF( DATA(I,IPERD)-DATA(I-1,IPERD) .GT. 0.01 ) THEN
       IF ( NPULS .EQ. 0 ) THEN
       ISTART = LCNT + 1
       END IF
       IF( NPULS .EQ. NPERD)THEN
       ISTOP = LCNT + 1
       GO TO 21
       END IF
       WRITE(IUNIT1,202) NPULS
 202   FORMAT('       NPULS = ',I5)
       NPULS = NPULS + 1
       END IF
       END IF
       LCNT=LCNT+1
    20 CONTINUE
       IF(NPULS .LT. NPERD)THEN
       WRITE(1,512)
 512   FORMAT(' WARNING, INSUFFICIENT PERIODS IN DATA',/
      &' INPUT SMALLER # OF PERIODS : ')
       READ(1,*) NPERD
       GO TO 14
       END IF
C
    21 CONTINUE
C
C
C      COMPUTE SAMPLE INTERVAL AND NUMBER SAMPLES
C      ------------------------------------------
       DELT=0.0
       DO 30 I=1,5
       DELT1=DATA(I+1,1)-DATA(I,1)
    30 DELT=DELT+DELT1
       DELT=DELT/5.0
       NSAM=(ISTOP-ISTART)
       WRITE(IUNIT1,201) DELT,NSAM
 201   FORMAT(' SAMPLE INTERVAL=',G12.5,20X,'NUMBER OF SAMPLES=',I5/)
       WRITE(IUNIT1,200) ISTART,ISTOP,TSTART,LINE
  200  FORMAT('      ISTART=',I5,5X,'ISTOP=',I5,5X,'TSTART=',G13.6,
      &'LINE=',I5)
C
       WRITE(IUNIT1,62)  (DATA(ISTART,J),J=1,M)
       WRITE(IUNIT1,62)  (DATA(ISTOP,J),J=1,M)
62     FORMAT(F8.5,10(1X,G11.4))
C
```

```
C      CALCULATE FOURIER SERIES NOW
C      ----------------------------
C
       DO 35 J=1,8
       SUMA(J)=0.0
35     SUMB(J)=0.0
       ISTRT1=ISTART+1
       ISTOP1=ISTOP-1
C
       OMEGA=376.99112
       TPERD=2*3.14159265/OMEGA
       DO 40 I=ISTRT1,ISTOP1
       SUMA(1)=SUMA(1)+ DATA(I,ICHAN)
       DO 50  N=1,7
       SUMA(N+1)=SUMA(N+1)+ DATA(I,ICHAN)*COS(N*OMEGA*DATA(I,1))
50     SUMB(N+1)=SUMB(N+1)+ DATA(I,ICHAN)*SIN(N*OMEGA*DATA(I,1))
40     CONTINUE
C      DC COMPONENT IS Ao/2 :
C      ----------------------
       A(1)=(DATA(ISTART,ICHAN)+DATA(ISTOP,ICHAN)+2.0*SUMA(1))
       A(1)=A(1)*DELT/(2*TPERD*NPERD)
       B(1)=0.0
       DO 60  N=1,7
       A(N+1)=DATA(ISTART,ICHAN)*COS(N*OMEGA*DATA(ISTART,1))+
      & DATA(ISTOP,ICHAN)*COS(N*OMEGA*DATA(ISTOP,1))+2.0*SUMA(N+1)
       A(N+1)=A(N+1)*DELT/(TPERD*NPERD)
       B(N+1)=DATA(ISTART,ICHAN)*SIN(N*OMEGA*DATA(ISTART,1))+
      & DATA(ISTOP,ICHAN)*SIN(N*OMEGA*DATA(ISTOP,1))+2.0*SUMB(N+1)
       B(N+1)=B(N+1)*DELT/(TPERD*NPERD)
60     CONTINUE
       DO 70  N=1,8
       IF(ABS(A(N)).LT.1.0E-08) A(N)=SIGN(1.0E-08,A(N))
       C(N)=SQRT(A(N)**2+B(N)**2)
       PHI(N)=-ATAN2(B(N),A(N))*180.0/3.14159265
70     CONTINUE
C      SAVE COEFFICIENTS FOR FURTHER CALCULATIONS.
C      -------------------------------------------
C
       IF(IPHASE.EQ.1) THEN
       DO 601 J=1,8
       AR(J)=A(J)
       BR(J)=B(J)
       CR(J)=C(J)
601    PHIR(J)=PHI(J)
       ELSE IF(IPHASE.EQ.2)THEN
       DO 602 J=1,8
       AS(J)=A(J)
       BS(J)=B(J)
       CS(J)=C(J)
602    PHIS(J)=PHI(J)
       ELSE IF(IPHASE.EQ.3)THEN
       DO 603 J=1,8
       AT(J)=A(J)
       BT(J)=B(J)
       CT(J)=C(J)
603    PHIT(J)=PHI(J)
       END IF
C
```

```
C
      WRITE(IUNIT0,704) (C(J),PHI(J),J=1,8)
704   FORMAT('       DC:MAG    =',F8.5,2X,'PHASE=',F7.2,2X,
     & '   60HZ:MAG=',F8.5,2X,'PHASE=',F7.2/
     & '       120Hz:MAG=',F8.5,2X,'PHASE=',F7.2,2X,' 180HZ:MAG=',
     & F8.5,2X,'PHASE=',F7.2/'         240HZ:MAG=',F8.5,2X,
     & 'PHASE=',F7.2,2X,' 300HZ:MAG=',F8.5,2X,'PHASE=',F7.2/
     & '       360HZ:MAG=',F8.5,2X,'PHASE=',F7.2,2X,' 420HZ:MAG=',
     & F8.5,2X,'PHASE=',F7.2/)
C
      IF(IPHASE.EQ.1) CLOSE(UNIT=18)
      IF(IPHASE.EQ.2) CLOSE(UNIT=19)
      IF(IPHASE.EQ.3) CLOSE(UNIT=20)
C
      IPHASE=IPHASE+1
5     CONTINUE
C
C     CALCULATE SEQUENCE COMPONENTS OF SVC CURRENTS
C     ---------------------------------------------
C     NOTE THAT A(N) IS ASSOCIATED WITH REAL AXIS(+ve X)
C     --------------------------------------------------
C     AND  -B(N) IS ASSOCIATED WITH IMG AXIS(+ve Y).
C     ----------------------------------------------
C
      DO  800 J=1,8
      CDO(J)=0.333*(CMPLX(AR(J),-BR(J))+CMPLX(AS(J),-BS(J))
     ,+CMPLX(AT(J),-BT(J)))
      CDP(J)=0.333*(CMPLX(AR(J),-BR(J))+CMPLX(AS(J),-BS(J))*(-0.5,0.866)
     &+CMPLX(AT(J),-BT(J))*(-0.5,-0.866))
      CDN(J)=0.333*(CMPLX(AR(J),-BR(J))+CMPLX(AS(J),-BS(J))*
     &(-0.5,-0.866)+CMPLX(AT(J),-BT(J))*(-0.5,+0.866))
800   CONTINUE
C
      DO 820 J=1,8
      CDOM(J)=CABS(CDO(J))
      CDPM(J)=CABS(CDP(J))
      CDNM(J)=CABS(CDN(J))
      A(1)=REAL(CDO(J))
      A(2)=REAL(CDP(J))
      A(3)=REAL(CDN(J))
      DO 821 K=1,3
      IF(ABS(A(K)).LT.1.0E-08) A(K)=SIGN(1.0E-08,A(K))
821   CONTINUE
      CDOA(J)=ATAN2(AIMAG(CDO(J)),A(1))*180.0/3.14159265
      CDPA(J)=ATAN2(AIMAG(CDP(J)),A(2))*180.0/3.14159265
      CDNA(J)=ATAN2(AIMAG(CDN(J)),A(3))*180.0/3.14159265
820   CONTINUE
C
      WRITE(IUNIT0,850)
850   FORMAT('       SYMMETRICAL COMPONENT ANALYSIS '/)
      WRITE(IUNIT0,851)
851   FORMAT('       ZERO SEQUENCE COMPONENTS'/)
      WRITE(IUNIT0,704) (CDOM(J),CDOA(J),J=1,8)
      WRITE(IUNIT0,853)
853   FORMAT('       POSITIVE SEQUENCE COMPONENTS'/)
      WRITE(IUNIT0,704) (CDPM(J),CDPA(J),J=1,8)
      WRITE(IUNIT0,854)
854   FORMAT('       NEGATIVE SEQUENCE COMPONENTS'/)
      WRITE(IUNIT0,704) (CDNM(J),CDNA(J),J=1,8)
      CLOSE(UNIT=IUNIT0)
      CLOSE(UNIT=IUNIT1)
      STOP
      END
C
```